### Targeted gene silencing/knockout of tomato phototropins to decipher their role in fruit carotenogenesis

Thesis to be submitted for the award of Ph.D. Degree

To

University of Hyderabad

By

Alekhya Dindu

(14LPPH17)

Supervisor: Prof. Y. Sreelakshmi



DEC, 2022

REPOSITORY OF TOMATO GENOMICS RESOURCES

DEPARTMENT OF PLANT SCIENCES

SCHOOL OF LIFE SCIENCES

UNIVERSITY OF HYDERABAD

HYDERABAD- 500 046

INDIA.



# DEPARTMENT OF PLANT SCIENCES SCHOOL OF LIFE SCIENCES UNIVERSITY OF HYDERABAD DECLARATION

I, D. Alekhya, hereby declare that the work described in this thesis entitled "Targeted gene silencing/knockout of tomato phototropins to decipher their role in fruit carotenogenesis" submitted by me under the supervision of Professor Y Sreelakshmi, Department of Plant Sciences, is an original research work. I also declare that it has not been submitted previously in part or in full to this University or any other University or Institution for the award of any degree or diploma. A report on plagiarism statistics from the University Librarian is enclosed.

Date 29/12/2014

Place: Hyderabad

D.Alekhya

Enrol. No. 14LPPH17

pr Y Sreelakshmi

Supervisor PROF. Y. SREELAKSHMI

Dept. of Plant Sciences School of Life Sciences University of Hyderabad Hyderabad-500 046, INDIA.



# DEPARTMENT OF PLANT SCIENCES SCHOOL OF LIFE SCIENCES UNIVERSITY OF HYDERABAD CERTIFICATE

This is to certify that the thesis entitled "Targeted gene silencing/knockout of tomato phototropins to decipher their role in fruit carotenogenesis" is based on the results of the work done by Ms D Alekhya for the degree of Doctor of Philosophy under my supervision. This work presented in this thesis is original and has not been submitted for any degree or diploma of any other University. A report on plagiarism statistics from the University Librarian is enclosed.

This thesis is free from plagiarism and has not been submitted previously in part or in full to this or any other University or Institution for award of any degree or diploma.

Further, parts of the thesis have been:

#### A. Published in the following publication:

Kilambi HV, Dindu A, Sharma K, Nizampatnam NR, Gupta N, Thazath NP, Dhanya AJ, Tyagi K, Sharma S, Kumar S, et al (2021) The new kid on the block: a dominant-negative mutation of phototropin1 enhances carotenoid content in tomato fruits. Plant J 106: 844-961

#### B. Presented in the following conferences:

1. Alekhya Dindu, Nizampatnam N.R, Neha Gupta, Rameshwar Sharma, Sreelakshmi Y Functional Genomics of phototropin1 gene in Tomato Poster

- presentation at the National Conference on Frontiers in Plant Biology (NCFIPB 2020), during 31<sup>st</sup> January–1<sup>st</sup> February 2020, in Hyderabad, Telangana, India.
- 2. Alekhya Dindu, Yellamaraju Sreelakshmi Functional Genomics of phototropin1 and 2 genes in Tomato. 11<sup>th</sup> Plant Science Colloquium-2019. Department of Plant Sciences, school of Life sciences, University of Hyderabad, Telangana, India.

Further, the student has passed the following courses toward the fulfilment of the coursework requirement for Ph.D. degree.

Sl. No.	Course Code	Name	Credits	Pass/Fail
1.	AS-801	Analytical Techniques	4	Pass
2.	AS-802	Research Ethics, Data Analysis and Biostatistics	3	Pass
3.	AS-803	Lab Work & Seminar	5	Pass

Head

Deproof by Harian Grees
School of Life Sciences
University of Hyderabad
Hyderabad-500 646 INDIA

Dean Dean

School of Life Sciences
School of Life Sciences
University of Hyderabad
Hyderabad-500 046.

Dr Y Sreelakshmi

Supervisor
PROF. Y. SREELAKSHMI
Dept. of Plant Sciences
School of Life Sciences
University of Hyderabad
Hyderabad-500 046, INDIA.

## Dedicated to My family members

#### ACKNOWLEDGEMENTS

It is the time to put down my feelings in words of thanks to many people who helped me throughout mu PhD journey. I owe my gratitude to all those people who have made possible to write this thesis but also helped in shaping up my carrier towards the next scientific endeavor.

First, my deepest gratitude to my supervisor Prof Y Sreelakshmi. I have been very fortunate to have a mentor like you who gave me constant support, freedom and encouragement to experiments and think in the better scientific perspective. Her enthusiasm, immense knowledge, constructive criticism and patience have helped me overcome many disastrous situations and finally finish this dissertation. I hope that one day I would be like you who can provide constant support and encouragement to people around me.

My co-supervisor Dr R P Sharma, who is always there to listen and give important guidance throughout this journey. My heartfelt thanks to you sir for your encouragement, insightful comments, and constant inspiration.

I also would like to thank Prof. Gopinath, my doctoral committee member for his guidance and timely suggestion throughout my research work.

My sincere thanks to Dean, Prof. S. Dayananda (Dean, School of Life Sciences), Prof. K.V.A. Ramaiah, Prof. P. Reddana (Former dean, School of Life Sciences); Prof. S. Rajagopal (Head Dept. of Plant sciences), and Prof. G. Padmaja, Prof.CH Venkataramana (Former head, Dept. of Plant Sciences) for providing me the opportunity to utilize the facilities of the Department and School.

I take this opportunity to thank Dr Arun Kumar Pandey, for designing and cloning the construct phot1 and phot2 RNAi constructs, and I thank Thanvitha for tissue culture with RNAi lines. I thank Dr Nizampatnam Narasimha Rao for the CRISPR phot1 construct, and thanks to Dr Neha Gupta for regenerating phot1 CRISPR lines. Thanks to Dr Prateek Gupta and Kapil Sharma for running the GCMS samples.

I am also thankful to all my past and present lab membersof RTGR for enduring me throughout my stay in the lab. I would like to mention Dr Himabindu, DR Kamal Tyagi, Dr Kapil Shrama, Dr Supriya, Dr Chaitanya, Dr Rachana, Dr Alka, Dr Suresh, Dr Rakesh Kumar, Dr Pallawi, Dr Prateek Gupta, Hema Latha, Dhanya, Anusha, Vikas, Adithi, Princy, Juveria, Sumi, Appus, Meenakshi, Dr Narasimha Rao, Dr Arun Kumar Pandey, Sravan, Dr Hymavathi, Thanvita, Dr Avanish, Dr Nidhi, Dr Amita, Dr Satyavathi, Dr Neha Gupta, Dr Mallikarjun, Dr Injang, Dr Durgeshwar for helping me in the one way or the other way to gain better insight into my work I extend my thanks to field assistant Narasimha, Zamir, Yadagiri and lab accountant Venkat Reddy.

Finally, and the most importantly, none of this would have been possible without the love and patience of my family. I am grateful to my late parents and my late grandmother. My heartfelt thanks must go to all my family member; my father, mother, grandmother, aunts and uncles, brothers and sister-in law for their moral support and encouragement and cooperation has allowed me to achieve this level. My special thanks to my husband Yuv Raj in my life. He has been a silent support in my life.

Finally, the financial support provided by the Department of Biotechnology in the form of DBT/JRF and SRF fellowship during Ph.D and even during covid times. I am also thankful to DBT- Tomato Ripening Network project to YS, DBT- CEIB projects to YS and RS, DST-SERB to YS for making me part of these projects.

Last but not least, I am highly grateful to God for his blesssings and strength which has helped me to successfully achieve this goal.

#### TABLE OF CONTENTS

Table of contents	
List of Abbreviationsxiv	V
Chapter 1: Introduction1-5	
Chapter 2: Review of literature	5
2.1 Tomato	
2.2 Tomato crop improvement	
2.3 Techniques to annotate gene function	
2.3.1 Induced mutagenesis	
2.3.2 Physical mutagenesis	
2.3.3 Chemical mutagenesis	
2.3.3.1 Limitations of Physical and chemical mutagenesis	
2.3.3.2 Oligonucleotide directed mutagenesis (ODM)	
2.3.3.3 Epigenome editing	
2.3.3.4 Transposons	
2.3.3.5 Zinc Finger Nucleases (ZFNs)	
2.3.3.6 Transcription activator-like effector nucleases (TALENs)	
2.3.3.7 CRISPR-Genome editing technique	
2.3.3.7.1 CRIPSR Genome editing in Plants	
2.3.3.7.2 CRISPR/Cas9 Genome editing approaches in tomato	
2.4 Tomato: A model of climacteric fruit ripening	
2.4.1 Fruit ripening	
2.4.2 Importance of fruit ripening	
2.4.3 Carotenoid biosynthesis	
2.4.4 Metabolic regulation of tomato fruit development and ripening	
2.4.4.1 Changes in the level of organic acids content	
2.4.4.2 Alternation in sugar and sugar alcohols abundance	
2.4.4.3 Amino acid expression and profiling	

2.5 Light
2.5.1 Photoreceptors
2.5.2 Carotenoid gene expression regulation in photosynthetic organs
2.5.3 Effect of photoreceptors on fruit ripening
2.5.4 Light signaling components affect fruit ripening
2.5.5 Phototropin homologs in other plants
2.5.6 Phototropin functions
2.5.7 Phototropin mutants in tomato
Chapter 3: Materials and Methods37-6
3.1.1 RNAi construct for <i>phot1</i> and 2 genes
3.1.2 cDNA amplification and cloning into the entry vector
3.1.3 Cloning of Entry Vector into Destination Vector
3.2 Plant genetic transformation using <i>phot1</i> , <i>phot2</i> and empty vector (pHellsgate) construct
3.2.1 Seed surface sterilization and germination
3.2.2 Explant preparation and preculture
3.2.3 Inoculum preparation and cocultivation
3.2.4 Callus induction, Regeneration and Selection
3.2.5 Root induction and hardening of plantlets
3.2.6 Plant materials and growth conditions
3.3 Development of CRISPR/Cas9 double gRNA constructs for targeting <i>phot1</i> gene
3.3.1 Selection of target site and vector construction
3.3.2 Plant genetic transformation using pCAMBIA2300-CAS9-phot1 construct
3.3.2.1 Seed surface sterilization and germination
3.3.2.2 Explant preparation
3.3.2.3 Preparation of inoculum for co-cultivation
3.3.2.4 Co-cultivation
3.3.2.5 Regeneration and selection
3.3.2.6 Rooting and hardening

3.4 plant material and growth conditions
3.5 DNA isolation
3.5.1 Primer design
3.5.2 Agrobacterium tumefaciens and nptII detection in transgenic plant material
3.5.3 PCR conditions
3.5.4 Analysis of CRISPR/Cas9 induced mutations
3.5.5 DNA sequencing
3.5.6 Multialignment
3.6 RNA isolation
3.6.1 Formaldehyde gel preparation
3.6.2 cDNA synthesis and Real-Time PCR
3.7 Monitoring of chloroplast movement in tomato leaflets
3.7.1 Off-target analysis
3.8 Screening for phototropism in <i>phot1<sup>CR</sup></i> lines
3.9.1 Phenotypic characterization of edited lines
3.9.2 Chlorophyll estimation
3.9.3 Chronological development of fruits
3.9.4 Estimation of ethylene
3.9.5 Estimation of CO <sub>2</sub>
3.9.6 Estimation of sugar content and pH of fruits
3.10 Carotenoids and Xanthophylls profiling from the fruit and leaf tissue
3.11 Metabolic profiling
Chapter 4: Results
Section I
4.1 Silencing of <i>phot1</i> and <i>phot2</i> genes using RNAi strategy
4.1.1 PCR based identification of transgene in T <sub>0</sub> lines
4.1.2 Endogenous <i>phot</i> 2 gene expression levels in <i>phot</i> 2 <i>RNAi</i> lines
4.1.3 Phenotypic characterization of <i>phot2 RNAi</i> lines

- 4.2 Generation of T<sub>1</sub> phot2 RNAi lines
- 4.2.1 Analysis of *phot2* gene expression in the T<sub>1</sub> generation
- 4.2.2 Chloroplast movement
- 4.2.3 Detection of transgene integration in T1 generation by PCR
- 4.2.4 Carotenoid levels in T<sub>1</sub> lines
- 4.2.5 Generation of T<sub>2</sub> lines and their evaluation at the phenotypic and functional level
- 4.3 phot2 gene expression in the T<sub>2</sub> RNAi lines
- 4.3.1 Time course study of chloroplast movement in the T<sub>2</sub> RNAi lines
- 4.3.2 Detection of transgene presence by PCR in the T<sub>2</sub> generation
- 4.3.3 Measurement of carotenoid levels in T<sub>2</sub> lines
- 4.4 Generation of T<sub>3</sub> lines and their evaluation at the phenotypic and functional level
- 4.4.1 *phot2* gene expression in the T<sub>3</sub> RNAi lines
- 4.4.2 Time course study of chloroplast movement in the T<sub>3</sub> lines
- 4.4.3 Detection of transgene by PCR in the T<sub>3</sub> generation
- 4.4.4 Study of fruit development and ripening in *phot2* RNAi lines.
- 4.4.5 °Brix and pH of ripe fruits of phot2 RNAi lines
- 4.4.6 phot2 positively influences carotenoid levels in T<sub>3</sub> lines
- 4.4.7 Gene expression for the rate-limiting enzymes of the carotenoid biosynthetic pathway in the  $T_3$  lines
- 4.4.8 Metabolite analysis in red ripe fruits of *phot2* RNAi lines

#### Section II

- 4.5 Generation of CRISPR/Cas9 edited *phot1* mutant lines
- 4.5.1 Identification of CRISPR/Cas9 induced mutations in T<sub>0</sub> generation
- 4.5.2 phot1<sup>CR</sup> lines show loss of function
- 4.6 Generation and characterization of  $phot1^{CR}$  alleles in the  $T_1$  generation
- 4.6.1 Loss of *phot1* function is stably inherited in the T<sub>1</sub> generation
- 4.6.2 Mutations in *phot1* affect the fruit carotenoid content
- 4.7 Generation and characterization of Cas9 free phot1<sup>CR</sup> lines in the T<sub>2</sub> generation

4.7.1 Identification of potential off-target in <i>phot1</i> <sup>CR</sup> homozygous Cas9 free alleles
4.7.2 Phototropism is affected in $phot1^{CR}$ alleles
4.7.3 <i>phot1</i> <sup>CR</sup> alleles show reduced chloroplast accumulation
4.7.4 Plant morphology of $phot1^{CR}$ alleles
4.7.5 Leaf morphology is altered in $phot1^{CR}$ alleles
4.7.6 phototropin1 affects leaf chlorophyll and carotenoid contents
4.7.7 Fruit development is altered in $phot1^{CR}$ alleles
4.7.8 Ethylene and $CO_2$ emissions from the fruits of <i>phot1</i> <sup>CR</sup> alleles
4.7.9 Acid and sugar levels in RR fruits of <i>phot1<sup>CR</sup></i> alleles
4.7.10 phot1 mutants show decreased carotenoid levels in fruits
4.7.11 Carotenogenic gene expression is not correlated content in $phot1^{CR}$ alleles
4.7.11.1 Mutations in <i>phot1</i> down-regulate the carotenoid sequestration genes
4.7.12 <i>phot1</i> mutations affect the primary metabolite levels
Chapter 5: Discussion83-91
Chapter 6: Summary and Conclusion93-103
6.1 Silencing of <i>phototropin1</i> and <i>phototropin2</i> genes using RNAi strategy
6.2 CRISPR/Cas9 mediated editing of phototropin1 gene
6.3 Conclusion
References

#### LIST OF ABBREVIATIONS

ABA Abscisic acid

AV Arka-Vikas

bp base pair

cDNA Complementary DNA

CRISPR Clustered Regularly Interspersed Palindromic Repeats

cDNA Complementary DNA

cry2 cryptochrome2

DNA Deoxyribonucleic acid

DNase Deoxyribonuclease

dNTP Deoxyribonucleotide triphosphate

DPA Days post anthesis

EMS Ethyl methyl Sulfonate

EtBr Ethidium bromide

FW Fresh weight

GC Gas chromatography

hr Hour

HPLC High performance liquid chromatography

Kb Kilo base

LED Light-emitting diode

min Minute

mRNA Messenger RNA

Nr Never-ripe

PCR Polymerase chain reaction

PHOT1 Phototropin1

PHOT2 Phototropin2

Phy Phytochrome

RNAi RNA interference

q-PCR Quantitative real-time PCR

RNA Ribonucleic acid

RNase Ribonuclease

SE Standard error

Sec second

Sl Solanum lycopersicum

UPLC Ultra-High performance liquid chromatography

UV Ultra-voilet light

UV-B resistance protein 8, UV-B receptor

v/v volume/volume

WT Wild Type

w/v weight/volume

#### 1. Introduction

Fruit ripening is a complex process involving many physiological and biochemical events that leads to the accumulation of pigments, metabolic changes related to flavor and nutrient composition, softening of the cell wall, etc. (Klee and Giovannoni 2011). The most studied model of fleshy fruit ripening is, without a doubt, the tomato Solanum lycopersicum. In tomato, fruit ripening is accompanied by pigment production, typically of carotenoids, like lycopene and  $\beta$ -carotene. This accumulation of carotenoids is therefore inhibited in non-ripening mutants like RIPENING INHIBITOR (RIN) (Vrebalov et al., 2002), COLORLESS NON-RIPENING (CNR) (Manning et al., 2006), and NON-RIPENING (NOR) (Yuan et al., 2016). These mutant loci encodetranscription factors that regulate fruit ripening, associated pigmentation, and softening, acting primarily through ethylene synthesis and signaling (Seymour et al., 2013). In tomato, ethylene differentially affects fruit ripening depending on the stage of development. In addition to ethylene, other hormones like ABA, JA, and auxin appear to be essential factors for fruit ripening and pigmentation (Galpaz et al., 2008; Liu et al., 2012; Su et al., 2015). Together, this network of transcriptional and hormonal regulators mediates the physiological changes that make the fruit attractive to seed-dispersing organisms. The availability of a high-quality tomato genome sequence is the foundation for expanding and refining our understanding of the genetic regulation of fruit development and ripening.

Besides these factors, light also has an auxiliary role in regulating fruit pigmentation. This is exemplified by the fact that the fruits developed on light-grown plants accumulate high levels of carotenoids than the dark-incubated fruits (Raymundo et al., 1976; Gupta et al., 2014). However, fruits of the light signaling defective mutants, such as *hp1* and *hp2*, accumulate high amounts of carotenoids, suggesting a negative regulation of light in this process. But, the increase in carotenoids in these mutants is primarily through the increased number and size of plastids and high levels of carotenoid sequestration proteins (Azari et al., 2010; Kilambi et al., 2013). Upstream to the light signaling components lie the photoreceptors that primarily sense the light and regulate plant growth and development. Among the five different photoreceptors, overexpression of either phytochrome, cryptochrome, or UVR8 increases the carotenoid content of tomato

fruits (Liu et al., 2018; Giliberto et al., 2005, Li et al., 2018, Alves et al., 2020). However, the loss of function of cryptochromes or phytochromes and UVR8 silencing reduces the carotenoid levels (Fantini et al., 2019, Gupta et al., 2014, Bianchetti et al., 2018, Li et al., 2018). In addition, downstream to phytochromes, COP1, HY5, and PIF1 regulate the light signaling and influence carotenoid accumulation (Liu et al., 2008; Bou-Torrent et al., 2015).

Phototropins are blue light sensing photoreceptors that are mainly involved in mediating the movements of plants and help optimize plants' photosynthetic efficiency. Some of the responses mediated by phototropins are phototropism of shoots (after which they are named),negative phototropism in case of roots, movement of chloroplasts in response to change in light intensities, movement of stomata for gaseous exchange, leaf positioning and flattening, etc (Christie et al., 1998, Wang et al., 2002, Sakai et al., 2001, Kinoshita et al., 2001, Inoue et al., 2008, Sakamoto and Briggs, 2002). All these responses help plants survive the best under changing environmental conditions by optimizing their photosynthetic efficiency. Also, all these processes have been studied using Arabidopsis as a model system and therefore are limited to vegetative tissues. The role of phototropins in organs such as fruits is relatively unknown as Arabidopsis lacks a fleshy fruit.

The functions of any gene can be studied by isolating mutants in it. Now that the genome sequences of various crop species are available, it is necessary to determine the role of previously uncharacterized genes. There are two methods for determining gene function. Forward genetics is the first strategy involving mutagenesis followed by phenotype screening to identify the locus contributing to a given function/phenotype. Eventually, either by mapping or candidate gene approaches, this strategy leads to identifying a gene. The reverse genetics strategy, on the other hand, is defined as finding a mutation first in a specific locus and then establishing its function through rigorous phenotyping and experimental research.

Because creating a mutagenized population takes a long time and requires a lot of resources, researchers have been focusing their efforts in recent years on developing genome-wide mutagenesis resources that the research community can use. Following the completion of the Arabidopsis and rice genome sequences, community resources such as T-DNA or transposon mutagenized lines were developed, which have tremendously benefited the community and assisted in

identifying multiple novel genes (The Arabidopsis Genome Initiative, 2000; Sasaki & Burr, 2000). Though the tomato genome was sequenced in 2012, the gene annotation phase is still behind schedule due to the restricted resources available in tomato for this purpose. Some of the strategies that can be used for functional genomics studies are TILLING, RNAi, VIGS, zinc finger nucleases, TALENS, and CRISPR/Cas9 (Till et al., 2003, Senthil Kumar and Mysore, 2010, Ruiz et al., 1998, Moon et al., 2010, Christian et al., 2013).

RNAi is widely utilized in plants as a reverse genetics technique to suppress the expression of specific genes. Using RNAi technology has some advantages over other technologies. One advantage is the possibility of targeting many genes in a family with a single RNAi-inducing transgene by selecting a conserved sequence in all members. This results in the specific silencing of any member of a multi-gene family. Another benefit is RNAi dominantly silences genes, whereas insertional or other loss of function mutations are generally recessive. The main feature of RNAi is that it may silence numerous genes in polyploid plants with more than two orthologous copies of each gene (Preuss & Pikaard, 2003). Orthologous genes can also be knocked down in the F<sub>1</sub> generation if one of the parents carries an RNAi-inducing transgene. Along with its dominant character, RNAi saves time by obviating the need for multiple generations of backcrossing to discover individuals homozygous for recessive loss of function alleles.

RNAi was extensively used in tomato for understanding gene regulation in carotenogenesis. When 9-cis-epoxycarotenoid dioxygenase (NCED), a crucial enzyme in the ABA production pathway, was silenced using RNAi, fruits from these lines exhibited deep red coloration compared to control fruit (Sun et al., 2012) and a reduction in ABA and an increase in ethylene levels. These results indicate that ABA may have controlled the level of pigmentation and the carotenoid content during ripening. In another study, RNAi of TAGL1 has shown that the gene is necessary for the genetic regulation of flower and fruit development (Gimenez et al., 2010). When zetacarotene desaturase (ZDS) was repressed by RNAi, the fruits lacked the distinctive red carotenoid, all trans-lycopene, and instead had beautiful yellow color due to increased 9,9' di-cis-carotene accumulation (McQuinn et al., 2020).

CRISPR/Cas9 these days has become more popular than the other techniques, primarily due to the ease of making construct, high efficiency of the

Cas9 nuclease in making cuts in the genomic DNA, and the subsequent repair process during which the mutations are generated. In addition, the availability of suitable transformation methods in many crops makes functional genomics studies feasible. CRISPR-Cas systems have emerged as a unique method to edit target genes in eukaryotes by exploiting this inherent property of prokaryotes (Wiedenheft et al., 2012). This technique needs Cas9 nuclease, and a synthetic single-guide RNA (sgRNA) made up of a short CRISPR RNA (crRNA) and a trans-activating CRISPR RNA (tracrRNA) to achieve cleavage in vitro (Jinek et al., 2012). For precise editing 20-bp sequence within the crRNA corresponding to the editing sequence followed by NGG (Proto-spacer Adjacent Motif or PAM) after the 3' end is necessary. Following successful sgRNA targeting, Cas9 creates a double-strand break three base pairs upstream of the PAM site, resulting in indels after the repair via error-prone nonhomologous end joining (NHEJ). Also, this can be used to fix an inserted transgene via homology-directed repair (HDR). By changing just one amino acid, Cas9 can be transformed into a nickase (Cas9n), favoring HDR over NHEJ (Cong et al., 2013; Mali et al., 2013).

The CRISPR system was effectively used to alter the genomes of mice, zebrafish, human cell lines, and higher plants (Wang et al., 2013, Hwang et al., 2013, Cong et al., 2013, Jinek et al., 2012). Currently, CRISPR/Cas9 is the gene editing method in plants, allowing for the insertion or deletion of genes by creating DNA breaks in addition to gene knockout (Filler Hayutet al., 2017; Roux et al., 2006; Cermak et al., 2015; Cermak et al., 2017). With the successful editing of the plant genome in 2013, the first gene to be edited in tomato was *Argonaute 7*, which resulted in the identification of edited lines due to a distinct wiry phenotype during the tissue culture stage itself (Brooks et al., 2014). After that, several publications were seen where CRISPR/Cas9-based genome editing was carried out to combat abiotic and biotic stresses, domestication of wild tomato species, and improvement of tomato nutrition-lycopene, anthocyanins, ascorbate, sugars, etc., and shelf life (Wang et al., 2019).

Compared to the other photoreceptors, the information about the role of blue light sensing phototropins in tomato fruit development and ripening is lacking mainly due to the scarcity of mutants. Our group isolated a single *nonphototropic* seedling 1 (Nps1) mutant in tomato phototropin1 from an EMS mutagenized population (Sharma et al., 2014). This mutant accumulates high levels of lycopene

in the fruits, which was tightly linked to the dominant negative nature of the R494H mutation (Kilambi et al., 2021). Considering the lack of alleles for *phototropin1* (other than *Nps1*) and *phototropin2* in tomato, we sought to use reverse genetic strategies like RNAi and CRISPR/Cas9 to generate additional alleles. We framed the following objectives for our study.

#### **Objectives:**

- To generate gene silenced/knockout mutations in *phototropin1* and *phototropin2* genes of tomato.
- To examine the effect of *phototropin1* and *phototropin2* mutations on fruit carotenogenesis.

#### 2. Review of literature

#### 2.1 Tomato

Lycopersicum esculentum was renamed Solanum lycopersicum by modern taxonomists and is one of the crucial members of the Solanaceae family. It is a diploid genome (n=12, ~950 Mb) with approximately 34,000 protein-coding genes (Tomato Genome Consortium 2012). It is commercially one of the essential crops due to its dietary value and industrial-originated products. The abundance of genetic and genomic resources also serves as the best link between model plants like Arabidopsis and other crops.

#### 2.2 Tomato crop improvement

On a global level, the domestication of tomatoes resulted in considerable breakthroughs. As a result, various *S. lycopersicum* cultivars with distinctive morphology have been produced. Unfortunately, some essential traits in wild tomatoes, such as resistance to biotic and abiotic effects, were diminished throughout domestication. Because of traditional breeding, genetic diversity and fitness were lost along with improved traits.

Diversification of the biological species is built on dissimilarities in the genetic pool (Mondini et al., 2009). Genetic variation in plant breeding is crucial for developing new cultivars and is the cornerstone for strengthening an organism's traits (Wenzel, 2006). Owing to DNA damage or errors occurring during DNA replication, genetic variations known as mutations occur spontaneously during evolution. This process is known as mutagenesis (Hidema et al., 2005). Breeding crops only with natural variations is impractical because of natural mutations' sporadic, random, and spontaneous nature (Brooks et al., 2014).

Modern genetics and breeding approaches have been used to understand better and develop tomato genome structure and functional traits (Just et al., 2013). The discovery of the genes responsible for the tolerance to heat, salt, and other fruit-related qualities has been made easier with the help of quantitative trait loci (QTL) mapping in tomatoes (Bai et al., 2018). Additionally, loci have been identified for characteristics like tomato fruit weight, shape, plant architecture, and fruit metabolites using genome wide association studies (GWAS) (Bauchet et al., 2017).

Recent efforts have secured the preservation of wild species and landraces that permitted the reintroduction of resistant traits (Gascuel et al., 2017). Breeders can also use artificial mutagenesis to produce genotypes with novel genetic and phenotypic variations, which helps to expand the limited genetic base (Just et al., 2013). Mutant collections, which offer an allelic series in a constant genetic background, provide a second option for identifying characteristics in tomatoes (Rothan et al., 2019). Various tomato cultivars have been used to produce mutant collections for the past ten years (Just et al., 2013; Ariizumi et al., 2014). Reverse genetic tools like Targeting induced local lesions in the genome (TILLING) aided the advancement of fruit crop breeding. Using the T-DNA/transposons, insertional mutagenesis is also vital to increase genetic diversity, a step essential for breeding operations.

Thanks to advancements in high-throughput sequencing technologies, the genomes of numerous wild tomato species, landraces, and the tomato have all been entirely sequenced (Bolger et al., 2014). Information on the genetic sequencing of wild tomato cultivars and additional accessions are provided at Sol Genomics Network (https://solgenomics.net/). The accessibility of high-quality genome sequences, the fast development of molecular biology, and genomics techniques have made it possible to precisely edit any desired genomic site by insertion/deletion or nucleotide substitution. Recombinant DNA technology also referred to as genetic engineering, involves the exchange of desirable genes between species, raising the possibility that crops can be improved (Gascuel et al., 2017; Chen et al., 2019). Pangenome accessibility might make it simpler to create gene-editing tools that would enable tomato breeding and development to assess the effects of target gene modifications.

#### 2.3 Techniques to annotate gene function

Before the advent of genome editing techniques, other techniques used to investigate the function of unannotated and uncharacterized genes are listed below (Vats et al., 2019).

#### 2.3.1 Induced mutagenesis

Induced mutagenesis permits the generation of new genetic variants for crop improvement as well as discovering new gene functions. Since Stadler's 1928 study

on mutation breeding, genetic breeding techniques have advanced significantly. Mutation breeding has been extensively used in species that cannot be raised using conventional methods and agricultural plants with little genetic variability. The mutagenized population is a limitless resource once it is developed. Due to their safety profile and lack of foreign DNA, plants generated by mutagenesis were exempted from the EU GMO restrictions. But producing a mutant population takes a lot of time and effort.

Depending on the mutagen used for creating mutations, the process can be classified into physical and chemical mutagenesis.

#### 2.3.2 Physical mutagenesis

Following the 1920s, ionizing radiation was recognized as a physical mutagen that can induce mutations.  $\gamma$ -rays are popular as they cause double-stranded breaks in DNA because of the free radical formation. As a result, enormous deletions and chromosomal rearrangements (Okamura et al., 2003) happen in the genome. For instance,  $\gamma$  -ray irradiation was used to develop 6301 mutant lines with various characteristics, providing invaluable genetic material for tomato breeding and functional genomics (Matsukura et al., 2007).

#### 2.3.3 Chemical mutagenesis

Chemical mutagens helps create point mutations or single base substitutions, which results in the loss or gain of function of genes resulting in new allelic variations as opposed to large deletions or chromosomal rearrangements caused by physical mutagens (Leitao, 2012). Ethyl methane sulphonate (EMS), an alkylating agent, is often used for mutagenesis. EMS creates G/C to A/T base-pair transition that account for most random point mutations (Till et al., 2007).

EMS has been used successfully to create mutagenized populations in tomato cultivars such as Moneymaker (Wisman et al., 1991), M82 (Menda et al., 2004), *S. lycopersicum* Mill (Kostov et al., 2007), Red setter (Just et al., 2013; Minoia et al., 2010)", and Arka Vikas "(Guptaet al., 2017), and Arka Vikas. A total of two EMS dosages (0.5 percent and 1 percent) were applied to the tiny dwarf tomato cultivar Micro-Tom to establish mutant populations for functional genomic investigations (Saito et al., 2011). Of the two doses, 1 percent of EMS was effective in producing

a mutant population for functional genomics studies (Just et al., 2013).

A mutation population can be screened for mutations within target genes using either forward or reverse genetics. TILLING is a well-known high-throughput reverse genetic tool for identifying point mutations in the DNA caused by chemical mutagenesis (Minoia et al., 2010). Three crucial phases are necessary for the TILLING method to yield the best results: first, proper pooling technique; second, a good gene model; third, a suitable protein conservation model that might aid in the primer selection process ranging between 1000-2000 bp. The discovered mutations in a gene will then be confirmed. Tobacco (Okabe et al., 2011), wheat (Slade et al., 2005), barley (Caldwell et al., 2004), maize (Till et al., 2004), Arabidopsis (Greene et al., 2003), lotus (Perry et al., 2003), and other plants have all benefited from TILLING. Since sequencing smaller amplicons (about 300 bp) allows for speedy and accurate screening of several amplicons in a short amount of time, next-generation sequencing (NGS) already replaced conventional TILLING (Marroni et al., 2011). The first use of NGS was by Rigola and colleagues to discover two novel SleF4E alleles in tomato, and they gave the technique the name "Key point" technology. A population of 2300 of tomato generated by EMS lines was screened using TILLING by NGS technology in 2017, and 64 mutations with a mutation frequency of 1 in 367 Kb were found (Gupta et al., 2017).

#### 2.3.3.1 Limitations of physical and chemical mutagenesis

The mutation spectrum of physical and chemical mutagenesis is poorly understood and involves random mechanisms. It is also necessary to identify the appropriate dose rate for each mutagen for each genotype. Since it requires a considerable population size for generating mutations in desired regions and high throughput methods which also take a lot of time and money. Additionally, ensuring the technicians' safety requires sophisticated infrastructure and technology that can only be found in labs with specialized facilities and massive funding.

#### 2.3.3.2 Oligonucleotide-directed mutagenesis (ODM)

ODM is also called site-directed mutagenesis (Sauer et al., 2016). It is a method for making precise adjustments to the desired target genes, causing substitutions, insertions, and deletions. Researchers used this technique on plants after it was successfully tested in mammalian systems (Yoon et al., 1996; Beetham

et al., 1999). The primary mechanism of ODM was analyzed in prokaryotes and eukaryotes. ODM's primary means of action is the passage of an oligonucleotide harboring a mutation through the target cell's cell and nuclear membranes. When the oligonucleotide reaches the nucleus, it binds to the matching DNA (Beetham et al., 1999). Following the repair of the DNA damage by the host's mismatch repair machinery, site-specific mutations are produced due to the alterations incorporated into the DNA. ODM techniques have a meager correction rate, although they were successfully utilized in plants for the generation of herbicide-resistant crops like wheat (Dong et al., 2006), rice (Okuzaki and Toriyama, 2004), tobacco (Kochevenko and Willmitzer, 2003), and maize (Zhu et al., 1999). However, there has been no information about ODM in tomatoes.

#### 2.3.3.3 Epigenome editing

Epigenetic gene regulation is a critical component of gene control. DNA methylation is a conserved process that regulates gene expression and prevents transposons from functioning (Chinnusamy and Zhu, 2009). Epigenome editing/epigenome engineering is the use of chemicals to alter the epigenetic state of a particular section of the genome. This editing is influenced by the genome's chromatin structure and methylation status. RNA-dependent DNA methylation (RdDM) carries out *de novo* DNA methylation. This system comprises RNA pol IV and RNA pol V (Zhanget al., 2018). Chromosomal methyl transferase, MET1, is the methyltransferase. Domain rearranged methyltransferase (DRM) is the other methyltransferase that maintains the CG/CHG/CHH cytosine methylation in plants (Greenberg et al., 2013).

The mechanism of DNA methylation involves two steps. Small interfering RNA is synthesized in the first step, and targeted methylation occurs in the second step (Xie and Yu, 2015). The two pathways by which RdDM methylation occurs are the non-canonical pathway in which chemicals and xenobiotics are involved, and the canonical pathway is a naturally occurring signaling channel inside a biological system (Dna et al., 2016). Using the traditional method, the RNA pol IV synthesizes single-stranded RNA (ssRNA) from heterochromatin. This ssRNA is transformed to double-stranded (dsRNA) using RNA-dependent RNA polymerase (RDR2) (Haag et al., 2012). RNA pol IV and RDR2, together with Dicer-like 3 (DCL3), cleave the

dsRNA fragments to create 24 nucleotide siRNAs (Xie and Yu, 2015). The non-canonical route does exist, but it is not very common (Dna et al., 2016). In a range of plant disciplines involving Arabidopsis (Brocklehurst et al., 2018), tobacco (Otagaki et al., 2011), maize (Li et al., 2014), potato (Kasai et al., 2016), and rice (Hu et al., 2014), numerous studies on epigenomic editing have been published.

Despite having the information on fruit epigenome, there have been few studies on the epigenome editing of tomatoes. The earliest studies of DNA methylation affecting fruit ripening comes from colorless non-ripening (*CNR*) mutant tomato. The *CNR* epimutant creates a colorless pericarp and hinders normal ripening by suppressing the expression of transcriptional factors relating to fruit ripening and carotenoid biosynthesis (Manning et al., 2006). Zhong et al., 2013 found that the methylation status of ripening- related genes substantially impacts tomato fruit development. Study from other group identified that DNA methylases (DMLs) with DEMETER-like properties regulate DNA methylation in tomato (Liu et al., 2015).

#### 2.3.3.4 RNA interference (RNAi)

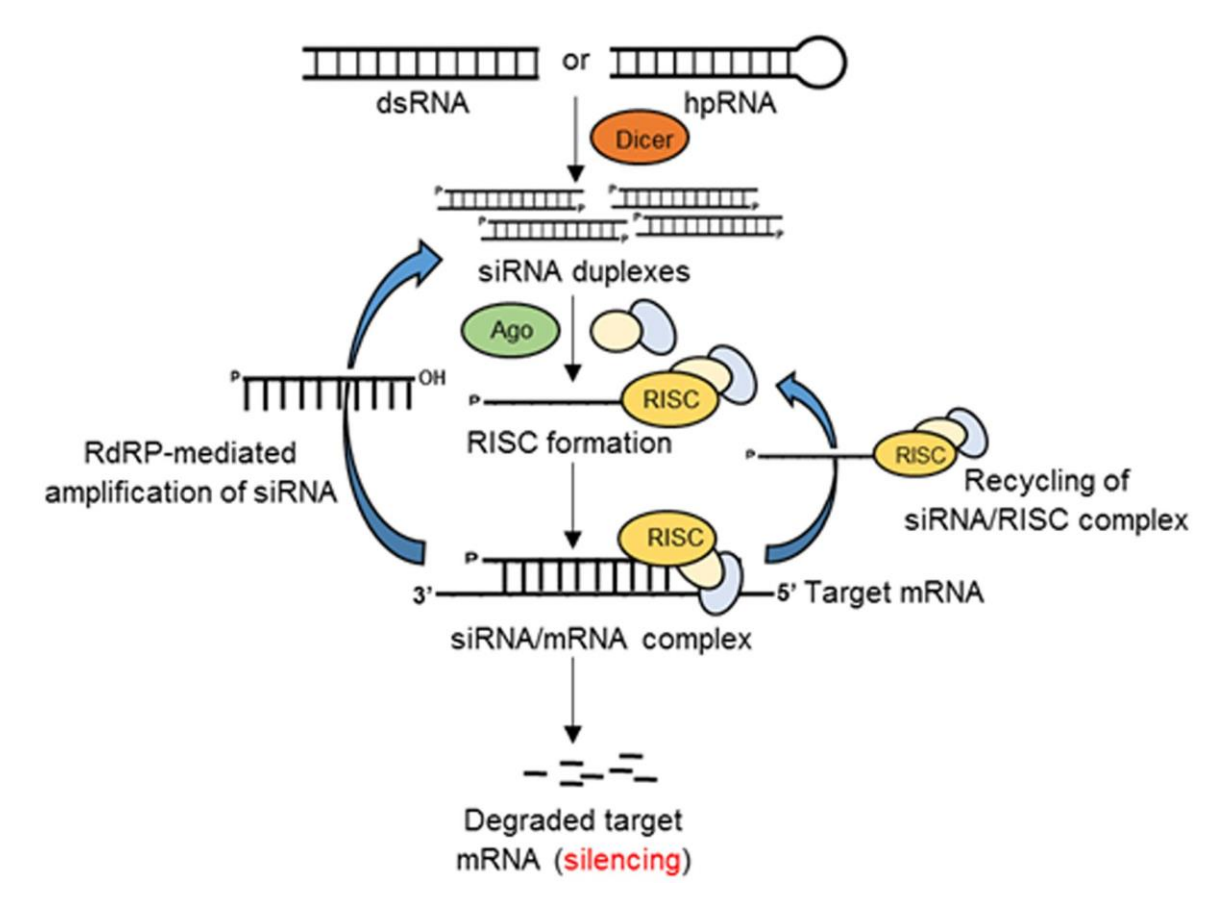


Figure 2.1 Schematic representation of RNAi-mediated gene silencing in eukaryotes. Double

**Figure 2.1** stranded RNAs or hairpin RNAs (hpRNAs) generate small siRNA duplexes by the action of Dicer. The guide RNA strand binds with Argonaute (Ago) and other proteins to form an RNA-induced silencing complex (RISC). The siRNA/RISC complex then binds the complementary sequence of the target mRNA resulting in the degradation of the target transcript or inhibition of translation. The components of siRNA/mRNA complex can be recycled to the RISC complex or generate siRNA duplexes by the cation of RNA-dependent RNA polymerase (RdRP). Adapted from Majumdar et al., 2017.

Many organisms, including protozoa, fungi, mammals, and crop plants, use RNA silencing as a natural defensive mechanism against pathogens like viruses (Voinnet O., 2001). This behavior was first noted in *Caenorhabditis elegans* in 1998 by Fire and his team. Genes can be silenced in two different ways: post-transcriptional gene silencing (PTGS) and transcriptional gene silencing (TGS) (Sijen et al., 2001). In TGS, promoter methylation inhibits mRNA degradation, while dsRNA induces mRNA degradation in PTGS (Baulcombe and English, 1996). There are many ways to decrease the target gene's expression in plants. Viral-induced gene silencing (VIGS) is one method used for the functional evaluation of plant genes through PTGS (Baulcombe, 1999). It is a reverse genetic technique that can be used in plants. To protect themselves, virus-infected plants use the PTGS mechanism to remove the viral RNAs (Burch-Smith et al., 2006).

In 1997, Van Kammen coined the phrase "VIGS." The mechanism of VIGS is the same as that of RNA-induced gene silencing, in which the target gene is silenced by dsRNAs produced by the host RNA-dependent RNA polymerase (RdRP). Here Double-stranded RNA (dsRNA) is transformed into short interfering RNA (siRNA), which has a length of 21–25 nucleotides and two nucleotides 3' overhangs, by the DICER-like enzyme (Bernstein et al., 2001). The RNA-induced silencing complex is then supplemented with these siRNAs (RISC). This combination then leads the siRNA to the corresponding RNA, ensuing RNA degradation and mRNA translation inhibition (Kawamata et al., 2009).

The first altered virus vector for "VIGS" is the Tobacco Mosaic Virus (TMV), which blocked *Nicotiana benthamiana's* phytoene desaturase (PDS) from expressing itself (Kumagai et al., 1995). Genes related to tobacco were successfully silenced utilizing modified TRV-based technology (Liu et al., 2002). Compared to other VIGS vectors, TRV has the benefit of being easier to introduce into plants,

especially Solanaceous plants (Liu et al., 2002). Another advantage is TRV infection spreads quickly throughout the plant.

VIGS analyzes gene function fast and efficiently, which is superior to other genome editing methods. Thorough population screening or plant transformations are necessary because it is a transitory procedure. The function of all the gene families in plant growth and development will be evident if a multigene family's conserved sequence is used for the VIGS. Alternately, choosing the VIGS sequence can also be used to target a gene member. In homologous gene families, the function of genes in many plant species can be studied using the same VIGS vector construct (Liuet al., 2002; Ramegowda et al., 2014).

#### 2.3.3.5Transposons

Transposable elements (TEs), also known as transposons and sometimes referred to as jumping genes," make up a large portion of a species' genome. In the 1950s, Barbara McClintock discovered TEs as mobile elements in maize (McClintock, 1950). TEs are the factors that move from one place to another in the chromosomal regions by creating transitions, transversions, and translocations in the genome. The abundance of TEs in the genome varies from species to species. TEs account for 80% of the genome in maize, 66.8% in wheat, 38.8% in, 80% in, and 20% in *Arabidopsis thaliana* (Iida and Terada, 2005).

Transposons are divided into retrotransposons and DNA transposons according to the intermediary RNA and DNA formed during the transposition. When RNA is reverse-transcribed into cDNA, the class I retrotransposons multiply throughout the genome and transpose themselves into numerous locations. The DNA transposons are class II transposons that move and integrate DNA into other sites in the genome using a "cut and paste" process. Ac/Ds (Activator/Dissociation) elements are the class II transposons. Transposons can contain either autonomous or non-autonomous transposable elements. Transposons are mobilized by autonomous elements using their encoded proteins, whereas non-autonomous elements utilize host machinery (Mirouze and Vitte, 2014).

Knockout mutant plants are typically produced by insertional mutagenesis employing transposon DNA (T-DNA). Most of the time, insertional mutagenesis

generates mutants devoid of any function, enabling us to ascertain the role of the gene. The transposed DNA will be present in all succeeding generations after the insertional mutants are created. The T-DNA insertion could determine a mutant's identity. In tomato, maize TEs were used as breeding tools (Grzebelus, 2018, Yoder, 1990). In a study, the enzymes through TEs from tomato were inserted into particular sites. In a study Polygalactouronase (PG) and dihydroflavonol 4 reductase (DHFR) introduced through TEs found that PG insertion rates were higher in Ds plant offspring than in other genes (Cooley et al., 1996). T-DNA insertions have been utilized to identify several *Solanum pennelli* mutants vulnerable to salt and drought stress (Atares et al., 2011). The *FEEBLY* (fb) mutant, which exhibits notable sensitivity to the herbicide phosphinothricin, was discovered using transposon tagging in tomato (Van Der Biezen et al., 1996).

#### 2.3.3.6Zinc Finger Nucleases (ZFNs)

ZFNs have been successfully exploited as site-specific genome editing tools (Bibikova et al., 2002). Zinc ions are coordinated to preserve the Cys2His2 motif, stabilizing ZFNs to have a length of roughly 30 amino acids (Persikov et al., 2015). The recognition of triple tandem nucleotides allows the ZFN arrays to adhere to the target site. The FokI restriction endonuclease in the cleavage domain of ZFNs generates a double-stranded break in the target DNA when ZFNs connect to it (Bitinaite et al., 1998). DSBs (double-stranded breaks) activate the DNA repair machinery, resulting in minute base alterations, deletions, or insertions (Mohanta et al., 2017). After being identified in1996, this technique was used in various plant species, like maize, tobacco, Arabidopsis, and soybean (Shukla et al., 2009; Kim et al., 1996).

ZFNs are precise and produce fewer off-targets. However, this approach also has some downsides (Mushtaq et al., 2018), like building zinc-finger arrays is hard, preventing its extensive application in regular laboratories (Gaj et al., 2016). ZFN design is a lengthy procedure that usually takes a long time. Because of its uniqueness, a distinct cloning technique must be employed every time, which is very costly (Mushtaq et al., 2018).

#### 2.3.3.7Transcription activator-like effector nucleases (TALENs)

Like ZFNs, TALENs have two domains, one for DNA binding and the other

for cleavage. A tandem repeat of 33-35 amino acids makes up the DNA binding domain, with highly variable amino acids (Moscou and Bogdanove, 2009). On the other hand, the DNA cleavage domain, like in ZFNs, called the FokI domain, cuts within the 12-19 bp spacer region. In the DNA binding domain, the highly variable amino acids are referred to as repeat variable residues (RVDs) and are intended to detect specific sequence (Guptaand Musunuru, 2014). Although it is simple to target any DNA sequence with TALENs, unlike ZFNs, there is a chance that they will go off-target and cause double-strand breaks in other regions of the genome (Mussolino et al., 2011). Since TALENs are much larger than ZFNs, it is also challenging to distribute them within cells.

However, it is possible to generate plants with beneficial and valuable traits utilizing TALENs (Reyon et al., 2013). Arabidopsis (Cermak et al., 2011), tobacco (Mahfouz et al., 2011), and rice (Li et al., 2012) are examples of plants where TALENs have been successfully used (Wendt et al., 2013). They observed somatic mutation rates of 2–15 percent in the transgenic plants and 1.5–12 percent in the transgenic offspring (Haag et al., 2012). Furthermore, there have been reports of somatic mutagenesis in rice and barley (Li et al., 2012, Wendt et al., 2013). Because rice has a high mutation frequency, transgenic plants with plant disease resistance were made (Wendt et al., 2013). TALENs were used to alter the anthocyanin gene (ANTI), which in tomato encodes a MYB transcription factor (Cermak et al., 2015). They used the Geminivirus for genetic transformation and obtained accurate insertions with no off-targets. The coupling of TALENs and CRISPR-Cas, also effectively altered the ANTI gene. The overexpression of the ANTI transgene led to the production of purple plant tissue (Cermak et al., 2015).

#### **2.3.3.8CRISPR-Genome editing Technique**

Genome editing is a hot topic in human illness prevention and treatment. Studies on this technique reveal that it can prevent and treat more complex diseases like genetic diseases, cancer, human immunodeficiency virus infection, and heart diseases. When CRISPR was utilized to change human genomes, ethical issues arose. However, most of the modifications brought about by genome editing affect somatic cells. Since somatic cell editing cannot be handed down to future generations, ethical issues can be circumvented. On the other hand, changes to the sperm or egg cell can be passed on to further generations.

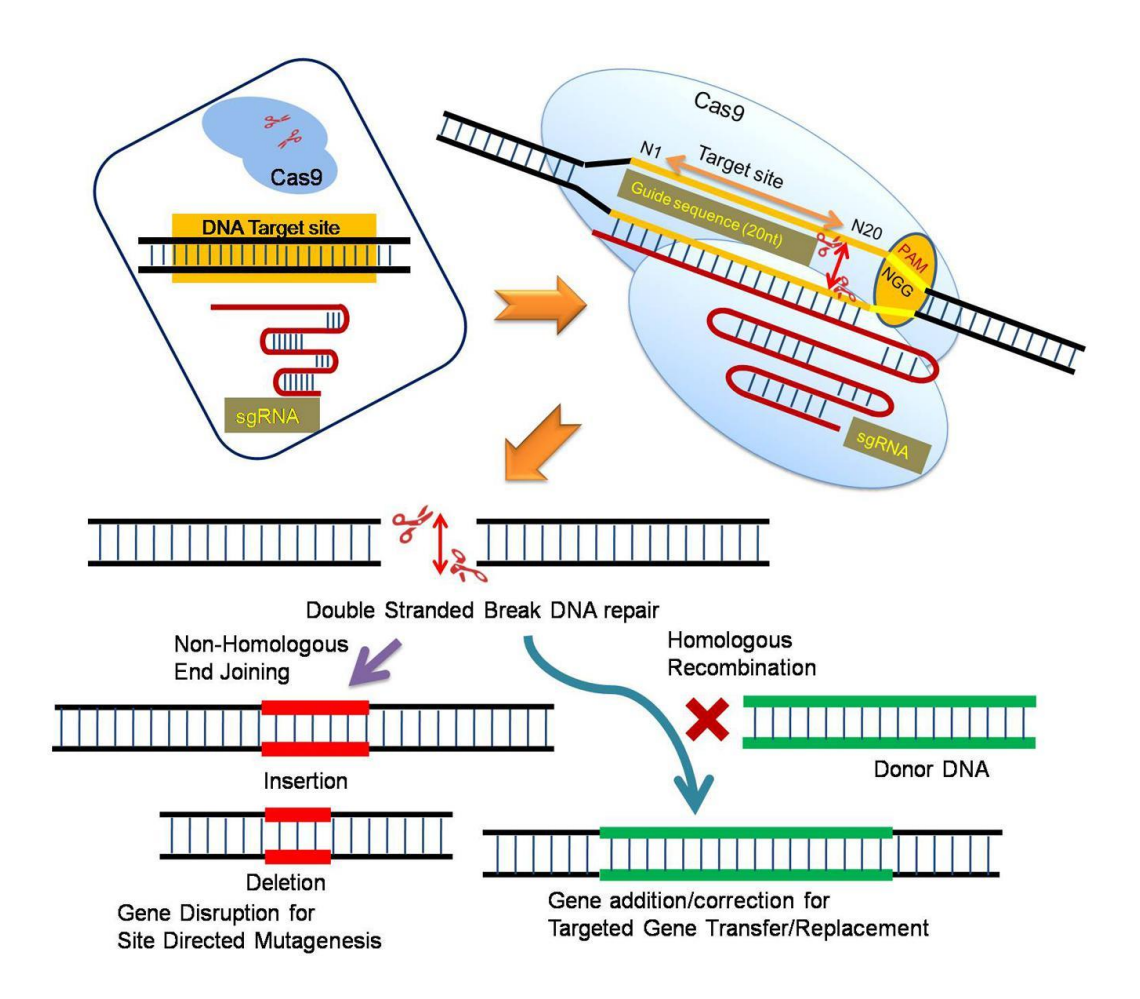


Figure 2.2 Schematic representation of Cas9/sgRNA system of CRISPR technology. The basic strategy of Cas9/sgRNA system. The Cas9 is a RNA guided endonuclease consists of two nuclease domains namely HNH and RuvC. The target specificity of Cas9 depends upon the guide sequence (20 nt) short guide RNA (sgRNA). The target sites must lay immediately 5' of a PAM (protospacer Adjacent Motif) sequence of the form N20-NGG (or N20-NAG). The Cas9 nuclease induces double stranded breaks (DSB) at the target site which can be repaired either by |Non-Homologous End Joining method or Homologous Recombination by cellular system which results in gene disruption by indels or gene addition/correction, respectively. Adapted from Khatodia et al., 2016

Genome editing (GE) techniques have changed the natural landscape by precisely editing the targeted sites leading to alteration of the genomic locations in the living organism, including bacteria, plants, and animals. The primary mechanism of GE involves the breakage of the double- stranded DNA by specially created nucleases. Homology-dependent recombination (HDR) or is used to repair the double-stranded breaks. HDR enables precise editing, while NHEJ is prone to errorprone DNA repair that, in theory, results in a gene knockout. However, both benefit

crop breeding (Veillet et al., 2019).

CRISPR/Cas9 is a rapidly evolving GE technique successfully utilized in various organisms. CRISPR/Cas technique was adapted from the bacterial immune system (Pennisi, 2013). The bacterium produces CRISPR array RNA segments when the virus attacks it for the first time. These arrays help bind and destroy the viral genome when exposed next time. A working CRISPR/Cas9 against a target gene requires a guide RNA, a Cas9 endonuclease, and an RNA- dependent DNA endonuclease (Shah et al., 2013). The Cas9 protein has two lobes: the nuclease lobe (NUC) and the recognition lobe (REC). NUC interacts with PAM domain, nickase domain, and HNH domains that cleave the complementary strand, on the other hand RUVC helps cleave the non-complementary stand. Cas9-sgRNA complex form REC lobe. After gRNA loading, Cas9 gets activated and forms a channel into which RNA-DNA heteroduplex is inserted. The Cas9- gRNA complex moves through the dsDNA to recognize the PAM sequence with the help of the PI domain. The matching DNA strand melts in the process, and a heteroduplex forms between RNA and DNA break the dsDNA before the PAM region following heteroduplex formation (Belhaj et al., 2015).

The *Streptococcus pyogenes* strain produces the type II Cas9 enzyme often used in CRISPR research (Jinek et al., 2012). The target gene's DSB caused by CRISPR/Cas9 is repaired by the host's DNA repair system (Jinek et al., 2014, Knott and Doudna, 2018). Despite being extremely accurate, CRISPR/Cas9 is not a perfect technique as it can induce off-target effects. However, off-targets in plants are relatively rare (Peterson et al., 2016).

Contrary to ZFNs and TALENs, CRISPR/Cas9 dramatically improves the feasibility and effectiveness of genome editing to produce knockout mutants (Mohanta et al., 2017). The CRISPR/Cas9 technique has many other uses, along with the generation of gene knockouts. The elimination of entire gene clusters is accomplished by simultaneously using two or more gRNAs. ZFNs and TALENs require the creation of nucleases, which takes time and is challenging, whereas the CRISPR/Cas9 editing method requires 18-20 bp gRNA.

#### 2.3.3.8.1 CRISPR Genome editing in plants

So far, CRISPR/Cas9 has been used on a variety of crops, including

climacteric fruits such as tomato (Brooks et al., 2014; Xu et al., 2016), apples (Nishitani et al., 2016), kiwifruit (Wang et al., 2018), and banana (Kaur et al., 2018). Non-climacteric fruits include sweet orange (Jia and Wang, 2014), duncan grapefruit (Jia et al., 2016), grapevine (Malony et al., 2016), watermelon (Tian et al., 2016), cucumber (Chandrasekaran et al., 2016). CRISPR has also been used in rice (Miao et al., 2013) and wheat (Shan et al., 2014).

#### 2.3.3.8.2 CRISPR/Cas9 Genome editing approaches in tomato

CRISPR Cas9 results in a variety of mutations. CRISPR/Cas has been shown to transport a variety of guide RNAs, allowing researchers to generate diverse alleles of genes to understand their functions better (Rodriguez-Leal et al., 2017). Tomato has become an attractive crop for gene editing in dicot crops due to high quality sequenced genome, easy transformation (Van Eck et al., 2006) and its economic importance. The first gene to be edited in tomato was *Argonaute 7*. The edited lines were identified due to a distinct wiry phenotype during the tissue culture stage (Brooks et al., 2014). After that, several publications can be seen in tomato where CRISPR/Cas9-based genome editing was carried out to combat abiotic, biotic stresses, domestication of wild tomato species, and improvement of tomato nutrition-lycopene, anthocyanins, ascorbate, sugars, etc. and shelf life (Wang et al., 2019).

In addition, CRISPR/Cas9 has been used in the generation of parthenocarpic fruit, altering plant architecture, inflorescence branching, and fruit size studies (Ueta et al., 2017; Li X et al., 2018; Leal et al., 2017). Instead of CDS, targeted Cisregulatory elements (CREs), resulting in various transgenic plant phenotypes (Leal et al. 2017). CRE mutations are common and have aided crop domestication (Meyer and Purugganan, 2013). As a result, it is possible to regulate gene activity without experiencing the pleiotropic consequences seen in mutants with complete loss of function.

Furthermore, CRISPR/Cas9 is proven to have a high editing efficiency, and homozygous alterations are passed down to successive generations in a stable manner (Zhang et al., 2014). CRISPR/Cas9 is more cost-effective, easier to design, and generates fewer off-targets than earlier gene-editing technologies (Xu et al., 2015). Its application to transcriptional factor coding sequences, hormones,

enzymes, and, in some cases, CREs, may allow for more accurate fruit ripening control.

#### 2.4 Tomato: A model of climacteric fruit ripening

Based on ethylene evolution and respiratory burst during ripening, fruits are categorized as climacteric and non-climacteric (Alexander and Grierson, 2002; Seymour et al., 2013). Tomatoes, bananas, apples, and melons come under climacteric fruits. Grapes, citrus, and strawberries are non-climacteric (Symons et al., 2012). Climacteric ripening is the physiological process indicating the end of fruit maturation and the start of the ripening stage.

#### 2.4.1 Fruit ripening

Anatomically, fruits are the swollen parts of the ovaries. They develop after fertilization and co-occur with seed maturation. Fruit ripening is a multi-step, irreversible process involving multiple biochemical, metabolic, physiological, and organoleptic changes. These changes increase the accumulation of sugars, metabolites, pigments, volatiles, and reduction of acids, making fruits more visually attractive for animal consumption (Gapper et al., 2013) and seed dispersal.

After fertilization, the developmental stages of fleshy fruits are separated into stages such as cell growth, division, maturation and ripening (Gillaspy et al., 1993; Seymour et al., 2013). Changes in metabolism, hormones and gene expression are recognized in these three stages. (Carrari and Fernie, 2006; Seymour et al., 2013). Because of the chloroplasts, which house the entire photosynthetic machinery, tomato fruits are green before they ripen. Loss of chlorophyll, softening of the cell wall, buildup of sugars, and extreme changes in volatile and pigment profiles characterize the transition from mature green to red ripe (Gapper et al., 2013). Most noticeably, chlorophyll degradation is associated with the transformation of chloroplast to chromoplast, which accumulates pigments like lycopene andβ-carotene, the health-promoting carotenoids. These carotenoids give the characteristic red and orange color to tomato fruits.

#### 2.4.2 Importance of fruit ripening

Ripening fleshy fruits is of considerable economic importance in agriculture. The significant demand for producers is to produce fruits with high nutritional quality and make them available to consumers with the same quality while consuming them. Thus, scientists focus on improved shelf life and nutritional quality through conventional breeding and gene editing.

#### 2.4.3 Carotenoid biosynthesis

During the ripening of fleshy fruit, carotenoids are synthesized, depending on the availability of precursors IPP and DMAPP (Chappell et al., 1995; Rodriguez-Concepcion and Boronat, 2002). Plants possess two separate ways of IPP and DMAPP synthesis. The methylerythritol 4-phosphate (MEP) route is found in the plastids while the "mevalonic acid (MVA) pathway" is located in the cytoplasm (Lichtenthaler, 1999, Eisenreich et al., 2001). IPP is produced from acetyl CoA through the cytosolic MVA pathway through MVA production. IPP isomerase transforms IPP into dimethylallyl pyrophosphate (DMAPP). Sesquiterpene (C15) and triterpene (C30) synthesis use DMAPP as a substrate. Geranyl pyrophosphate is created when one molecule of DMAPP and one molecule of IPP condense (GPP). The plastidial MEP route is the primary source of IPP and DMAPP necessary for Hsieh and Goodman 2005plant carotenoid production (Eisenreich et al., 2004). IPP and DMAPP in plastids produce a variety of metabolites (Rodriguez- Concepcion 2010). Nuclear-encoded enzymes participate in the production of carotenoids on the plastid membrane, and it has been proposed that the location of these enzymes is essential for their active function (Cunningham and Gantt, 1998; Cuttriss et al., 2011).

The reaction between pyruvate and glyceraldehyde-3-phosphate is catalyzed by the enzyme DXP (1-deoxy-D-xylulose-5-phosphate) synthase (DXS), which is the initial step in the plastidial MEP route, to produce IPP. DXP reductoisomerase (DXR) performs intramolecular rearrangement and reduction to make MEP from DXP. DXS is the pathway's rate-limiting enzyme, controlling the flux (Lois et al., 2000; Pulido et al., 2013). Through a succession of phosphorylations and reductions, IPP created from MEP condenses with DMAPP under the influence of isopentenyl diphosphate isomerase (IPI), resulting in GPP. The enzyme GGPP synthase catalyzes the reaction in which two molecules of IPP are added to GPP to create the C20 chemical known as geranylgeranyl pyrophosphate (GGPP) (GGPPS; Fraser and Bramley 2004). The first step in the route is two GGPP molecules condensing to form 15-cis-phytoene in the presence of the enzyme phytoene synthase (PSY1)

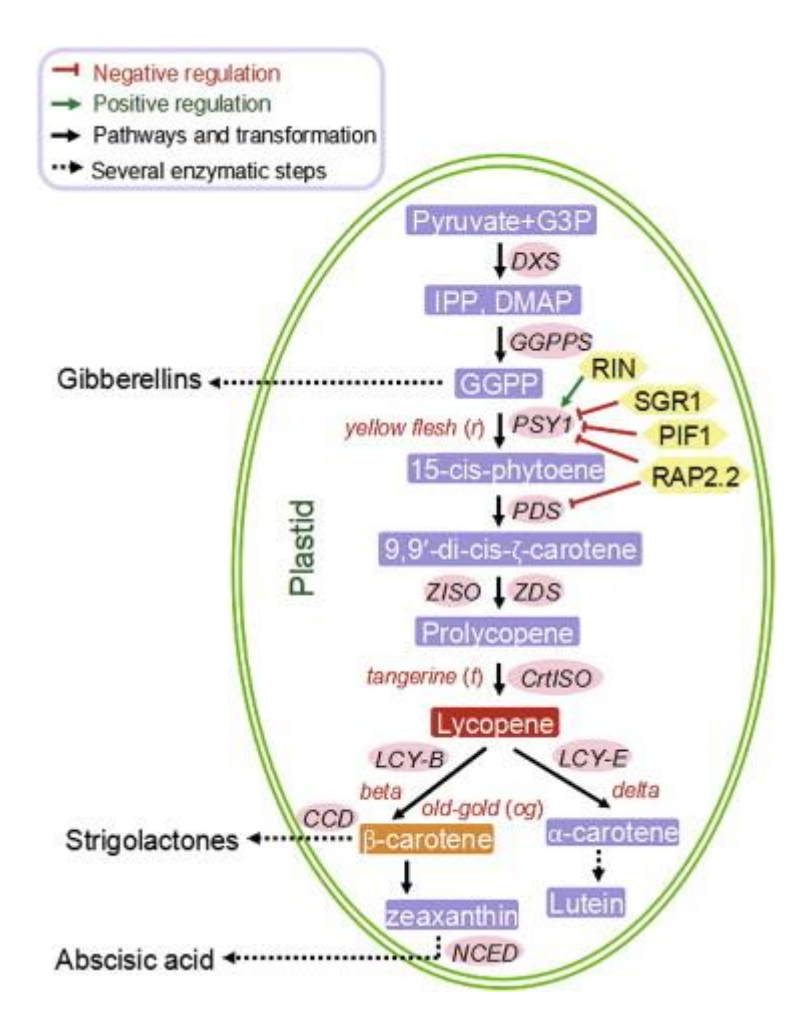


Figure 2.3 Carotenoid biosynthesis pathway with associate enzymes and regulatory genes.

Mutants related to carotenoid biosynthesis are indicated in italic red type. The rounded rectangles represent the substrates involved in carotenoid biosynthesis. The pink ellipses represent carotenoid pathway genes localized in plastids. The hexagons represent transcription factors regulating carotenoid biosynthesis. *CCD*, *carotenoid cleavage dioxygenases*; *CrtISO*, *carotene isomerase*; DMAPP, dimethylallyl diphosphate; *DXS*, *1-deoxy-d-xylulose-5-phosphate synthase*; G3P, glyceraldehyde-3-phosphate; GGPP, geranylgeranyl diphosphate; *GGPPS*, *geranylgeranyl pyrophosphate synthase*; IPP, isopentenyl diphosphate; *LCY-B*, *lycopene*  $\beta$ -cyclase, *LCY-E*, *lycopene*  $\varepsilon$ -cyclase, NCED,  $\beta$ -cis-epoxycarotenoid dioxygenase; PDS, phytoene desaturase; PIF1, phytochrome interacting factor 1; *PSY1*, phytoene synthase; RAP2.2 related to ap2; RIN, ripening inhibitor; SGR1, stay-green; *ZDS*,  $\zeta$ -carotene desaturase; ZISO, carotene isomerase. Adapted from Liu et al., 2015.

(Cunningham and Gantt 1998). Lycopene is produced in plants by four steps that entail consecutive dehydrogenations and isomerizations. The enzymes phytoene

desaturase (PDS) and  $\zeta$ -carotene desaturase (ZDS) inject double bonds into the chromophore and change the colorless phytoene into red-colored lycopene. PDS, an enzyme, transforms phytoene into tri-*cis*-carotene by producing phytofluene. The *cis-trans* isomerization of 9,15,9'-tri-*cis*- $\zeta$ -carotene into 9,9'-di-*cis*- $\zeta$ - carotene is catalyzed by  $\zeta$ -carotene isomerase (ZISO) (Li et al., 2007). Although this isomerization phase can occur in the light, an examination of mutations in Arabidopsis showed that ZISO is still necessary (Ruiz-Sola and Rodriguez-Concepcion 2012). The enzyme " $\zeta$ -carotene desaturase (ZDS) converts 9,9'-di-*cis*- $\zeta$ -carotene into 7,9,9',7' tetra-*cis*-lycopene (pro-lycopene) by forming 7,9,9'-tri-cisneurosporene. The final stage in the synthesis of lycopene involves a process mediated by the enzyme carotenoid isomerase (CRITSO), which changes *cis*-lycopene into all-*trans*-lycopene (Isaacson et al., 2004). Green tissues can convert the above pro-lycopene to all-*trans*-lycopene without any enzymatic action on light exposure (Park et al., 2002).

Two cyclase enzymes use lycopene as their substrate to add  $\beta$ - or  $\epsilon$ -ionone rings to the isoprenoid backbone. LCYB (lycopene  $\beta$ -cyclase B) catalyzes the cyclization of  $\gamma$ -carotene, which results in the synthesis of  $\beta$ -carotene at the opposite end (Pecker et al., 1996). LCYE (lycopene  $\epsilon$ -cyclase) catalyzes the inclusion of an  $\epsilon$ -ring to lycopene to make  $\delta$ -carotene. At the same time, LCYB then cycles the other end of lycopene to produce  $\alpha$ -carotene (Cunningham and Gantt 2001). The tomato chromoplast-specific gene *cycb*, expressed in the fruit and flowers, controls the composition of carotenes in particular tissues (Ronen et al., 2000). In tomato and Arabidopsis, the expression of *lcyb* and *lcye* holds the ratio of  $\beta$ -carotene to  $\alpha$ -carotene, which modulates the cyclase activity (Yu and Beyer, 2012; Giorio et al., 2013).

The hydroxylation of  $\alpha$ - and  $\beta$ -carotenes results in the production of xanthophylls, the oxygenated hydrocarbons. Zeaxanthin is formed when  $\beta$ -carotene is converted to zeaxanthin by  $\beta$ - carotene hydroxylase (BCH). Lutein is produced when  $\epsilon$ - and  $\beta$  -ionone rings of  $\alpha$ -carotene are hydroxylated by the cryptochrome P450 hydroxylases CYP97A3 and CYP97C1 (Kim et al., 2009). Zeaxanthin epoxidase (ZEP) converts zeaxanthin into antheraxanthin, which is then converted into violaxanthin in a reversible process facilitated by violaxanthin de-epoxidase (VDE). Together, these processes make up the xanthophyll cycle (Niyogi et al.,

1998) where epoxidation and de-epoxidation reactions are light-dependent, dissipate surplus light energy, and help plants acclimate to different light intensities (Latowski & Grzyb 2004; Jahns et al., 2009). Young tomato fruits also undergo the reversible de-epoxidation of lutein epoxide to lutein, or lutein epoxide cycle, in addition to the violaxanthin cycle (Rabinowitch et al., 1975). The production of neoxanthin from violaxanthin is the last stage in the carotenoid pathway (Parry and Horgan 1991).

## 2.4.4 Metabolic regulation of tomato fruit development and ripening

Tomato captures the attention of researchers studying ripening and maturation as it undergoes substantial metabolic changes during fruit development. Metabolic complements of the tomato fruit help identify the developmental stages (Carrari and Fernie, 2006). GC-MS is widely deployed to measure the metabolite content of pericarp in tomato transgenics (Roessner-Tunali et al., 2003), analyze the metabolic diversity of tomatoes from wild species (Schauer et al., 2005), and quantify tomato metabolite composition at different developmental stages (Carrari andFernie, 2006). The goal of comprehensive metabolomic research is to determine the chemical elements present in the tissue quickly. Metabolic profiling techniques have improved our understanding of the qualitative changes in the metabolite pool as fruit matures from green to ripe.

It was believed that manipulating essential enzyme activities would affect fruit growth by changing carbon metabolism and partitioning photoassimilates. Overexpression of the *hexokinase1* (*AtHXK1*) gene from Arabidopsis in tomato showed specific biochemical and phenotypic changes (Menu et al., 2004). Due to this overexpression, the resulting inadequate carbon supply decreased cell proliferation and fruit size during fruit maturation. The sucrose given to these fruits was used for cell wall metabolism rather than starch storage. As a result of the decreased respiratory levels, the fruits revealed severe metabolic disturbances.

In tomato, silencing a fruit-specific isoform of *sucrose synthase* (*SuSy*) has been studied to identify its function in fruit development (D' Aoust et al., 1999). Early fruit development and fruit set were disrupted by SuSy inhibition resulting in decreased sucrose unloading capacity (D' Aoust et al., 1999). *Lin5* is a major QTL affecting the sugar and weight of fruit, and the gene that codes for cell wall-bound invertase has been discovered (Fridman et al., 2000; Fridman et al., 2004). Fruit

yield, size, and seed quantity drastically reduced when *Lin5* was RNAi silenced (Zanor et al.,2009). The transgenic plants exhibited metabolic changes limited to sugar, as an increased sucrose content was observed with a decrease in glucose and fructose content at the red ripe stage.

#### 2.4.4.1 Changes in the level of organic acids content

In tomato, organic acids play an important part in providing flavor and quality of the fruit. The predominant fruit acid is citric acid, followed by malic acid. Other organic acids like ascorbic acid, citra-malic acid, dehydroascorbic acid, fumaric acid, gluconic acid, isocitric acid, lactic acid, maleic acid, shikimic acid, succinic acid, saccharic acid, and tartaric acids are less prevalent (Oms-Oliu et al., 2011). The organic acids fumarate, isocitrate, and succinate act as precursors for amino acids. Shikimic acid is only found in very young fruit and is quite plentiful. Acids like citrate, malate, and saccharate are absent until later development. However, fumaric and lactic acids are discovered after harvest (Carrari and Fernie, 2006).

During maturation and ripening, the concentration of malic acid falls (Oms-Oliu et al., 2011). The increased malic enzyme activity forms pyruvate by decarboxylating malic acid at fruit maturity and ripening. Malate dehydrogenase and citrate synthase continue to work, resulting in decreased levels of malic acid and a preferred citric acid accumulation. Phenotyping of *aconitase* (*ACO*) and *mitochondrial malate dehydrogenase* (*mMDH*) mutants in tomato revealed significant alteration in the metabolism of the leaf and performance of the plant (Carrari et al., 2003; Nunes-Nesi et al., 2005). There was a reduction in TCA cycle flux and an increase in photosynthetic activity (Carrari and Fernie, 2006).

The metabolism of citric and malic acids is regulated by ethylene. In antisense *LeACS2* lines, malic and citric acid metabolism is boosted, but ethylene production is repressed. In addition, organic acids such as ascorbic, succinic, isocitric and dehydroascorbic acids are increased at ripening, whereas their levels reduced during postharvest storage, returning to pre-ripening levels (Oms-Oilu et al., 2011). This indicates the exclusive increase of metabolites through the climacteric ripening process. The TCA pathway is well-established in plants, but the regulation remains a mystery (Fernie et al., 2004). During ripening, glycolysis and TCA cycles provide

the necessary carbon fluxes in the fruit. Through the fruit ripening process, a higher concentration of intermediates of the TCA cycle, like isocitric and succinic acid, could be explained by enhanced respiration, exclusive of climacteric fruit.

Tartaric acid builds up throughout the ripening process and rises during storage (Oms-Oilu et al., 2011). The tartaric acid synthesis may be linked to the lower levels of ascorbic acid in the later maturation stage. During postharvest storage, compounds, including gluconic and 2-keto-L- gluconic acid, accumulate and may function as an intermediate in tartaric acid production via ascorbic acid (DeBolt et al., 2006). Ascorbic acid degradation could lead to the buildup of gluconic acid, 2-keto-L- gluconic acid, and tartaric acid. Postharvest tomatoes exhibit consistency with decreased levels of ascorbic acid (Oms-Oilu et al., 2011).

#### 2.4.4.2 Alternation in sugar and sugar alcohols abundance

Glucose, fructose, galactose, sucrose and inositol are the most abundant sugars and sugar alcohols, while glucose-6-phosphate, maltose, mannitol, sorbitol, and raffinose are found in trace amounts in tomato fruit (Oms-Oliu et al., 2011). As the fruit ripens, starch stored in plastids is broken down into smaller components that account for the fruit's respiration. During ripening, glucose and fructose are in identical amounts and linked to invertase activity which breaks down sucrose (Richardson et al., 1990; Oms-Oliu *et al.*, 2011).

Although the rapid turnover rate restricts its concentration, sugar phosphates are vital intermediate components in central metabolic pathways. According to Oms-Oliu *et al.* (2011), the glucose-6-phosphate levels decreased primarily during the postharvest stages. Sugar and its phosphates are catabolized via the glycolysis and TCA cycle, and their amounts may rise with changes in climacteric respiration. Respiration causes most carbon fluxes in red fruits containing minimal starch (Rontein *et al.*, 2002).

Galactose, galacturonic acid, and mannose are the primary cell wall constituents linked to ripening-associated softening. Their levels rise in tandem with decreasing hardness during maturation and ripening (Oms-Oliu et al., 2011), indicating a cell wall complex breakdown (Oms-Oliu et al., 2011). During the tomato fruit's climacteric stage of growth, significant alterations in cell wall constituents related to polysaccharide-degrading enzyme activity shift (Carrari et al.,

2006). Among these enzymes, polygalacturonase has received considerable attention. During tomato ripening, pectins break down to galacturonic acid with the help of this enzyme, and its activity rises steeply. Early in the ripening process, galactosidase activity was reduced to lower softening and galactose losses (Bremmell and Harpster, 2001).

During the early phases of fruit maturation and ripening, the concentration of galactinol, myo-inositol, and raffinose increases (Oms-Oliu et al., 2011). Myo-inositol is an essential precursor in producing several cell wall polysaccharides. Raffinose family oligosaccharides (RFOs) are another carbohydrate type linked to the development of plants. In the RFOs biosynthesis, the first step is catalyzed by galactinol synthase forming galactinol from UDP-galactose and Myo-inositol. Raffinose synthase catalyzes the donation of galactose to sucrose from galactinol, resulting in RFOs (Zhao et al., 2004).

#### 2.4.4.3 Amino acid expression and profiling

Oms-Oliu et al. (2011) found that amino acid concentrations fluctuate depending on the ripening stage. The substantial rise in aspartic and glutamic acid, phenylalanine, methionine and threonine are apparent throughout maturity and ripening, whereas GABA, alanine, glycine, and valine levels decline. Amino acid levels, including asparagine, isoleucine, glutamine, serine, and leucine, rise throughout the breaker phases but fall during the postharvest stages.

During ripening, the amino acid content and levels and the enzyme activities to convert them to esters are critical factors for the ensuing specific aroma in fruits such as bananas (Wyllie and Fellman, 2000). Compounds like, which describe the profile of banana volatile, are primarily associated with the rising levels of free alanine, leucine, and valine throughout the climacteric period (Wyllie and Fellman, 2000). Oms-Oliu et al. (2011) found that tissues with higher phenylalanine, leucine, and isoleucine produced the most ethylene. An increase in free amino acid leucine may encourage the formation of 3-methyl butanal and 3-methyl butanol. Similarly, isoleucine may form 2-methyl butanal and 2-methyl butanol (Mathieu et al., 2009).

Aspartate, glutamate, glutamine, and GABA are the free amino acids with the most significant relative amounts in mature and ripe tomato (Oms-Oliu et al., 2011). Others have experienced similar outcomes (Boggio et al., 2000; Pratta et al.,

2004). Glutamic acid accounts for the major amino acid detected in the growing fruit's pericarp region (Valle et al., 1998). N- GABA is the most prevalent form during the growing stage and reduces after the breaker stage. Glutamine, which is noticeable in mature green fruit, drops dramatically as the fruit matures and ripens (Oms-Oilu et al., 2011).

As glutamine is known to transport nitrogen molecules in plants, it could alter the requirement of this element when developmental processes are gradually replaced with ripening- related processes (Boggio et al., 2000). Glutamic acid is highly abundant throughout ripening and postharvest stages of fruit ripening. Glutamic acid levels are lower before the breaker stage, but as the fruit ripens, its level gradually increases (Oms-Oilu et al., 2011). With a nearly 40-fold increase in glutamic acid level during ripening, glutamic acid content was the most affected of all the amino acids studied (Oms-Oilu et al., 2011). In tomato the amount of glutamic acid generated during ripening was inversely related to the shelf life (Pratta et al., 2004).

Methionine levels rise at the beginning of ripening (Oms-Oilu et al., 2011), a significant ethylene precursor (Adams and Yang, 1977). Nevertheless, methionine content gradually rises during storage following harvest while the production of ethylene decreases (Oms-Oliu et al., 2011).

#### 2.5 Light

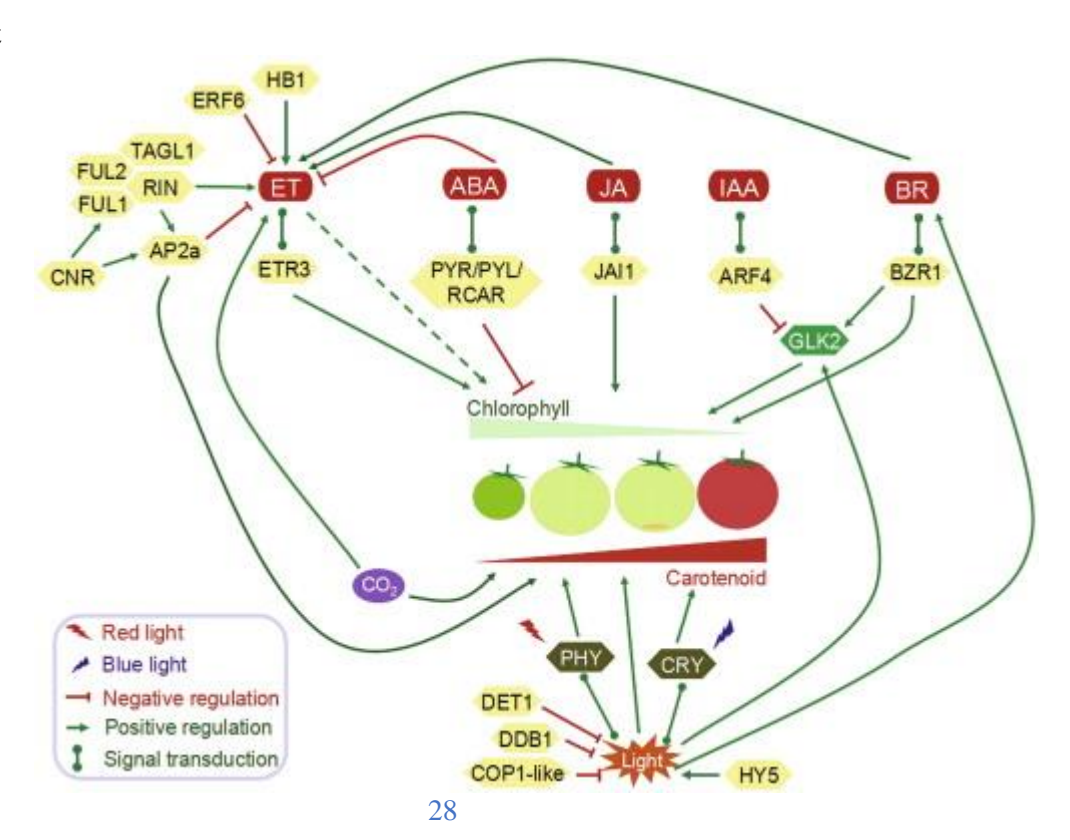


Figure 2.4 Roles of plant hormones, CO<sub>2</sub>, light, and their interplay in carotenoid accumulation during tomato fruit ripening. The picture is adapted from Liu et al., 2015.

The ability of single and multicellular organisms to sense and respond to the extracellular environment is critical for their survival. Numerous species have developed complex photosensory systems that respond effectively to light, which is a significant environmental component. Plants that are sessile and photoautotrophic are highly vulnerable to environmental conditions. In plants, light is an energy origin for photosynthesis and a climate cue influencing germination, photomorphogenesis, circadian rhythms, and phototropism (Chen et al., 2004).

#### 2.5.1 Photoreceptors

Photoreceptors can detect light quality, quantity, direction, and duration. The photoreceptors' photonic data collected by plants are subsequently translated into changes in the

gene expression levels influencing plant growth, development, and reproduction (Jiao etal., 2007). Plants have five types of photoreceptors. UV8 functions in the UV-B (280-315 nm) range, while cryptochromes, phototropins, ZTL (zeitlupe), LKP2 (LOV Kelch repeat protein 2), and FKF1 (Flavin-binding, Kelch repeat, F-box) perceive blue light (390-500 nm) and ultraviolet-A (320-390 nm) wavelengths. Phytochromes react in a dynamic photo equilibrium governed by the red (R) to farred (FR) wavelength range "(R-660 nm and FR-730 nm)". Phototropins are a pair of photoreceptors crucial for various light responses leading to optimal photosynthesis, such as chloroplast movement, phototropism, and stomatal opening (Briggs andChristie, 2002; Wada et al., 2003).

Physiological and genetic research on single phytochrome mutants and different phytochrome mutant combinations have revealed redundant synergistic and antagonistic functions for phytochromes in Arabidopsis growth and development (Casal and Sanchez, 1998). Physiological processes like floral induction and seedling development are controlled by interconnected networks of phytochrome and cryptochrome, as opposed to shade avoidance response and seed germination, which are entirely regulated by phytochromes (Casal and Mazella, 1998; Neff and Chory, 1998). Photoreceptors assist plants in adjusting their growth and development to the ambient light environment throughout their development.

Photoreceptor activation triggers a transcriptional cascade by controlling a set of master transcriptional factors that regulate transcriptional reprogramming during photomorphogenesis (Tepperman et al., 2001, 2004). While these photoreceptors directly impact individual light responses, there is usually a lot of crosstalk across the various photosensory systems. In Arabidopsis, gain and loss of function tests on zeitlupe, LKP2, and FKF1 revealed that these proteins are necessary for proper circadian clock operation and photoperiod-dependent blooming (Imaizumi et al., 2003; Yanovsky and Kay, 2003). Photoperiod-dependent flowering induction and circadian oscillator resetting are crucial functions of the cryptochromes photoreceptor (Cashmoreet al., 1999; Yanovsky and Kay, 2003).

#### 2.5.2 Carotenoid gene expression regulation in photosynthetic organs

The light activates several genes involved in photosynthesis and photomorphogenesis. Because carotenoids are necessary for photosynthesis in plants and algae, light regulates their gene expression in these organisms (Welch et al., 2000). The extent of gene expression and carotenoids produced in dark- grown plants were compared to plants brought out of the dark and into the light. The expression of the *ggpps* and *pds* genes is mainly steady during the de-etiolation of *A. thaliana*. In contrast, the single-copy gene expression such as *psy* and *hdr*, was dramatically increased (Von Lintig et al., 1997). Evidence suggests that *psy*, *dxs*, and *dxr* transcriptional activation is required to stimulate carotenoid production in green organs (Toledo-Ortiz et al., 2010).

Continuous white-light illumination for 3-5 h activates xanthophyll biosynthetic genes in plants (Simkin et al., 2003; Woitsch and Romer, 2003). Tomato *lcy* mRNA levels increased five times after seedlings were moved from low to high-intensity light (Hirschberg, 2001). Regardless of the light quality utilized, considerable activation of carotenogenic gene expression was seen in etiolated seedlings of tobacco by red, blue, or white light illumination (Woitsch and Romer, 2003). Phytochrome and cryptochrome activities influenced the expression level. However, following continuous red and white illumination, significant changes in expression levels were identified concerning the kind of light, indicating that various photoreceptors are involved in regulating their expression levels (Woitsch and Romer, 2003). In maize (Zea mays) seedling photoinduction, PHY modulates the

upregulation of psy2 gene expression (Li et al., 2008).  $Lcy\beta$ , cycb, and vde were also generated by red light exposure. However, in the presence of red or blue light, zep exhibits identical transcriptional activity (Woitsch and Romer, 2003).

Photo-oxidation contributes significantly to the quantity of carotenoids generated in leaves as opposed to the normal light-induced activation of the carotenogenic genes. Carotenoids are formed in the presence of light. However, the photo-oxidation increases in response to the increased light intensity from 150 to 280 µmol/m²/s and exceeds the synthesis rate, and carotenoids are obliterated to a specific level (Simkin et al., 2003). Following sustained irradiation at moderate light levels, the various carotenogenic gene expression levels are similarly decreased (Woitsch and Romer, 2003). The biosynthesis of carotenoids in leaves stops in the dark, as there is no photooxidation of carotenoids.

#### 2.5.3 Effect of photoreceptors on fruit ripening

Regular tomato fruit coloration during ripening needs phytochrome-mediated light signal transduction (Alba et al., 2000). Due to lycopene buildup, carotenoid content increases 10 to 14 times during tomato fruit ripening (Fraser et al., 1994). An increase in carotenoid synthesis occurs during the transition from MG (mature green) to RR (Red ripe) stages of tomato fruit ripening. A synchronized overexpression of dxs, hdr, pds, and psy1 was detected during the process, while the expression of  $lcy\beta$ ,  $cyc\beta$ , and  $lcy\varepsilon$  decreased (Fraser et al., 1994; Botella-Pavia et al., 2004). The psy1 gene also controls carotenoid production throughout flower development (Zhu et al., 2003), fruit growth, and ripening (Giuliano et al., 1993; Fraser et al., 1999). The phytoene synthase genes psy1 and psy2 are distantly related in tomato. The former was transcriptionally initiated in flower petals and fruits under continuous blue or white light illumination (Welsch eta l., 2000; Giorio et al., 2008). Fruit carotenoids were reduced by 97 percent in transgenic tomato plants, having reduced psy1 expression by RNAi, but leaf carotenoids were unaffected since the production of psy2 is unaffected (Fraser et al., 1999).

Studies report that light impacts carotenoid accumulation in several different species, including tomato. PHY activation with red light stimulates carotenoid production, but treatment with far-red light inhibits it (Alba et al., 2000; Schofield and Paliyath, 2005). Fruits that have not been exposed to sunlight since their early

stages of development generate fruits utterly free of pigments (Cheung et al., 1993). Phytochromes also control the transition of distinct ripening phases and influence the carotenoid content in tomato fruits. The overexpression of phytochromes, cryptochrome, and UVR8 increased the carotenoid content in tomato fruits (Liu et al., 2018; Giliberto et al., 2005, Li et al., 2018, Alves et al., 2020). Contrarily, the loss of function of cryptochromes or phytochromes and silencing of UVR8 reduces the carotenoid levels. A dominant negative mutation of *phot1* in tomato fruits resulted into enhanced the carotenoid (Kilambi et al., 2021); however, no other alleles are available for tomato *phot1* or *phot2* and thus form the main focus of the present study.

#### 2.5.4 Light signaling components affect fruit ripening

Several reports in the literature highlight the importance of fruit-localized photosensory pathways as crucial participants in fruit ripening regulation and the possibility of manipulating them to increase nutritional quality (Azari et al., 2010). The tomato high pigment (*hp*) mutants, *hp1* (*DDB1*) and *hp2* (*DET1*), are the two best characterized among the several light signaling mutants with altered fruit phenotypes. The mutants derive their name from deep pigmentation due to the increase in size and number of plastids, which in turn accumulate a high level of carotenoids (Yen et al., 1997; Levin et al., 2003). In addition, extraplastidial metabolites such as flavonoids were found in significant amounts in *hp1* and *hp2* mutants. Other signaling components that participate in light signaling with *DDB1* and *DET1* include *CUL4*, *COP1*, and *HY5*, and they also affect fruit carotenogenesis (Wang et al., 2008; Schwechheimer and Deng, 2000; Liu et al., 2004).

#### 2.5.5 Phototropin homologs in other plants

From *Chlamydomonas reinhardii* to higher plants, phototropins were identified in several plant species (Briggs et al., 2001). In the fern, Adiantum, a hybrid phytochrome and phototropin protein called PHY3, mediates both red and blue light responses (Nozue et al., 1998). Like PHY3, green algae *Mougeotia scalaris* has two genes, *NEOCHROME1*, and *NEOCHROME2*, which show considerable homology to PHY3 (Suetsugu et al. 2005) and serve as a chimeric photoreceptor for red and blue light perception. In higher plants, phototropins are represented by two members, phot1 and phot2, and they share considerable sequence

homology. While in rice, two copies of phot1 exist- phot1a and phot1b- but it has a single *phot2* (Kanegae et al., 2000; Iinoand Haga, 2005). Tomato has two members, phot1 and phot2 (Sharma and Sharma 2006; Sharmaand Sharma, 2007).

## 2.5.6 Phototropin functions

Plants use phototropins to sense the visible spectrum's unidirectional UVA/Blue light. While phot1 senses low fluence blue light (up to 0.1 μmole/m²), phot2 can detect light intensities higher than 1 μmole/m², beyond which both can detect redundantly (Briggs and Christie 2002; Kagawa et al. 2001; Sakai et al. 2001). Consistent with this, phot1 mediates phototropism towards low fluence blue light, while phot2 mediates high fluence phototropism. In addition to phototropism, phototropins also mediate other tropic responses, such as negative phototropism of roots, stomatal movements (Kinoshita et al., 2001), chloroplast relocation responses (Sakai et al., 2001), and nuclear positioning (Iwabuchi et al., 2007). Also, they mediate leaf expansion (Ohgishi et al., 2004), movements (Inoue et al., 2005), positioning, and flattening (Sakamotoand Briggs, 2002).

While phot1 and phot2 redundantly mediate stomatal opening, phototropism, chloroplast accumulation, and leaf expansion, they retain their differential sensitivity to varying light fluences. Consistent with this, phot1 and 2 mediate the accumulation of chloroplasts under low fluence blue light. At higher fluence, avoidance response is mediated by phot2 (Jarillo et al., 2001; Kagawa et al., 2001). Similarly, phot1 alone is responsible for the rapid inhibition of elongation of hypocotyl in blue light (Folta and Spalding, 2001).

Molecular analysis of phot1 and phot2 revealed them to be serine/threonine protein kinases, as both have a kinase domain in the C-terminal domain. N-terminal has two LOV (light, oxygen, or voltage sensing) domains, and these are essential for blue light perception as the oxidized chromophore FMN (flavin mononucleotide), binds here. Of the two LOV domains, LOV2 is critical for kinase activity and function (Christie, 2007). Upon BL perception by the LOV domains, the kinase domain gets activated. It causes autophosphorylation of phot at multiple sites, such as the kinase domain, the linker region between LOV1 and LOV2, and the upstream sequences to LOV1. This autophosphorylation causes a conformational change resulting in the movement of the LOV2 domain away from the kinase domain. As a then phosphorylate result, activated phot can substrates like PKS4

(PHYTOCHROME KINASE SUBSTRATE1), ABCB19 (ATP binding cassette (ABC) transporter family member 19), and BLUS1 (BLUE LIGHT SIGNALING1) to mediate responses like phototropism, and stomatal movements (Kharshiing et al., 2019).

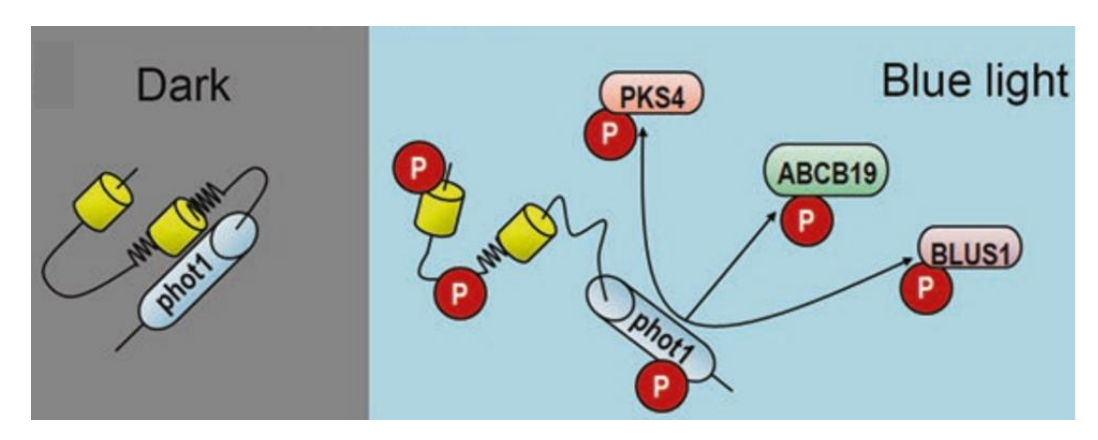


Figure 2.5. Blue light induces autophosphorylation of phototropin (phot1) at multiple residues resulting in conformation change, which moves the LOV2 domain away from the kinase domain. This relieves the dark-state inhibition of the kinase domain, which allows the activated protein to phosphorylate substrate targets, including PKS4, ABCB19, and BLUS1. Yellow barrels indicate LOV domains, and blue barrel shows the kinase domain. This figure is adapted from Kharshiing et al., 2020.

#### 2.5.7 Phototropin mutants in tomato

Searching for non-phototropic seedlings under continuous blue light from an EMS mutagenized population led to identifying *Nps1* (non-phototropic seedling 1), a dominant negative mutant of phototropin1 in tomato. Molecular characterization of *Nps1* revealed that the Arg494His mutation in the A-α-helix located in the hinge region between LOV1 and LOV2 domains causes the dominant nature of phot1. Similar to the Arabidopsis *phot1* mutant, *Nps1* showed the loss of phototropism, and chloroplast relocation. In addition, the leaf shape, flattening, and stomatal opening (Sharma et al., 2014) were also affected. Surprisingly, this mutant dominant-negatively affected the fruit carotenoid content (Kilambi et al., 2021). The stimulation of carotenogenesis was tightly linked to the *phot1* mutation as the introgression of *Nps1* into two local cultivars also elevated the carotenoid content. In addition to influencing carotenogenesis, *Nps1* mutation also affected the fruit proteome, metabolome, and volatile profiles (Kilambi et al., 2021). Given the lack of additional alleles for *phot1* and no existing alleles for *phot2*, this thesis attempts to isolate gene-silenced lines/knockout alleles for *phot1* and *phot2* to decipher their

functions in fruit carotenogenesis. As Arabidopsis lacks a fleshy fruit, understanding the influence of phototropins on fruit carotenogenesis in tomato paves the way for such studies in other crops to uncover hidden and novel functions..

#### Materials and methods

#### 3.1.1 RNAi construct for *phot1* and 2 genes

Both *phot1* (Solyc11g072710.1.1) and *phot2* (Solyc01g097770.2.1) gene sequences were retrieved from Solanaceae Genome Network (SGN); <a href="http://www.sgn.cornell.edu">http://www.sgn.cornell.edu</a>). RNAi construct was designed with the help of Gateway<sup>TM</sup> technology for cloning the genes (Figure 3.1A & B). For silencing *phot1* and *phot2*, 250 bp regions unique to each of these genes in tomato were selected (Figure 3.2A and B).

#### 3.1.2 cDNA amplification and cloning into the entry vector

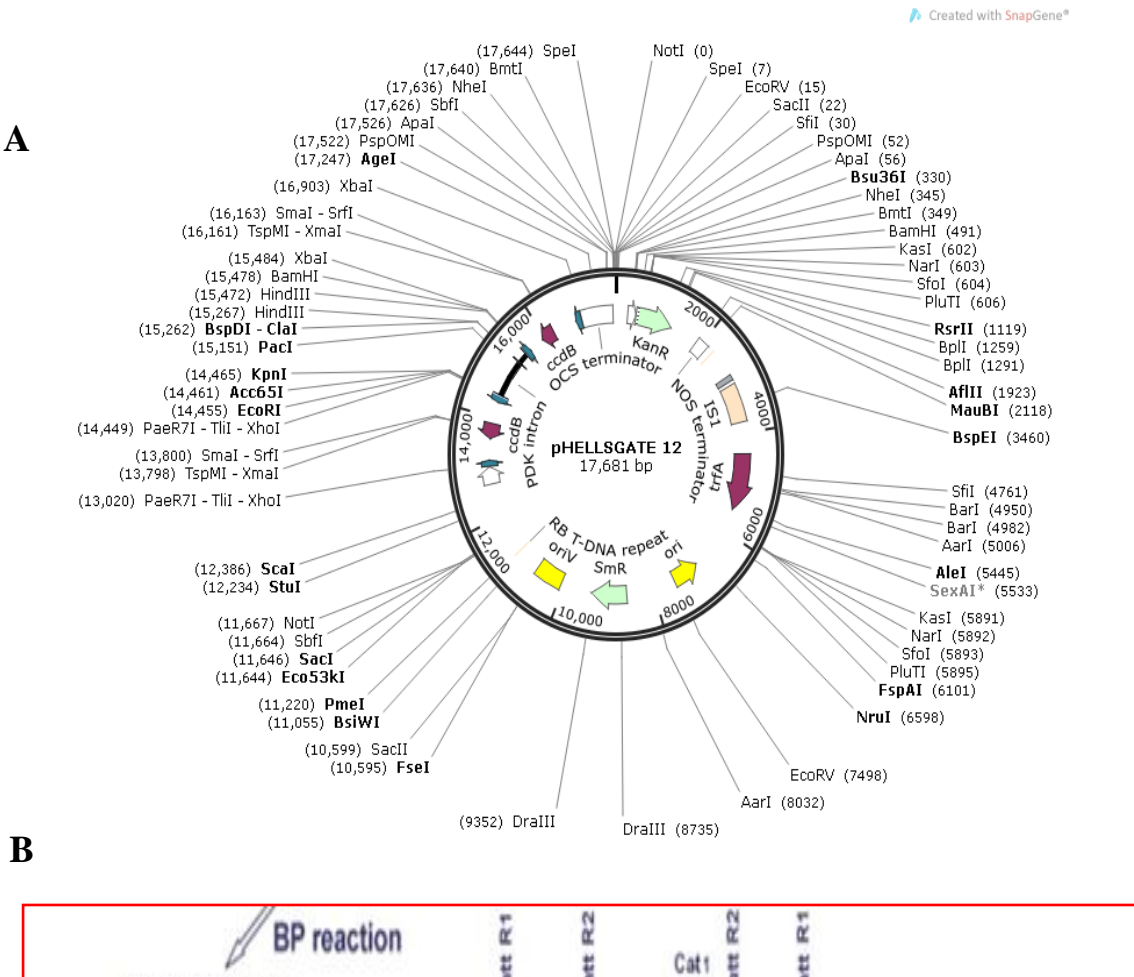
Using standard protocols, the total RNA from tomato leaves was isolated and converted to cDNA. The unique 250 bp region (for *phot1* and 2) from cDNA was amplified using a set of primers (Table 3.1) having an additional attB sequence at the 5' end of primers of both *phot1* and *phot2* (Figure 3.2C). The PCR products were cloned into pDONR201 vector having attP1 and attP2 sites, and positive colonies were confirmed by PCR using gene-specific primers (Figure 3.3). In addition, using M13 primers, the plasmid sequencing from the positive clones confirmed the presence of *phot1* and *phot2* sequences in the pDONR201 vector (Figure 3.4).

Table: 3.1. Primers used for isolating *phot1* and 2 fragments from cDNA.

S.No	Gene	Forward Primer	Reverse Primer	
1	phot1	AGAGAGCAGCCGAGTGGGGAC	ATGTTTGTTGAAATGTAGATAAGGCATC	
	gene			
2	phot2	GGACAGGAACAGACAAGTTAATTAAC	TGATCCAACTGAATTCTTCTCAAT	
	gene			

#### 3.1.3 Cloning of entry vector into Destination Vector (pHellsgate 12)

The gene fragment from the pDONR201 vector was then transferred to the pHellsgate vector (CSIRO, Australia). This was done by recombination between attL1/attL2 and attR1/attR2, mediated by LR Clonase enzyme (*Invitrogen*). Colony PCR confirmed that *phot1* and 2 were transferred into the destination vector (Figure 3.5). In both constructs, many clones showed the gene of interest. Thereafter, positive clones were confirmed by digestion using restriction enzymes *Xba1* (Figure 3.6). The positive clones were reconfirmed by sequencing the positive clones'



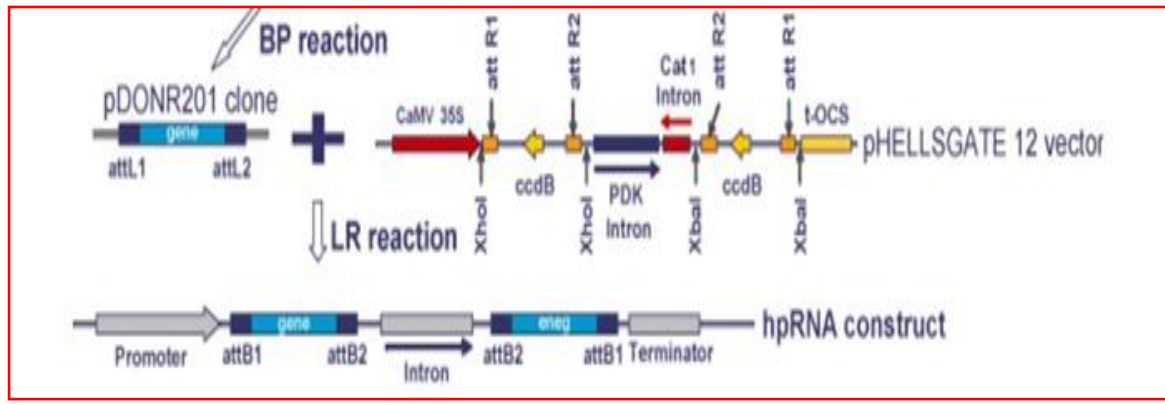
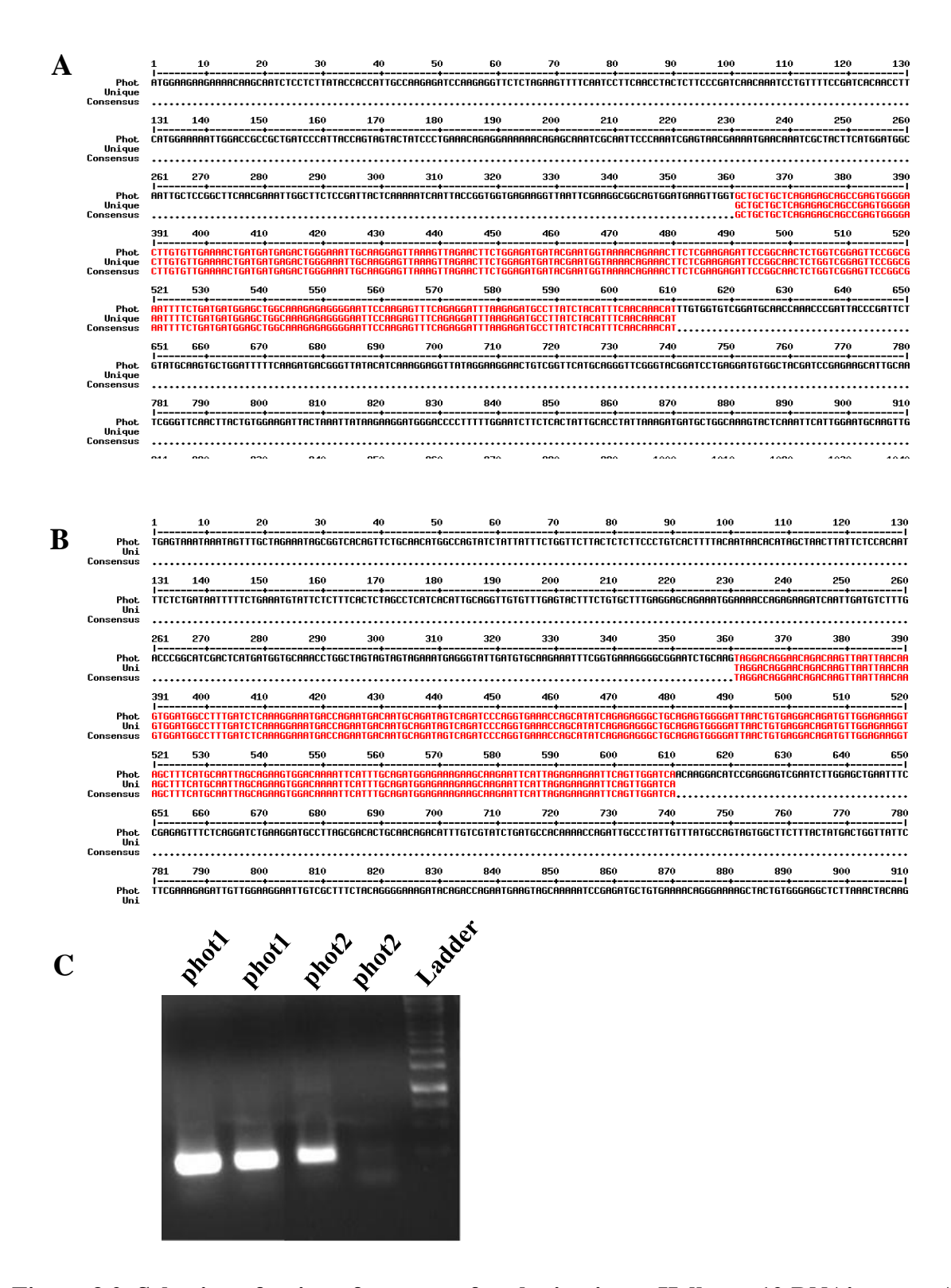
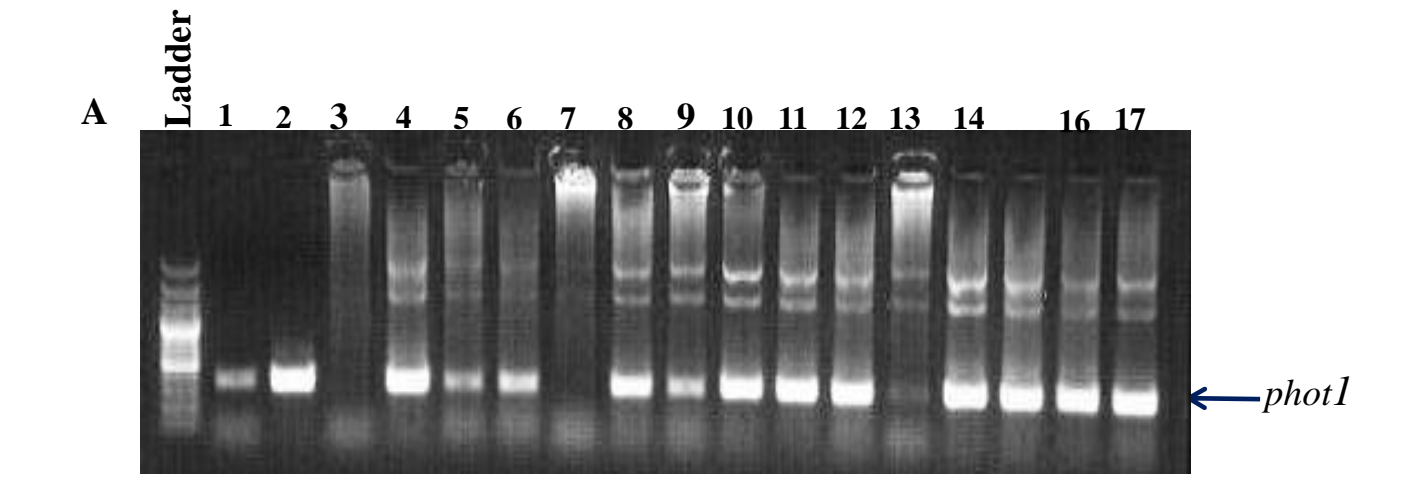


Figure 3.1. Schematic representation of restriction map of construct used for silencing of *phot1* and *phot2* genes in tomato. A, Schematic representation of pHellsgate 12 construct. B, Schematic representation of Gateway<sup>TM</sup> cloning strategy.



**Figure 3.2. Selection of unique fragments for cloning into pHellsgate12 RNAi vector. A**, Unique region of *phot1* was selected from 461-610 (249 bp) **B**, Unique region of *phot2* was selected from 360-610 (250bp). **C**, Unique fragments were isolated from cDNA with specific primers.



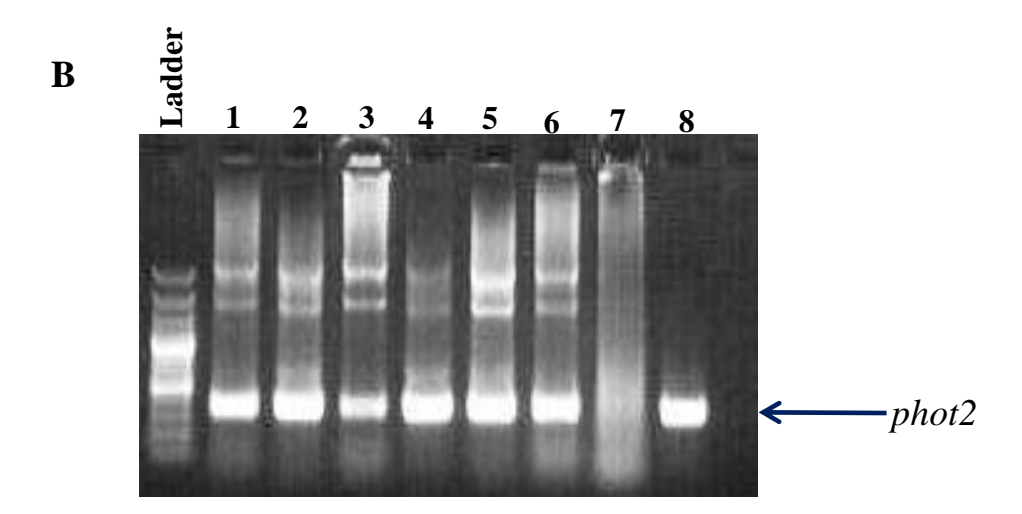


Figure 3.3. Colony PCR in *phot1* (A) and *phot2* (B) clones with the help of gene-specific primers to know their presence in the pDONAR201 entry vector. A, 1 and 2 lanes are positive control, 3, blank, 4-17 shows *phot1* clones. B, Lane 1-6 shows *phot2* clones, lane 7 is blank, 8- positive control.

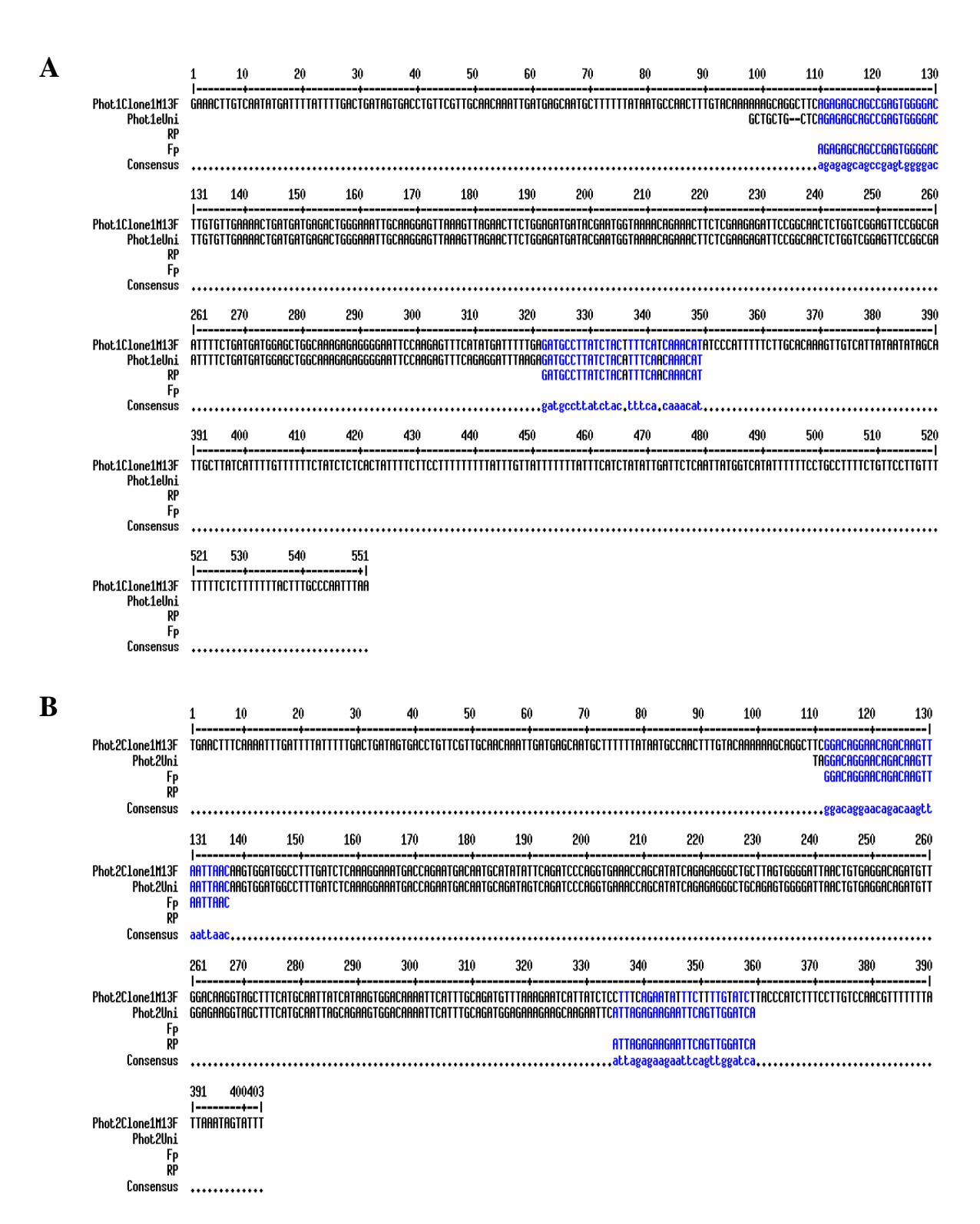
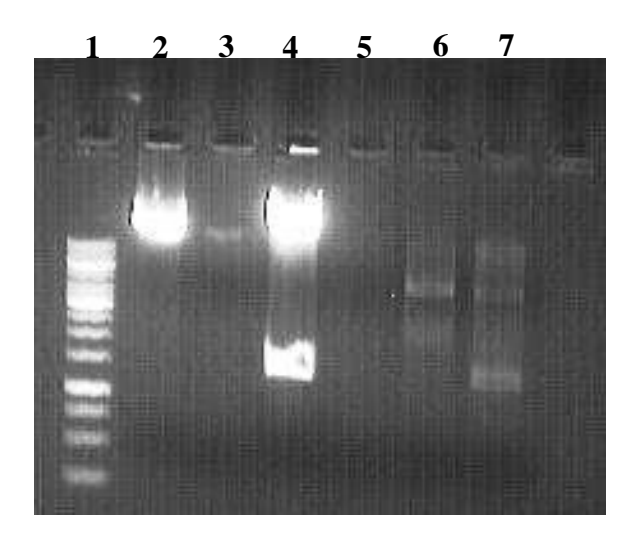


Figure 3.4. Sequencing analysis of phot1 (A) and phot2 (B) clones in pDONAR201 entry vector.

Figure 3.5. Colony PCR in *phot1* (A) and *phot2* (B) clones with the help of gene-specific primers to know their presence in the pHellsgate12 destination vector. A, Lane 1-13 shows *phot1* clones, lane 14 is positive control, 15-16 are negative control, lane 17 is blank. B, Lane 1-13 shows *phot2* clones, lane 14 is positive control, 15-16 are negative control, lane 17 is blank.



**Figure 3.6. Restriction analysis of PCR confirmed positive clones.** Lane 1 - 1 Kb Ladder, lane - 2 un-digested *phot1* clone, lane 3 – un-digested *phot2* clone, lane 4 - *phot1* clone digested with *Xba*I, lanes 5-7 - *phot*2 clone digested with *Xba*I.

plasmid using *CaMV 35S* primers. The sequencing result showed that *phot1* and 2 were ligated into pHellsgate12 vectors (Figure 3.7). The confirmed clones were transformed into *Agrobacterium tumefacians* C58CI strain (Figure 3.8). The transformation of Arka Vikas was initiated with these clones (Figures 3.9 & 10). In addition, an empty vector, pHellsgate, was also used for tomato transformation to serve as a control (Figure 3.11). Dr. Arun Pandey cloned the *phot1* and 2 genes, and Ms. Thanvitha did the tomato transformation. The hardened plants were handed over to me when I started my Ph.D. work and were analyzed by me and taken forward to subsequent generations.

# 3.2 Plant genetic transformation using *phot1*, *phot2* and empty vector (pHellsgate) constructs

Different steps involved in the protocol for tissue culture transformation and regeneration of the plants (Sharma et al., 2009) are described below.

#### 3.2.1 Seed surface sterilization and germination

Tomato (*S. lycoperscicum cv* Arka Vikas) seeds were washed with 5% (v/v) Teepol with vigorous shaking for 20 min. Then, the seeds were then treated with sodium hypochlorite 4% (v/v) for 10 min with intermittent mixing by shaking and were finally washed with autoclaved distilled water for five times. Then the seeds were dried on the filter paper. These seeds are then placed in the jam bottles containing the ½ MS media for germination in the dark for 2-3 days. After the radical emergence, the bottles were placed under the light for the growth of the seedlings. These seedlings were maintained at 16 h light/8 h dark cycle.

#### 3.2.2 Explant preparation and pre-culture

Cotyledons of 10-day-old seedlings were cut carefully, ensuring they were not bruised. The cotyledons of approximately 0.7 to 1 cm in length were placed on the nutrient media with their adaxial surface facing the light for two days. The cotyledons were maintained at controlled conditions of 25°C temperature for 16 h light and 8 h dark conditions. The explants that showed swelling at the cut edges and expansion were considered healthy and taken forward for co-cultivation.

#### 3.2.3 Inoculum preparation and Co-cultivation

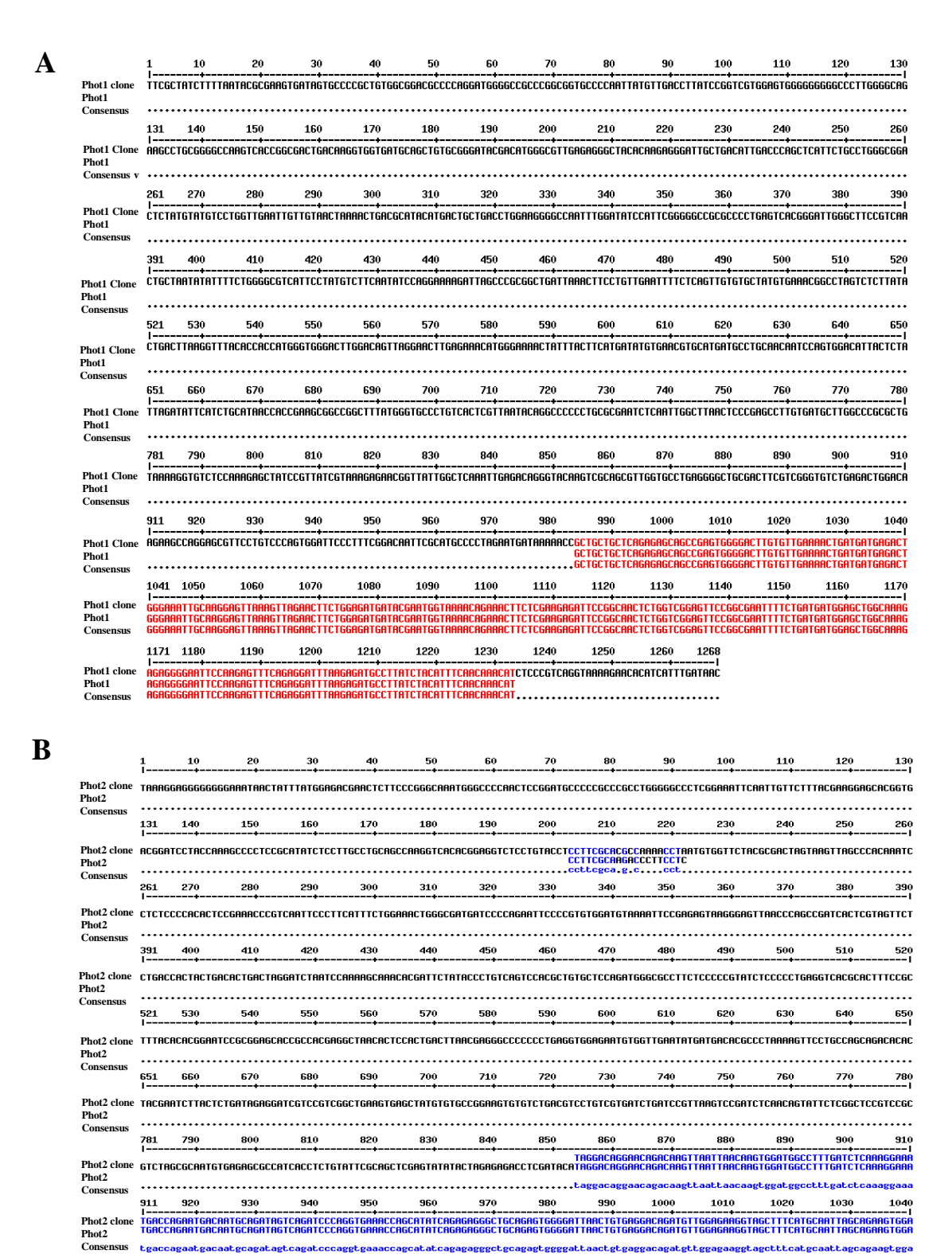


**Figure 3.7.** Sequencing analysis of *phot1* (**A**) and *phot2* (**B**) clones in pHellsgate12 destination vector.

Phot2 clone

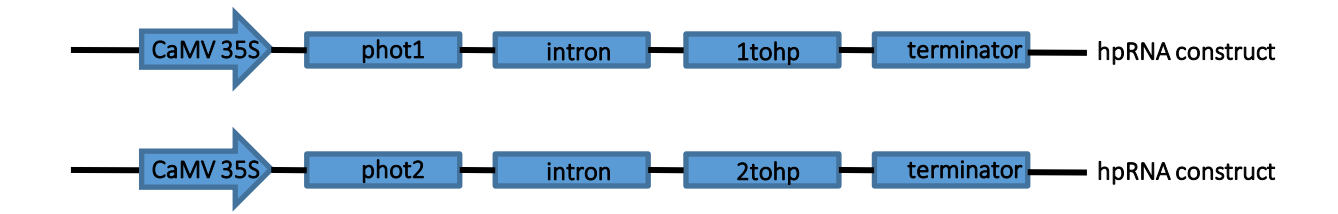


**Figure 3.8.** The *phot1* and *phot2* cassettes having CaMV 35S promoter, Nos terminator, intron structure for gene silencing in pHellsgate vector.

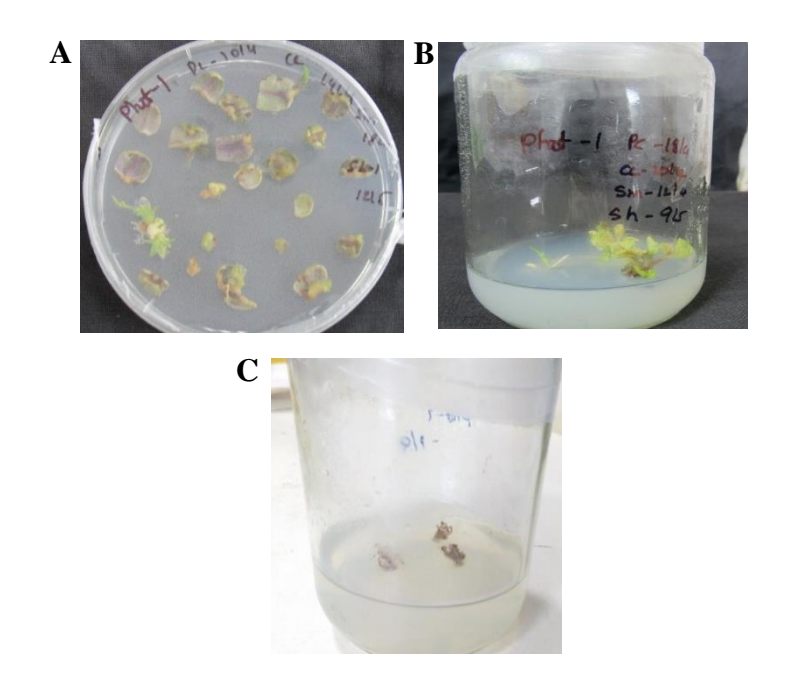


**Figure 3.9. Transformation and regeneration of tomato with** *phot1* **RNAi construct**. A, *phot1* callus, B, *phot1* explants on shooting medium, C, *phot1* explants on rooting medium. Note: The *phot1* explants failed to regenerate on rooting medium even after multiple attempts.

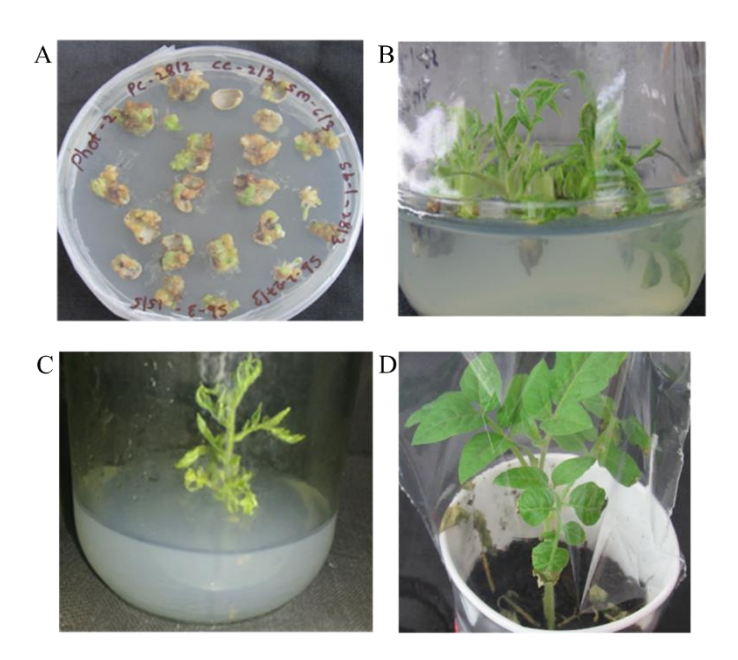


**Figure 3.10. Transformation and regeneration of tomato with** *phot***2 RNAi construct**. A, *phot***2** callus, B, *phot***2** explants on shooting medium, C, *phot***2** explants on rooting medium, D, *phot***2** regenerated plant in cup.

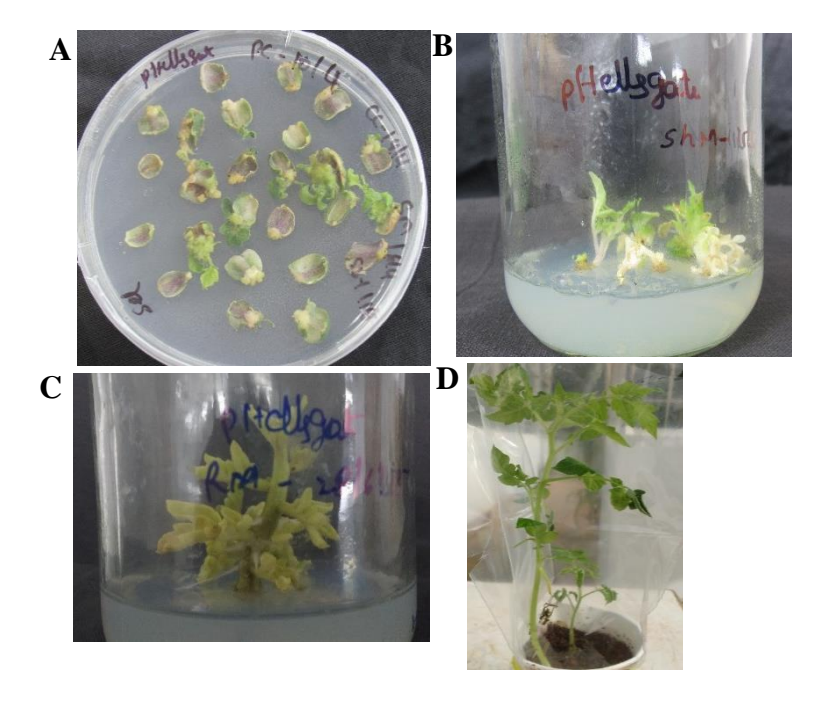


**Figure 3.11. Transformation and regeneration of tomato with pHellsgate12 RNAi construct (empty vector control)**. A, pHellsgate12 callus, B, pHellsgate12 explants on shooting medium, C, pHellsgate12 explants on rooting medium, D, pHellsgate12 regenerated plant in cup.

phot1, phot2, and empty vector (pHellsgate) constructs were transformed in the C58C1 strain of Agrobacterium tumefaciens (Holsters et al., 1980). The above constructs were further used for tomato transformation, and they contain kanamycin as the selection marker. Two days before the co-cultivation, a single colony of Agrobacterium harboring the respective construct was grown in 5 mL of LB media containing 25 mg/L of rifampicin and 50 mg/L of kanamycin for 24- 36 h under constant rotation at 200 rpm and 28°C. 2 mL of the culture was used as the inoculum for 50 mL of LB broth with equated antibiotic concentartions as mentioned above. The culture was grown until the O.D reached 0.5-0.8 at 600 nm. After that, the culture was pelleted at 3000g for 10 min. This pellet was washed with 1X MS media once and then resuspension in 1X MS media having sucrose. The culture having 1x10<sup>8</sup> cells per mL of the media with each of the *phot1*, *phot2*, and empty vector (pHellsgate) constructs were used for the transformation of tomato explants. The pre-cultured cotyledonary explants were immersed in bacterial suspension for 30 min, then the explants were placed on the sterile filter paper to remove excess bacteria. After that expants were placed on the same pre-culture plate before and incubated on the pre-culture media for another 48 h.

## 3.2.4 Callus induction, Regeneration, and selection

After 48 h of incubation, the explants were transferred into callus induction media having one mg/L Zeatin, 500 mg/L cefotaxime, and 100 mg/L kanamycin. The explants were sub-cultured every 10-12 days. The explants forming shoots were transferred into regenerative media containing kanamycin to select only the transformed shoots for each construct. As the non-transformed shoots show bleaching on kanamycin, they were discarded.

## 3.2.5 Root induction and hardening of plantlets

The shoots which survived the selection were transferred into MS media which doesn't contain hormones to induce roots. After the root formation, the plants were transferred into cups containing autoclaved coco-peat. Plants with good growth were transferred into greenhouses for hardening for one week and then moved into pots.

#### 3.2.6 Plant materials and growth conditions

Transgenic plants, after tissue culture, were transferred into the greenhouse and maintained along with NpsI, a phototropin1 mutant, and used as the control for chloroplast movement analysis. All the above plants were kept at  $25\pm2^{\circ}$ C.

## :3.2. Composition of media.

Name of the	Seed	Pre-culture and	Selection	Rooting
reagent	germination	co-cultivation		
MS salts	0.5 x	1 x	1 x	1 x
B5 Vitamins	0.5 x	1 x	1 x	1 x
Sucrose (g/L)	15	30	30	30
Agar (%w/v)	0.8	0.8	0.8	0.8
BAP mg/L	0	2	0	0
IAA mg/L	0	0	0.1	0
Zeatin mg/L	0	0	1	0
Kanamycin	0	0	100	100
Cefotaxime	0	0	500	500

## 3.3 Development of CRISPR/Cas9 double gRNA constructs for targeting phot1 gene

## 3.3.1 Selection of target site and vector construction

Two target sequences located in the first exon of the *phot1* gene (Solyc11g072710) were selected using the CRISPR-P web tool (http://cbi.hzau.edu.cn/crispr) to introduce mutations (Lei etal., 2014) (Figure 3.12 & 3.13 A). For better editing efficiency, the score of the selected gRNA should be higher than 0.5, with the GC content between 40-60%, and gRNA should have fewer off-targets (Figure 3.12). Once the gRNAs were selected, their folding was predicted using the **RNA** fold server (http://mfold.rna.albany.edu/?q=mfold/RNA-Folding-Form2.3) (Figure 3.13 B). The following two guide RNAs with adjacent protospacer motif (PAM) were chosen for GAGAAGGTTAATTCGAAGG, targeting phot1, sgRNA-1: and sgRNA-2: GGAACTCCGACCAGAGTTGC.

The cassette harboring a U6 promoter for a functional gRNA and a spacer sequence to enable the binding of gRNA to Cas9 and the U6 terminator sequence (Nekrasov et al., 2013) was commercially synthesized (Macrogen Inc) (Figure 3.14 A and B). The overlap extension PCR was used to amplify the 130 bp long primers to assemble into a perfect complementary DNA strand (Figure 3.14C) containing U6 promoter, gRNA scaffold, and U6 terminator. The cassette region thus generated is

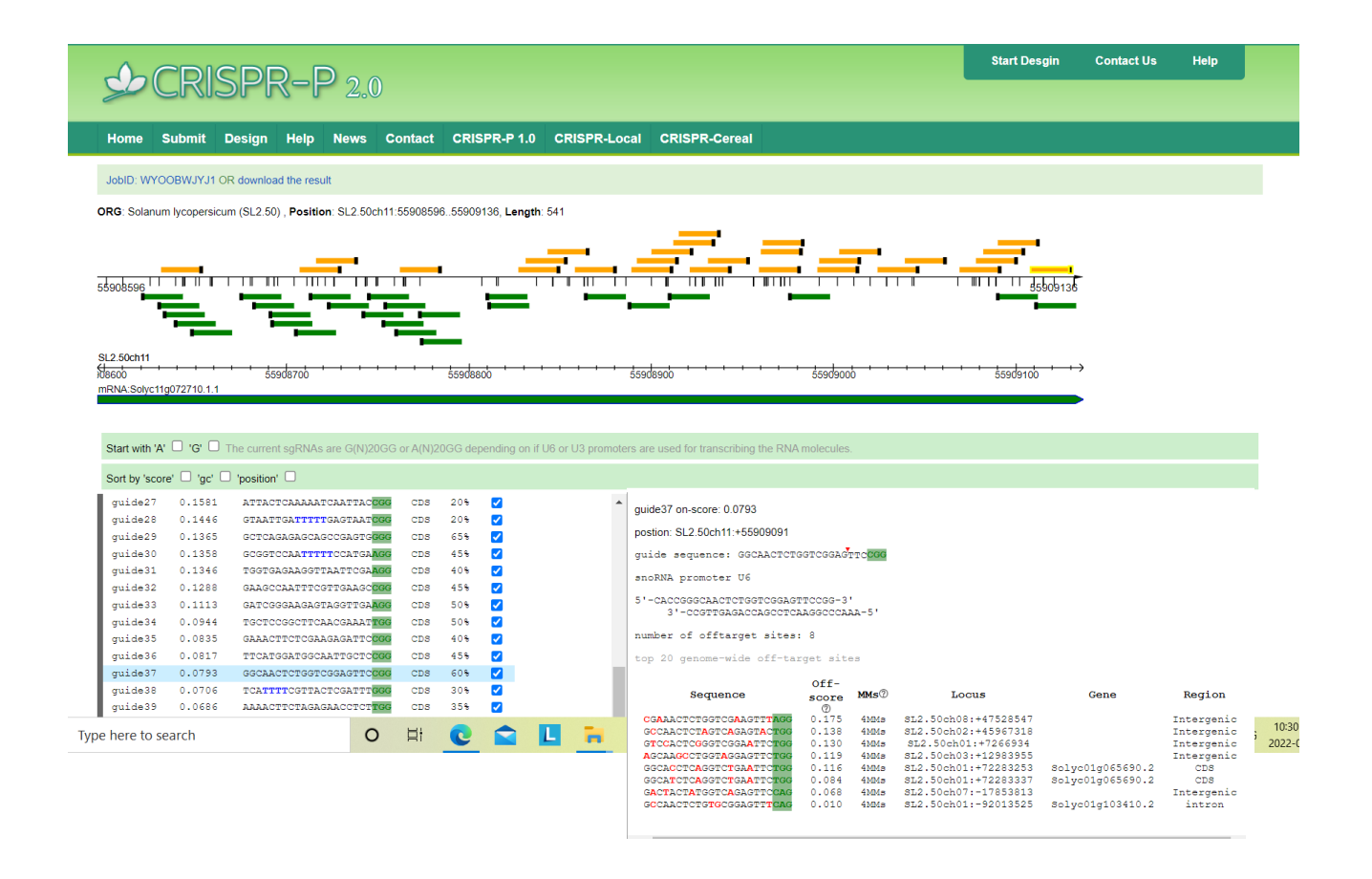
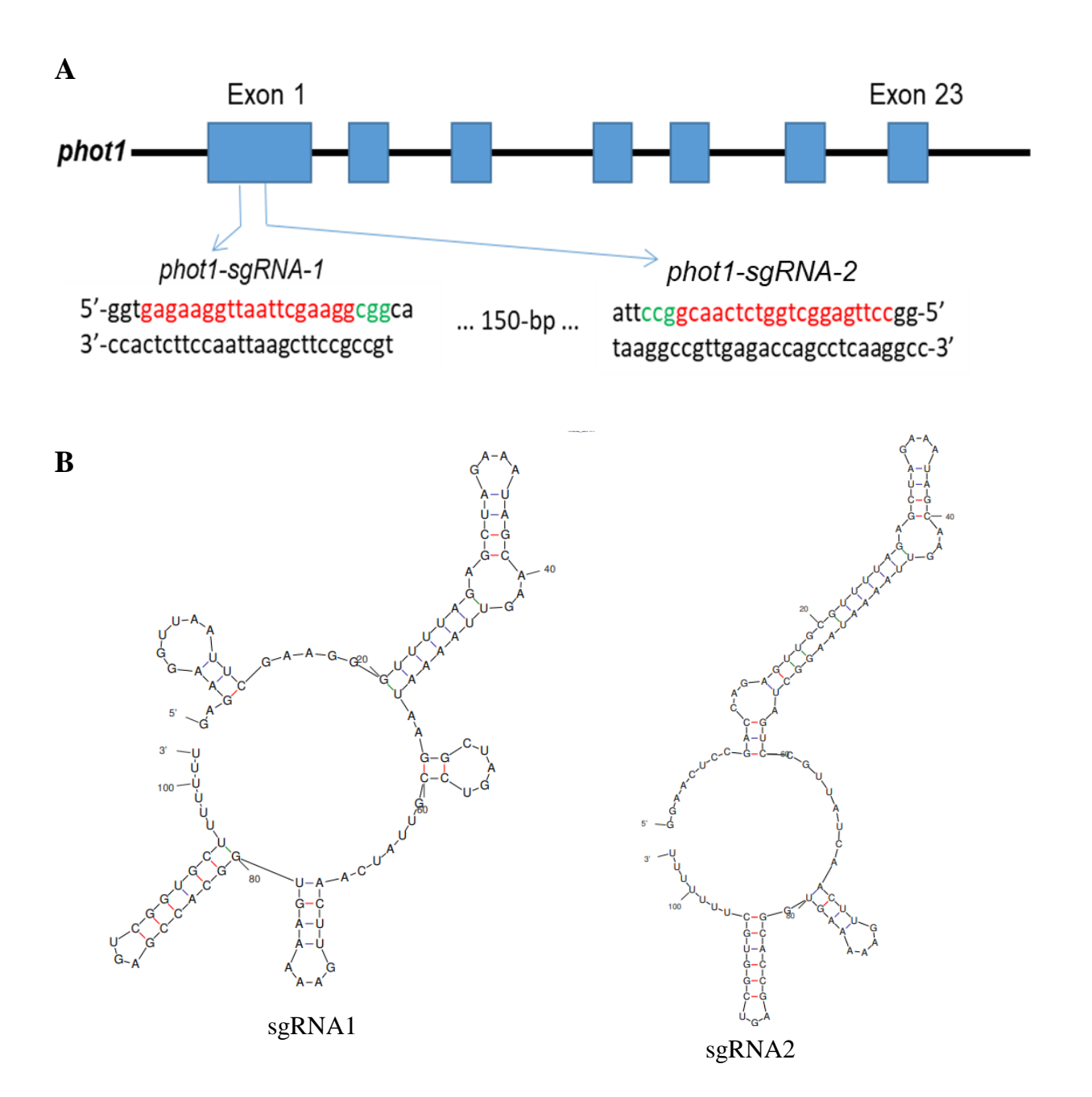


Figure 3.12. Selection of gRNAs from the *phot1* gene using CRISPR-P web tool. This tool helps in screening all possible sgRNA in the target sequence. Green and red bar on top of the target sequences indicates the sgRNA predicted on the + and – strands of the target region. The on-target efficiency of the gRNA is determined by the scoring and the best ones score > 0.5. 30-80% CG content is recommended. PAM sequences are in high lightened in green color in the predicted gRNA sequences. These sgRNA sequences are scanned for off-target matches throughout the selected genome. Then, top 20 off-target scored genome locus and its mismatches (MMs) to target sequence are listed for every sgRNA (mismatches are high lightened in red color).



**Figure 3.13. A**, Schematic view of sgRNA1 and sgRNA2 target sites in the *phot1* gene. Boxes indicate exons, red color indicates 19-20 bp target sequences and green indicates the protospacer-adjacent motif (PAM). **B**, Secondary structures of *phot1* gRNA1 and gRNA2 visualized using RNA fold server, Mfold. The best gRNA in stable complex with Cas9 for gene editing should have i) no more than 12 base pairs with the other bases of sgRNA, ii) no more than 7 consecutive base pairs and iii) no more than 6 internal base pairs. Based on this, the selected gRNAs have good secondary structure and ideal for editing.

## A phot1\_guide2

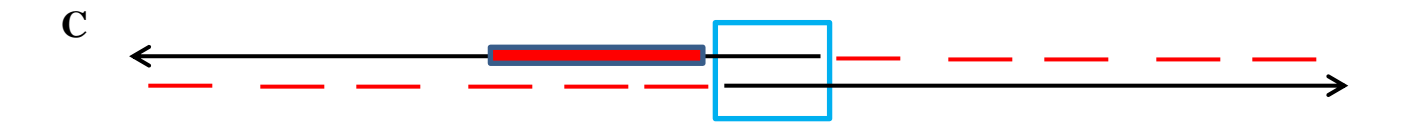
PacI

TTAATTAAGGAGTGATCAAAAAGTCCCACATCGATCAGGTGAT
ATATAGCAGCTTAGTTTATATAATGATAGAGTCGACATAGCGA
TTGAGAAGGTTAATTCGAAGGGTTTTAGAGCTAGAAAATAGC
AAGTTAAAAATAAGGCTAGTCCGTTATCAACTTGAAAAAAGTG
GCACCGAGTCGGTGCTTTTTTTCTAGACCCAGCTTTCTTGTA
CAAAGTTGGCATTACGCTACTAGT
Spel

B phot1\_guide2

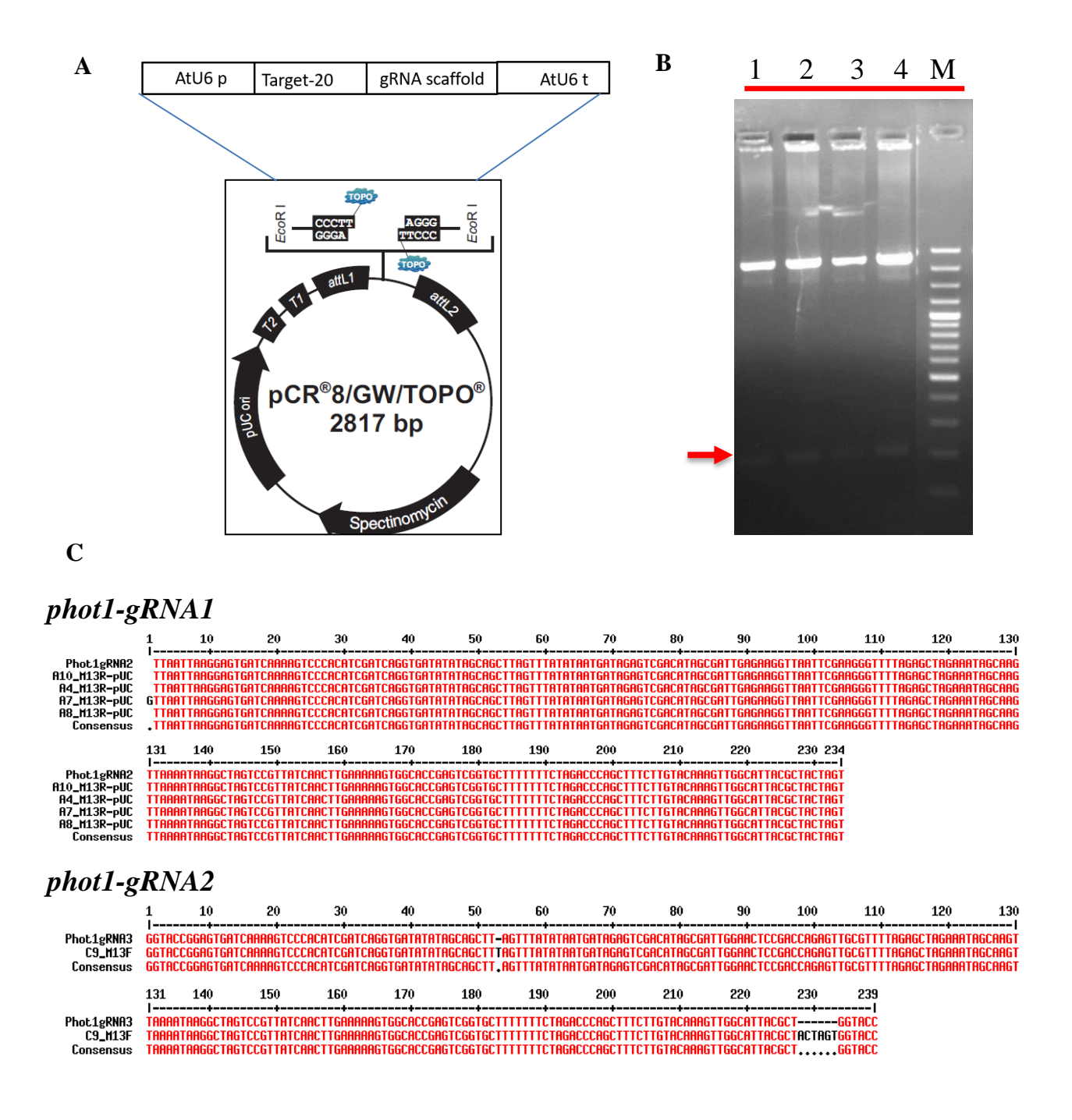
Kpn1

GGTACCGGAGTGATCAAAAGTCCCACATCGATCAGGTGATAT
ATAGCAGCTTAGTTTATATAATGATAGAGTCGACATAGCGATT
GGAACTCCGACCAGAGTTGCGTTTTAGAGCTAGAAATAGCAAG
TTAAAATAAGGCTAGTCCGTTATCAACTTGAAAAAAGTGGCA
CCGAGTCGGTGCTTTTTTTCTAGACCCAGCTTTCTTGTACAA
AGTTGGCATTACGCTGGTACC Kpn1

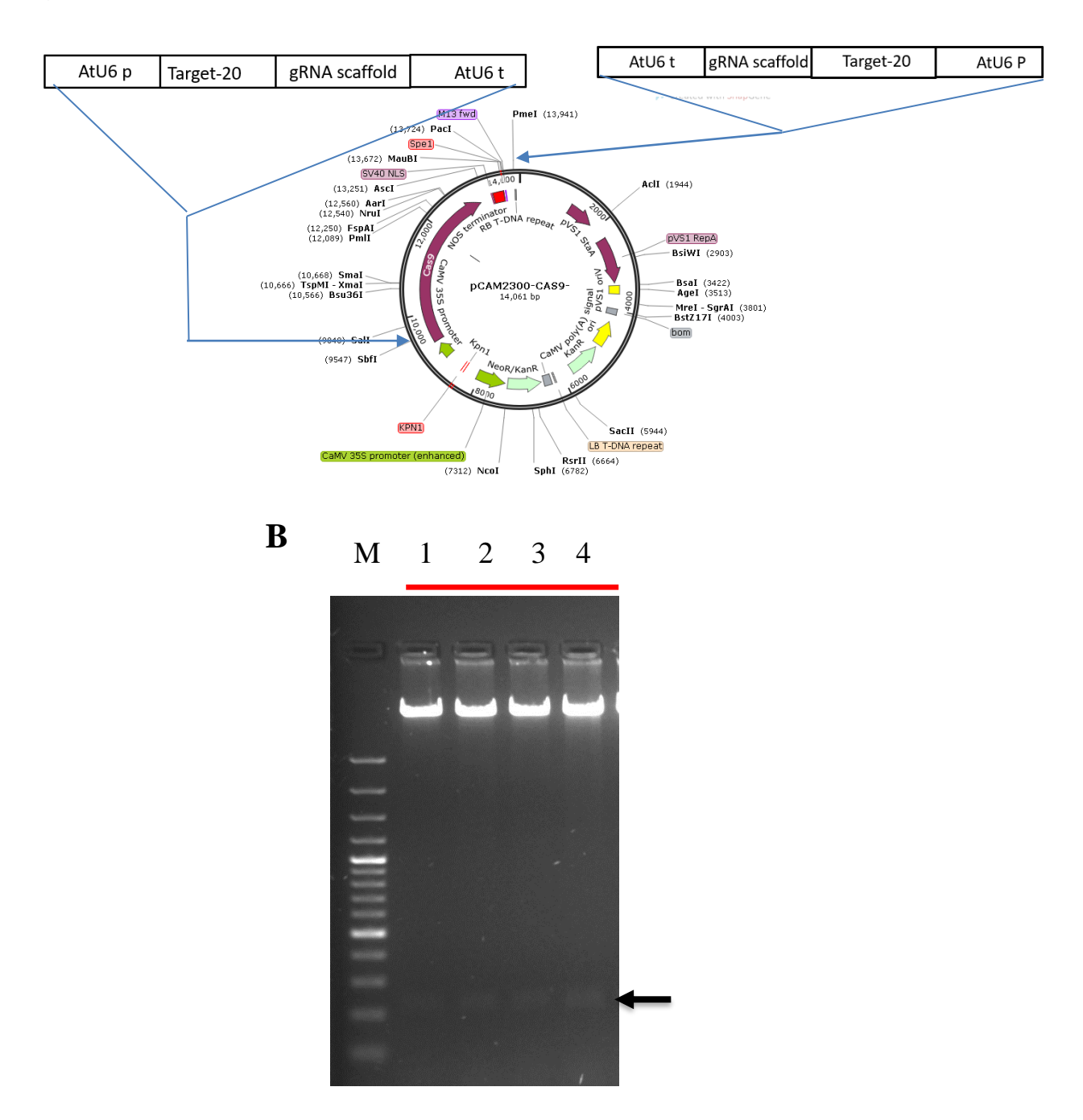


**Figure 3.14. A & B,** Sequences used for generation of gRNA expression cassette. Sequences in blue color indicate At*U6* promoter, red sequence indicate guide sequence, green sequence indicates scaffold sequence, black sequence indicate At*U6* terminator sequence; **C,** 130 bp long primers used to generate expression cassette through overlap extension PCR.

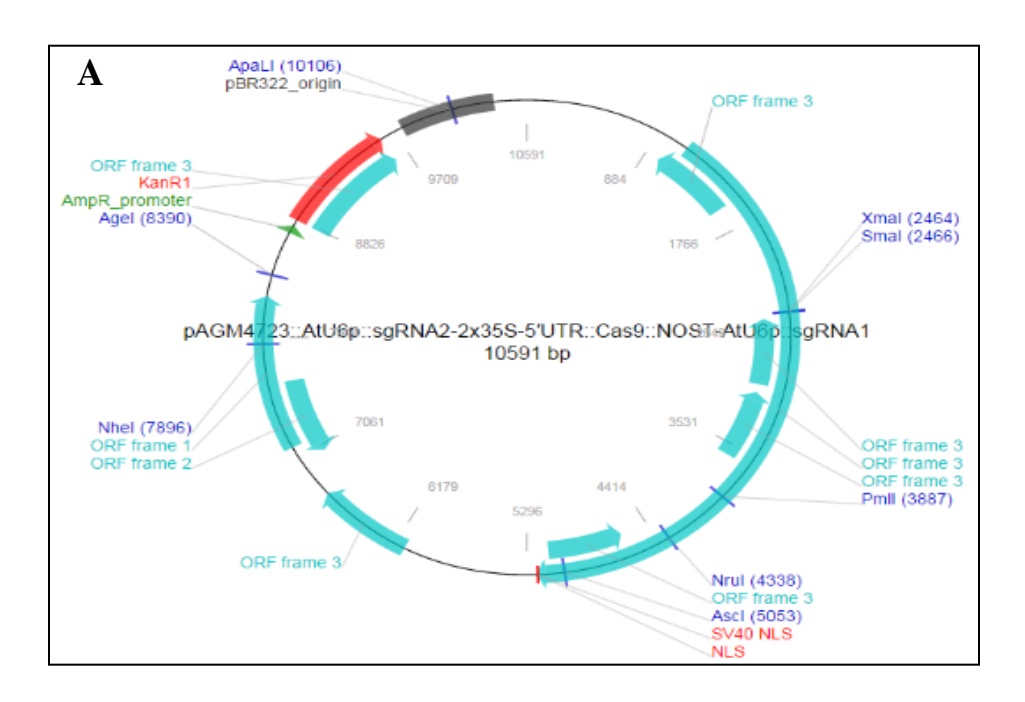
**Figure 3.14. D,** Schematic representation of gRNA1 *phot1* expression cassette and gRNA2 *phot1* expression cassette.



**Figure 3.15. A,** Cloning of sgRNA1 *phot1* and sgRNA2 *phot1* into pCR8/GW/TOPO-TA vector. **B,** Confirmation of *sgRNA1-phot1*, *sgRNA2-phot1* in pCR8/GW/TOPO-TA vector using *EcoRI* enzyme. Lane 1 and 2 indicate restriction fragments (red arrow) of *sgRNA1-phot1* and lane 3 and 4 indicate restriction fragments (red arrow) of *sgRNA2-phot1*, Lane M: 100 bp marker. **C,** Sequence alignment of *pCR8/GW/TOPO-TA-sgRNA1-phot1*, gRNA2-*phot1*.



**Figure 3.16. A,** Cloning of sgRNA1 phot1 sgRNA2 phot1 cassette into pCAM2300 vector. **B,** Confirmation of pCAM2300-sgRNA1, sgRNA2-phot1 using PacI + SpeI and KpnI enzymes. Lane 1 and 2 shows restriction digestion for PacI + SpeI. Lane 3 and 4 shows restriction digestion for KpnI enzyme and black arrow indicates the fragments formed after digestion with these enzymes.



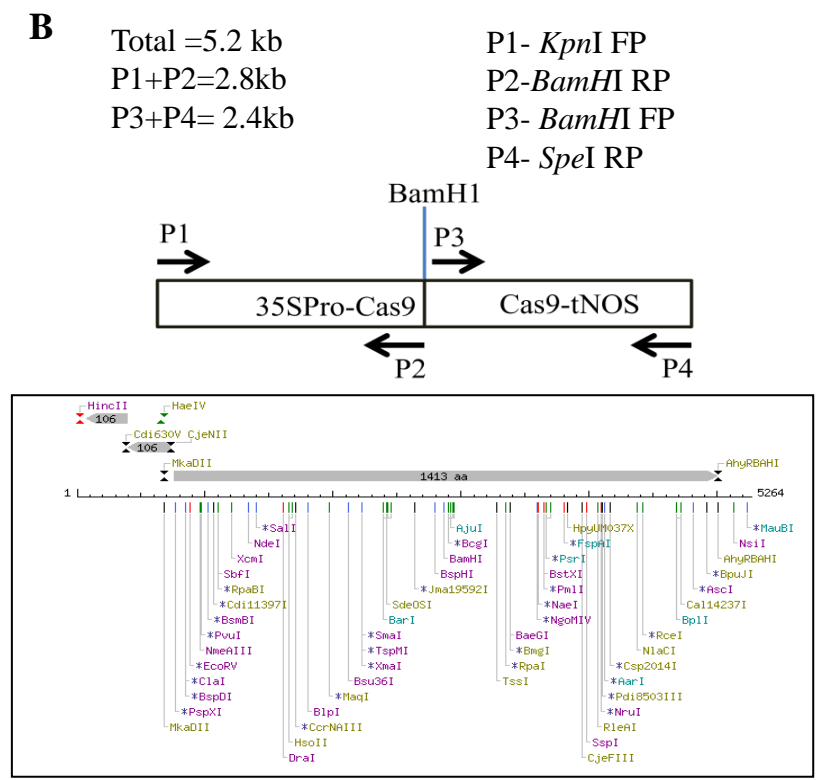


**Figure 3.17. A**, CRISPR/Cas9 construct from Addgene (# 49772). **B**, PCR amplification of human codon optimized Cas9 with 2X35S CaMV promoter and nos terminator from pAGM4723 plasmid (Addgene# 49772) using *Kpn*I FP, *Bam*HI RP for Cas9-I region and *Bam*HI FP, *Spe*I RP for Cas9-II region generating two amplicons each of 2.8 kb (Cas9-I) and 2.4 kb (Cas9-II) respectively.

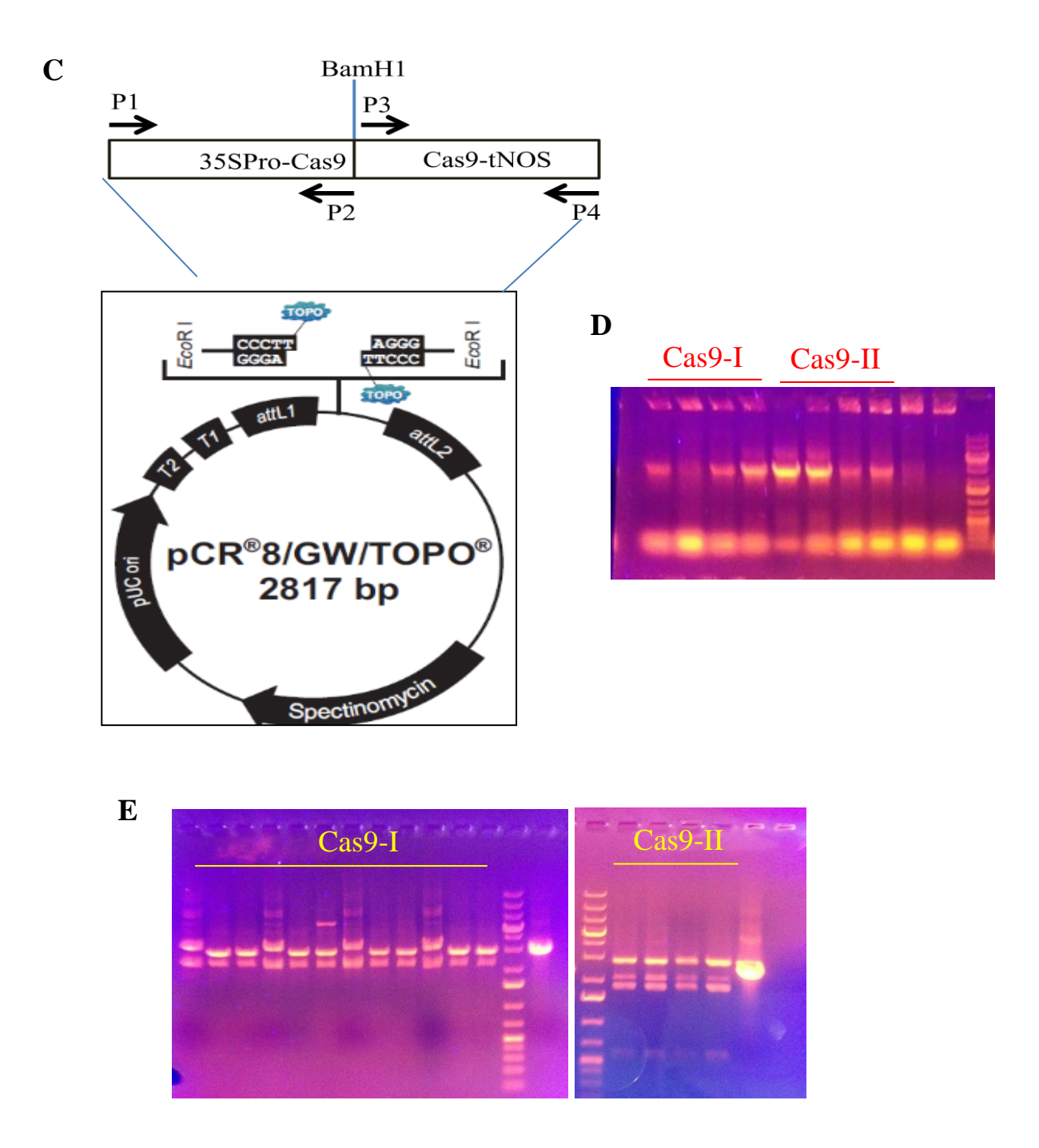


**Figure 3.17.** C, Cloning of Cas9-I and Cas9-II into pCR8/GE/TOPO cloning vector. **D**, Confirmation of cloning using colony PCR which gave a product size around 1.1 Kb for both Cas9-I and Cas9-II. **E**, Confirmation of Cas9-I (*Kpn*I and *BamH*I) sequence and Cas9-II (*BamH*I and *Spe*I) using restriction digestion.

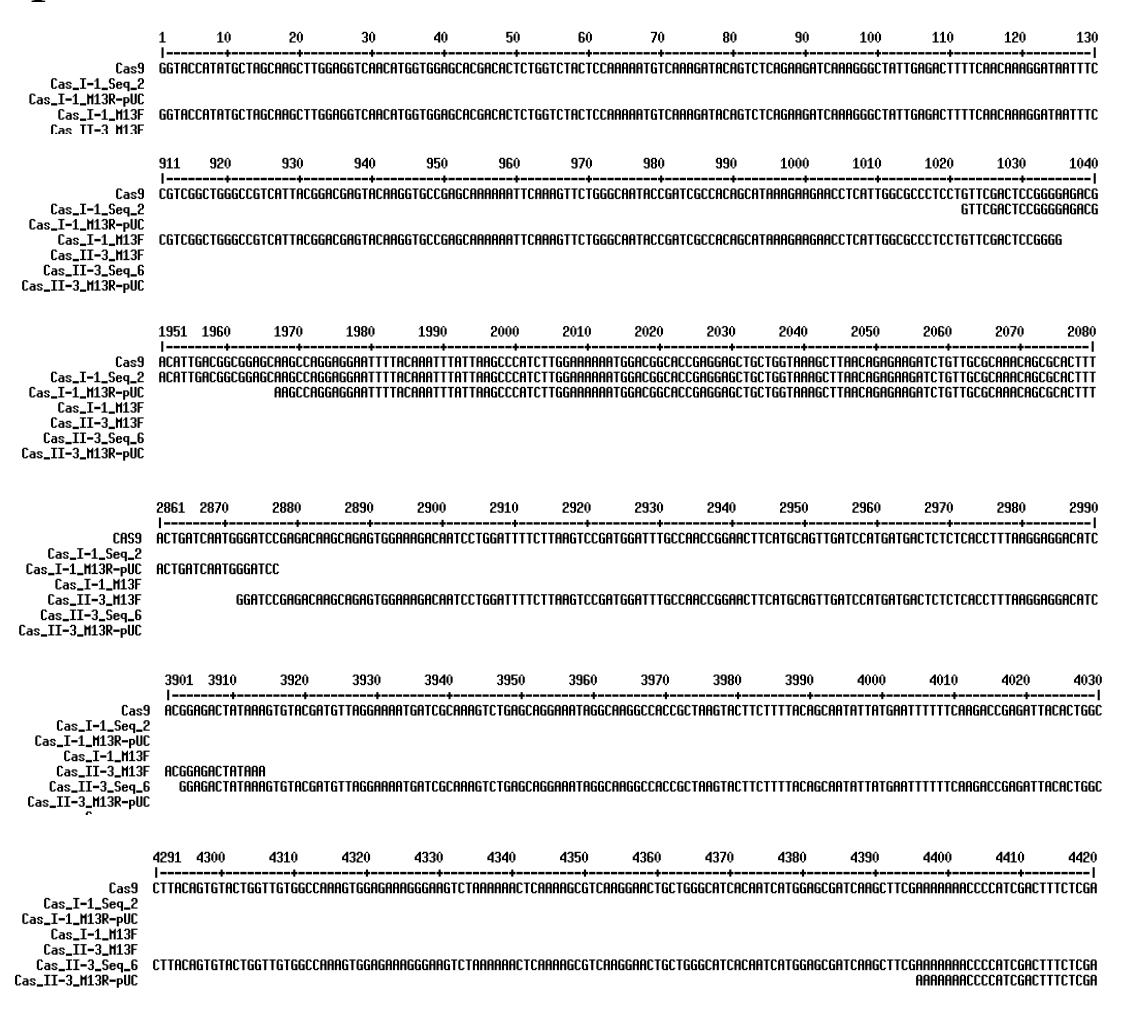
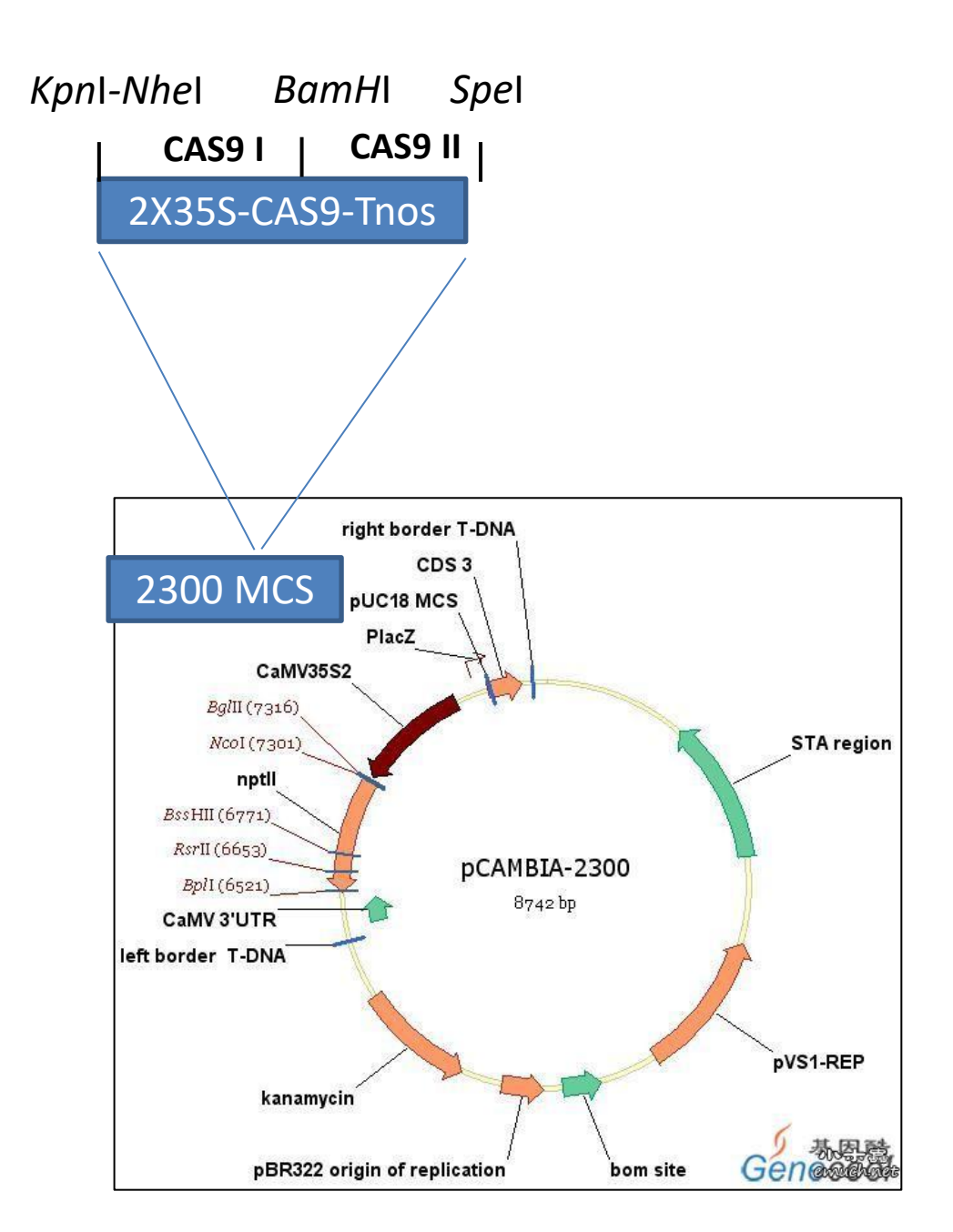
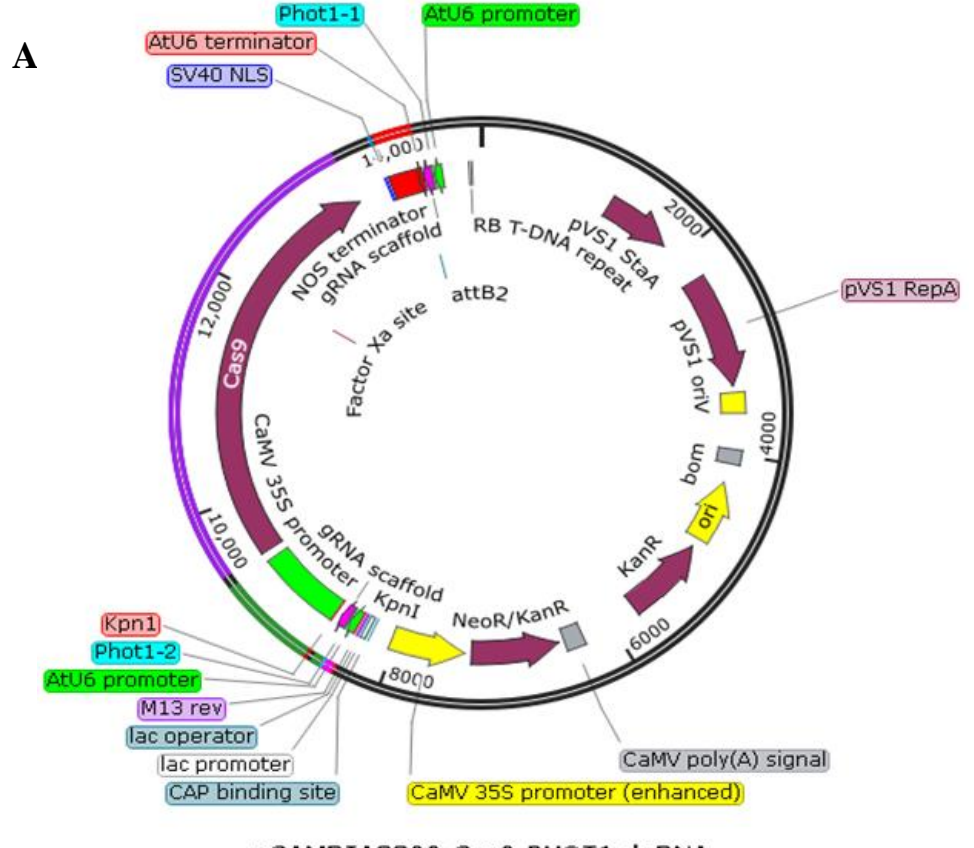


Figure 3.17. F, Confirmation of cloning using sequence alignment.



**Figure 3.18.** Schematic view of the cassette having 2X35S-Cas9-Tnos cloned into the pCAMBIA-2300 vector.



pCAMBIA2300-Cas9-PHOT1.dgRNA 14,432 bp

B

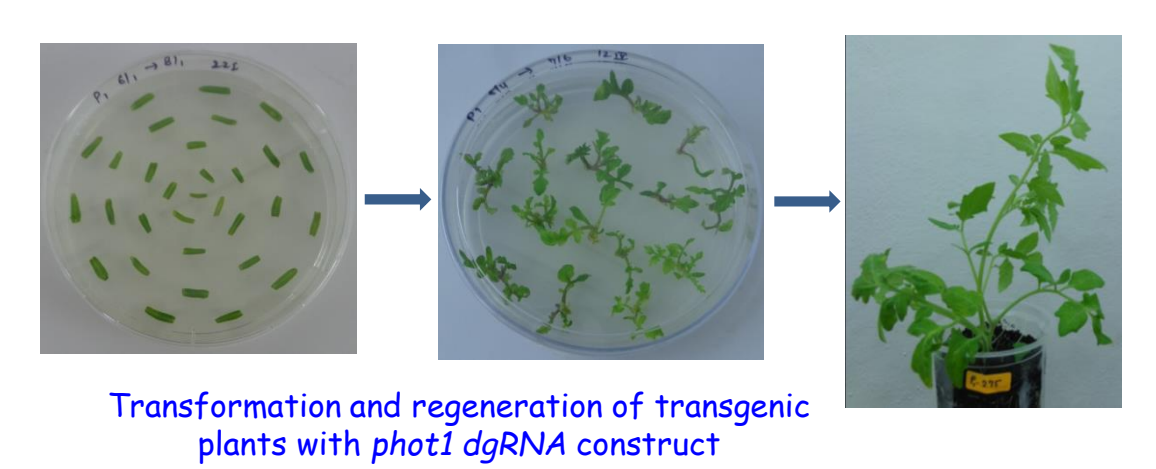


**Figure 3.19. A,** Vector map of *phot1* CRISPR construct. The construct contains Cas9 gene driven by CaMV 35S promoter, flanked by two gRNA cassettes driven by AtU6 promoter to target the Cas9 protein to the respective site in target genome. It also contains kanamycin gene as a selection marker for selection of transgenic lines. **B,** Transformation and regeneration of transgenic plants with *phot1* dgRNA construct.

further amplified to include restriction sites using *Pac*I forward, *Spe*I reverse primers" for *phot1*-sgRNA-1 and *Kpn*I forward, and *Kpn*I reverse primers for *phot1*-sgRNA-2 (Figure 3.14D) and cloned into the pCR8/GW/TOPO vector (Figure 3.15 A). The vectors were checked using restriction digestion and sequencing (Figure 3.15 B and C). Two-way cloning was used to construct the CRISPR/Cas9 gRNA vector, in which first the cassette was cloned into the TOPO-TA vector and then into the pCAMBIA-2300 vector. So, the two gRNAs from the TOPO-TA vector were transferred to pCAMBIA-2300, and the confirmation was done using restriction digestion (Figure 3.16).

As the pCAMBIA-2300 construct lacks the Cas9 for the editing to proceed, we took human codon-optimized Cas9 and 2X35s CaMV promoters (Figure 3.17B) from pAGM4723 (Addgene# 49772) (Figure 3.17 A) using PCR amplification and cloned into the pCR8/GW/TOPO vector (Figure 3.17 C). These vectors are further transformed into E. coli DH5α cells. The cloning was confirmed by performing Cas9-I and Cas9-II specific colony PCR (Figure 3.17 D). Cas9-specific PCR primers were designed by including restriction sites at their ends. Cas9-I primers had KpnI forward, and BamHI reverse sites, and Cas9-II sites were created by including restriction sites like BamHI forward, and SpeI reverse. The Cas9 PCRs resulted in the generation of amplified products of sizes around 2.5 kb. Secondly, restriction digestion (Figure 3.17 E) was used for Cas9 cloning confirmation using KpnI and BamHI for Cas9-I, BamHI, and SpeI for the Cas9-II region. We also confirmed Cas9 presence by Sanger sequencing (Figure 3.17F). 2X35S-Cas9-Tnos was further cloned into pCAMBIA-2300 (Figure 3.18). After sequence confirmation, the gRNA cassettes were further transferred into the pCAMBIA-Cas9 vector (Figure 3.19). The final vector pCAMBIA2300-CAS9-phot1 is shown in Figure 3.19, and the primers are listed in Table 3.3. pCAMBIA2300-CAS9-phot1 vector was transferred into Agrobacterium strain LBA4404 using the freeze-thaw method. The primers used to make the phot1 dgRNA construct are mentioned in Table 3.3

## 3.3.2 Plant genetic transformation using pCAMBIA2300-CAS9-phot1 construct

The transformation of tomato with pCAMBIA2300-CAS9-phot1 construct in *Agrobacterium* strain LBA4404 was done using Van Eck et al. (2019) protocol (Figure 3.19B).

Table:3.3. List of primers used for making CRISPR constructs for *phot1* gene, for sequencing the editing events, and the primers used for detecting off-target effects in the current study.

Name	Primer sequence (5' to 3')	Usage
Phot1-gRNA-1-F	TTAATTAAGGAGTGATCAAAAGTCCCACATCGATCAGG	sgRNA template
	TGATATAGCAGCTTAGTTTATATAATGATAGAGTCGA	for overlap
	CATAGCGATTGAGAAGGTTAATTCGAAGG	extension PCR
	GTTTTAGAGCTAGAAATAGCAAG	
Phot1-gRNA-2-F	GGTACCGGAGTGATCAAAAGTCCCACATCGATCAGGTG	
	ATATATAGCAGCTTAGTTTATATAATGATAGAGTCGAC	
	ATAGCGATTGGAACTCCGACCAGAGTTGC	
	GTTTTAGAGCTAGAAATAGCAAG	
Un-sgRNA-R	GGATCCACTAGTAGCGTAATGCCAACTTTGTACAAGAA	
	AGCTGGTCTAGAAAAAAAGCACCGACTCGGTGCCACTT	
	TTTCAAGTTGATAACGGACTAGCCTTATTTTAACTTGCT	
	ATTTCTAGCTCTAAAAC	
Un-gRNA-PacI-F	TTAATTAAGGAGTGATCAAAAGTCCC	Amplification of
Un-gRNA-SpeI-R	ACTAGTAGCGTAATGCCAAC	phot1-gRNA-1
		cassette
Un-gRNA-KpnI-F	GGTACCGGAGTGATCAAAAGTCCC	Amplification of
Un-gRNA-KpnI-R	GGTACCAGC GTA ATG CCA AC	phot1-gRNA-2
		cassette
CAS9-F	CGTCACAGAAGGGATGAGAAAGC	CAS9
CAS9-R	TGACAACTTCTTCTGAGGGGACG	confirmation
Kan-M	CGATGTTTCGCTTGGTGGTCG	Kanamycin
35S-M	CCATTGCCCAGCTATCTGTCAC	confirmation
SlPh1-F	AGCAAATCG CAATTC CCAAATC	Amplification of
SlPh1-R	CCCCTCTCTTTGCCTGTATTTTTACG	phot1 gene
Ph1-off-1F	GTGCAAAGAAGGTCTAGCATG	Off-target 1
Ph1-off-1R	TGCTCTTAGGCTGAGTTTCC	amplification for
		gRNA-1
Ph1-off-2F	GTTGCTGCATCATTCTCTCC	Off-target 2
Ph1-off-2R	ACCCTCGAGCCAAAACAC	amplification for
		gRNA-1
Ph1-off-3F	CCTTTGGTGGATATTGGAACC	Off-target 3
Ph1-off-3R	AACGAGTGTTCCTAACCCTC	amplification for
		gRNA-1
Ph1-off-4F	CAAAGTCCTTCGAAGATCTGC	Off-target 4
Ph1-off-4R	AGGTCGCTTTATCTCCAGC	amplification for
		gRNA-1
Ph1-off-5F	TGTCCGAGTGTTTGGTCAAG	Off-target 5
Ph1-off-5R	AGCATTGACCAACTCACAAG	amplification for
		gRNA-2
Ph1-off-6F	GAGCATGTTCAAACACTGTTG	Off-target 6
Ph1-off-6R	TGATGTGCAAAGATCAACACC	amplification for
		gRNA-2
Ph1-off-7F	GCCGTAGAAGCTATATGGAGAC	Off-target 7
Ph1-off-7R	CAGGATTAGGGAGTGCCAC	amplification for
		gRNA-2

.

## 3.3.2.1 Seed surface sterilization and germination

The tomato seeds of AV were washed with 5% (v/v) Teepol and then washed with distilled water followed by 4% sodium hypochlorite (v/v) solution for 10 min. seeds were washed again with distilled water and blotted dry on sterile filter paper, placed in a petri dish and transferred to glass bottles containing ½ strength MS medium. About 30 to 40 seeds were kept in each bottle for seed germination. These bottles were kept in the dark for 4-5 days until the hypocotyls emerged and moved to light one day before co-cultivation.

## 3.3.2.2 Explant preparation

The 4-5 days old unopened cotyledons were used as explants for co-cultivation. The cotyledons were carefully cut from the seedlings to avoid injury. Then both the base and tip of the cotyledon were cut and used for co-cultivation.

## 3.3.2.3 Preparation of inoculum for co-cultivation

Agrobacterium tumefaciens strain LBA4404 harboring pCAMBIA2300-CAS9-phot1 construct was used for transformation. The Agrobacterium colony was inoculated into YEM broth containing 25 mg/L rifampicin and 50 mg/L kanamycin and was grown two days before the co-cultivation. This primary culture was used as an inoculum for growing the secondary culture. The culture was grown till it reached 0.5 O.D. The culture was centrifuged at 3000g for 10 minutes at 4°C, then the pellet was washed with ½ MS medium. The pellet was then resuspended in a 2% MSO medium and used for co-cultivation.

#### 3.3.2.4 Co-cultivation

The excised cotyledonary leaves were incubated in bacterial suspension for 20 minutes with intermittent mixing. After drying the explants were placed in petri plates containing a solid KCMS medium, with the adaxial side of the explants facing upwards. The explants were co-cultivated in the dark for two days.

Table :3.4. Composition of YEM broth.

Constituents	Concentration (g/L)
Yeast Extract	1.0
Mannitol	10.0
Dipotassium Phosphate	0.5
Magnesium Sulphate	0.2
Sodium Chloride	0.1

pH-7.0±0.02 at room temperature.

Table: 3.5. Composition of YEM Agar.

Constituents	Concentration (g/L)
Yeast Extract	1.0
Mannitol	10.0
Dipotassium Phosphate	0.5
Magnesium Sulphate	0.2
Sodium Chloride	0.1
Agar	15

pH-7.0±0.02 at room temperature

## 3.3.2.5 Regeneration and selection

The explants were transferred to 2Z media after two days of co-cultivation, which allowed the plants to expand and grow. The explants were sub-cultured three times to 2Z medium once every 15 days, transferred to a 1Z medium for 15 days each. In 1Z medium, the transformed explants begin to form shoots, while non-transformed explants bleach and die.

# 3.3.2.6 Rooting and hardening

The elongated shoots were transferred into rooting media. The rooted plants were transferred to cups containing autoclaved coco-peat. After a few days, these plants were moved into the greenhouse for hardening, and then they were transferred into pots.

Table :3.6. Composition of half-strength Murashige and Skoog (MS) medium.

Constituents	Concentration (mg/L)
--------------	----------------------

Ammonium Nitrate	825
Potassium Nitrate	950
Calcium Chloride	220
Magnesium Sulphate	185
Potassium dihydrogen Phosphate	85
Manganese sulfate	11.15
Boric acid	3.1
Zinc sulphate	4.3
Potassium Iodide	0.415
Sodium Molybdate	0.125
Copper Sulphate	0.015
Ethylene diamine tetra acetate	18.65
Ferrous Sulphate	13.9
Nicotinic acid	0.25
Pyridoxine HCl	0.25
Thiamine HCl	0.5
Glycine	1.0
Myo-inositol	50
Sucrose	15
Agar	4.0

pH-5.8±0.03 at room temperature

Table:3.7. Composition of 2.0% MSO liquid medium.

Constituents	Concentration (Per Litre)
MS salts	4.3 g
Myo-inositol	100 mg
Glycine	2.0 mg
Nicotinic acid	0.5 mg
Pyridoxine HCL	0.5 mg
Thiamine HCL	0.4 mg
Sucrose	20 g

pH-5.6±0.03 at room temperature

Table:3.8. Chemical composition of KCMS (Potassium containing callus inducing Murashige and Skoog) Medium.

Constituents	Concentration
MS salts	4.3 g
Myo-inositol	100 mg
KH <sub>2</sub> PO <sub>4</sub> (1 mg/mL)	200 mg
2,4-D Stock (1 mg/mL)	200 μL
Kinetin stock (1.0 mg/mL)	1.3 mL
Sucrose	30 g
Agar	5.2 g

pH-5.5±0.03 at room temperature.

Table: 3.9. Chemical composition of 2Z medium.

Constituents	Concentration (Per Liter)
MS salts	4.3 g
Myo-inositol	100 mg
Nitsch vitamin stock (1000X)	1.0 mL
Sucrose	20 g
Agar	8 g

pH-6.0±0.03 at room temperature

**Note:** The following filter-sterilized components were added after autoclaving:

Zeatin (2 mg/L), Timentin (300 mg/L), and Kanamycin (100 mg/L).

**Chemical composition of 1Z medium:** The basic recipe was the same as the 2Z medium; however, the final concentration of Zeatin was 1 mg/L, and kanamycin concentration was reduced to 75 mg/L.

Table: 3.10. Chemical composition of rooting medium.

Constituents	Concentration (Per Liter)
MS salts	4.3 g
Nitsch vitamin stock (1000X)	1.0 mL
Sucrose	30 g

Agar 8 g	
----------	--

pH-6.0±0.03 at room temperature

**Note:** The following filter-sterilized components were added after autoclaving- Timentin (300 mg/L) and kanamycin (50 mg/L).

### 3.4 Plant material and growth conditions

The transgenic *phot1* CRISPR plants and wild-type Arka Vikas (AV) and *Nps1* (non-phototropic mutant1) were grown in greenhouses maintained at 25±2°C during the day and 14-18°C at night. Seeds of the Arka Vikas were procured from IIHR (Indian Institute of Horticulture, Bangalore, India). *Nps1* is a *phot1* mutant isolated in the lab described earlier (Sharma et al., 2014). *Nps1* and Arka Vikas were used as controls in the experiments.

### 3.5 DNA isolation

Approximately 100 mg of leaf tissue was taken for DNA extraction by NEATILL PROTOCOL (Sreelakshmi et al., 2010). The mechanical disruption of the tissue was done in a mini-bead beater using steel balls for 1 min 20 sec with preheated extraction buffer consisting of Tris 0.1M Tris-HCl of pH 7.5, 0.05 M EDTA of pH 8.0, 1.25% (w/v) SDS. Additionally, 0.2 M β-mercaptoethanol and a small spatula full of insoluble polyvinylpolypyrrolidone (PVPP) were added. The tubes were incubated at 65°C for 30 min and then brought to room temperature for cooling down. 4 µL of RNAase from 10 mg/mL stock was added to the extract and was incubated at 37°C for half an hour to remove RNA from the extract. 400 μL of cold Ammonium acetate was added to the extract to precipitate proteins. After that, tubes were incubated at 4°C for 15 min subsequently centrifuged for half an hour at 13000 rpm. After centrifugation, the supernatant was collected into another tube that had DNA. The pellet contained the cell debris and precipitated proteins and was discarded. To the collected supernatant equal volume of isopropanol was added and incubated at -20°C for two hours. DNA was pelleted after incubation followed by washing the pellet with 70% (v/v) ethanol twice to remove salts. Pellet was air-dried and then dissolved in 200 µL TE having 10 mM Tris of pH 7.5 and 1 mM EDTA of pH 8.0 supplemented with 3.2 µg/mL RNase. DNA quality was checked using Nanodrop-1000 and quantity using agarose gel 1% (w/v) electrophoresis.

### 3.5.1 Primer design

For designing the primers, Primer3 (<a href="http://bioinfo.ut.ee/primer3-0.4.0">http://bioinfo.ut.ee/primer3-0.4.0</a>" software was used. Many parameters such as primer length, % GC content, avoiding complementary sequences, and secondary structures like hairpin formation were considered during the primer design. The length of the primers was adjusted between 19-25 bp, and the GC content varied between 40-50%. The Tm for the designed primers varied between 50-65°C. The primers were verified using IDT "(<a href="http://eu.idtdna.com/analyzer/applications/oligoanalyser/">http://eu.idtdna.com/analyzer/applications/oligoanalyser/</a>)" and Oligocalc "(<a href="http://www.basic.northwestern.edu/biotools/oligocalc.htmL">http://www.basic.northwestern.edu/biotools/oligocalc.htmL</a>)". NCBI blast was used to verify the primer to check for homology with untargeted sites to avoid non-specific amplification.

## 3.5.2 Agrobacterium tumefaciens and nptII detection in transgenic plant material

PCR was used to identify transformed plants early to check the transformation efficiency of the transgenic plants raised by tissue culture. The PCR product formation using primer pair specific for kanamycin (*nptII* gene), an antibiotic selection marker, indicates the construct presence in the transformed lines. The second primer pair is specific for *chv* gene detection, the Agrobacterium chromosomal virulence gene. PCR product formation with this primer indicates the presence of the Agrobacterium contamination in the transformed lines.

Table: 3.11. List of primers used for screening.

Name of	Forward Primer (5'-3')	Reverse Primer (5'-3')
the gene		
ChvA	CGAAACGCTGTTCGGCCTGTGG	GTTCAGCAGGCCGGCATCCTGG
nptII	TGCTCGACGTTGTCACTGAAGC	AGCAGGCATCGCCATGGGTCAC

### 3.5.3 PCR conditions

PCR reaction mixture contained 1 μL of the template DNA (10 ng), 1X PCR buffer, 2.5 mM MgCl<sub>2</sub>, 0.2 mM dNTPs, 0.1 pmol *nptII* FP, 0.1 pmol *nptII* RP, 0.1 pmol *ChvA* FP, 0.1 pmol *ChvA* RP, 1 U *Taq* polymerase, and MilliQ water to make it 20 μL final volume. The program included an initial denaturing followed by denaturation, annealing, extension step for 40 cycles at 94°C for 40 s, 66°C for 40 s, 72°C for 2 min respectively, and a final extension at 72 °C for 10 min. The samples were analysed on 1.2% agrose gels having 0.5 μgmL<sup>-1</sup> ethidium bromide in 1X Tris-

acetate-EDTA buffer.

# 3.5.4 Analysis of CRISPR/Cas9-induced mutations

The plants were screened for Cas9 and *nptII* genes using PCR. The primers used for PCR are listed in Table 3.12. PCRs for *Cas9* and *nptII* PCRs follow the same steps as mentioned above 3.5.3, except for the change in the annealing temperature as per the specific primer requirement and extension time depending on the product size. So for the Cas9 gene, annealing is at 56°C, and the extension time is 45 s. In the case of *nptII*, annealing is at 56°C, and extension is for 1 min.

The homozygous Cas9 positive and Cas9 negative plants of *phot1* CRISPR alleles were grown in greenhouses along with the wild-type plants PCR confirmation of the editing was done before carrying out the phenotypic characterization of the plants. The primers used for the screening are mentioned in Table 3.12

Table: 3.12. List of primers used for screening.

Primer Name	Gene Name (SOL ID)	Orientatio n	Sequence (5'3')
phot1 exon1	Phototropin 1 (Solyc11g072710.1)	Fp	AGCAAATCGCAATTCCCAAATC
		Rp	CGTAAAAATACAGGCAAAGAGAGGGG
Cas9 Set 1	CRISPR-associated protein 9	Sequence 4	GCTACGCCGGATACATTG
		Reverse I	GGATCCCATTGATCAGTTTTCTTGACAGC
nptII	Kanamycin	Fp	ATGGATTGCACGCAGGTTC
		Rp	CAAGAAGGCGATAGAAGGCG

## 3.5.5 DNA sequencing

To confirm the nature of editing, the PCR products obtained after the gene-

specific amplification targeting the gRNA region of the *phot1* gene were subjected to sequencing. The DNA sequencing was carried out by outsourcing it to Macrogen, Korea.

# 3.5.6 Multialignment

To ascertain the editing in the transformants, DNA sequences obtained after the sequencing analysis were compared with the *phot1* sequence of the wild type by using a multiple alignment tool, multalin (http://multalin.toulousie.inra.fr/multalin/).

### 3.6 RNA isolation

RNA was isolated from the silenced (leaf and red ripe fruit) or edited plants (fruittissue at different ripening stages) to check the gene expression level. RNA was extracted by the TRIZOL method: 100 mg liquid nitrogen frozen sample (leaf/fruit) was collected from the transgenic plants and homogenized. Then samples were centrifuged and supernatant was collected. To the supernantant 0.2 ml of chloroform was added and vortexed vigorously for 15 seconds. Then samples were centrifuged at 12,000g for 15 min at 4°C. The upper phase was transferred to a new tube and RNA was precipitated by adding 0.5 mL of isopropanol and allowed to rest at -20°C for 15 min. The sample was centrifuged and the pellet was washed with 75% alcohol for 5 min at 7,500g at 4°C. The air-dried RNA pellet was dissolved in DEPC-treated water by heating at 55°C for 5 min. Nanodrop measurement and visualization on formaldehyde agarose gel electrophoresis helped estimate RNA concentration and quality.

## 3.6.1 Formaldehyde gel Preparation

1.2% Formaldehyde agarose gel was made with 10X FA (formaldehyde) buffer containing 200 mM MOPS, 50 mM Sodium Acetate, 10 mM of EDTA with pH adjusted to 7 in DEPC treated water. All the samples of RNA were taken in an equal quantity of 1 volume, and four volumes of 5X loading dye (0.4% of saturated bromophenol blue, 1mM EDTA of pH 8, 50% glycerol, 1 mg/mL Ethidium bromide, 720 μL of 37% formaldehyde, 3084 μL of formamide, 4 mL of 10X FA gel buffer, RNAse free water to make it to 10 mL) was added. The RNA and the loading dye were mixed and incubated at 65°C for 3-5 min and chilled on ice. After that, the above mixture was loaded onto a gel for separation at 5-7 Vcm<sup>-1</sup>.

## cDNA synthesis and Real-Time PCR

To remove genomic DNA contamination, 2 µg RNA was treated with DNase (Promega). Using the ABI cDNA synthesis kit (ThermoFisher Scientific, India), 2 µg RNA was converted to cDNA. Ariamax real-time PCR detection system (Agilent) was used in standard mode with Kappa SYBR Green Supermix (Takara, Japan). Melting curve analysis (Ct) was used to analyze the product. The mRNA abundance was analyzed using the relative standard curve with normalization to *SlActin* and *SlUbiquitin*. All primer sequences used for real-time PCR are given in

Table:3.13. List of primers used for real-time PCR.

Name of	Forward Primer (5'-3')	Reverse Primer (5'-3')
the gene		
phot2	TTGGTGGGCTTTAGGAATCTT	ACCGGAATGCTACTAGGAAA
dxs	AAATGGGATCGGTGTAGAGC	TGCTGAGCCATATCCCAATA
psy1	TGAATTAGCACAGGCAGGTC	TCAATTCTGTCACGCCTTTC
psy2	AATTCCGAGGTCTCATACGG	CCTTTCCACATCGAATTCCT
cycb	TCTTCTCAAGAATTTTCCATC	TGGTGGGACTTAGAAAAGAAGG
β-actin	TGTCCCTATTTACGAGGGTTATGC	CAGTTAAATCACGCCAGCAAGAT
Ubiquitin3	GCCGACTACAACATCCAGAAGG	TGCAACACAGCGAGCTTAACC

## 3.7 Monitoring of chloroplast movement in tomato leaflets

Chloroplast movement analysis in tomato plants was monitored indirectly by measuring red light transmittance through the leaf discs placed in microtiter plate wells using a microplate reader as described by Wada and Kong (2011). The time course of change in the leaf transmittance was monitored at different intensities of blue light. Using this assay, since the microplate reader can simultaneously read 96 samples, the chloroplast movement in many samples can be simultaneously monitored. The leaf discs were subjected to blue light (~470 nm wavelength) to detect the chloroplast movement, and transmittance was measured using weak red light (~660 nm wavelength). Briefly, leaf discs of 0.3-0.4 cm in size were punched from the leaves that were dark-adapted overnight under subdued darkness. To protect the leaf discs from dehydration, they were immediately floated in a beaker filled with water till all the discs were punched. After punching, leaf discs were blotted on tissue paper to remove excess water. After that, leaf discs were carefully placed on the 0.5% (w/v) agar filled in a 96-well plate. Eight leaf

discs were taken from each edited/silenced plant and wild- type (control) plants to monitor chloroplast movement. Once all the leaf discs were placed in the 96- well microtiter plate, the plate was placed in the microplate reader (Biotek, Synergy HT), and the transmittance of red light through leaf discs was measured in the dark for the next 30 minutes at an interval of 1 min at 660 nm wavelength.

Subsequently, leaf discs were irradiated with weak blue light (~3.2 µmol/m²/s) for 1 min to initiate the chloroplast accumulation response, followed by transmittance measurement 70 times in case of continuous measurement. Later, leaf discs were irradiated with high-intensity blue light (60- 80 µmol/m²/s) for 2 min to initiate chloroplast avoidance response, followed by transmittance measurement 40 times in continuous measurement (Figure 3.20). *Nps1* and wild-type (pHellsgate/AV) leaves were used as control. The wild-type leaves showed normal accumulation and avoidance response, while the *Nps1* leaf showed no accumulation and little avoidance (Figure 3.20). The machine's internal temperature was maintained at 25°C during the experiment. Numerical analysis was performed using the chart data obtained from the microplate reader.

A three-point chloroplast measurement is a modified version of the above continuous measurement assay. This was used to rapidly screen lines to assess the loss of function. In this modified assay, the first three readings were taken at the end of half an hour incubation in the dark at 25°C. The subsequent three readings were taken after exposing the test sample to continuous low-intensity light (~3.2  $\mu$ mol/m²/s) for 45 min. Then final readings for accumulation were taken three times at 1 min intervals. After this, the plate was exposed to a high-intensity blue light for another 45 min (60-80  $\mu$ mol/m²/s) to measure transmittance for avoidance response.

## 3.7.1 Off-target analysis

A list of 33 potential off-targets was predicted with a minimum of 4 bp mismatches for the target gRNA region using CRISPR-P (<a href="http://cbi.hzau.edu.cn/crispr">http://cbi.hzau.edu.cn/crispr</a>) web tool (Lei et al., 2014; Haeussler et al., 2016) Further "high cutting frequency distribution (CFD) off-target score (Haeussler et al., 2016)" was used to select eight potential off-target sites for each target site. The primers were designed for the off-target sites (Table 3.14). The sites were analyzed by PCR amplification followed by sequencing the amplified product.

**Table: 3.14** Off-target sites for *phot1gRNA1* and *phot1gRNA2* were predicted using CRISPR-P and CRISPOR web tools (<a href="http://crispor.tefor.net">http://crispor.tefor.net</a>). Mismatch nucleotides are marked in green, and the PAM sequence (NGG) is highlighted in yellow.

# sgRNA-1 (GAGAAGGTTAATTCGAAGG<mark>CGG</mark>)

ontarget_mm0_exon_ mRNA:Solyc11g07271 0.2.1_SL3.0ch11_5620 3511	CATGGATGCCAATTGCTCCGGCTTCAACGAAATTGGC TTCTCCGATTACTCAAAAATCAATTACCGGTGG <b>TGAG</b> AAGGTTAATTCGAAGGCGGCAGTGGATGAAGTTGGTG CTGCTGC	CFD Score 1.0
mm4_intergenic_mRN A:Solyc03g044625.1.1  mRNA:Solyc03g04463 0.2.1_SL3.0ch03_1025 5031	TGCCAAAGTCAAAGAGGCCATTGAAAAGAATAATTCA AAGGTGGCCATTCAAAAAAAATCGAGGAAGAAAGGAAG TGTTCTTCAATGCAGGTGATTGGGTGTGAG  >SL3.0ch03 SL3.0ch03:1025480010255257 TTGATGGTTTTTTTGTGCAAAGAAGGTCTAGCATG TATGGACATGAGCTCATAAAGAGAGGTCTAGCATG TATGGACATGAGCTCATAAAGAGAGTTATTTGTCA AAGAGGTTCATAGTGGTGGTTTGATTGGACTCTTT GGGGTGCCAAAAATACTTGATATTCTTAAGGAGCA GTTTCTTTGTCTAGCCATATTGTTGGGAGCCTAGA TGCCAAGAAAAGAGCAAAAGAGATGATGAAAATTC ATGCCAAAGTCAAAGAGGCCATTGAAAAGAATAT TCAAAGGTGGCCATTCAAAAAAAATCGAGGAAGAAA GGAAGTGTTCTTCAATGCAGGTGATTGGGTGTGA GTGCATTTTCGAAAGGAGAGATTCCACAAGTACG AAAAGGGAAACTCAGCCTAAGAGCAGATGAAACCT TCGAAGTACTCAAGATAATTAATGACAATGCTCAC ATGATTGACCTACCAAGTGAGTATAATGTTCATAAT GTT  Ph1-off1-F: GTGCAAAGAAGGTCTAGCATG Ph1-off1-R: TGCTCTTAGGCTGAGTTTCC  PCR product size: 360 bp	0.83
mm4_exon_mRNA:Sol yc08g006870.3.1_SL3. 0ch08_1415680	AGCTGCAGAAATCTTTGAAATTAGTGTCTTTTGTATAGTTAAAAAAAA	0.64

TTCTGCATGTGGGGTTTGTTCAAAGTTGAGTATTTT GTGGTTTAGTGTTAATGGGAGTTTATAAAGGGATT ATGGGTATTGAAATTTTGGTGTTTTTGGCTCGAGGG TCGAGGTGGGGGTGGGAGCAAAAGCAAAATCAAG ATTATGCTCTGTTAGTCTGGTGTT

Ph1-off2-F: GTTGCTGCATCATTCTCTCC Ph1-off2-R: ACCCTCGAGCCAAAACAC

PCR product size: 456 bp

mm4\_intergenic\_mRN A:Solyc03g063320.3.1| mRNA:Solyc03g06334 0.3.1\_SL3.0ch03\_3648 7010

### GAGAAGGTTAATTCGAAGG<mark>CGG</mark>

TCCACACCCTGGTCATCTTTTCATTCAGAACATCTT
CCCTCATTCGAATTAAACTTTCCACAACTAAGTTCTC
AATAGCAGCAAGAATATTAGACTCCGACGACTCGTC
TTGGGAAGGTCTCC

>SL3.0ch03 SL3.0ch03:36486781..36487200
TTGGTGGAGGGCCTTTTTCTAGGTGTATCTTAATC
ACCTTTTCCTTCCCTTTGGTGGATATTTGGAACCATT
CTCTTCTGAAGCATCCACTTGAGTGGACATTATCC
TCATAATTGTTAGTGGAATCGATGAAGAGTAGCCA
CCGATCTCAGGAGTTCGATCAAACATCGGTCGAG
ATCCATCAAGTAAATCTTCCACACCCTGGTCATCT
CTTTCATTCAGAACATCTTCCCTCATTCGAATTAAA
CTTTCCACAACTAAGTTCTCAATAGCAGCAAGAAT
ATTAGACTCCGACGACTTCGTCTTGGGAAGGTCTC
CCTAAAAAAGATGGTCAGAGAGCATCTCAGAACAG
GGACCAGGTTGATATGAGGGTGCTCATCTATTATT
GTAGAAAGAGGAAAAGAGGGTTAGGAACACTCGTT

Ph1-off3-F: CCTTTGGTGGATATTGGAACC Ph1-off3-R: AACGAGTGTTCCTAACCCTC

PCR product size: 373 bp

mm3\_intergenic\_mRN A:Solyc06g016770.3.1| mRNA:Solyc06g01678 0.1.1\_SL3.0ch06\_1354 0421

### GAGAAGGTTAATTCGAAGG<mark>CGG</mark>

TGTGCCCAGGAGTGACAAAAAAGATCCATGAATGTTA
ATGTGTTGCC**TGCGAAGTTTAATACGAAGGAGG**GCAC
GAAGAAAAATGTGAGAATGAATCTTCAAG<u>AACGTTTG</u>
AACCAAAAGTTGACT

>SL3.0ch06 SL3.0ch06:13540200..13540650
TATTGGGAGCATCTTTACATCTTACAAGGAATAAA
GCCAAAGTCCTTCGAAGATCTGCTACTCGTTCCCA
TGATATCGAGTTGAGCATGTCCTCTGCTGGGAAAG
ATGTGAATTCTATCCATGATCCCCGTAAAGGAAGA
GAAAAGCAAGAGCCAAGAGAAGATGGAGTAAATTT
GTGCCCAGGAGTGACAAAAAAGATCCATGAATGTT
AATGTGTTGCCTGCGAAGTTTAATACGAAGGAGG
CACGAAGAAAAAATGTGAGAATGAATCTTCAAGAAC

0.22

0.16

	GTTTGAACCAAAAGTTGACTTTATGAGAGATGCAA GAAAAGGAATACCCCTTCTTGGATTCTGACGTTTC TGATATTTTTGATGAGTTACTAGAGTTAAAGCTCAT TGAGTTGCTGGAGATAAAGCGACCTGATGAAGCT GGTAAAGCTGATGACCCAAATTATTGCAAG  Ph1-off4-F: CAAAGTCCTTCGAAGATCTGC Ph1-off4-R: AGGTCGCTTTATCTCCAGC  PCR product size: 374 bp	
mm4_intergenic_mRN A:Solyc09g055670.1.1  mRNA:Solyc09g05570 0.3.1_SL3.0ch09_4381 3156	GAGAAGGTTAATTCGAAGGCGG  ACATACCGTGGACTTAACTTCCAATTTTTGCAAAATT  TTACAACATCTTTCATAGGTCAGATCATCAAATACAC CATATCACCTACTTCGAATTCAACATCTCACCTTCTA  TTGTCAGCAAACGATTTTGGCT  >SL3.0ch09 SL3.0ch09:4381300043813400 ACCAAAGATAGTTCACTAGGTAGTCTCAACTCATA TGCAACCTCTCCAAAACTTTGCAAAAAACCTCATA GCAACCTCTCCAAAACTTTGCAAAAAACCTCATAG GAACCCACATACCGTGGACTTAACTTCCAATTTT GCAAAATTTTACAACATCTTTCATAGGTCAGATCAT CAAATACACCATATCACCTACTTCGAATTCAACATC TCACCTTCTATTGTCAGCAAACGATTTTGGCTGAC TATAGGCTATTTTCAATCTATCCCTTATCACTCAAA CCTTCTTAAAATCTTCATAGATAATTTTCTGACCAA GAGTGAAGACTCACAAACCTCAAACCATCCAACCG GAGACCTACATATCCAACCATAAAGTCTTCGAATG GATCCACTTAAATGCTTGAATGATAGCTATAATTAT AAGAGAACTC  Ph1-off5-F: CCAAAGATAGTTCACTAGGTAGTCTC Ph1-off2-R: GGATGGTTTGAGGTTTTGTGAG  PCR product size: 313 bp	0.15

# $sgRNA-2 \ ( {\color{red}CCG} {\color{blue}CCG} {\color{blue}GCAACTCTGGTCGGAGTTCC} )$

ntarget_mm0_exon_m RNA:Solyc11g072710. 2.1_SL3.0ch11_56203 684	TGAGACTGGGAAATTGCAAGGAGTTAAAGTTAGA ACTTCTGGAGATGATACGAATGGTAAAACAGAAA CTTCTCGAAGAGATT CCGGCAACTCTGGTCGGAG TTCCGGCGAATTTTCTGATGATGAGGAGCTGGTAAG C	CFD Score 1.0
mm4_intron_mRNA:So lyc10g011985.1.1_SL3 .0ch10_4271015	AGGCATAGAGAAGCCCAAAGGGCCACTTGAGGCA CTTCGGCCAAAGTTGCTGG TATTACATCAATTTC GTTCCATCTCTTTTCGCCT	0.14
	>SL3.0ch10 SL3.0ch10:42707864271200 GAATGTCCGAGTGTTTGGTCAAGTTCTCTG	

	TTTTAAGTAACCCATATTTGTGTTAGGATCATG TGTGTGCTTATTTTGATTCTGCTGATTGGGATC TTGGAAAGGTAGTGGTCCACTTTATAGTCTCA CAATTTTGTTAAGTTGATGCTTATATTATGGTT ATCACGTAACCCTTAATATGGTTCATGATCACA ACAAGGCATAGAGAAGCCCAAAGGGCCACTT GAGGCACTTCGGCCAAAGTTGCTGGTATTACA TCAATTTCGTTCCATCTCTTTTCGCCTAGAGTT GTTTTTGATAACCATTCTTTTGGTCATTCTGCTG CAAATTTGAACCCTTAAAGTACATTGTTTGATA GGTTGTTTTTTCTTGTGAGTTGGTCAATGCTAA AAGACATTAATTCCTCGGTTAAA  Ph1-off6-F: TGTCCGAGTGTTTGGTCAAG Ph1-off6-R: AGCATTGACCAACTCACAAG  PCR product size: 386 bp	
mm4_intron_mRNA:So lyc04g045470.3.1_SL3 .0ch04_33467753	CCGGCAACTCTGGTCGGAGTTCC  AATCCTAGATCTAGCCGCGCGTGAGGGATCTGCG  ACCAGCGATGCTGGTTGGCCTTTGGTCGCTGGAG  GTTGCCAGACCATTAGGTG  >SL3.0ch04  SL3.0ch04:3346752433467981  GAGCATGTTCAAACACTGTTGGAAAACATAG ATATGTCGGAAAATAGCACAACTGTCTGTAGAA AGTGATCAAAATTGGGTACAAAAATATATGGATT GTGTGGAAACCAAAAGGGGTGTTGATGGA ATAATAAAGTTGCCAAAAAACTGATTAGATAG GCTGACACATCACACATCAACACATGGTATTG ATGCAGCTGTTGGAATCCTAGATCTAGCCGCG CGTGAGGGATCTGCGACCAGCGATGCTGGTT GGCCTTTGGTCGCTGGAGGTTGCCAGACCAT TAGGTGGTGTTGATCTTTGCACATCATTGACG ACAGTTGAAATTATGTAAGTCACATCATGAGAA GTCAATAAAAAGACGCATGGATCTACGCTAAT AAATCTGAGGAGTCAATGAAAAATGCACGGT GCTACGCAATTCAGATATGAGAAAGTCACATATGAGAA  Ph1-off7-F: GAGCATGTTTCAAACACTGTTG Ph1-off2-R: TGATGTGCAAAGATCAACACC  PCR product size: 312 bp	0.04
mm4_exon_mRNA:Solyc03 g083440.3.1_SL3.0ch03_54 769089	CCGGCAACTCTGGTCGGA GTTCC  CGTCAGAAGTGATGGAGCGATGTTTCAATGGAACTCC  TAGCAGAGTGGAGGGTGCAACTTTTGAGGCACTTGCC AAAGATGCACTCAATCTGCATGGACTTGCATTTCCAT CACGGGC	0.02
	>SL3.0ch03 SL3.0ch03:5476880054769317	

GAGAAGTGCACCATTTCTGTACATTGGTAGGA TTTGGTGCTGATGCTATCTGCCCTTATTTAGC CGTAGAAGCTATATGGAGACTACAGGTTGATG GAAAAATCCCACCCAAGTCAACCGGTGAGTTT CATTCCAAGGATGAGCTTGTCAAGAAATACTT CAAAGCAAGTCACTATGGCATGATGAAGGTTC TTGCAAAAATGGGCATATCAACATTGGCATCG TACAAGGGTGCTCAGATATTTGAGGCTGTTGG TCTTTCGTCAGAAGTGATGGAGCGATGTTTCA ATGGAACTCCTAGCAGAGTGGAGGGTGCAAC TTTTGAGGCACTTGCCAAAGATGCACTCAATC TGCATGGACTTGCATTTCCATCACGGGCCTTG GCTCCAGGAAGTGCAGAAGCTGTGGCACTCC CTAATCCTGGTGATTATCATTGGAGAAAGGGT GGTGAGATTCACCTTAACGATCCATTTGCCAT TGCAAAATTGCAGGAGGCTGCGCAATCTAATA **GTGTAGCT** 

Ph1-off8-F: GCCGTAGAAGCTATATGGAGAC Ph1-off2-R: CAGGATTAGGGAGTGCCAC

PCR product size: 361 bp

# 3.8 Screening for phototropism in *phot1<sup>CR</sup>* lines

The seeds of *phot1*<sup>CR2</sup>, *phot1*<sup>CR3</sup>, and *phot1*<sup>CR5</sup> lines, AV, and *Nps1* were treated with sodium hypochlorite (4% v/v) for 10 min, followed by a thorough water wash. Then the seeds were germinated on filter paper in germination boxes kept at room temperature under dark conditions. A spectroradiometer (International Light Technologies) was used to measure the emission spectrum of blue light (465 nm). After measuring the light intensity and adjusting to desired intensity with a light meter (Skye Instruments, UK) attached to a quantum sensor, the blue light was used to screen the seedlings. In the darkroom, the seedlings were arranged using green, safe light, and when the seedlings reached a proper height of 2-3 cm, they were transferred to egg trays containing cocopeat and exposed to 0.3 µmol/m²/s intensity of unilateral blue light. The seedlings' position at zero time point and after 16 h of blue light exposure were recorded to see the phototropic response. The seedlings were kept under the white light for another week before being transferred to pots in the greenhouses.

## 3.9.1 Phenotypic characterization of the edited lines

The *phot1*<sup>CR2</sup>, *phot1*<sup>CR3</sup>, and *phot1*<sup>CR5</sup> lines and AV plants were grown in the greenhouse. The difference in the plant height and the internode length between AV

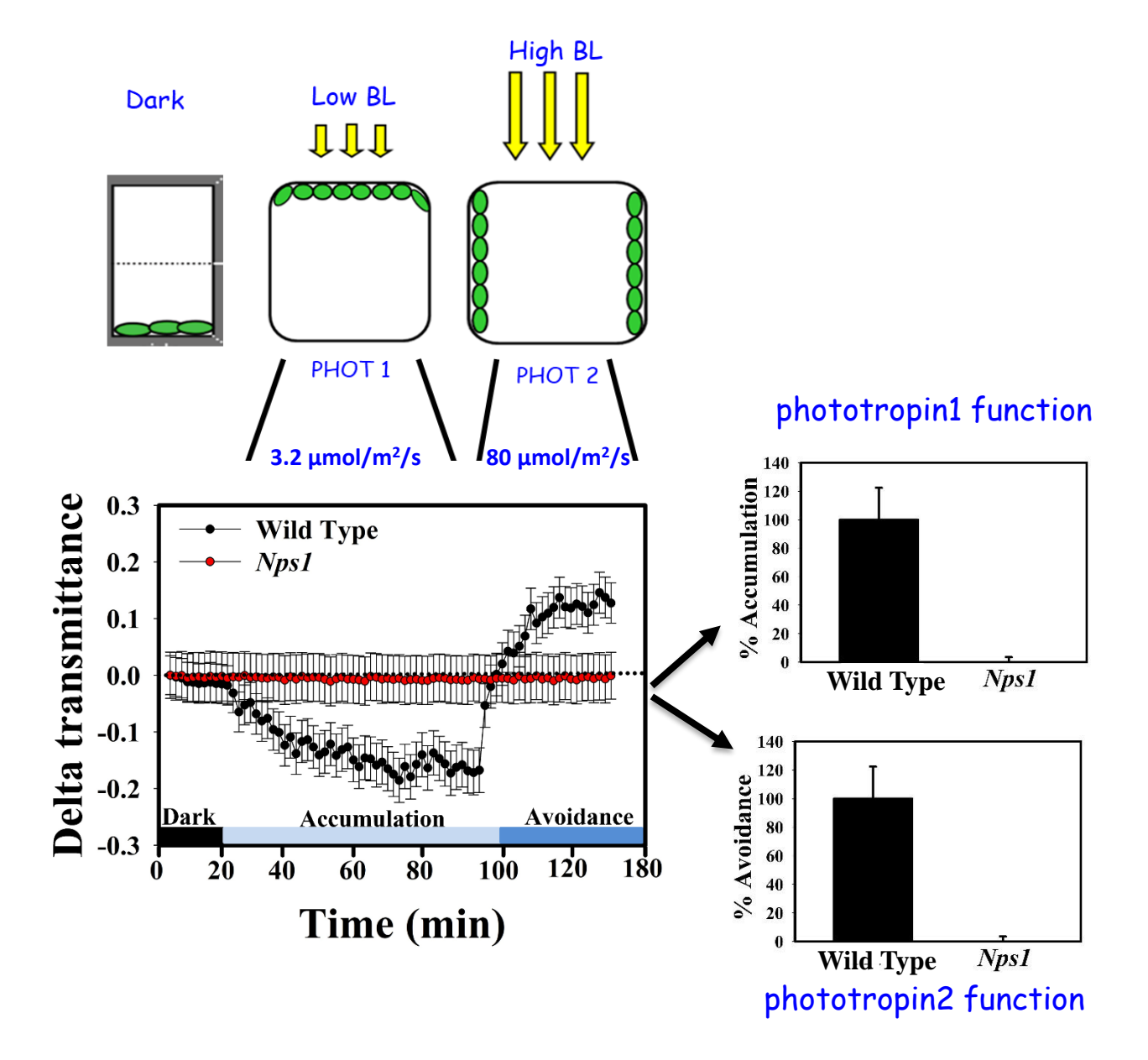


Figure 3.20. Measurement of chloroplast movement in response to blue light in the leaves of wild type and Nps1. Leaf discs from the dark adapted leaves of wild type and Nps1 mutant were collected and placed on the 0.5% (w/v) agar filled in a 96-well plate. Eight leaf discs were taken from Nps1 (shown here) or each edited/silenced plant and wild-type (control) plants to monitor chloroplast movement. Once all the leaf discs were placed in the 96-well microtiter plate, the plate was inserted in the microplate reader (Biotek, Synergy HT), and the transmittance of red light through leaf discs was measured in the dark for the next 30 minutes at an interval of 1 min at 660 nm wavelength. Subsequently, leaf discs were irradiated with weak blue light (~3.2  $\mu$ mol/m²/s) for 1 min to initiate the chloroplast accumulation response, followed by transmittance measurement and this process is repeated 70 times. Later, leaf discs were irradiated with high-intensity blue light (60-80  $\mu$ mol/m²/s) for 2 min to initiate chloroplast avoidance response, followed by transmittance measurement and this is repeated 40 times. While the wild type leaves show normal chloroplast accumulation and avoidance responses, both are hindered in the Nps1

**Figure 3.20** mutant. In the mutant, % accumulation and avoidance were calculated with reference to the wild type. In the case of  $phot1^{CR}$  lines, accumulation response will be affected, indicating loss of phot1 function, while in  $phot2^{RNAi}$  lines, chloroplast avoidance will be affected, signifying loss of phot2 function. Each data point is a representation of the mean value  $\pm$ SE, n=8.

and mutants was recorded using a measuring tape. To monitor the difference in leaf morphology, leaves were collected from the 10<sup>th</sup> node of 60 days-old wild-type and mutant plants and photographed.

## 3.9.2 Chlorophyll estimation

The chlorophyll content in the leaves collected from the 10<sup>th</sup> node of 60 days-old wild-type and mutant plants was estimated using 80% (v/v) acetone, as described by Wellburn (1994). Frozen leaf tissue from the plants was ground using a motor and pestle with liquid nitrogen. A known amount of tissue (50 mg) was weighed. To this, 2 ml of 80% (v/v) acetone was added and stored in darkness overnight. The next day, the samples were centrifuged at 5000 rpm at 4°C for 5 min to collect supernatant. The absorbance was recorded at 663 nm and 645 nm using a UV/VIS spectrophotometer (Perkin Elmer). The chlorophyll a and b amounts were calculated using the following formulae:

Chl a (
$$\mu g/gFW$$
) = (12.25 X A<sub>663</sub> - 2.79 X A<sub>645</sub>)

Chl b (
$$\mu g/gFW$$
) = (21.5 X A<sub>645</sub> – 5.1 X A<sub>663</sub>),

where A is the absorbance at 663 nm and 645 nm.

## 3.9.3 Chronological development of fruits

The flowers from the first and second truss in the wild-type and mutant plants were tagged at the time of anthesis to precisely determine the age of fruits and was considered zero DPA (days post anthesis). Fruits were visually monitored for color changes during ripening to record the transition intervals between MG, BR, and RR stages. The number of days taken for fruit color change was recorded. A minimum of 10 fruits for every ripening stage per allele were monitored, and the data were recorded.

### 3.9.4 Estimation of ethylene

The fruits at different maturity stages were collected from the *phot1*<sup>CR</sup> mutants and AV. The fruits were then incubated in an airtight container at room temperature for 2-4 h to collect ethylene emitted in the headspace. After that, one mL volume of ethylene was collected from the container's headspace and injected into the gas Chromatogram (model GC-17A, Shimadzu, Kyoto, Japan) fitted with an activated "Porapack T" column and flame ionization detector. The amount of

ethylene released from the fruits was calculated by comparing the peak area of the experimental fruit with the standard of 1 mL ethylene injected into the column. For ethylene estimation, three biological replicates were taken for each line at each fruit maturity stage.

## 3.9.5 Estimation of CO<sub>2</sub>

For estimation of  $CO_2$  emission, fruits at different stages were collected from the  $phot1^{CR}$  mutants and AV. The collected fruits were confined in a container connected with a  $CO_2$  sensor (Vernier, OR, USA) for 10 min. Then the  $CO_2$  emission from the fruits was examined using Graphical analysis software.

## 3.9.6 Estimation of sugar content and pH of fruits

The total soluble sugar content of the fruit is measured as °Brix, and this is measured with the help of a "pocket refractometer (ATAGO, Tokyo, Japan)". One unit of °Brix equals 1% (w/v) of total soluble solids (Tieman et al., 1992). To measure °Brix, the whole pericarp of the fruit was ground to make a homogenized paste. This paste was taken into an Eppendorf for centrifugation at 13000g for 15 min to collect the supernatant. From this supernatant, approximately  $200 \, \mu L$  of the homogenate was used for measuring the sugar content. Simultaneously, a pH strip was used to measure the pH of the fruit.

## 3.10. Carotenoids and Xanthophylls profiling from the fruit and leaf tissue

The carotenoids were profiled using the Accela U-HPLC system (Thermo Fischer Scientific, Bremen, Germany). Fifteen different carotenoid standards were used in this study – violaxanthin, neoxanthin, antheraxanthin, lutein, zeaxanthin, phytoene,  $\beta$ -carotene,  $\beta$ -carotene,  $\beta$ -carotene,  $\gamma$ -carotene, neurosporene, and lycopene. For chromatographic separation by HPLC, a YMC polymeric C30 column (250 mm x 4.6 125 mm I.D., 3  $\mu$ m particle size) and YMC guard cartridge (23 mm x 4.0 mm I.D., 3  $\mu$ m particle size) from YMC Co. (Kyoto, Japan) were used.

All the steps of carotenoid extraction were done under dim light. About 150 mg $\pm 10$  mg of powdered tissue (fruit or leaf) was weighed and taken into 2 mL Eppendorf. To this powder, 1000  $\mu$ L of chloroform and 500  $\mu$ L of dichloromethane were added, and the resultant suspension was mixed in thermomixer at 4°C for 20 min. Afterward, 500  $\mu$ L of saturated NaCl was added to the mixture, mixed well,

and centrifuged for 10 minutes at 5000g. The organic phase, which formed the lower phase, was collected with the pipette into a new Eppendorf tube. The aqueous phase was reextracted with 500  $\mu$ L chloroform and 250  $\mu$ L of dichloromethane. The organic phase extract was collected, pooled with the earlier fraction, and dried using Speed Vac. The residue was stored at -80°C till UHPLC analysis. The dried residue was suspended in 1 mL methanol: tert-methyl butyl ether (MeOH: MTBE) (25:75) for red ripe fruit or leaf samples and 200  $\mu$ L for green and breaker fruit samples (Gupta et al., 2014).

Chromatographic separation of carotenoids was carried out on Thermo ACCELA ultra- high performance liquid chromatography (UHPLC) unit with a photodiode array (PDA) detector. Data was collected and analyzed using X-caliber software. The spectra were monitored continuously from the 200-700 nm range throughout the chromatography by maintaining column temperature at 20°C. The retention times of the samples were compared with that of the standards, and the area under the peak was used to quantify individual carotenoids. A minimum of 3-5 biological replicates per sample were used for carotenoid profiling.

# 3.11 Metabolite profiling

The metabolites were extracted using a modified protocol of Rosenner et al. (2000). The fruit tissue from the mutants and wild type was frozen in liquid nitrogen and ground into fine powder. Approximately  $100\pm10$  mg of fruit powder was extracted with  $1.4\,\mu\text{L}$  of 100% methanol, and  $60\,\mu\text{L}$  of ribitol ( $0.2\,\text{mg/mL}$ ) was added as an internal standard. The samples were maintained at  $70^\circ\text{C}$  for 15 minutes before mixing thoroughly with  $1.4\,\mu\text{L}$  of pre-chilled MilliQ water. The contents were centrifuged at 2200g for 10 min at  $4^\circ\text{C}$  in a GL-14 Schott Duran glass vial. The upper phase of  $150\,\mu\text{L}$  was taken in a glass tube and vacuum dried for two hours. The dried pellet was treated with  $80\,\mu\text{L}$  of  $20\,\text{mg/mL}$  o-methoxyamine hydrochloride ( $20\,\text{mg}$  diluted in  $1\,\text{mL}$  pyridine) at  $37^\circ\text{C}$  for  $90\,\text{min}$ , followed by derivatization with  $80\,\mu\text{L}$  of N-methyl-N- (trimethylsilyl) trifluoroacetamide (MSTFA) at  $37^\circ\text{C}$  for  $30\,\text{min}$ .  $100\,\mu\text{L}$  of derivatized samples were transferred to vials, and of this,  $1\,\mu\text{L}$  was injected onto the GC column.

A GC7890A (Agilent Technologies, Palo Alto, CA, USA) detector was used in conjunction with an MS Pegasus 4D with Time of Flight for primary metabolite analysis (LECO Corporation, MI, USA). The GC system utilized a capillary column

(30 m RXi- 5 ms column with a 0.25 mm inner diameter and 0.25 µm) film thickness (LECO, Restek, USA). The following program was used to separate the metabolites: 5 min at 70°C with a 4°C/min linear ramp to 250°C and 5 min at that temperature. The injector and detector were both at a temperature of 280°C. The carrier gas was helium. Ionization energy (EI) of 70 eV, source temperature of 200°C, and a scan range of 50-600 m/z were used for metabolite profiling. To identify the metabolites, the mass spectra were compared to that present in the mass spectral library (NIST 11) of of the National Institute Standards and **Technology** (https://chemdata.nist.gov/mass-spc/ms-search/) as well as the Golm metabolite database (http://gmd.mpimp-golm.mpg.de/). Only those metabolites whose fragmentation pattern and the retention index matched that of standards and those consistently present in the majority of the biological replicates were considered. The data were normalized against ribitol, the internal standard used in the experiment. A minimum of 5-8 biological replicates were used for GC-MS profiling.

### Results

### **Section I**

## 4.1 Silencing of *phot1* and *phot2* genes using RNAi strategy

RNAi strategy was employed to silence both *phot1* and *phot2* genes in tomato. The pHellsgate vector containing the cDNA targeted towards the 3' ends of the *phot1* and *phot2* genes driven by CaMV35S promoter was used for gene silencing. *Agrobacterium tumefaciens* mediated transformation was used for targeting the construct into wild-type tomato (*S. lycoperscicum* cv Arka Vikas) cotyledons. The cotyledons transformed with the *phot1* construct did not regenerate even after multiple attempts, and we could not generate *phot1* gene silenced lines. On the other hand, in the case of *phot2* construct transformed cotyledons, we could regenerate 21 *Slphot2* RNAi lines, which were transferred to the greenhouse (Figure 4.1C, D). The phenotypes of these plants were monitored throughout the life cycle. Out of 21 *phot2* RNAi lines, seven died due to *Tuta absoluta* infection, and three did not set any fruit even after repeated manual pollination. The rest 11 lines were used for further analysis, as mentioned below.

Similarly, four lines were raised with the pHellsgate empty vector; out of these, only one line survived, set fruit, and gave seeds (Figure 4.1A, B). This line was used for further analysis. DNA isolated from *Slphot2* RNAi and pHellsgate lines was used for PCR.

## 4.1.1 PCR-based identification of transgene in $T_0$ lines

To check whether the RNAi cassette for silencing the *phot2* gene got integrated into genomic DNA, a PCR-based screening was carried out using primers specific to the neomycin phosphotransferase (*nptII*) gene. When the genomic DNA of 11 *Slphot2*RNAi lines and one pHellsgate line (empty vector control) was amplified with *nptII* primers, a 353 bp PCR product could be seen on agarose gels in all the lines and positive control (plasmid DNA) except in no template (NT) control and wild type (AV; negative control) plants (Figure 4.2B). This confirms the integration of the RNAi cassette in all the lines.

In addition, during Agrobacterium-mediated transformation, tumor-inducing and chromosomal virulence genes like *chvA* and *chvB* are required to insert a foreign gene into the plant genome. Of these, the *chvA* gene is crucial for crown gall tumor

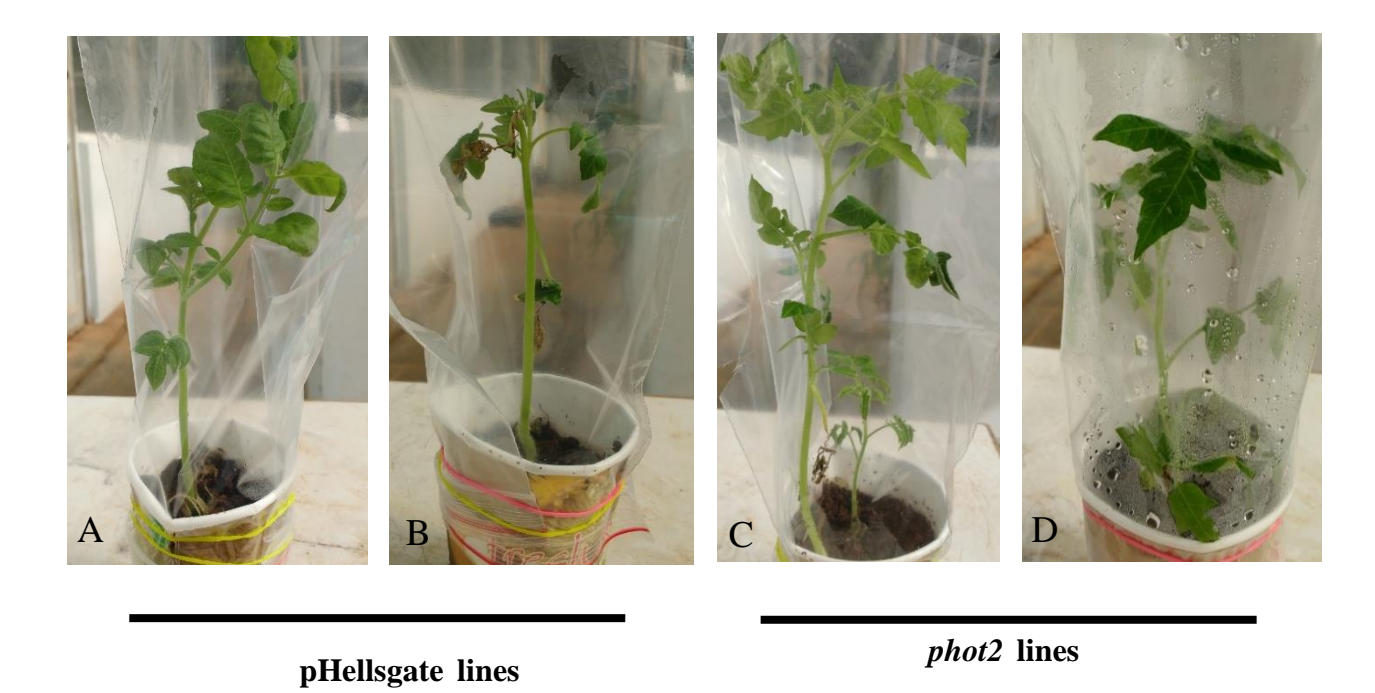


**Figure 4.1. Representative images of the plants transferred to green houses.** A, B represent the pHellsgate lines (empty vector). C, D represent *phot2* RNAi lines

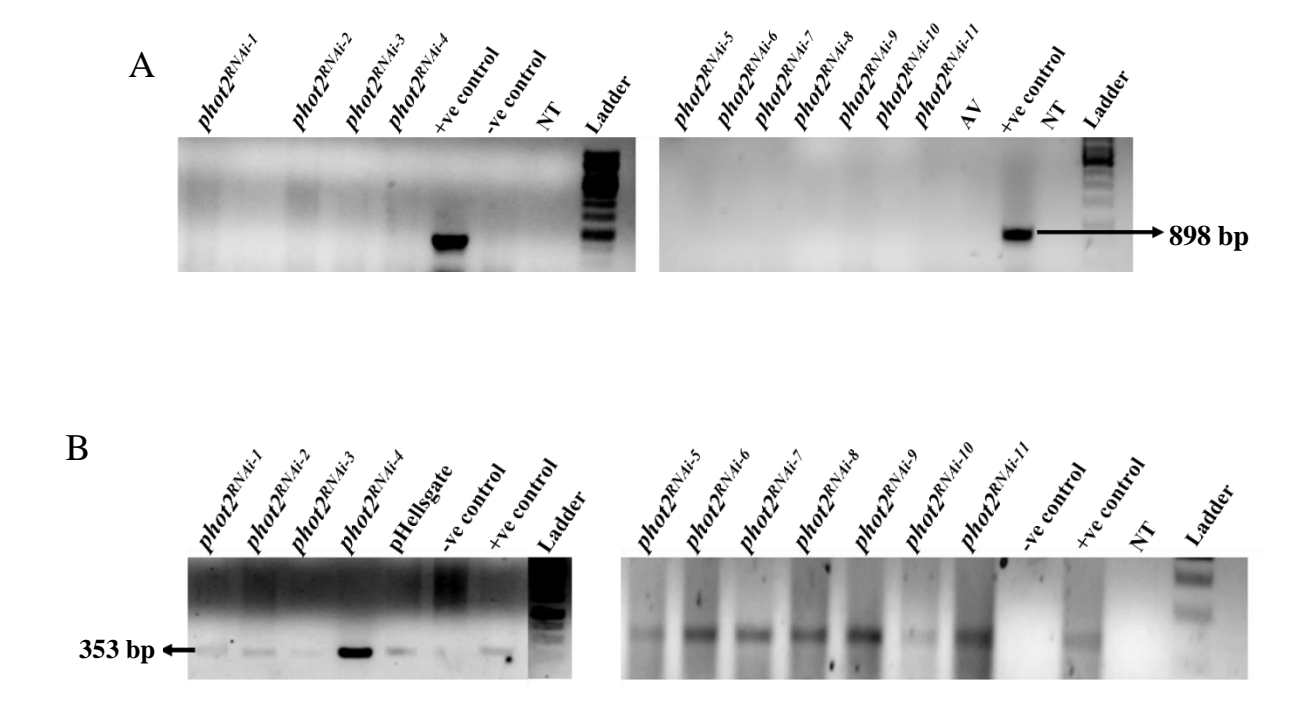


**Figure 4.2. PCR based gene detection in** *Slphot2*  $T_0$  **RNAi lines. A,** Expression analysis of chromosomal virulence gene, *chv* in *phot2*  $T_0$  transgenic lines. PCR primers specific to *Chv* shows amplification of 898 bp product. **B,** Expression analysis of transgene, *nptII* gene in *phot2*  $T_0$  transgenic lines. PCR primers specific to *nptII* shows amplification of 353 bp product in all the transgenic lines.

formation and its residual in plant cells can be easily detected by PCR of *chvA* gene fragment. Amplifying the genomic DNA from 11 *phot2* RNAi and one pHellsgate line using primers specific to the *chvA* gene revealed the presence of 898 bp product only in positive control but not in any of the RNAi lines (Figure 4.2A). This suggests that the transgenic lines do not harbor any residual agrobacterial contamination.

## 4.1.2 Endogenous *phot2* gene expression levels in *phot2 RNAi* lines

As the integration of the transgene in the genome is very random, the expression of the transgene can be widely influenced by the position of integration, the regulatory sequences present in its vicinity, and the copy number of the transgene. Based on this, it is expected that the extent of endogenous *phot2* silencing will not be uniform in all the lines and can vary. Consistent with this, the *phot2* expression analysis using real-time qPCR from the leaf of the RNAi lines revealed variable expression. Of the 11 *phot2 RNAi* lines examined the line numbers. 2, 3, 7 and 11 did not show any silencing, while line numbers 1 (50%), 5 (80%), 6 (87%), 8 (60%), 9 (75%) and 10 (44%) showed significant silencing of *phot2* gene (Figure 4.3, Table 4.1).

### 4.1.3 Phenotypic characterization of *phot2 RNAi* lines

We compared the eleven *phot*2 RNAi T<sub>0</sub> lines with the empty vector control plant (pHellsgate) for any phenotypic changes. Most of the *phot*2 RNAi lines were similar to pHellsgate barring a few exceptions in fruit phenotypes. The *phot*2<sup>RNAi-8</sup> plant showed some fused flowers (Figure 4.4), and most of the fruits of this line were parthenocarpic. Fruits of *phot*2<sup>RNAi-2 & 6</sup> showed ridges, while fruits of *phot*2<sup>RNAi-11</sup> were small and shiny (Figure 4.4). Interestingly, highly silenced lines gave very few seeds, while the moderately silenced lines and lines which showed no silencing gave a good amount of seeds. These phenotypic differences should be analyzed more thoroughly in the subsequent generations, as some of the observed changes could be due to somaclonal variations generated during tissue culture. A tight co-segregation of the genotype % silencing and the phenotype/function must be ascertained before any detailed characterization of the silenced lines is carried out.

## 4.2 Generation of T<sub>1</sub> phot2 RNAi lines

Out of the 11 independent *phot2* RNAi lines, three lines ( $phot2^{RNAi-5}$ ,  $phot2^{RNAi-6}$ , and  $phot2^{RNAi-9}$ ) were selected (Figure 4.5 shows representative pictures

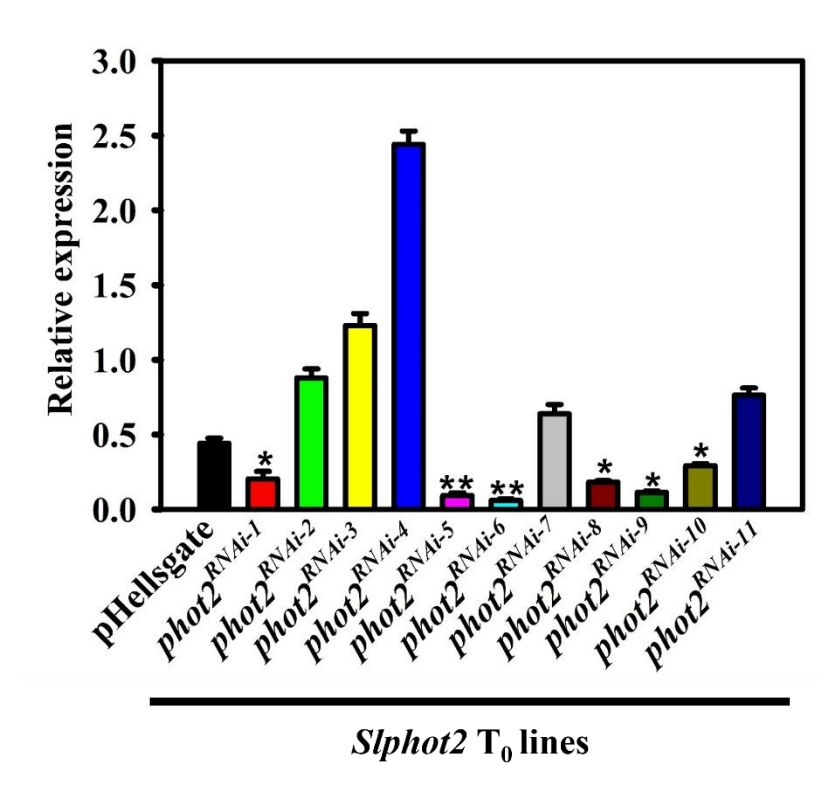


Figure 4.3. Relative expression of *phot*2 gene in phot2 RNAi lines in  $T_0$  generation.

Relative levels of *phot*2 gene expression was determined using qRTPCR with reference to internal controls: actin and ubiquitin genes. Since each transgenic plant is an independent event, the values represent the average of at least three technical replicates  $\pm SE$  taken from same plant. The star mark shows statistically significant reduction in phot2 expression. The statistically significant differences were determined by Student's t-test with  $*P \le 0.05$ ,  $**P \le 0.01$  and  $***P \le 0.001$ .

phot2 RNAi line #	Silencing of <i>phot2</i> expression	Fruit set and seed availability
phot2 <sup>RNAi-1</sup>	50%	yes
phot2 <sup>RNAi-2</sup>	No silencing	yes
phot2 <sup>RNAi-3</sup>	No silencing	yes
phot2 <sup>RNAi-4</sup>	No silencing	yes
phot2 <sup>RNAi-5</sup>	80%	yes, few seeds
phot2 <sup>RNAi-6</sup>	87%	yes, few seeds
phot2 <sup>RNAi-7</sup>	No silencing	yes
phot2 <sup>RNAi-8</sup>	60%	Mostly parthenocarpic very few seeds
phot2 <sup>RNAi-9</sup>	75%	yes, few seeds
phot2 <sup>RNAi-10</sup>	44%	yes
phot2 <sup>RNAi-11</sup>	No silencing	yes

Table 4.1. Details of percentage silencing of phot2 gene, fruit set seed availability in phot2 RNAi lines  $T_0$  generation. Note that highly silenced lines gave very few seeds.

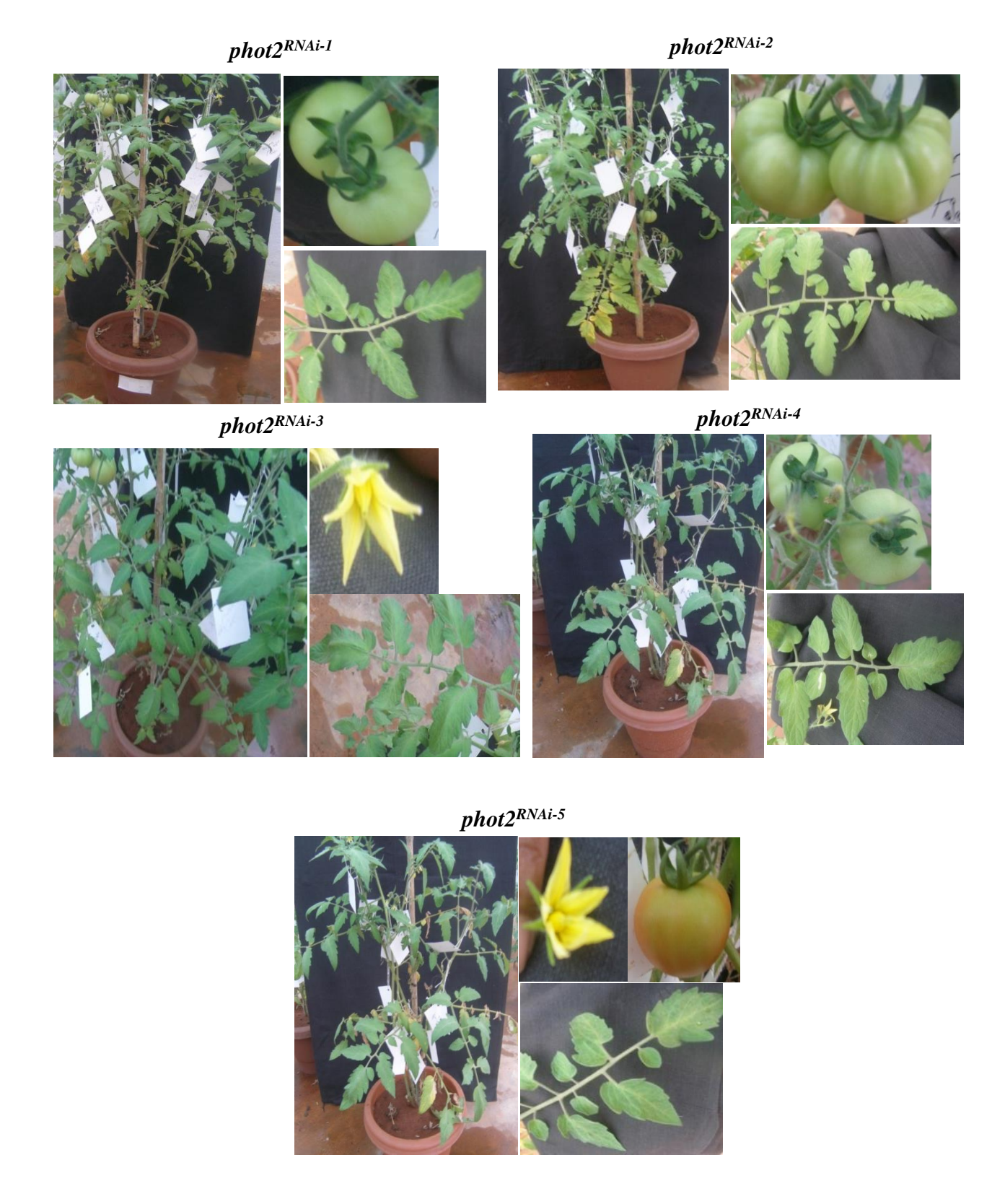


Figure 4.4. Phenotypes of *phot2* silenced in lines in  $T_0$  generation. Representative pictures for whole plant architecture, leaf, flower and fruit were given for each of the transgenic line.

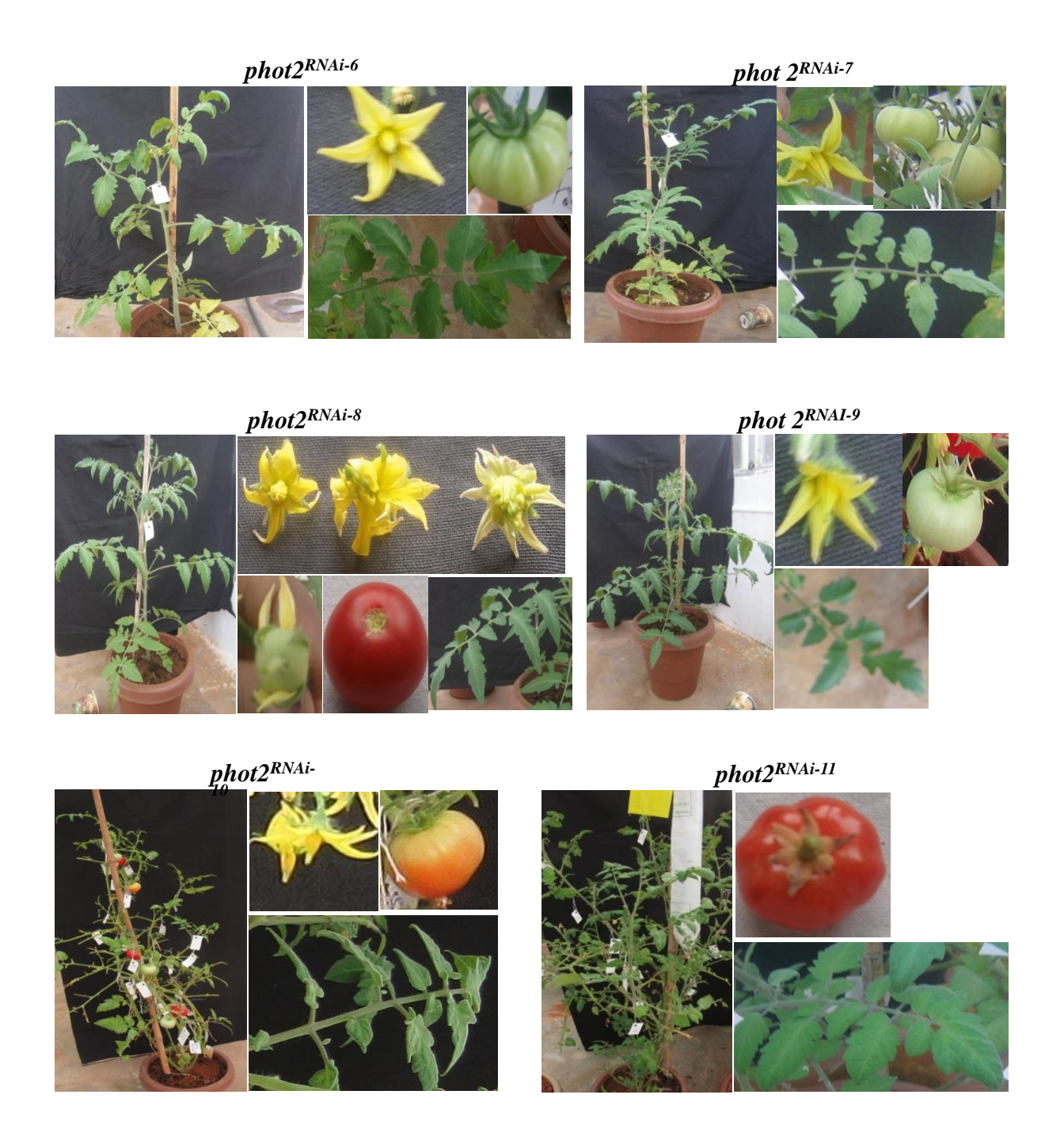


Figure 4.4. Phenotypes of *phot2* silenced lines in  $T_0$  generation. Representative pictures for whole plant architecture, leaf, flower and fruit were given for each of the transgenic line.

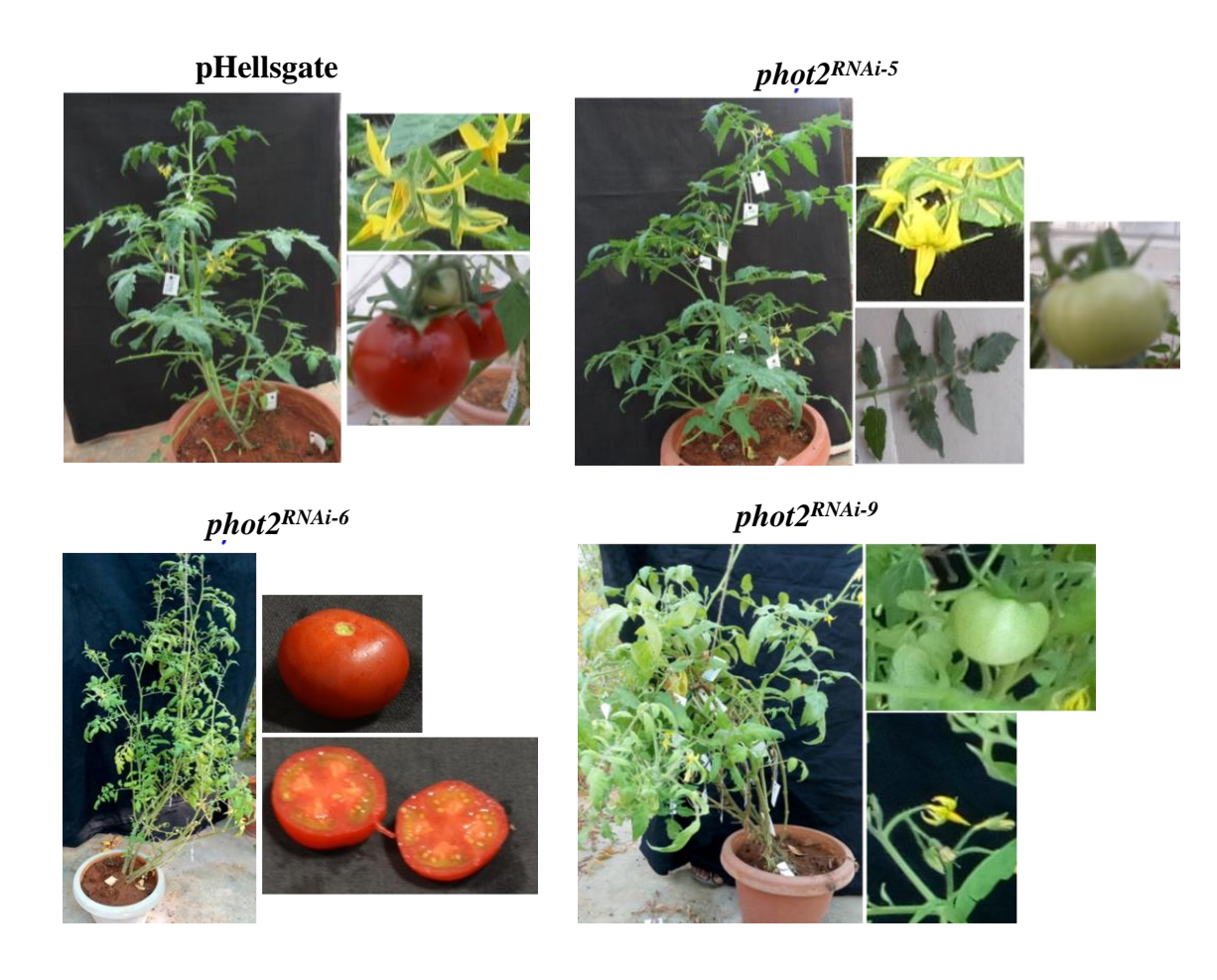


Figure 4.5. Phenotypes of phot2 RNAi lines in  $T_1$  generation. No drastic differences could be seen between these silenced lines and empty vector control, pHellsgate.

from each line) for advancing to  $T_1$  generation for further characterization as they had high silencing of *phot2* gene in  $T_0$ . About 8-10 seeds were germinated per line, and the DNA and RNA were extracted from these plants for further analysis, as described below. These plants were also observed for any noticeable phenotypic differences from the pHellsgate plant in the  $T_1$  generation. In the  $T_1$  generation, no significant phenotypic differences were observed between *phot2* RNAi lines and pHellsgate plants.

### 4.2.1 Analysis of *phot2* gene expression in the T<sub>1</sub> generation

One of the ways to ascertain the silencing of a gene of interest is by monitoring the expression of that endogenous gene. So, when we examined *phot2* expression in the T<sub>1</sub> progeny of *phot2*<sup>RNAi-5</sup>, *phot2*<sup>RNAi-6</sup>, and *phot2*<sup>RNAi-9</sup>, the expression varied between them and the progeny of single lines (Figure 4.6). To elaborate, for *phot2*<sup>RNAi-5</sup> progeny, #2 (65%), #3 (67%), #5 (52%) and #7 (56%) showed significant silencing while the rest did not show any effect (Figure 4.6A). For *phot2*<sup>RNAi-6</sup> progeny, only two plants out of eight showed silencing-#3 (60%) and #7 (90%) (Figure 4.6B). For *phot2*<sup>RNAi-9</sup> progeny, out of 8 plants, only four showed significant silencing- # 4 (50%), #5 (70%), #7 (54%) and #8 (60%) (Figure 4.6C). Such a disparity regarding the expressivity and penetrance of transgene silencing was expected as many studies using RNAi approaches reported a similar behavior earlier (Varsha Wesley et al., 2001; Wang et al., 2005). As we did not observe any noticeable phenotypic changes in the silenced lines, we then proceeded to assess the function of *phot2* in highly silenced lines among the T<sub>1</sub> progeny as that would indicate whether RNAi silencing affected the gene function.

### 4.2.2 Chloroplast movement

Of the different photoreceptors present in plants, phototropins perceive the blue light and help the plants optimize their photosynthetic efficiency and growth. They do this by mediating chloroplast movements in response to low light intensity (chloroplast accumulation) and high light intensity (chloroplast avoidance) (Briggs et al., 2001; Sakai et al., 2001). These characteristic chloroplast movements help plants maximize the light uptake for efficient photosynthesis in low light and protect them from photooxidative damage in high light (Jarillo et al., 2001; Kagawa et al., 2001). While phot1 and phot2 contribute to low light-induced chloroplast

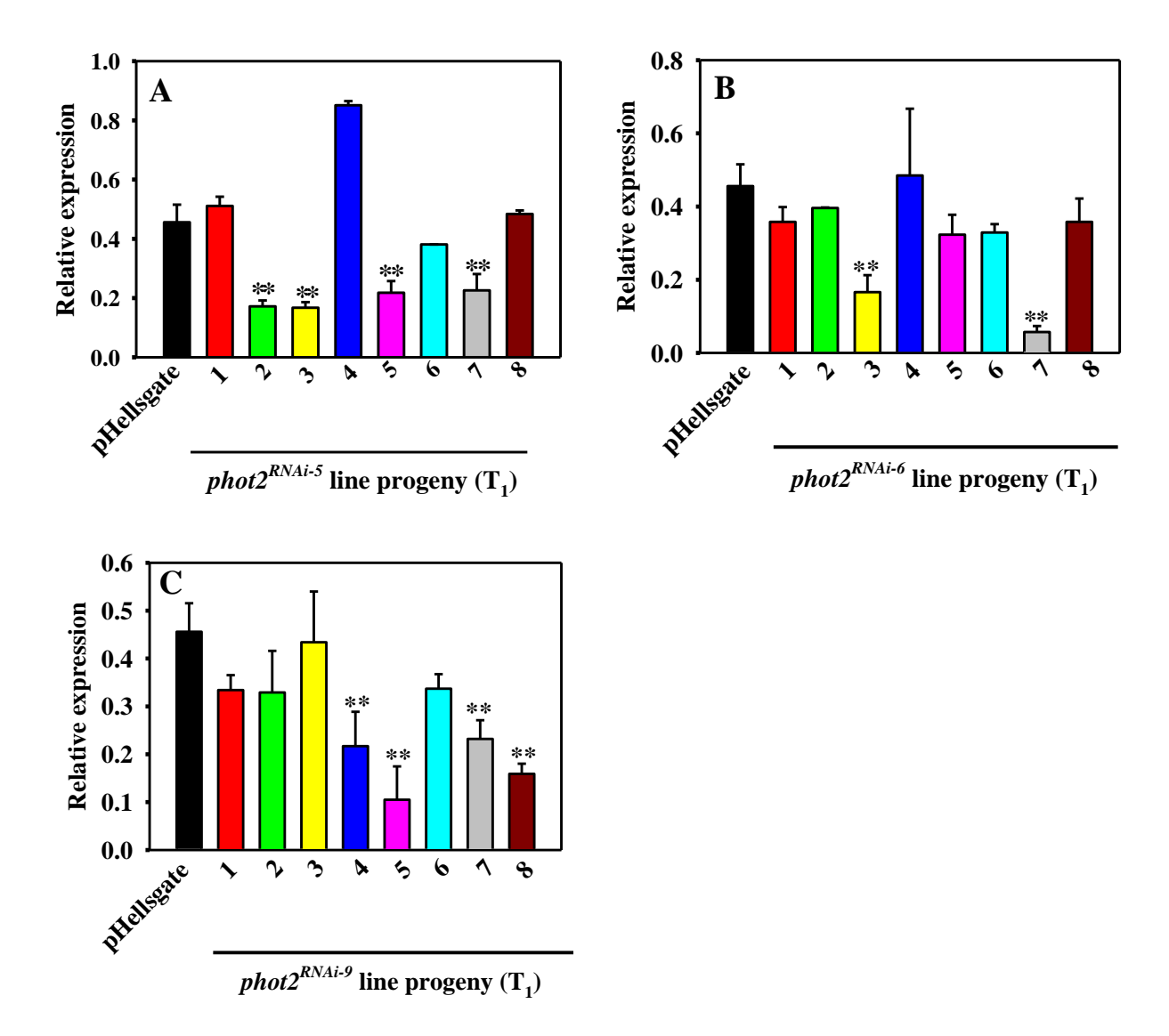


Figure 4.6. Quantitative Real time PCR analysis for measuring endogenous phot2 transcript abundances in phot2 RNAi  $T_1$  lines. A, B and C figures shows phot2 gene expression analysis in  $phot2^{RNAi-5}$ ,  $phot2^{RNAi-6}$  and  $phot2^{RNAi-9}$  RNAi lines. Relative levels of phot2 gene expression was determined by qRT-PCR with reference to internal control genes actin and ubiquitin. The values represent the average of three biological replicates from different progeny of each line  $\pm$  SE. A statistically significant reduction in endogenous phot2 was observed in  $phot2^{RNAi-5}$ ,  $phot2^{RNAi-6}$  and  $phot2^{RNAi-9}$  RNAi lines. Statistical significance was determined by Student's t-test with  $*P \le 0.05$ ,  $**P \le 0.01$  and  $***P \le 0.001$ .

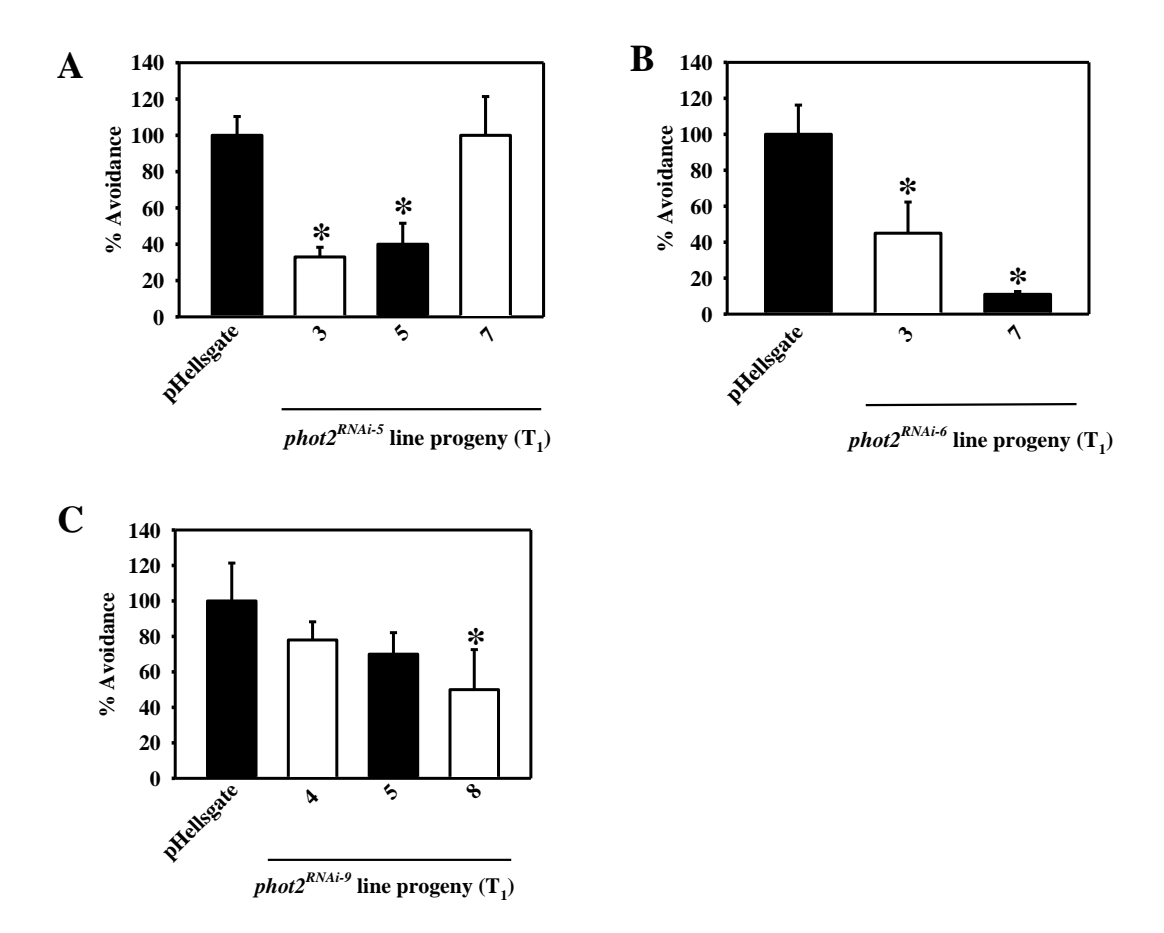


Figure 4.7. % of avoidance of chloroplast movement in leaves of *phot2* RNAi plants in  $T_1$  generation in comparison to pHellsgate under BL pulses. A, B and C figures shows chroroplast analysis in  $phot2^{\text{RNAi-5}}$ ,  $phot2^{\text{RNAi-6}}$  and  $phot2^{\text{RNAi-9}}$  RNAi lines. Dark adapted tomato leaves were placed in 96 well microplate well in the dark, and then red light transmittance was recorded for 20 min (Dark). The leaf was then irradiated sequentially with weak blue light (3.2  $\mu$ mol /m2/s) for 1h 20min for accumulation induction (Accumulation) and strong blue light (60-80  $\mu$ mol /m2/s) for 40 min each for avoidance induction (Avoidance). The blue light was given during the interval periods between red light transmittance measurements. % accumulation and avoidance was calculated with reference to positive control, pHellsgate. Note that chloroplast avoidance response mediated phot2 is affected in the *phot2* RNAi lines, suggesting impaired function of phot2. Each data point is a representation of the mean value  $\pm$ S.E of eight replicates.

accumulation, phot2 specifically plays a role in avoidance responses under high light intensity (Jarillo et al., 2001; Kagawa et al., 2001; Sakai et al., 2001).

Taking advantage of the specific role of phot2 in mediating chloroplast avoidance response under high fluence, we used this assay to assess the loss of phot2 function in the highly silenced phot2 RNAi lines. The red-light transmittance was measured for the dark-adapted leaves of pHellsgate and highly silenced progeny from each of the phot2 RNAi lines for dark measurement. After that, the leaf discs were exposed to low intensity blue light (3.2 µmol/m<sup>2</sup>/s), which induced the chloroplast accumulation response, and reflected in the reduction of red light transmittance. This was followed by high fluence blue light exposure (60-80 μmol/m<sup>2</sup>/s), which triggers chloroplast avoidance response, and the red light transmittance was measured. Based on this assay, the progeny of phot2<sup>RNAi-5</sup>: #3 (33%), #5 (42%), and #7 (100%) showed variable avoidance response compared to 100% avoidance recorded for pHellsgate plant (Figure 4.7A). Similarly, the progeny of phot2<sup>RNAi-6</sup>: #3 (45%) and #7 (11%) phot2<sup>RNAi-9</sup>: # 4 (78%), #5 (70%), and #8 (50%) showed variable chloroplast avoidance compared to pHellsgate control (Figure 4.7 B & C). As the highly silenced lines showed variable loss of phot2 function, the lines which showed a maximal loss of phot2 function were examined for the presence of transgene and other downstream analyses. These lines were also

## 4.2.3 Detection of transgene integration in T<sub>1</sub> generation by PCR

advanced to T<sub>2</sub> generation for further stabilization and characterization.

In the T<sub>1</sub> generation, *phot2*<sup>RNAi-5</sup> #2, *phot2*<sup>RNAi-6</sup> #7, and *phot2*<sup>RNAi-9</sup> #7 were analyzed for the presence of the transgene by using primers specific for the *nptII* gene. In all these lines, PCR product for *nptII* was detected along with pHellsgate (positive control) but was absent in Arka Vikas (negative control) plants suggesting that they were transgenic Figure 4.8B). Since Agrobacterium can survive longer than a year and even in multiple generations in transformed plants (Mogilner et al., 1993; Cubero and Lopez, 2004; Charity and Klimaszewska, 2005), the possibilities of contamination of Agrobacterium DNA with genomic DNA are considerable. So, we checked for Agrobacterium contamination in the above plants using *chvA* primers, and this revealed an absence of Agrobacterium contamination in these plants (Figure 4.8A).

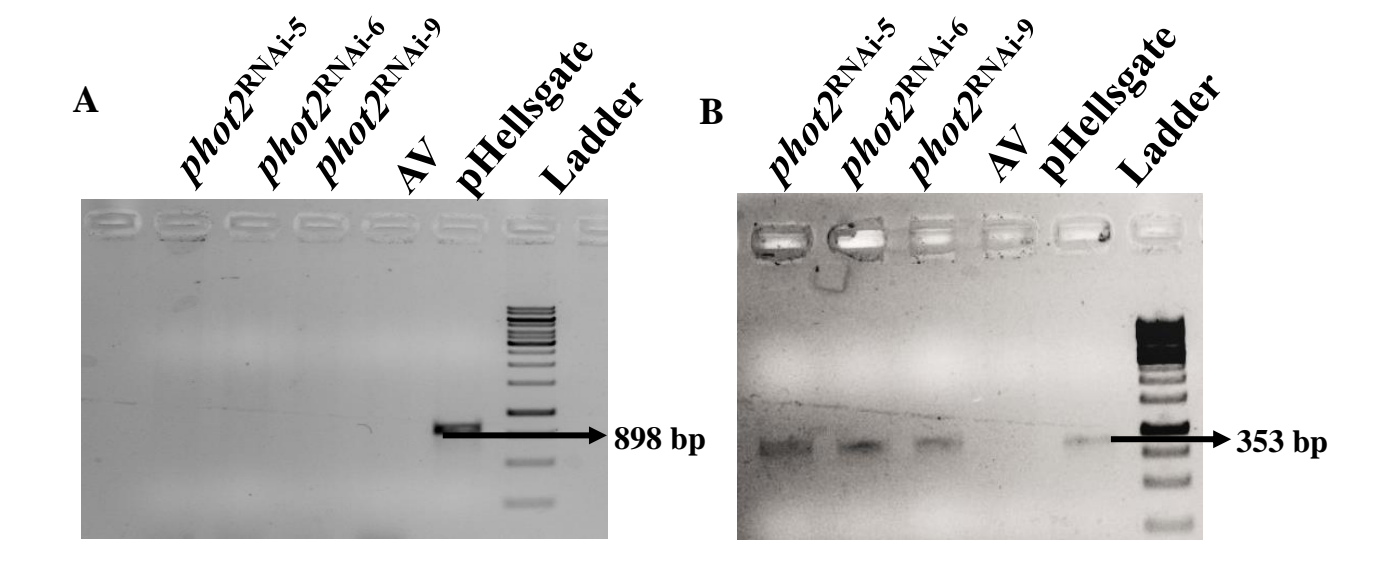


**Figure 4.8. PCR based detection of transgene in** *Slphot2*  $T_1$  **generation RNAi lines. A,** Expression analysis of chromosomal virulence gene, *Chv* in *phot2*  $T_1$  transgenic lines. PCR primers specific to *chv* shows amplification of 898 bp product. **B,** Expression analysis of transgene, *nptII* in *phot2* transgenic lines. PCR primers specific to *nptII* shows amplification of 353 bp product while AV doesn't show any amplification.

#### 4.2.4 Carotenoid levels in T<sub>1</sub> lines

To examine the effect of *phot2* silencing on fruit phenotype, we estimated carotenoid content in the ripe fruits of these plants. In the  $T_1$  generation, the ripe fruits of  $phot2^{RNAi-5}$  and  $phot2^{RNAi-9}$  had similar lycopene levels to that of pHellsgate fruits, while  $phot2^{RNAi-6}$  fruits showed slightly elevated lycopene (Figure 4.9A). The  $\beta$ -carotene levels in all three lines were either lower or equal to that of pHellsgate fruits (Figure 4.9B). As the lines need to be stabilized, this is only preliminary data and indicative. This needs to be confirmed in stabilized lines in future generations.

# 4.2.5 Generation of $T_2$ lines and their evaluation at the phenotypic and functional level

Eight to ten seeds were germinated from each of the lines  $phot2^{RNAi-5}$  - #3;  $phot2^{RNAi-6}$  -#7, and  $phot2^{RNAi-9}$  - #8 as these showed maximal loss of phot2 function and silencing to raise T2generation along with pHellsgate plants. After transferring to the greenhouse, these lines were characterized for any phenotypic variations from the control plants. The phenotypes of most RNAi lines were similar to control plants. In addition, these lines were analyzed for the inheritance of phot2 gene silencing and loss of chloroplast avoidance to confirm the disruption of phot2 gene function in these plants.

#### 4.3 phot2 gene expression in the T<sub>2</sub> RNAi lines

Real-time PCR analysis to assess the *phot2* silencing in  $T_2$  lines revealed segregation of silencing. In the progeny of *phot2*<sup>RNAi-5</sup> - #3, of the eight plants grown, only 50% showed silencing- #2 (40%), #3 (45%), #4 (52%) and #8 (50%) compared to that of pHellsgate. Similarly, in *phot2*<sup>RNAi-6</sup> - #7 progeny, 5 plants showed silencing out of 8 grown – #1 (50%), #4 (65%), #6 (52%), #7 (67%) and #9 (56%). In *phot2*<sup>RNAi-9</sup> - #8 progeny, out of six plants that survived, only 3 plants- #2 (50%), #4 (56%), and #5 (90%) showed silencing. (Figure 4.10). These highly silenced lines were then assessed for loss of *phot2* function as described below.

#### 4.3.1 Time course study of chloroplast movement in the T<sub>2</sub> RNAi lines

In highly silenced  $T_2$  lines, the chloroplast movement was studied under blue light and compared with pHellsgate under three conditions: dark, low-intensity blue light, and high-intensity blue light. Similar to the segregation seen in the case of *phot2* 

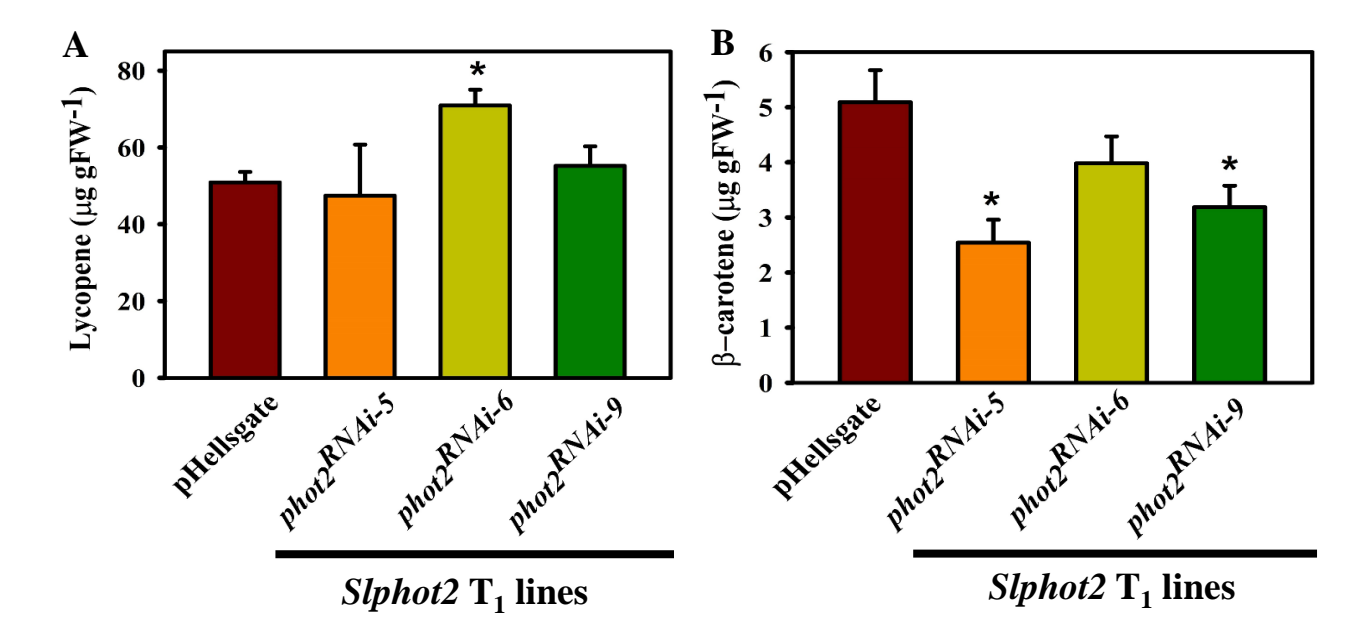


Figure 4.9. Carotenoid profiling in RR fruits of *phot2* RNAi plants in comparison pHellsgate. Figure A shows Lycopene content and B shows  $\beta$ -Carotene content. Carotenoids were extracted from RR fruits of pHellsgate and *phot2* RNAi lines. Data are means of n=5-8±SE, \*P value  $\leq 0.05$ .

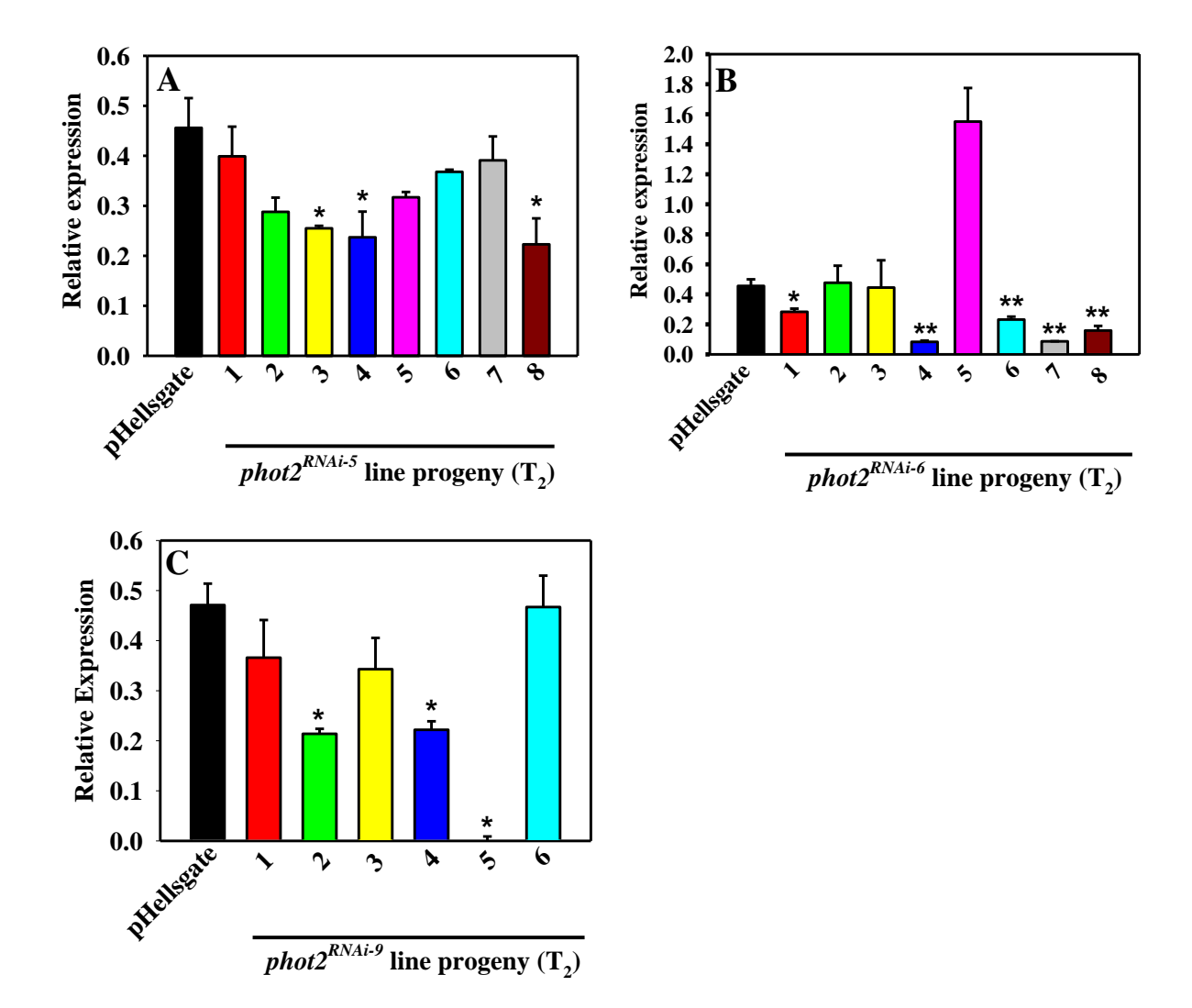


Figure 4.10. Relative expression of *phot2* gene in the *phot2* silenced lines in  $T_2$  generation A, B and C figures shows phot2 gene expression analysis in *phot2*<sup>RNAi-5</sup>, *phot2*<sup>RNAi-6</sup> and *phot2*<sup>RNAi-9</sup> RNAi lines. Relative levels of *phot2* gene expression after normalization with actin and ubiquitin genes was determined by RTPCR. The values represent the average of at least three biological replicates from different progeny of each line  $\pm$  SE. The star mark shows statistically significant reduction in *phot2* expression. The statistically significant differences were determined. Data are means  $\pm$ SE (n=3; \*P  $\leq$  0.05, \*\*P  $\leq$  0.01 and \*\*\*P  $\leq$  0.001).

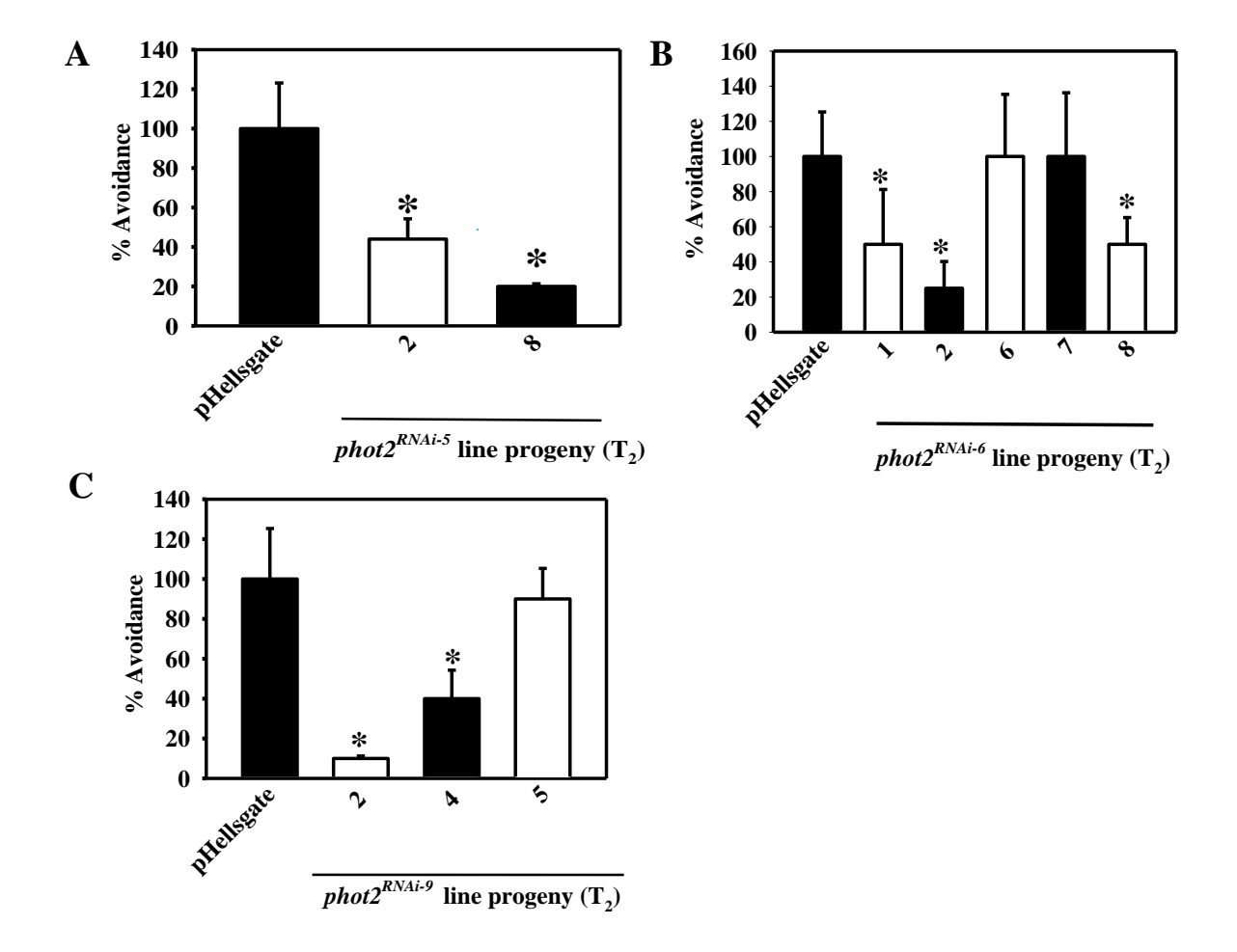


Figure 4.11. % avoidance of chloroplast movement in leaves of phot2 RNAi plants in  $T_2$  generation in comparison to pHellsgate under BL pulses. A, B and C figures shows chroroplast analysis in  $phot2^{RNAi-5}$ ,  $phot2^{RNAi-6}$  and  $phot2^{RNAi-9}$  RNAi lines. Dark adapted tomato leaves were placed in 96 well microplate well in the dark, and then red light transmittance was recorded for 20 min (Dark). The leaf was then irradiated sequentially with weak blue light (3.2  $\mu$ mol /m2/s) for 1h 20 min for accumulation induction (Accumulation) and strong blue light (60-80  $\mu$ mol /m2/s) for 40 min each for avoidance induction (Avoidance). The blue light was given during the interval periods between red light transmittance measurements. % accumulation and avoidance was calculated with reference to positive control, pHellsagte. Note that chloroplast avoidance response mediated phot2 is affected in the phot2 RNAi lines, suggesting impaired function of phot2. Each data point is a representation of the mean value  $\pm$ S.E of eight replicates.

silencing, segregation was observed in the disruption of *phot2* function even in the highly silenced lines (Figure 4.11). In the T<sub>2</sub> progeny of *phot2*<sup>RNAi-5</sup> - #2, plants #4 (44%) and #8 (22%) showed reduced chloroplast avoidance compared to 100% avoidance seen in pHellsgate plants suggesting around 56 and 78% loss of *phot2* function in these lines respectively (Figure 4.11A). Similarly, in *phot2*<sup>RNAi-6</sup> - #7 T<sub>2</sub> progeny, #1, #4 and #8 showed 50%, 75% and 50% loss of *phot2* function respectively, while in *phot2*<sup>RNAi-9</sup> - #7 T<sub>2</sub>progeny, #2, #4, and #5 plants showed 90%, 60% and 10% loss of *phot2* function (Figure 4.11B & C). Interestingly, the loss of chloroplast accumulation response has also been affected in a few lines. This is not unexpected as though *phot1* is mainly responsible for chloroplast accumulation, *phot2* has also been shown to affect this response together with *phot1* under low fluence blue light.

# 4.3.2 Detection of transgene presence by PCR in the T<sub>2</sub> generation

The ge under blue lightnomic DNA from the T<sub>2</sub> *phot2* RNAi transgenic plants exhibiting both *phot2* silencing and maximal loss of *phot2* function was isolated. The presence of *nptII* was examined using PCR employing *nptII*-specific primers. The *nptII* gene amplification in these lines confirmed the transgene presence (Figure 4.12).

#### 4.3.3 Measurement of carotenoid levels in T<sub>2</sub> lines

The lycopene and  $\beta$ -carotene content in the ripe fruits of  $T_2$  RNAi lines was measured and compared with pHellsgate control (Figure 4.13). The  $T_2$  progeny of  $phot2^{RNAi-5}$ -#8 showed similar levels of lycopene to that of pHellsgate fruits but showed a significant reduction in  $\beta$ -carotene content. The fruits of  $phot2^{RNAi-6}$  # 1, # 8 (#4 did not set any fruit), and  $phot2^{RNAi-9}$ #2 showed areduction in both lycopene and  $\beta$ -carotene contents compared to the control (Figure 4.13).

# 4.4 Generation of T<sub>3</sub> lines and their evaluation at the phenotypic and functional level

Three T<sub>2</sub> lines that showed a significant reduction in *phot2* expression and maximal loss of *phot2* function and gave seeds were taken forward to the next generation, T<sub>3</sub>. Eight seeds were sowed from the lines, *phot2*<sup>RNAi-5</sup>-#8, *phot2*<sup>RNAi-6</sup>-#1 and *phot2*<sup>RNAi-9</sup>-#2 and control, pHellsgate. After transferring to the greenhouse, these lines were characterized for any phenotypic variations that were considerably different from the control plants. No significant alterations in phenotype or

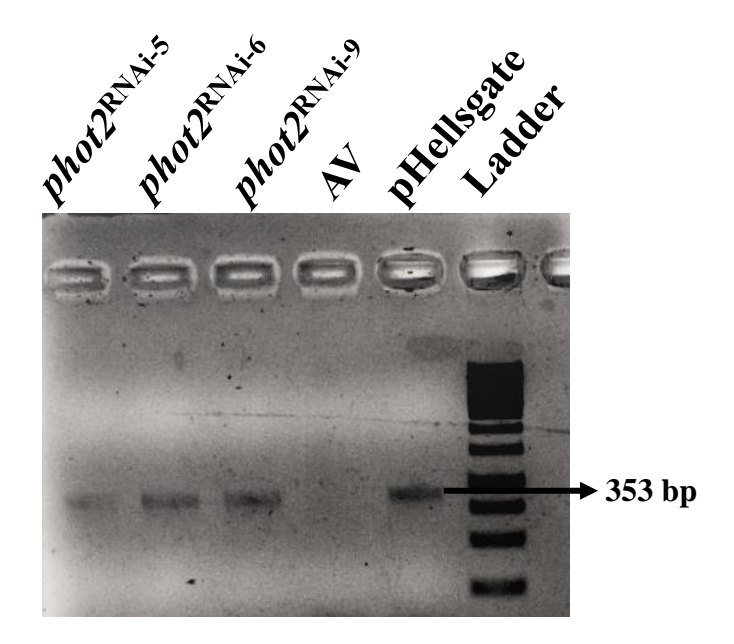


Figure 4.12. PCR based detection of *nptII* in *Slphot2* RNAi lines in  $T_2$  generation. Expression analysis of *nptII* gene in *phot2*  $T_2$  transgenic lines. PCR primers specific to *nptII* shows amplification of 353 bp product in RNAi lines but not in AV.

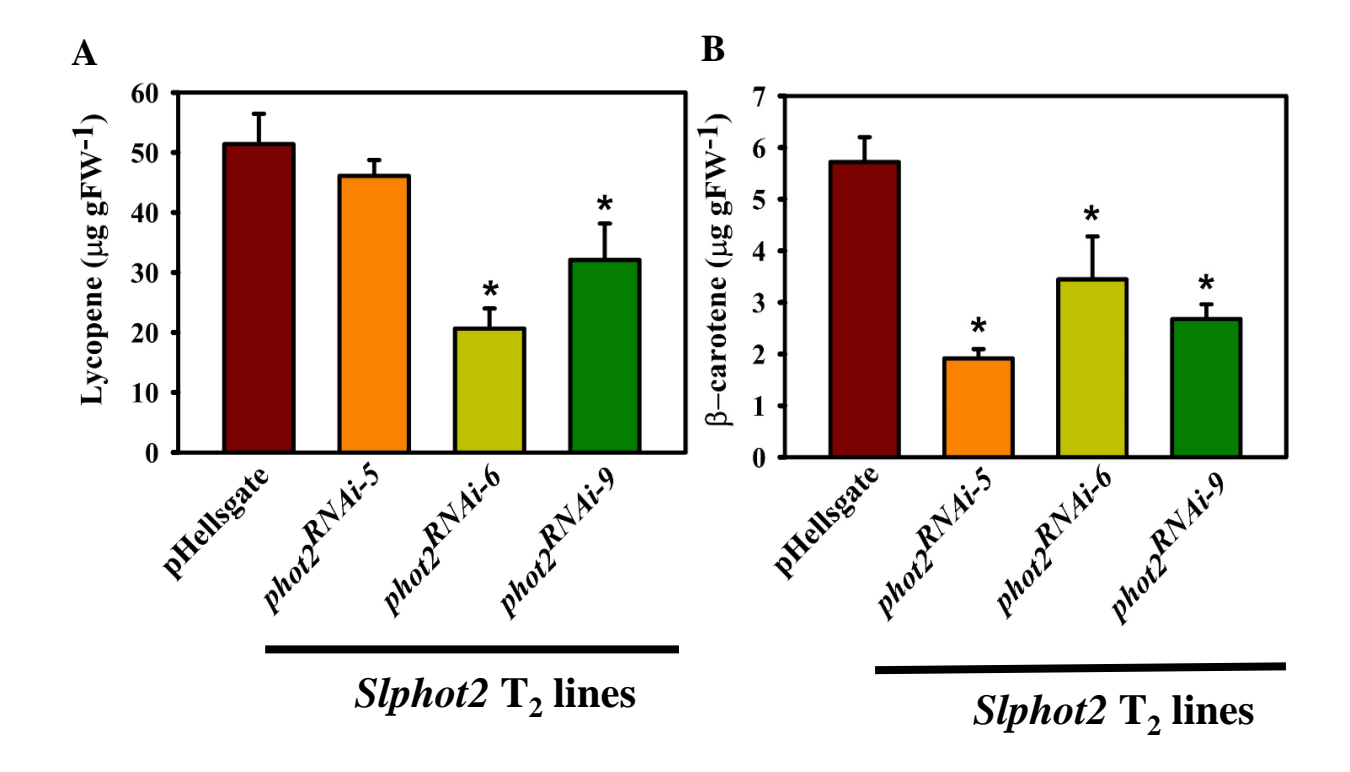


Figure 4.13. Carotenoid profiling in RR fruits of *phot2* RNAi plants in comparison pHellsgate. Figure A shows Lycopene content and B shows  $\beta$ -Carotene content. Carotenoids were extracted from RR fruits of pHellsgate and *phot2* RNAi lines. Data are means of n=5-8±SE, \*P value  $\leq 0.05$ .



Figure 4.14. Phenotype of phot2 RNAi lines in  $T_3$  generation. Representative images are shown here.

development were observed when these three *phot2* transgenic lines were compared to control pHellsgate lines. Even though these lines had low levels of *phot2* expression, the plants had a normal phenotype (Figure 4.14).

#### 4.4.1 phot2 gene expression in the T<sub>3</sub> RNAi lines

To assess the level of silencing in the T<sub>3</sub> RNAi lines, the transcript abundances of *phot2* were measured. Though the transcript levels were variable between the T<sub>3</sub> lines, a majority of the progeny of the three T<sub>3</sub> lines showed a significant reduction in *phot2* gene expression compared to the control, pHellsgate. The percentage decrease in *phot2* transcript levels in *phot2*<sup>RNAi-5</sup> progeny varied between 45-80%, with most lines showing a 75% reduction in *phot2* expression compared to control (Figure 4.15A). However, in *phot2*<sup>RNAi-6</sup> progeny, of the eight lines, five lines showed significant *phot2* silencing, which varied between 40-80% (Figure 4.15B). In *phot2*<sup>RNAi-9</sup> progeny, of the ten plants, six showed a substantial reduction in *phot2* expression, which varied between 40-66% (Figure 4.15C).

### 4.4.2 Time course study of chloroplast movement in the T<sub>3</sub> lines

In  $T_3$  lines, the blue light-induced chloroplast movement was studied under same conditions as in  $T_2$ . All the  $T_3$  progeny of the 3 RNAi lines showed a significant reduction in *phot2* function, given that the chloroplast avoidance response was impaired compared to control (Figure 4.16).

#### 4.4.3 Detection of transgene integration by PCR in the T<sub>3</sub> generation

T<sub>3</sub> generation plants were analyzed for transgene presence, as in the previous generation using *nptII* primers. All the progeny germinated in the T<sub>3</sub> generation were kanamycin positive. A representative image with the *nptII* amplicon in the lines showing maximal silencing and loss of *phot2* function is given in Figure 4.17.

# 4.4.4 Study of fruit development and ripening in phot2 RNAi lines

Given that different photoreceptors influence fruit ripening and pigmentation, it was interesting to examine the influence of *phot2* on fruit development and ripening. Flowers from T<sub>3</sub> generation plants were tagged at the anthesis, and the fruit developmental stages were monitored. The color transition between different ripening stages was visually observed during the on-vine ripening and recorded. Compared to pHellsgate, *phot2*<sup>RNAi-6</sup> and *phot2*<sup>RNAi-9</sup> lines required a longer duration to attain the mature green stage (MG), while *phot2*<sup>RNAi-5</sup> fruits

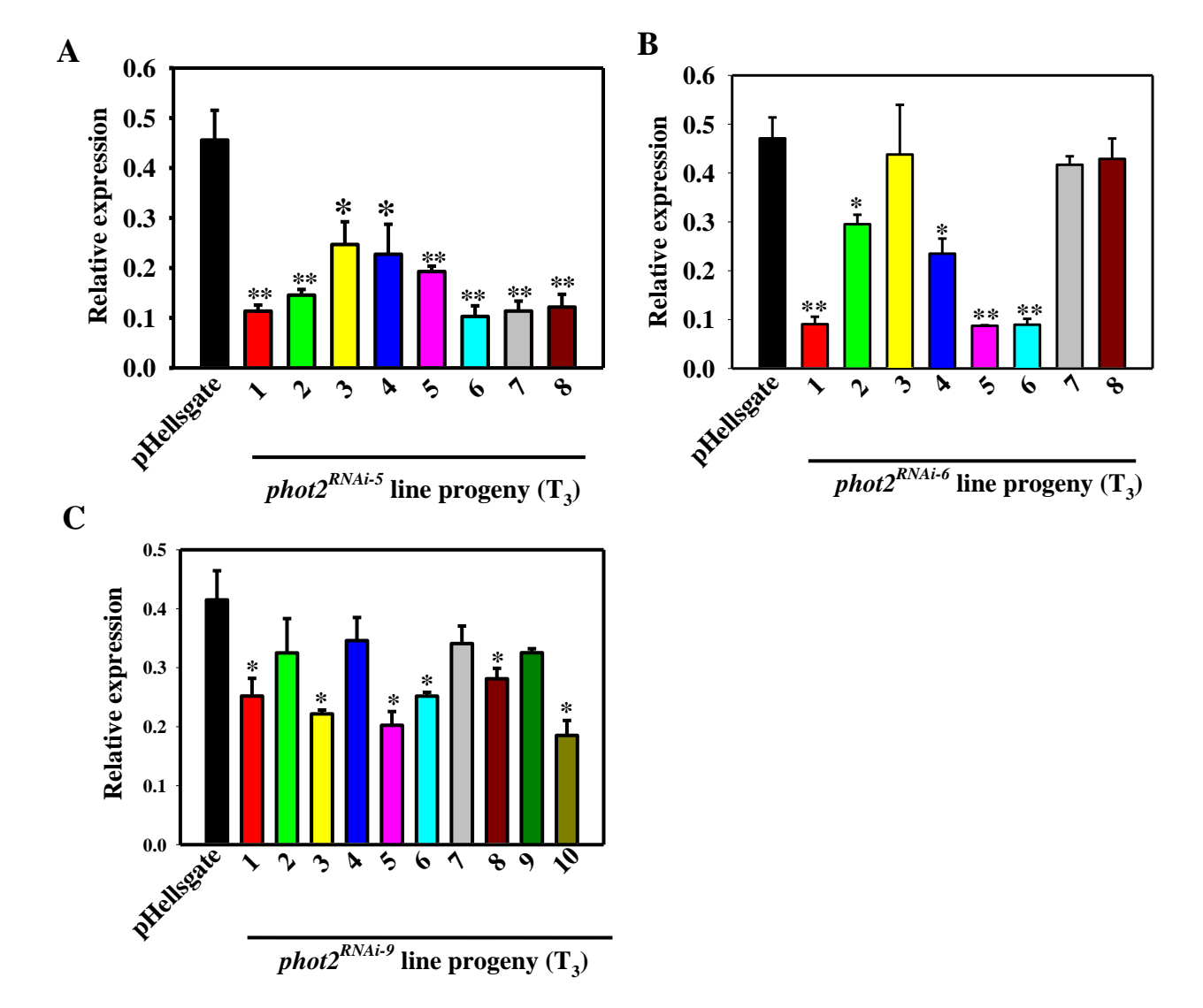


Figure 4.15. Relative expression of *phot*2 gene.

A, B and C figures shows phot2 gene expression analysis in  $phot2^{RNAi-5}$ ,  $phot2^{RNAi-6}$  and  $phot2^{RNAi-9}$  RNAi lines. Relative levels of phot2 gene expression was determined by RTPCR. Since each transgenic plant is an independent event, the values represent the average of at least three biological replicates from different progeny of each line  $\pm$  SE. The star mark shows statistically significant reduction in  $phot2^{RNAi-5}$ ,  $phot2^{RNAi-6}$  and  $phot2^{RNAi-9}$  RNAi lines. The statistically significant differences were determined by Student's t-test with  $*P \le 0.05$ ,  $**P \le 0.01$  and  $***P \le 0.001$ .

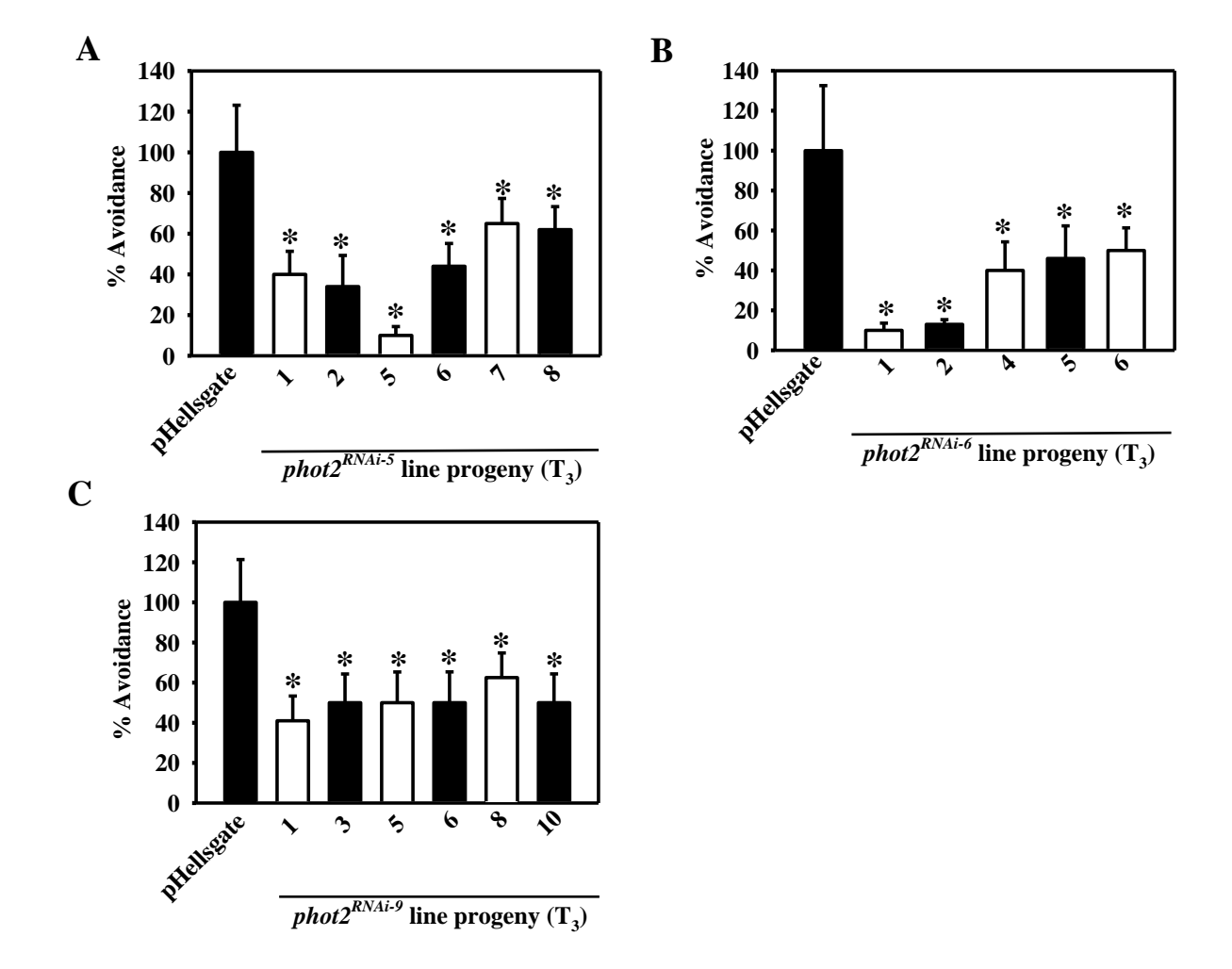


Figure 4.16. % avoidance of chloroplast movement in leaves of *phot2* RNAi plants in  $T_3$  generation in comparison to pHellsgate under BL pulses. A, B and C figures shows chroroplast analysis in  $phot2^{RNAi-5}$ ,  $phot2^{RNAi-6}$  and  $phot2^{RNAi-9}$  RNAi lines. The leaves were placed in 96 well microplate well in the dark, and then red light transmittance was recorded for 30 min (Dark). The leaf was then irradiated sequentially with weak blue light (3.2  $\mu$ mol/m²/s) for 45 min for accumulation induction (Accumulation) and strong blue light (60-80  $\mu$ mol/m²/s) for 45 min each for avoidance induction (Avoidance). The blue light was given during the interval periods between red light transmittance measurements. Note that chloroplast avoidance response mediated phot2 is affected in the phot2 RNAi lines, suggesting impaired function of phot2. Each data point is a representation of the mean value  $\pm$  S.E of eight replicates.

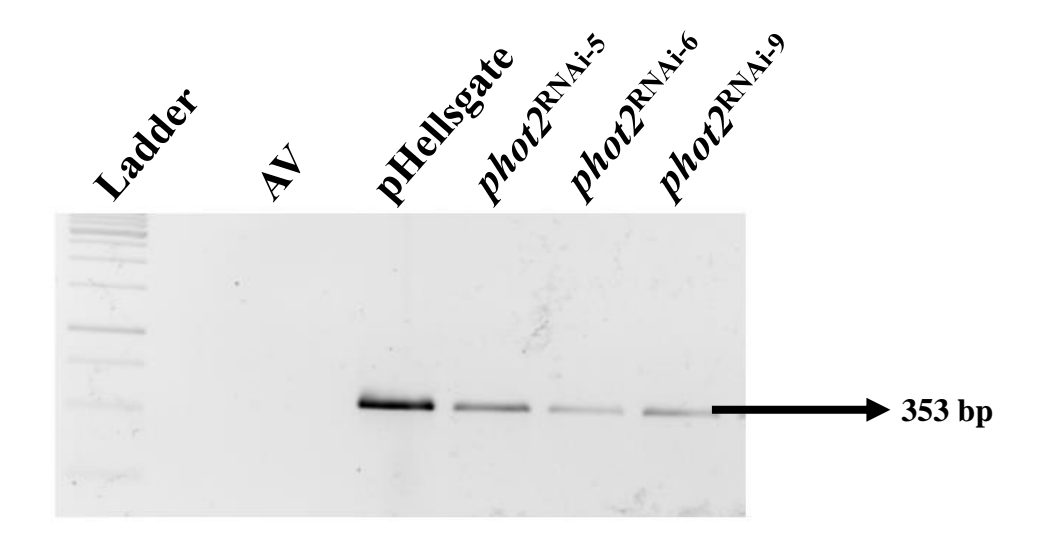


Figure 4.17. PCR based detection of *nptII* in *Slphot2* RNAi lines in  $T_3$  generation. Expression analysis of *nptII* gene in *phot2*  $T_3$  transgenic lines. PCR primers specific to *nptII* shows amplification of 353 bp product in RNAi lines but not in AV.

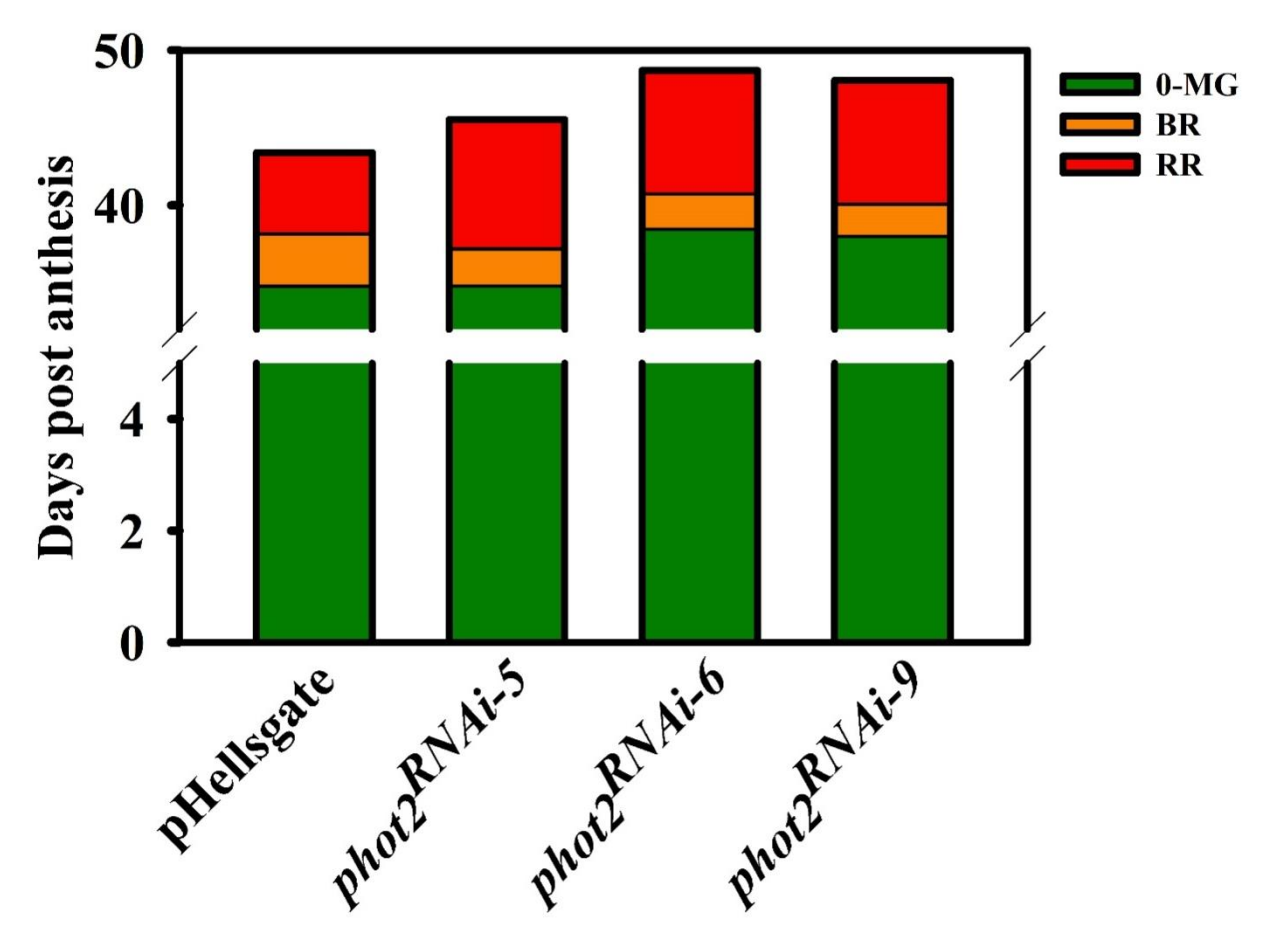


Figure 4.18. Chronological development of tomato fruit during ripening in pHellsgate and *phot2 RNAi* lines (n=8 fruits). Fruits were tagged at anthesis and their development is visually monitored. Once the mature green (MG) stage is reached, the time taken for transition to BR and then RR is subsequently recorded. At every stage, data is means  $\pm$  SE (n=8). Note that attainment of MG stage is delayed in  $phot2^{RNAi-6}$ , and  $phot2^{RNAi-9}$  and subsequent MG-BR transition is hastened but BR-RR is extended.

behaved like control in reaching MG. Thereafter, the fruits of all the three RNAi lines required a slightly lesser duration (~1 day) to attain the breaker stage (BR) than the control, and the subsequent transition from breaker to the red ripe stage (RR) in the RNAi lines was longer (~2-3 days) than the control fruits (Figure 4.18).

#### 4.4.5 °Brix and pH of ripe fruits of *phot2* RNAi lines

°Brix indicates the total soluble sugar content and can affect the fruits' taste and quality. The higher the °Brix, the better the fruit quality. In addition to °Brix, the pH of the fruits also indicates the acid levels, especially the citrate and malate levels. These acids also affect the fruit quality and taste. Examination of °Brix and pH of the ripe fruits of the *phot2* RNAi lines revealed no significant change from the pHellsgate fruits (Figure 4.19), suggesting that *phot2* did not affect these parameters.

# 4.4.6 phot2 positively influences carotenoid levels in T<sub>3</sub> lines

As photoreceptors like phytochromes, cryptochromes and UVR8 are positive regulators of carotenogenesis in tomato fruits, and tomato *phot1* mutant exhibits high carotenoid levels, it was of interest to examine the influence of *phot2* on fruit carotenogenesis. Analysis of total carotenoid content in ripe fruits of *phot2* RNAi lines revealed a decrease compared to pHellsgate fruits (Figure 4.20). Specifically, compared to red ripe fruits of pHellsgate, fruits of *phot2* RNAi lines had about 2-fold high phytoene, 1.5-1.6 fold high phytofluene, but lycopene (~1.6-2.2 fold),

β-carotene (~1.53-2.36 fold) and lutein (~1.6-2 fold) levels were reduced. These results signify *phototropin2* as a positive regulator of fruit carotenoid accumulation since disruption of this gene resulted in low carotenoid levels (Figure 4.20).

# 4.4.7 Gene expression for the rate-limiting enzymes of the carotenoid biosynthetic pathway in the $T_3$ lines

In tomato fruits, carotenoids are synthesized from the plastidic methylerythritol-4- phosphate (MEP) pathway and the enzyme deoxy-xylulose-5-phosphate synthase (dxs) is the rate- limiting enzyme that drives the MEP-derived geranylgeranyl diphosphate (GGPP) towards carotenoids biosynthesis. When tomato fruits ripen, the chloroplast-specific carotenoid biosynthesis switches to a chromoplast-specific pathway. This involves activating fruit-specific phytoene synthase (psy1), the key to lycopene synthesis, and chromoplast-specific lycopene  $\beta$ - cyclase (cycb), vital for  $\beta$ -carotene formation. As phot2 acts as a positive

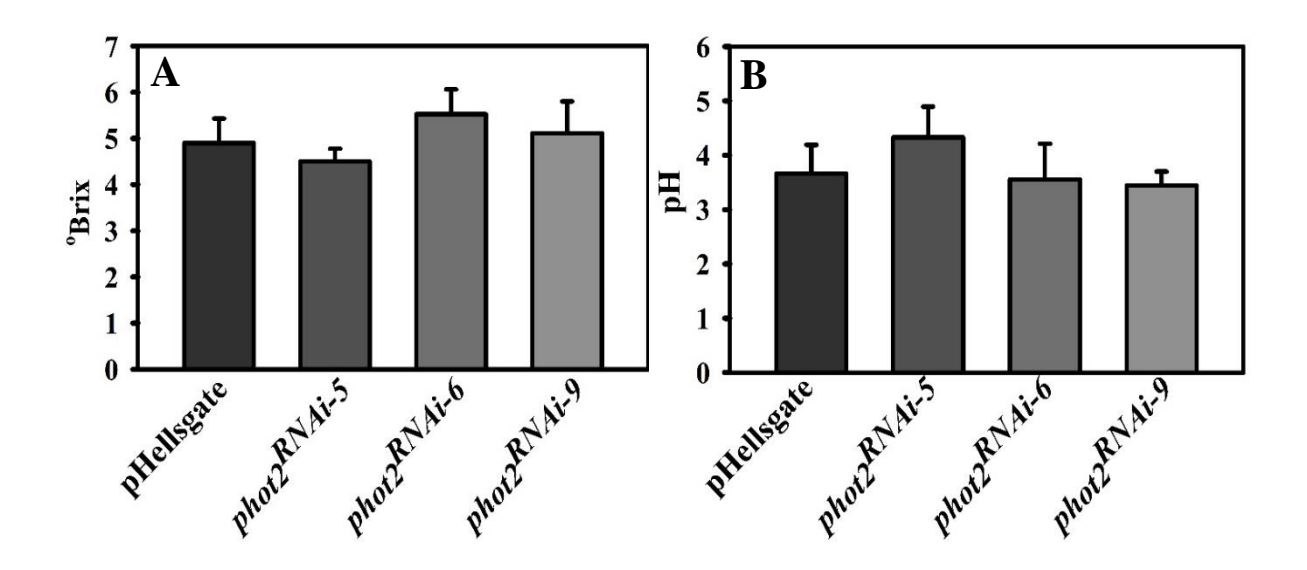


Figure 4.19. pH (A) and °Brix (B) comparison of fruits at red ripe stage in *phot2* RNAi and pHellsgate lines. Data are means  $\pm$ SE (n=5 fruits). \*P  $\leq$  0.05, \*\*P  $\leq$  0.01 and \*\*\*P  $\leq$  0.001. Note that the pH and °Brix of silenced lines are similar to that of empty vector control.

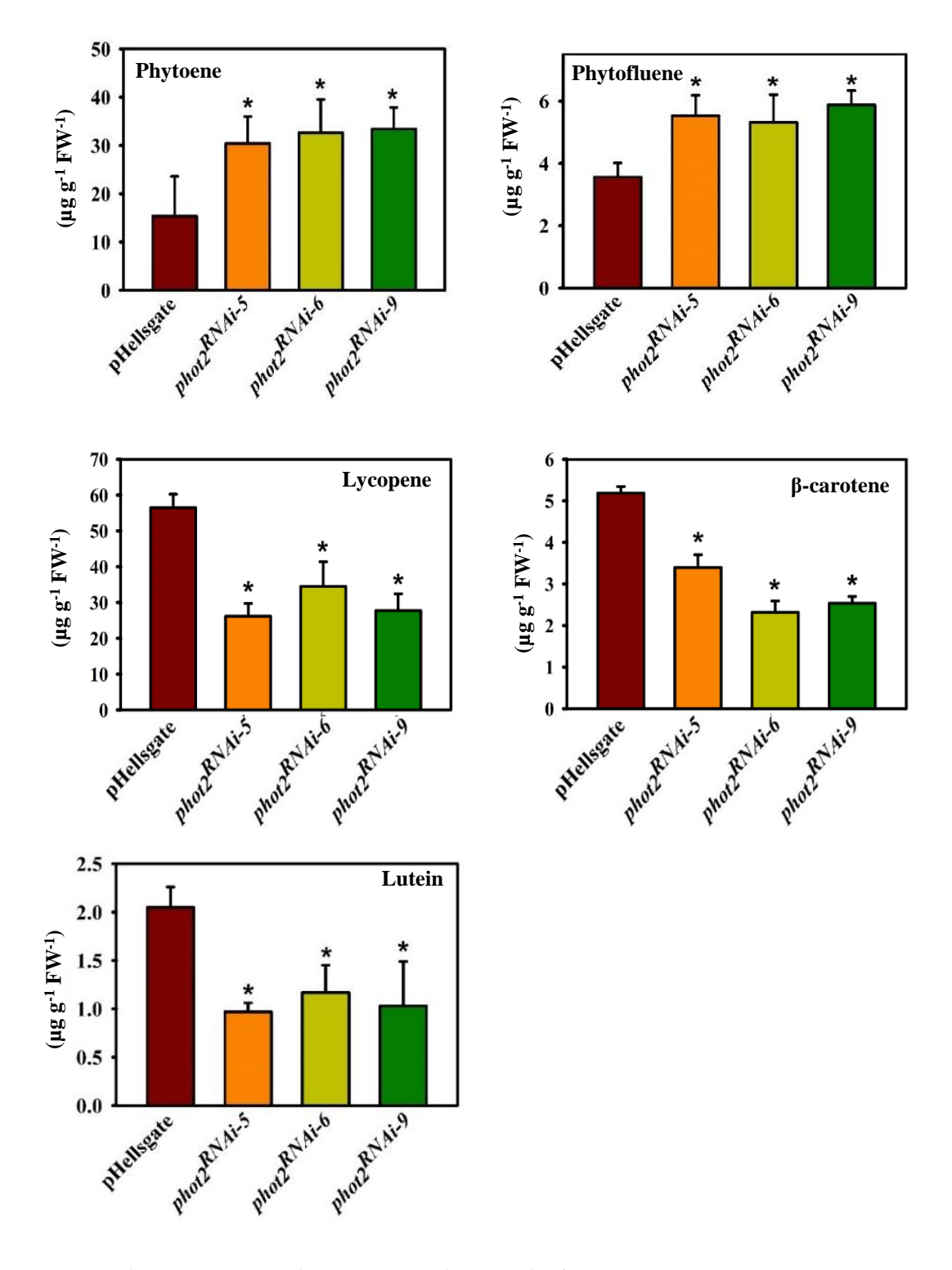


Figure 4.20. Carotenoid profiling in RR fruits of *phot2* RNAi plants in comparison pHellsgate. Carotenoids were extracted from RR fruits of pHellsgate and *phot2* RNAi lines. Data are means  $\pm$ SE (n=5-8).

# Pyruvate + Glyceraldehyde-3-phosphate

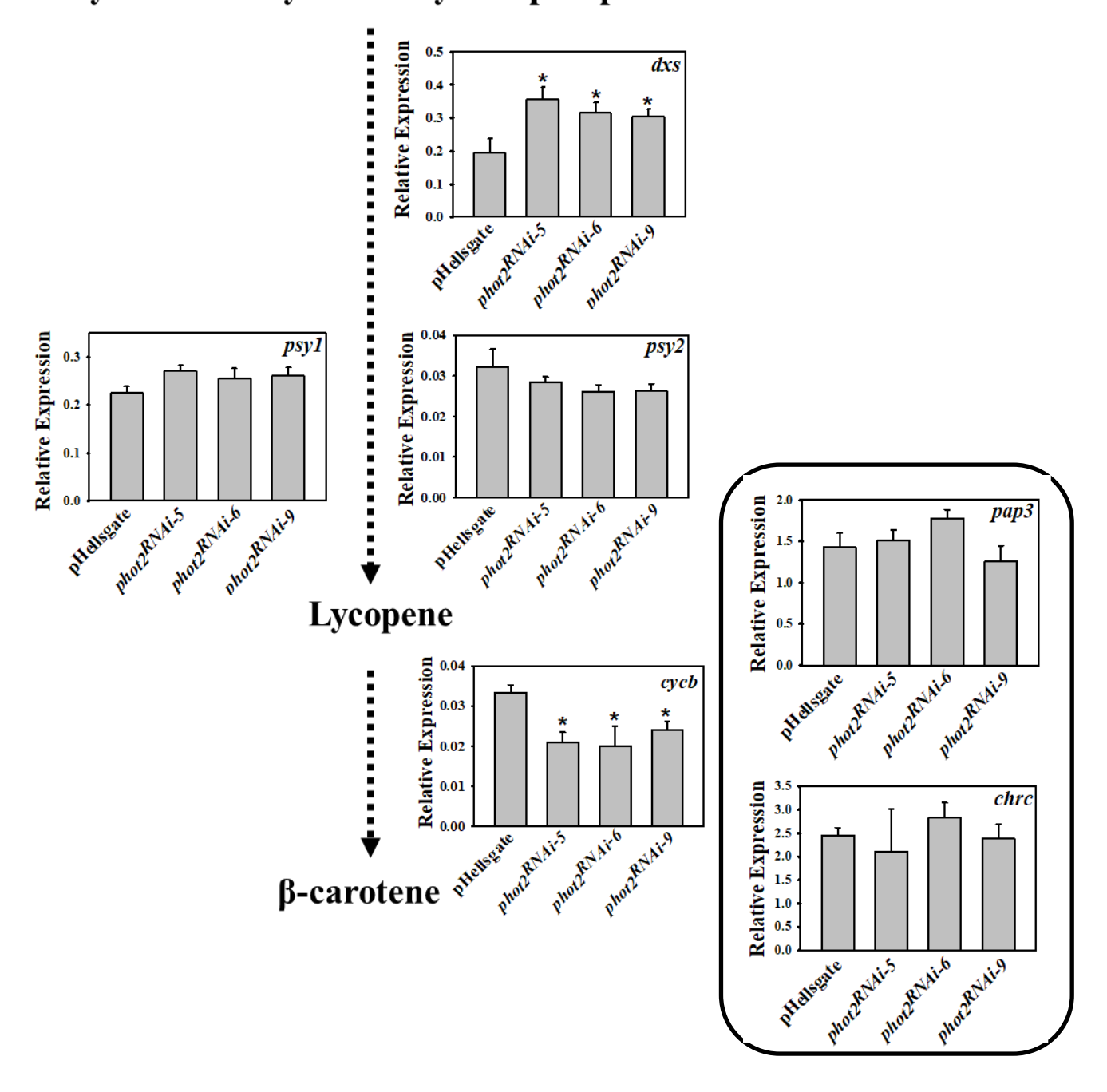


Figure 4.21. Relative gene expression of carotenoid biosynthesis and sequestration genes in *phot2* RNAi lines. The y-axis indicates relative expression of genes obtained after normalization with actin and ubiquitin. Data are means  $\pm SE$  (n=3), \*P  $\leq$  0.05.

regulator of carotenoid synthesis, it was of interest to examine its influence on the expression of carotenogenic genes.

Compared to the pHellsgate fruits, *dxs* expression was higher in the ripe fruits of *phot2* RNAi lines. Thereafter, despite high levels of phytoene and low levels of lycopene in the *phot2RNAi* lines, the *psy1* and *psy2* expression levels were similar to that of the control (Figure 4.21). As β-carotene amounts were lower, it is expected that the *cycb* expression also would be lower in the silenced lines. However, no significant difference in the *cycb* expression was observed in the silenced lines. In addition, expression of carotenoid sequestration genes, *chromoplast- specific carotenoid-associated protein (chrc)*, and *plastid lipid-associated protein 3 (pap3)* were similar to that of control. This suggests that carotenogenesis in *phot2RNAi* lines is not regulated at the transcriptional level and could be regulated post-transcriptionally.

#### 4.4.8 Metabolite analysis in red ripe fruits of phot2 RNAi lines

Apart from the dramatic color changes that occur during fruit ripening, several metabolic changes also occur to improve taste, flavor, and palatability. Most of these responses are mediated by the plant hormone ethylene with a cross-talk from other hormones and other factors, includinglight. To check the influence of *phot2* on metabolite profiles of tomato fruit, we used GC-MS to detect the primary metabolite levels in the red ripe fruits of *phot2* silenced lines. We identified around sixty-five metabolites belonging to different classes such as organic acids, carbohydrates, fatty acids, amino acids, and amines. We used principal component analysis (PCA) of the primary metabolites to determine if the profiles of control and *phot2* RNAi fruits differ at the RR stage. The PCA showed overlapping profiles of *phot2* RNAi lines with pHellsgate lines (Figures 4.22). Then we did a detailed analysis of the different classes of metabolites to understand the effect of *phot2* silencing.

Of the eight amino acids detected, only three: Glycine,  $\beta$ -alanine, and  $\gamma$ -aminobutyric acid (GABA), showed significantly high abundance in *phot2* RNAi lines, while the rest were similar in abundance to that of pHellsgate fruits, and many were below the detection limits (Figure 4.23). Similarly, in the case of organic acids, only citrate and aconitate were high in abundance in the fruits of *phot2* silenced lines, and malate levels were similar. In contrast, gluconate levels were lower than the pHellsgate fruits. Most of the twenty-one sugars detected were similar in

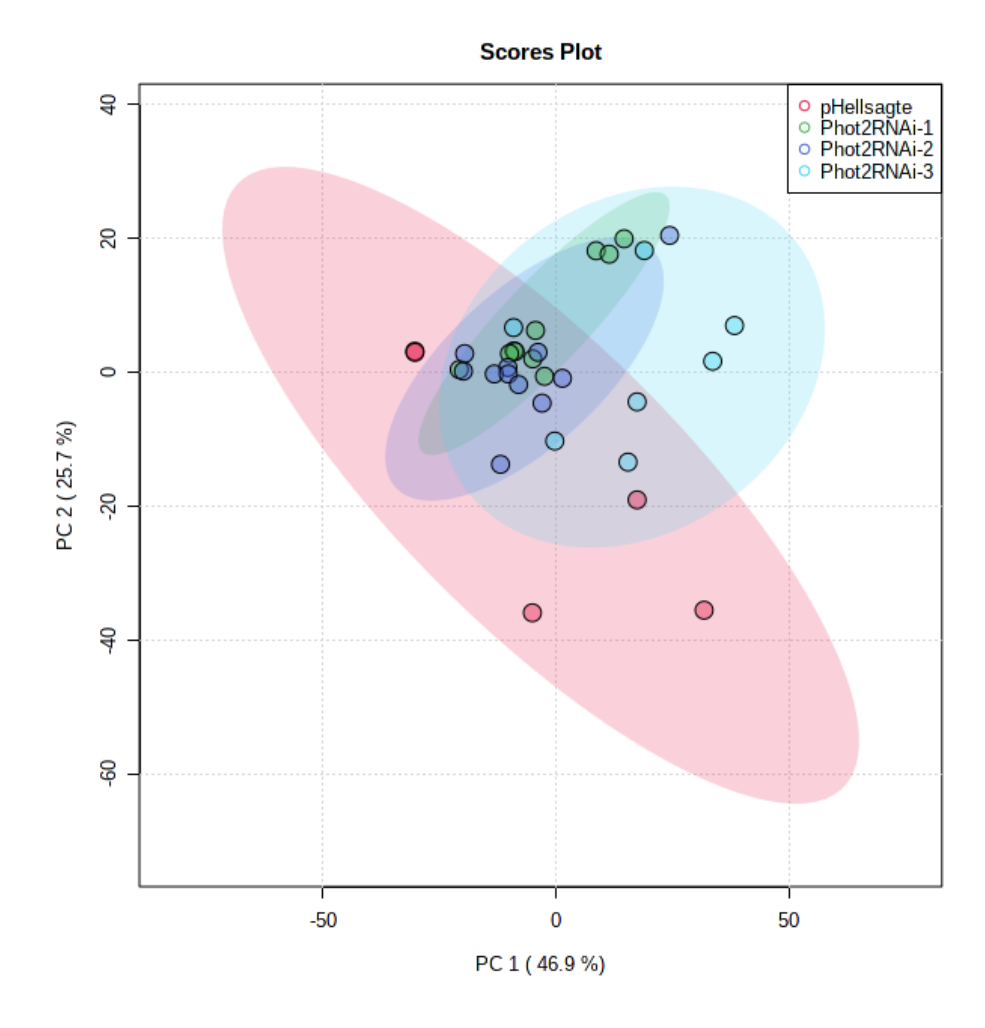


Figure 4.22. The principal component analysis (PCA) of metabolites extracted from RR fruits *phot2* RNAi lines and control pHellsgate fruits. The symbols in PCA plot represent individual biological replicates of RNAi lines and pHellsgate fruits.

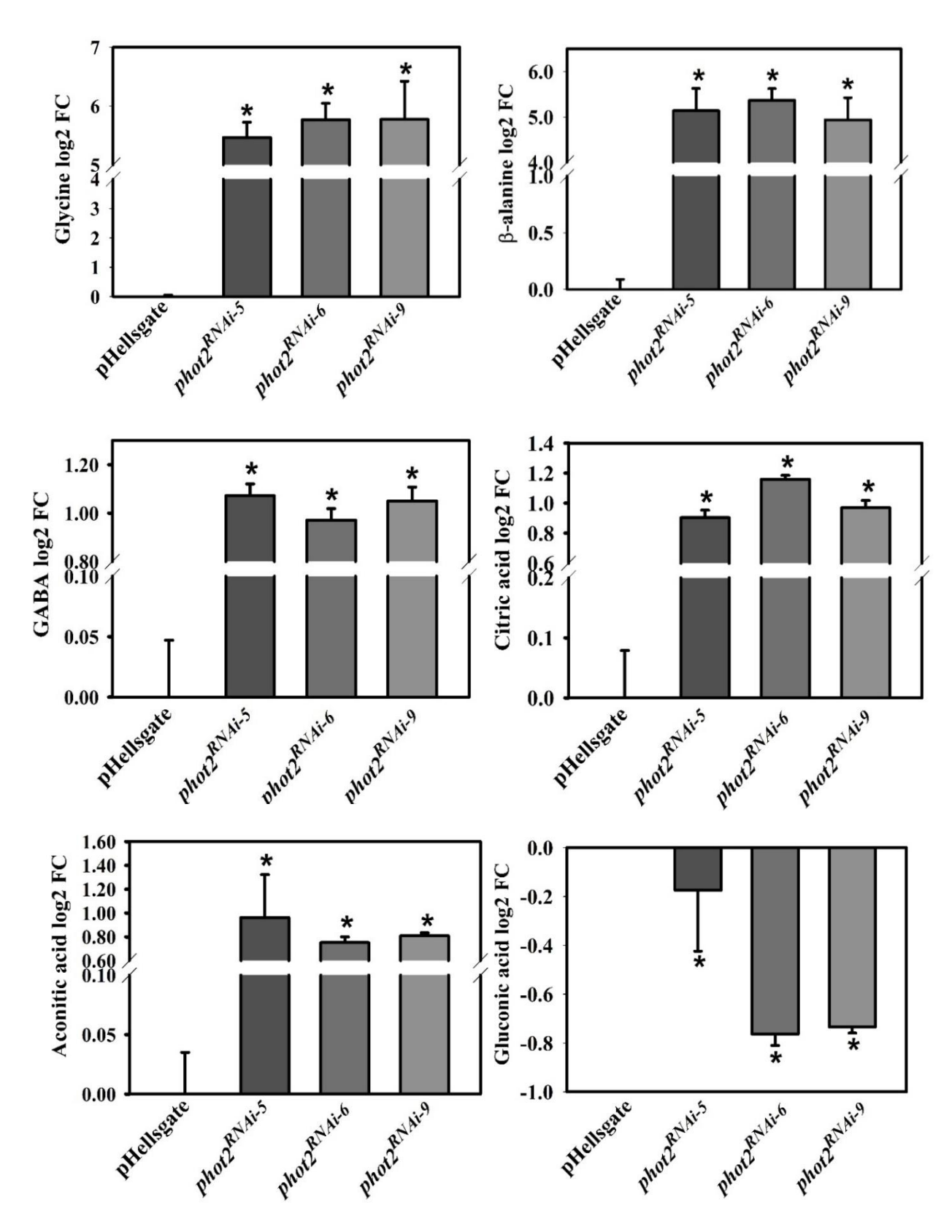


Figure 4.23. Primary metabolites in RR fruits of pHellsgate and RNAi lines. Only significantly different metabolites are depicted in graphs. Data means  $\pm$  SE (n=5-8), \*P  $\leq$  0.05.

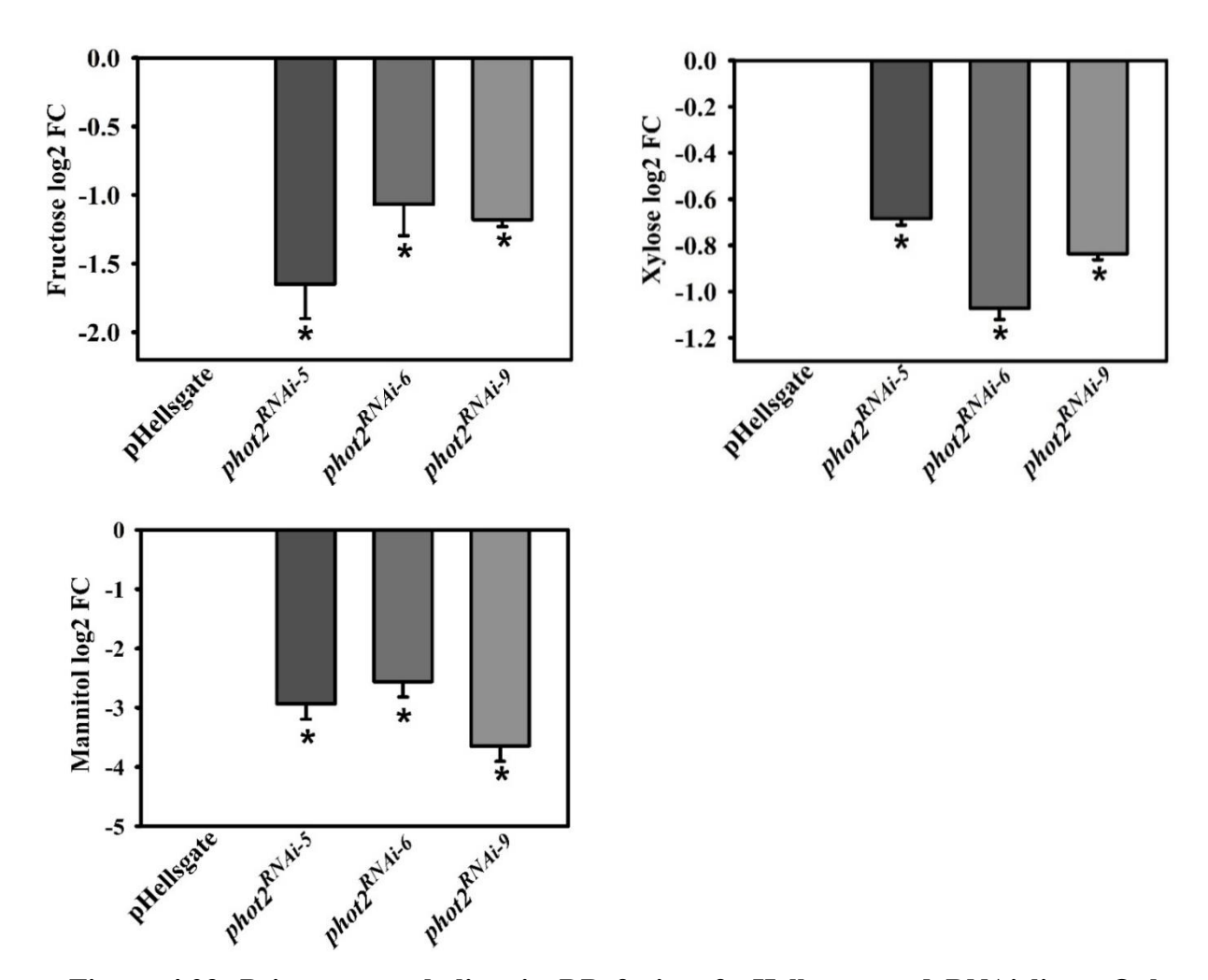


Figure 4.23. Primary metabolites in RR fruits of pHellsgate and RNAi lines. Only significantly different metabolites are depicted in graphs. Data means  $\pm$  SE (n=5-8), \*P  $\leq$  0.05.

abundance to control, and only fructose, xylose, and mannitol were significantly lower in *phot2* silenced lines. All these results suggest a mild influence of *phot2* on the primary metabolome.

#### **Section II**

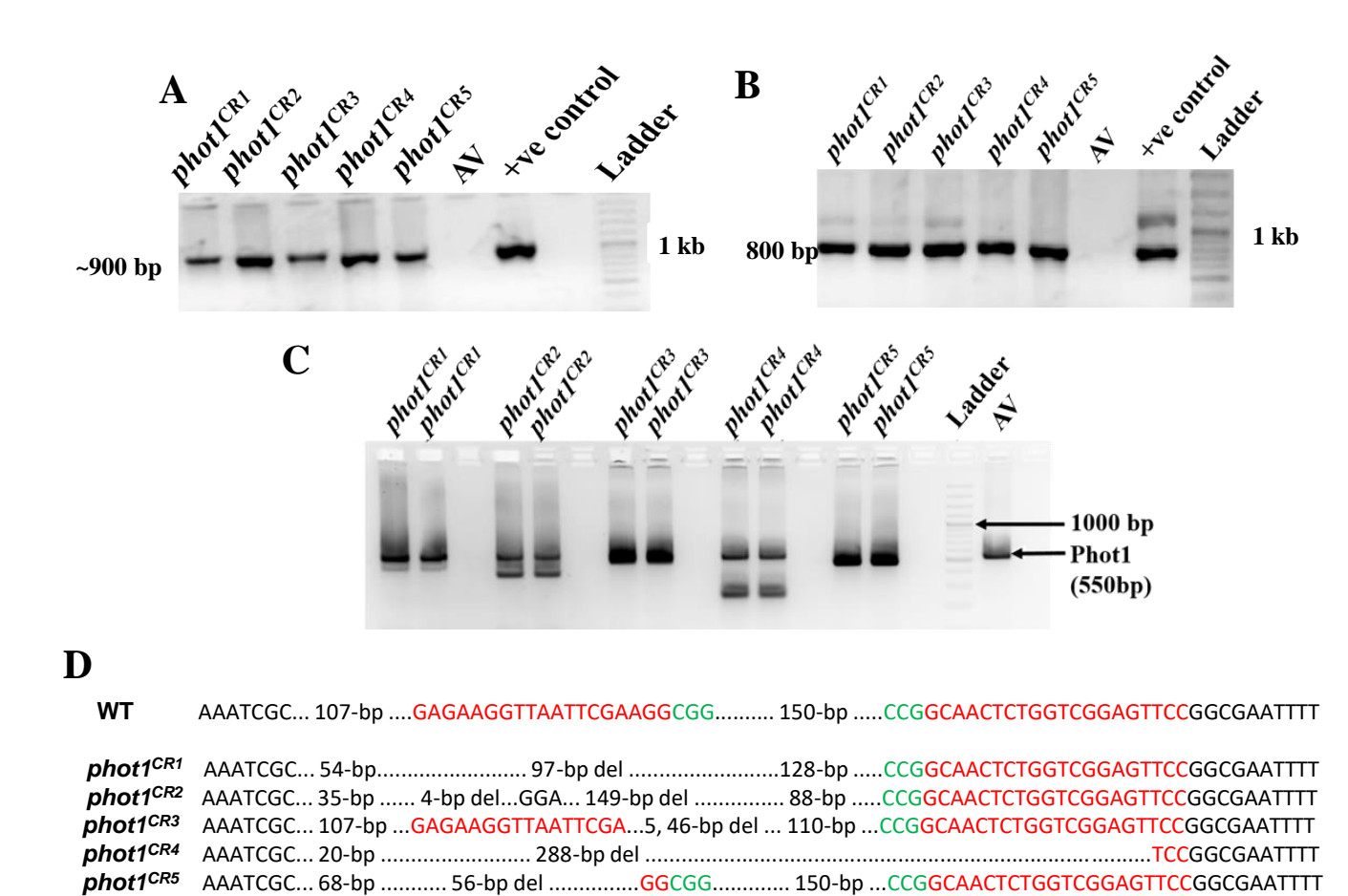
To develop tomato lines with different allelic variations in the *phot1* gene and mainly to create knockouts, we targeted the first exon using the CRISPR/CAS9 strategy. We used a double guide RNA-based approach rather than a single guide RNA-based for high editing efficiency.

# 4.5 Generation of CRISPR/Cas9-edited phot1 mutant lines

The *Agrobacterium tumefaciens* harboring the *phot1*-dgRNA construct was used to transform tomato cultivar Arka Vikas (AV) following Van Eck et al.'s (2006) protocol. In brief, tomato seeds sterilized with 4% NaOCl were germinated on 1/2 MS media. After 7-10 days of growth, semi-opened cotyledons were co-cultivated with Agrobacterium suspension of  $OD_{600} = 0.5$ -0.6. The explants were allowed to grow on the kanamycin selection media. The plants regenerated on kanamycin were screened for the presence of CRISPR/Cas9 cassette and *nptII* gene before transferring to the greenhouse. *Cas9* and *nptII* primers used for PCR are listed in Table 3.12.

According to Sreelakshmi et al.'s (2010) protocol, genomic DNA was isolated from the regenerated explants. This DNA was used for the PCR amplification of *Cas9* and *nptII* genes. The detection of Cas9 amplicon in the explants indicates that CRISPR/Cas9 binary expression cassette was successfully delivered to tomato plants by Agrobacterium transformation. As kanamycin is the selection marker for the plants transformed with *phot1*-dgRNA construct, the presence of *nptII* amplicon indicates the successful transformation of plants. The explants that test negative for *Cas9* and *nptII* are not transgenic and were discarded from the many explants tested at a very young age, for example, at the shooting stage. Using this method, we can screen many explants in the tissue culture room when they are very young. The above step helps in saving time, money, and energy. Editing is further confirmed in the transgenic lines when the explants start rooting and when the plants are transferred to the greenhouse by gene-specific PCR.

# 4.5.1 Identification of CRISPR/Cas9-induced mutations in T<sub>0</sub> generation



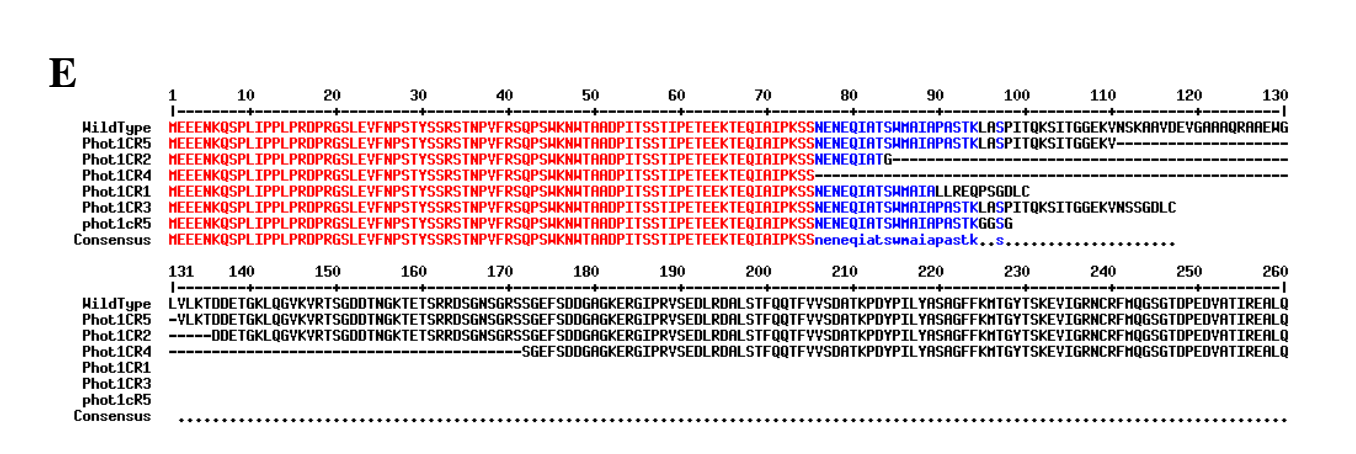


**Figure 4.24. PCR based screening of CRISPR** *phot1*  $T_0$  **plants. A**, shows amplification of CAS9 gene. **B**, shows amplification for *nptII* gene. **C**, shows *phot1*-specific PCR. **D**, Sequence alignment of the target regions. The wild type sequence is shown at the top with the target sequence in red and the PAM in green. Nucleotide variations at the targets of  $T_0$  mutant lines, 'del' -base deletion. **E**, shows the allelic variation in protein sequence alignment of edited lines compared to wild type sequence by Multialign software.

To investigate the role played by *phot1* in tomato fruit development and ripening, we generated phot1 CRISPR edited lines. After confirming that the explants were positive for both Cas9 and nptII, these were further screened using phot1-specific PCR to check the editing (for primer details, see Table 3.12, Figure 4.24A, B). Analysis of *phot1* amplicons on 2% (w/v) agarose gel revealed a few smaller fragments than the expected size suggesting editing (Figure 4.24C). Sequencing of these smaller fragments revealed large deletions consistent with the observed gel mobility of the corresponding PCR fragments. However, this gel-based method makes deletions smaller than 50 bp difficult to visualize compared to large deletions. In such cases, the PCR amplified fragments were further confirmed by sequencing. The sequencing step is essential to visualize smaller deletions and the point mutations. In cases with no significant mobility shift in the PCR amplicons, we could observe a few base pair changes on sequencing. This strategy helped us to identify at least eight editing events in the T<sub>0</sub> generation, including five large deletions and two small deletions of 4-5 bp. None of these events were homozygous in the  $T_0$  generation; they were either heterozygous or chimeric with one wild-type band and smaller fragments. The eight editing events upon sequence confirmation include phot1<sup>CR1</sup> (97 bp deletion; heterozygous), phot1<sup>CR2</sup> (4, 149 bp deletion; heterozygous), phot1<sup>CR3</sup> (5, 46 bp deletion; chimera), phot1<sup>CR4</sup> (288 bp deletion, heterozygous) and phot1<sup>CR5</sup> (56, 63 bp deletion; chimera) alleles (Figure 4.24D). No inversions or insertions in the edited regions were observed in the *phot1* explants. The *phot1*- specific screening of the adult plants (after transferring the hardened rooted explants to the greenhouse) was also carried out to rule out any successful repair of the editing event. At least in the T<sub>0</sub> generation, all the initially observed editing events were also confirmed at the adult stage.

The mutated gene sequences of *phot1* were translated to protein sequences with the EXPASY tool and aligned with the AV PHOT1 protein sequence using MULTIALIGN (<a href="http://multalin.toulouse.inra.fr/multalin/">http://multalin.toulouse.inra.fr/multalin/</a>) software. The above-aligned sequences revealed that the deletions induced by CRISPR/Cas9 affected the PHOT1 protein sequence (Figure 4.24E). Among eight editing events, mutations in *phot1* prematurely truncated the PHOT1 protein due to frameshifts resulting in Thr100Cys\* (*phot1*<sup>CR1</sup>), Ala115Gly\*, and Asp117Cys\* (*phot1*<sup>CR3</sup>) and Pro98Gly\* (*phot1*<sup>CR5</sup>). In addition, a Ser84Gly substitution and in-frame deletion of 50 aa from

85-135 aa  $(phot1^{CR2})$ , in-frame deletion of 96 aa from 76-171 aa  $(phot1^{CR4})$ , and 21 aa from 111- 131 aa  $(phot1^{CR5})$  were observed (Figure 4.24E, Table 4.2).

# 4.5.2 phot1<sup>CR</sup> lines show loss of function

As phototropin mediates chloroplast relocation responses when exposed to low and high fluence blue light, it was interesting to examine whether the mutations in *phot1*<sup>CR</sup> alleles affected the function of PHOT1 protein. The blue light-induced chloroplast movement was studied in *phot1*<sup>CR</sup> alleles and compared with controls, AV, and *Nps1* under three conditions: dark, low intensity, and high-intensity blue light. As expected, *phot1*<sup>CR1-5</sup> lines showed loss of *phot1* function as evidenced by the 75%, 66%, 40%, 71% and 72% reduction in the chloroplast accumulation response (partial loss) respectively (Figure 4.25). This suggests that the mutations induced by CRISPR/Cas9 affected the *phot1* function. These plants and AV were monitored for any phenotypic changes throughout their life cycle. The seeds were collected for all the alleles to advance them to the next generation.

# 4.6 Generation and characterization of *phot1<sup>CR</sup>* alleles in the T<sub>1</sub> generation

Fifty seeds from each allele were germinated to raise  $T_1$  *phot1*<sup>CR</sup> lines. These plants were screened to identify the homozygous edited lines that are also Cas9-free. Out of 8 editing events observed in  $T_0$ , five were recovered in the homozygous condition in the  $T_1$  generation (Table 4.2). From these, only *phot1*<sup>CR2</sup> became Cas9-free in the  $T_1$  generation (Figure 4.26B).

In the  $T_1$  generation, though homozygous edited plants were obtained for  $phot1^{CR1}$ ,  $phot1^{CR3}$ ,  $phot1^{CR4}$ , and  $phot1^{CR5}$  alleles, these plants were both Cas9 and nptII positive (Figure 4.26A, C, D& E). All the homozygous lines were monitored for any phenotypic changes compared to AV, and the loss of phot1 function was also assessed by monitoring chloroplast movement responses.

#### 4.6.1 Loss of *phot1* function is stably inherited in the $T_1$ generation.

As five homozygous edited alleles were recovered in the  $T_1$  generation, the effect of *phot1* mutation on its function was examined in them. All the homozygous progeny in every allele were monitored for chloroplast relocation response in dark, low, and high fluence blue light using a three-point measurement for rapid scanning. The mean chloroplast relocation response showed the loss of *phot1* function in all the alleles with 31%, 30%, 40%, 35%, and 29% reduction in the chloroplast accumulation response in the progeny of *phot1*<sup>CR1-5</sup> respectively (Figure 4.27). This

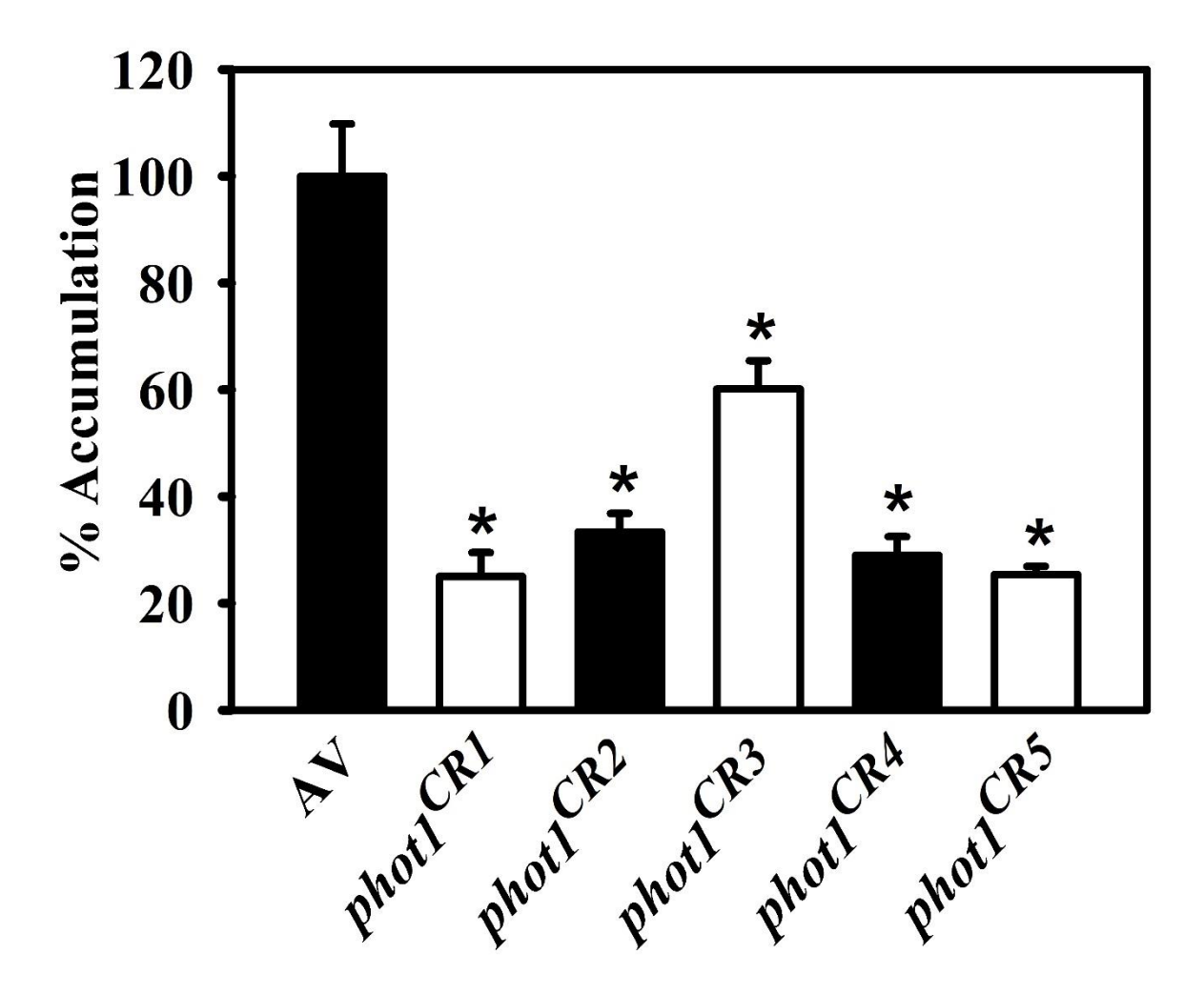
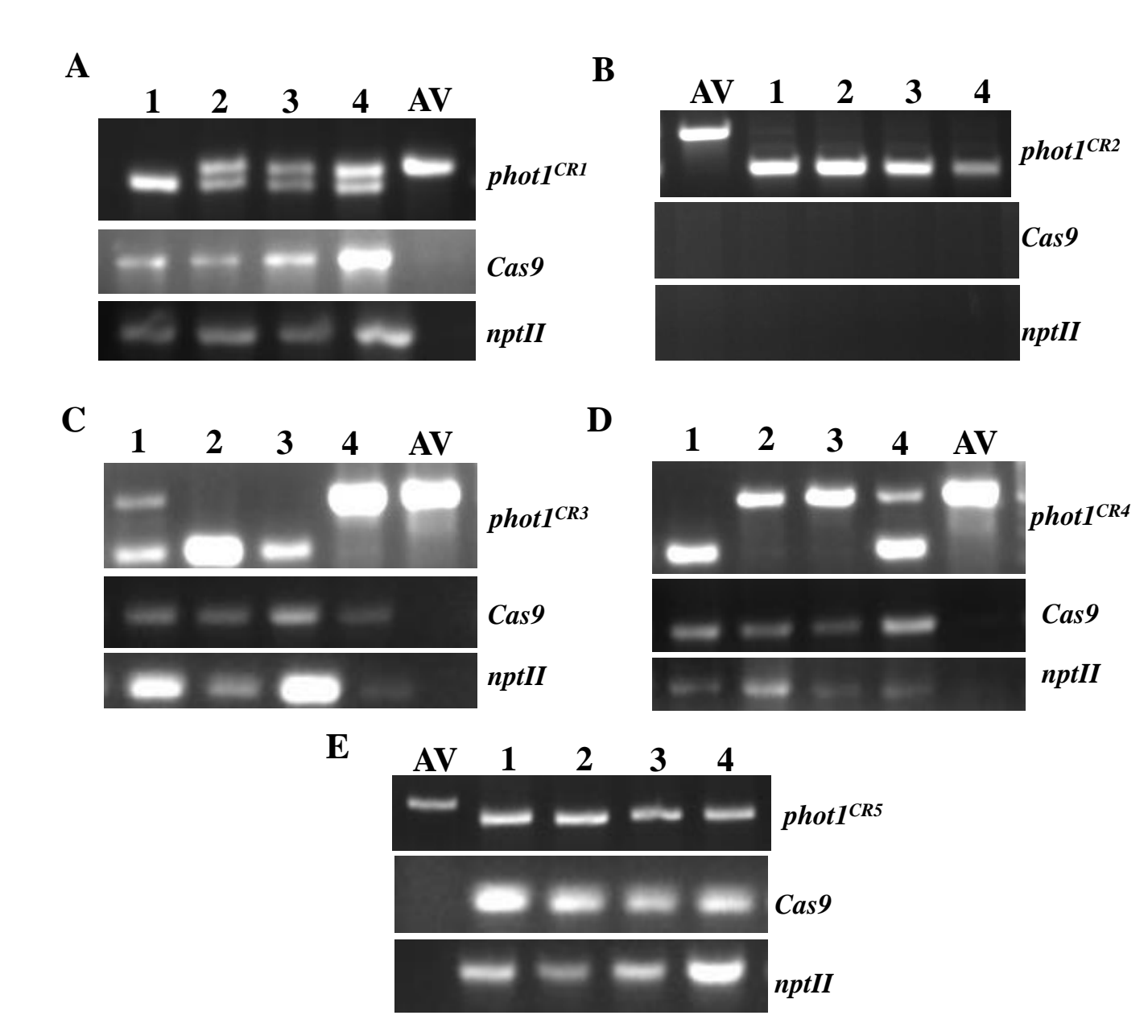


Figure 4.25. % accumulation and avoidance of chloroplast movement in leaves of *phot1* CRISPR plants in  $T_0$  generation in comparison to AV under BL treatment. Dark adapted tomato leaf discs were placed in 96 well microplate well in the dark, and then red light transmittance was recorded for 20 min for dark reading. The leaf discs were then irradiated sequentially with weak blue light (3.2  $\mu$ mol/m²/s) for 80min for accumulation induction (Accumulation) and strong blue light (60-80  $\mu$ mol/m²/s) for 40 min each for avoidance induction (Avoidance). The blue light was given during the interval periods between red light transmittance measurements. % accumulation and avoidance was calculated with reference to positive control, AV. Note that chloroplast accumulation response mediated by phot1 is affected in the phot1 CRISPR lines, suggesting impaired function of phot1. Each data point is a representation of the mean value  $\pm$ S.E of eight replicates. \*P  $\leq$  0.05.



**Figure 4.26.** A representative image showing the identification of homozygous, free and *nptII* free plants in T<sub>1</sub> generation by PCR. A, Lane 1-4 display PCR amplicons of *phot1*<sup>CR1</sup> progeny. Lane 1 is homozygous edited and 2, 3 and 4 are heterozygous for editing. All the plants are *Cas9* and *nptII* positive. B, For *phot1*<sup>CR2</sup> progeny, lane 1, 2, 3 and 4 are putative homozygotes and free of Cas9 gene. C, Lane 1-4 display PCR amplicons of *phot1*<sup>CR3</sup>. Lane 1 is heterozygous plant and 2, 3 are homozygous edited plants. 4 is homozygous wild type. All the plants are *Cas9* and *nptII* positive. D, Lane 1-4 display PCR amplicons of *phot1*<sup>CR4</sup>. Lane 1 is homozygous edited. 2, 3 are homozygous wild type and 4 is heterozygous. All the plants are *Cas9* and *nptII* positive. E, Lane 1-4 display PCR amplicons of *phot1*<sup>CR5</sup>. Plant number 1, 2, 3,4 are homozygous. All are *Cas9* and *nptII* positive. \*- indicates homozygous edited lines, \*- indicates wild type

Alleles	Effect of gene sequence in exon 1	Zygosity in T <sub>0</sub>	Effect on translated Protein	Homozygous alleles recovered in $T_1$ generation
phot1 <sup>CR1</sup>	97 bp deletion	Heterozygous	Thre100Cys*	97 bp deletion (Thre100Cys*)
phot1 <sup>CR2</sup>	4 and 149 bp deletion	Heterozygous	Ser84Gly and in- frame deletion of 50 aa from 85-135 aa	4 and 149 bp deletion (Ser84Gly and 50 aa deletion from 85-135 aa)
phot1 <sup>CR3</sup>	5 bp and 46 bp deletion	Chimera	Ala115Gly* Asp117Cys*	46 bp deletion (Asp117Cys*)
phot1 <sup>CR4</sup>	288 bp deletion	Heterozygous	In-frame deletion of 96 aa from 76- 171 aa	288 bp deletion (95 aa deletion from 76-171 aa)
phot1 <sup>CR5</sup>	56 and 63 bp deletion	Chimera	Pro98Gly* In-frame deletion of 21 aa from 111- 131 aa	63 bp deletion (20 aa deletion from 111-131 aa)

Table 4.2. Summary of editing events recovered alleles to homozygosity in  $T_1$  generation. Effect of editing was also examined on the translated protein and mentioned here.

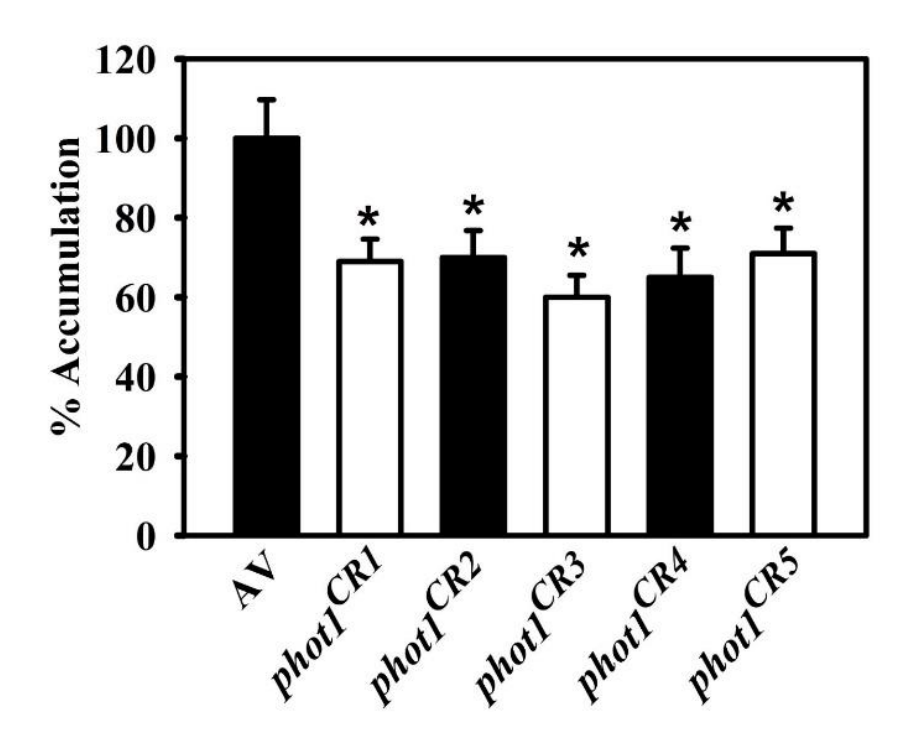


Figure 4.27. Assessment of loss of phot1 function by monitoring the chloroplast movement in response to varying BL intensity. Dark adapted tomato leaf discs were placed in 96 well microplate well in the dark, and then red light transmittance was recorded for 20 min for dark reading. The leaf discs were then irradiated sequentially with weak blue light (3.2  $\mu$ mol/m²/s) for 80 min for accumulation induction (Accumulation) and strong blue light (60-80  $\mu$ mol/m²/s) for 40 min each for avoidance induction (Avoidance). The blue light was given during the interval periods between red light transmittance measurements. % accumulation and avoidance was calculated with reference to positive control, AV. Note that chloroplast accumulation response mediated by phot1 is affected in the phot1 CRISPR lines, suggesting impaired function of phot1. Each data point is a representation of the mean value  $\pm$  S.E of eight replicates.

reveals the stable inheritance of loss of function in *phot1* alleles from  $T_0$  to  $T_1$  generation.

# 4.6.2 Mutations in *phot1* affect the fruit carotenoid content.

As *Nps1* mutant is dominant-negative and its fruits show high carotenoid levels, especially lycopene content at the ripe stage, it was interesting to know whether mutations in *phot1* affect the fruit carotenoid content. The fruit development and ripening were monitored in all the five homozygous *phot1*<sup>CR1-5</sup> alleles. When the fruits reached the ripe stage, carotenoid content was measured compared to AV. All the *phot1*<sup>CR1-5</sup> alleles showed a significant reduction of lycopene compared to AV (Figure 4.28A), while  $\beta$ -carotene content increased in all the alleles than AV except *phot1*<sup>CR3</sup> (Figure 4.28B). This suggests the potential role of phototropins in fruit carotenogenesis.

# 4.7 Generation and characterization of Cas9-free *phot1<sup>CR</sup>* lines in the T<sub>2</sub> generation

All the five *phot1*<sup>CR</sup> alleles recovered in homozygous conditions in T<sub>1</sub> were advanced to T<sub>2</sub> generation by growing a minimum of 30 plants per line. The genomic DNA was isolated from these plants and was initially screened using PCR for the presence of Cas9. Upon screening for the existence of Cas9, few of the progeny of *phot1*<sup>CR3</sup> and *phot1*<sup>CR3</sup> became Cas9-free, and all the progeny of *phot1*<sup>CR2</sup> were Cas9-free since this line became transgene-free in T<sub>1</sub> generation itself (Figure 4.29 B, C & E). The other two alleles, *phot1*<sup>CR1</sup> and *phot1*<sup>CR4</sup>, still harbored the transgene and were not taken forward for further studies (Figure 4.29 A & D). In addition, the editing was also confirmed in these Cas9-free plants by using *phot1*-specific PCR and subsequent analysis of PCR fragments on agarose gel electrophoresis and Sanger sequencing. All the progeny of these three alleles were homozygous for editing.

# 4.7.1 Identification of potential Off-target editing in $phot1^{CR}$ homozygous Cas9-free alleles

CRISPR/Cas system has become indispensable for functional genomics studies in recent years. However, the mutations created by this system are not always intended, as mutations can occur in the unintended regions in the genome other than the target site and were often reported in several studies. Such off-target mutations can be detrimental as they can affect the function/regulation of un-targeted genes.

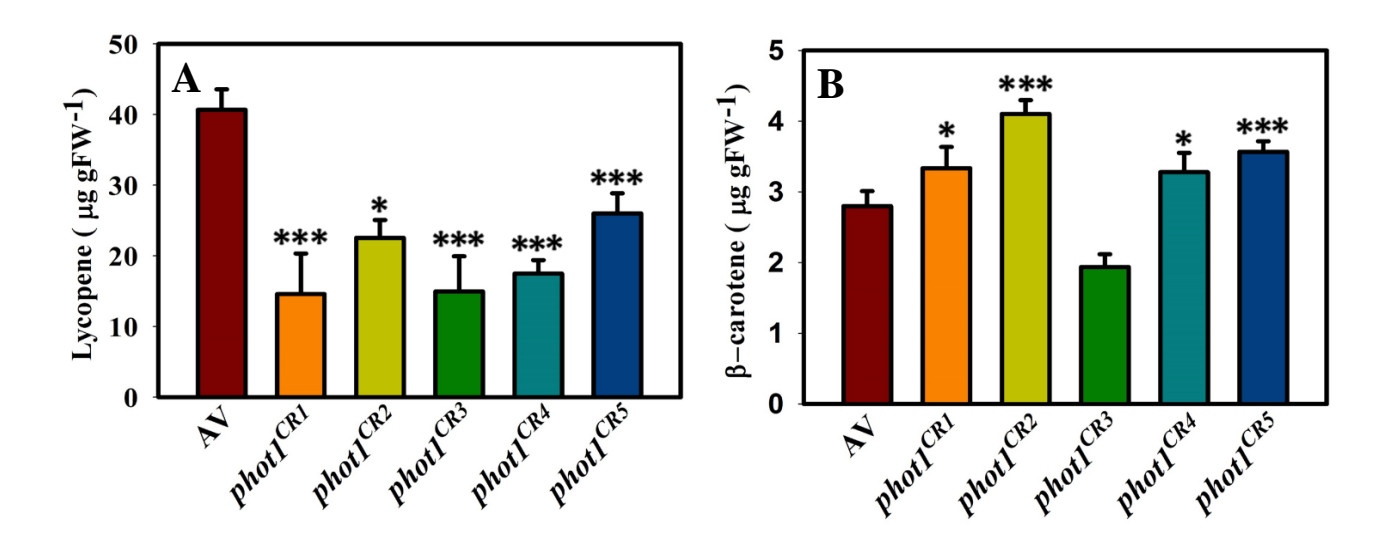


Figure 4.28. Carotenoid profiling in RR fruits of phot1 CRISPR lines in T<sub>1</sub> generation in comparison to AV. Figure A shows lycopene and B shows  $\beta$ -carotene content content in *phot1* CRISPR lines. Data are means of n=5-8  $\pm$  SE, \*P  $\leq$  0.05, \*\* P value  $\leq$  0.01, \*\*\*P value  $\leq$  0.001.

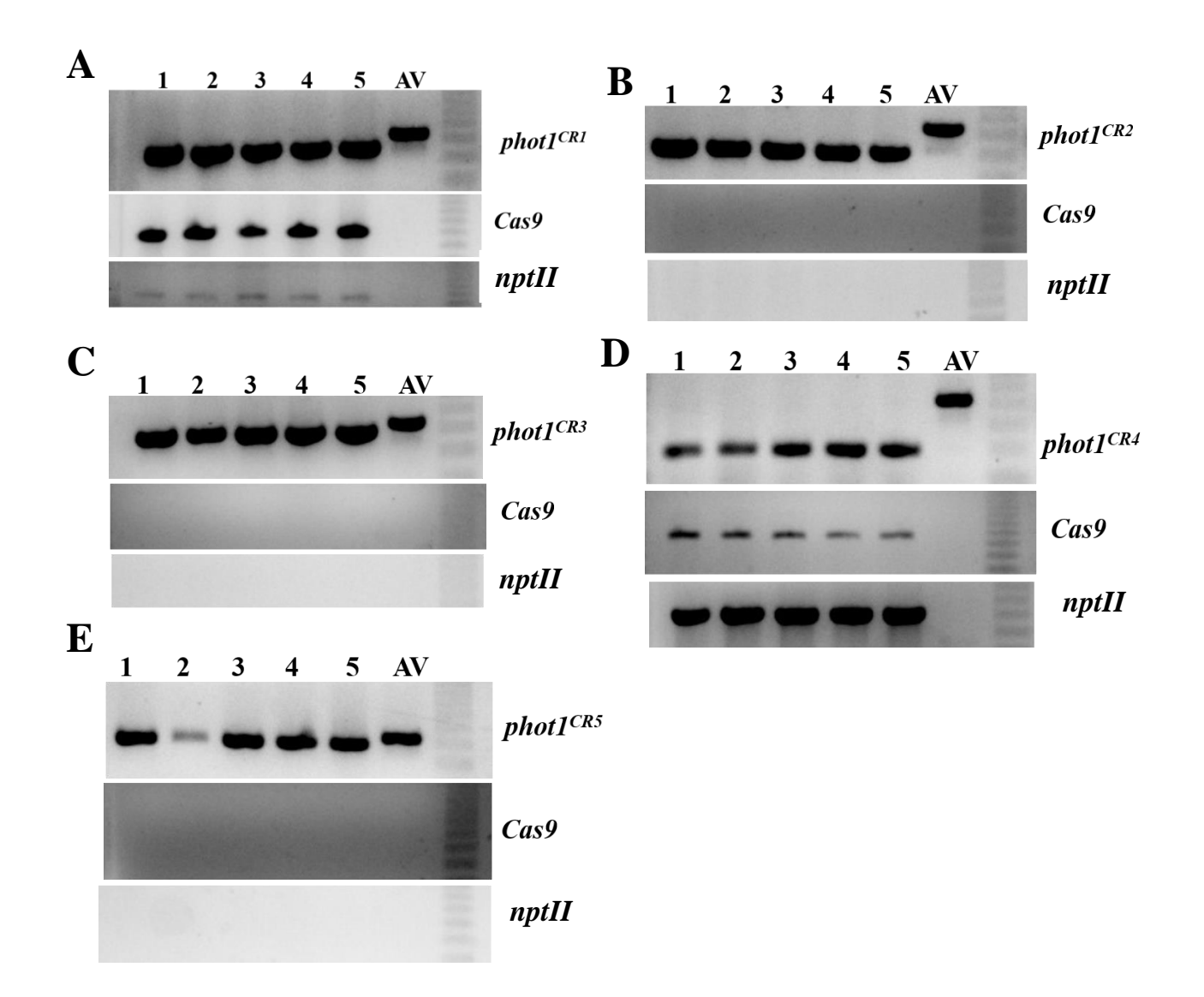


Figure 4.29. PCR based screening of  $phot1^{CR}$  plants in T2 generation specific, Cas9 and kanamycin. A, B, C, D and E shows PCR amplification in  $phot1^{CR1}$ ,  $phot1^{CR2}$ ,  $phot1^{CR3}$ ,  $phot1^{CR4}$  and  $phot1^{CR5}$  plants. The DNA from all the above lines was amplified with primers specific for phot1, Cas9 and nptII genes. As can be seen from  $phot1^{CR1}$ ,  $phot1^{CR2}$ ,  $phot1^{CR3}$ ,  $phot1^{CR4}$  and  $phot1^{CR5}$  all the five are homozygous edited and but  $phot1^{CR2}$ ,  $phot1^{CR3}$ , and  $phot1^{CR5}$  are Cas9 and nptII free. This suggests that the three alleles are transgene free.

Off-tai	rget-1
---------	--------

WT	${\sf TCATGCCAAAGTCAAAGAGGCCATT}{\underline{\sf GAaAAGaaTAATTCaAAGG}}{\sf TGGCCATTCAAAAAAAATCGAGGAAG}$
phot1 <sup>CR2</sup>	${\sf TCATGCCAAAGTCAAAGAGGCCATTGAaAAGaaTAATTCaAAGGTGGCCATTCAAAAAAAATCGAGGAAG}$
phot1 <sup>CR3</sup>	${\sf TCATGCCAAAGTCAAAGAGGCCATTGAaAAGaaTAATTCaAAGGTGGCCATTCAAAAAAAATCGAGGAAG}$
phot1 <sup>CR5</sup>	TCATGCCAAAGTCAAAGAGGCCATTGAaAAGaaTAATTCaAAGGTGGCCATTCAAAAAAAATCGAGGAAG

# Off-target-2

WT	$AAAAAAGAAGAAGAAATTTTTAGGT\underline{GAaAtaGTTAATTCaAAGG}CGGCTACAAATTTAAGACTGAACCA$
phot1 <sup>CR2</sup>	AAAAAAGAAGAAGAAATTTTTAGGTGAaAtaGTTAATTCaAAGGCGGCTACAAATTTAAGACTGAACCA
phot1 <sup>CR3</sup>	AAAAAAGAAGAAGAAATTTTTAGGTGAaAtaGTTAATTCaAAGGCGGCTACAAATTTAAGACTGAACCA
phot1 <sup>CR5</sup>	AAAAAAGAAGAAGAAATTTTTAGGTGAaAtaGTTAATTCaAAGGCGGCTACAAATTTAAGACTGAACCA

#### Off-target-3

WT	CTCTTTCATTCAGAACATCTTCCCT <u>CaTTCGAATTAAaCTTtcC</u> ACAACTAAGTTCTCAATAGCAGCAA
phot1 <sup>CR2</sup>	$\tt CTCTTTCATTCAGAACATCTTCCCTCaTTCGAATTAAaCTTtcCACAACTAAGTTCTCAATAGCAGCAACTAAGTTCTCAATAGCAACTAAGTTCTCAATAGCAACTAAGTTCTCAATAGCAACTAAGTTCTCAATAGCAACTAAGTTCTCAATAGCAACTAAGTTCTCAATAGCAACTAAGTTCTCAATAGCAAACTAAGATAGAAT$
phot1 <sup>CR3</sup>	$\tt CTCTTTCATTCAGAACATCTTCCCTCaTTCGAATTAAaCTTtcCACAACTAAGTTCTCAATAGCAGCAACTAAGTTCTCAATAGCAACTAAGTTCTCAATAGCAACTAAGTTCTCAATAGCAACTAAGTTCTCAATAGCAACTAAGTTCTCAATAGCAACTAAGTTCTCAATAGCAACTAAGTTCTCAATAGCAACTAAGTTCTCAATAGCAACTAAGTTCTCAATAGCAATAGA$
phot1 <sup>CR5</sup>	CTCTTTCATTCAGAACATCTTCCCTCaTTCGAATTAAaCTTtcCACAACTAAGTTCTCAATAGCAGCAA

# Off-target-4

WT	$ATCCATGAATGTTAATGTGTTGCCT\underline{GcGAAGtTTAATaCGAAGG}AGGGCACGAAGAAAAATGTGAGAAT$
phot1 <sup>CR2</sup>	ATCCATGAATGTTAATGTGTTGCCTGcGAAGtTTAATaCGAAGGAGGGCACGAAGAAAAATGTGAGAATGTAGAGAATGTGAGAATGTAGAATGTAGAATGTAGAGAATGTAGAGAATGTAGAGAATGTAGAGAATGTAGAGAATGTAGAGAATGTAGAGAATGTAGAGAATGTAGAGAATGTAGAGAATGTAGAGAATGTAGAGAATGTAGAATGAATGAATGAATGTAGAATGAATGAATGAATGTAGAAT
phot1 <sup>CR3</sup>	ATCCATGAATGTTAATGTGTTGCCTGcGAAGtTTAATaCGAAGGAGGGCACGAAGAAAAATGTGAGAATGTGAATG
phot1 <sup>CR5</sup>	ATCCATGAATGTTAATGTGTTGCCTGcGAAGtTTAATaCGAAGGAGGGCACGAAGAAAAATGTGAGAATGTAGAGAATGTGAGAATGTAGAGAAGA

# Off-target-5

WT	$TAGAGAAGCCCAAAGGGCCACTTGA\underline{GGcACTtCGgCCAaAGTTGC}\\TGGTATTACATCAATTTCGTTCCAT$
phot1 <sup>CR2</sup>	TAGAGAAGCCCAAAGGGCCACTTGAGGCACTtCGgCCAaAGTTGCTGGTATTACATCAATTTCGTTCCAT
phot1 <sup>CR3</sup>	TAGAGAAGCCCAAAGGGCCACTTGAGGCACTtCGgCCAaAGTTGCTGGTATTACATCAATTTCGTTCCAT
phot1 <sup>CR5</sup>	${\sf TAGAGAAGCCCAAAGGGCCACTTGAGGcACTtCGgCCAaAGTTGCTGGTATTACATCAATTTCGTTCCAT}$

# Off-target-6

WT	${\tt AATCCTAGATCTAGCCGCGCGTGAG} \underline{{\tt GGAtCTgCGACCAGcGaTGC}} {\tt TGGTTGGCCTTTGGTCGCTGGAGGT}$
phot1 <sup>CR2</sup>	A ATCCTAGATCTAGCCGCGCGTGAGGGAtCTgCGACCAGcGaTGCTGGTTGGCCTTTGGTCGCTGGAGGT
phot1 <sup>CR3</sup>	A ATCCTAGATCTAGCCGCGCGTGAGGGAtCTgCGACCAGcGaTGCTGGTTGGCCTTTGGTCGCTGGAGGT
phot1 <sup>CR5</sup>	${\tt AATCCTAGATCTAGCCGCGCGTGAGGGAtCTgCGACCAGcGaTGCTGGTTGGCCTTTGGTCGCTGGAGGT}$

# Off-target-7

WT	$\textbf{AGAAGTGATGGAGCGATGTTTCAAT} \underline{\textbf{GGAACTCCtAgCAGAGTgGa}} \textbf{GGGTGCAACTTTTGAGGCACTTGC}$
phot1 <sup>CR2</sup>	A GAAGTGATGGAGCGATGTTTCAATGGAACTCCt Ag CAGAGTgGaGGGTGCAACTTTTGAGGCACTTGC
phot1 <sup>CR3</sup>	A GAAGT GATGGAGCGATGTTT CAATGGAACTC C tAg CAGAGT g GaGGGTGCAACTTTT GAGGCACTTGC
phot1 <sup>CR5</sup>	AGAAGTGATGGAGCGATGTTTCAATGGAACTCCtAgCAGAGTgGaGGGTGCAACTTTTGAGGCACTTGC

**Figure 4.30.** A representative image showing the off-target sequencing results in *phot1*<sup>CR2, 3 & 5</sup>. Mutation patterns were examined in 7 most potential off-target sites for sgRNA1 (1-4) and sgRNA2 (5-7) by PCR amplification followed by sanger sequencing. Target sequence of potential off-target sites was underlined, with lowercase letters representing mismatches. Note that no off-target editing events were detected.

Several factors are known to affect off-target editing, such as the selection of gRNA, the number of mismatches between the targeted sequence and the gRNA, GC content of the selected gRNA, type of nuclease used for editing, delivery method of nuclease system in plants, etc. (Modrzejewski et al., 2020). The gRNA with up to 4 mismatches with the target sequence can be selected, and also, only those gRNAs are selected which do not have any predicted off-target effects in the coding sequence of un-targeted genes. This is done initially during the gRNA selection for making the CRISPR constructs by using CRISPR-P and CRISPOR web tools (please see methods for more details). In case no predicted off-targets can be avoided with the selected gRNA having the desired features, it is essential to rule out the presence of such off-target editing by sequencing the potential off-target sites in the edited transgene-free plants. This can be done by designing specific primers from the region surrounding the predicted off-target site, followed by PCR amplification of this site and Sanger sequencing. If no mutations are detected for all the predicted offtarget sites in this experiment, we can conclude that the edited plants have only the desired mutations. Such plants can be characterized in detail for further analyses.

The homozygous Cas9-free plants from *phot1*<sup>CR2</sup>, *phot1*<sup>CR3</sup>, and *phot1*<sup>CR5</sup> alleles were checked for unwanted editing by amplifying the off-target gene sequences predicted by CRISPR- P and CRISPOR web tools. Sanger sequencing of the amplified PCR products was carried out, and the obtained sequences were further analyzed by Chromas software compared to AV for off-target analysis. Our results revealed the absence of any off-target editing events in *phot1*<sup>CR2</sup>, *phot1*<sup>CR3</sup>, and *phot1*<sup>CR5</sup> alleles (Figure 4.30).

Based on the above experiments, three alleles,  $phot1^{CR2}$ ,  $phot1^{CR3}$ , and  $phot1^{CR5}$ , were characterized in detail at phenotypic, genotypic, functional, metabolite, and transcript levels. These alleles were also advanced to the next generation to finish the pending experiments that could not be completed in the  $T_2$  generation. For convenience sake, from now onwards, all further studies were carried out in  $phot1^{CR2}$ ,  $phot1^{CR3}$ , and  $phot1^{CR5}$  alleles that are homozygous, Cas9-free, and off-target-free in  $T_2/T_3$  generations.

# 4.7.2 Phototropism is affected in *phot1<sup>CR</sup>* alleles.

Phototropism is one of the fundamental movement responses of plants

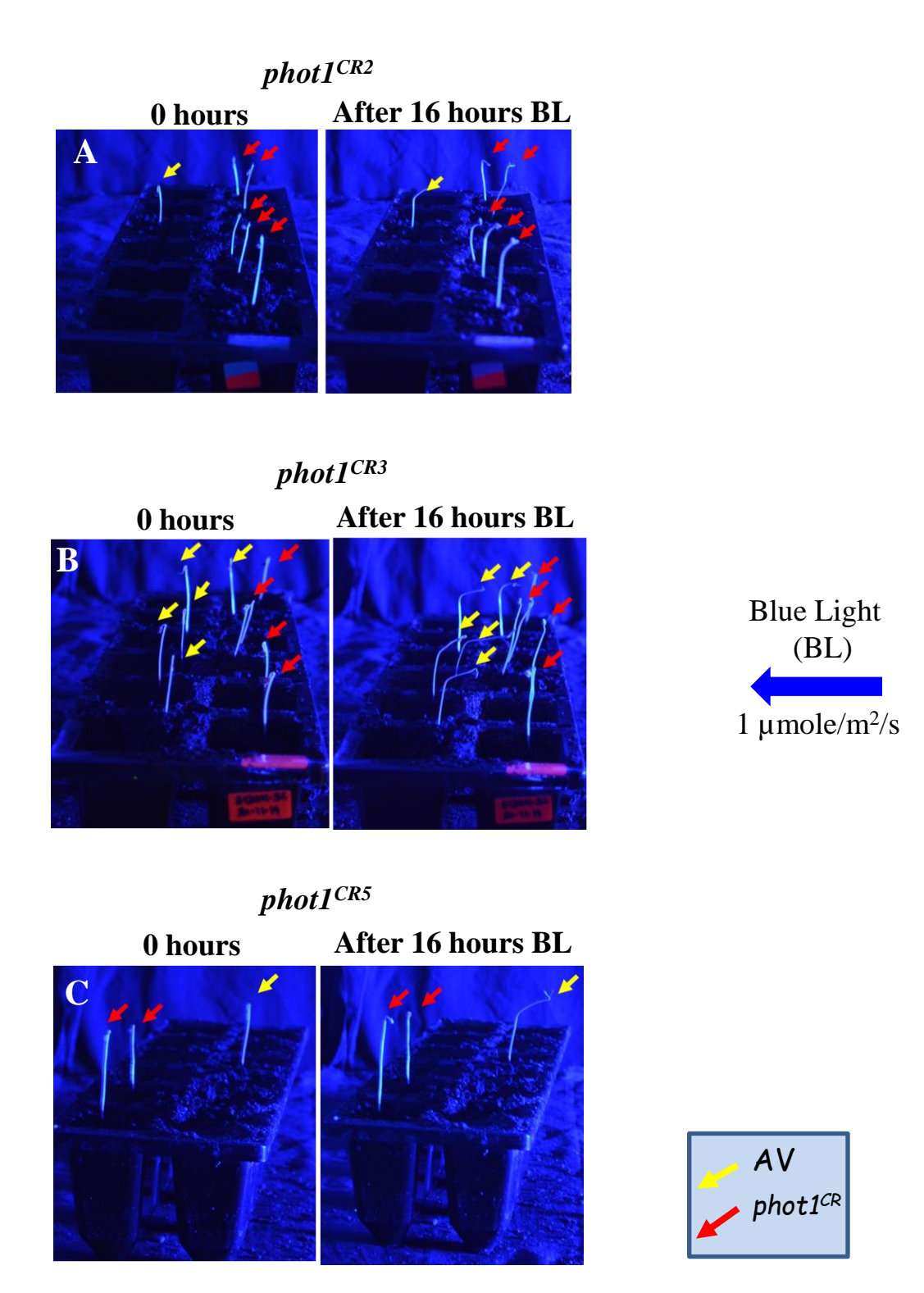


Figure 4.31. Screening for phototropism in  $phot1^{CR}$  alleles at the seedling stage. Seedlings are exposed to 1  $\mu$ mol/m²/s intensity of blue light. A, B and C shows  $phot1^{CR2}$ ,  $phot1^{CR3}$  and  $phot1^{CR5}$  along with AV seedlings. phot1 CRISPR seedlings though shows phototropism but the extent of the bending is reduced compared to AV seedlings. Red arrows indicate the phot1 CRISPR lines and yellow arrows indicate wild type (AV). Blue arrow indicate the direction of blue light and the direction.

towards the direction of light, and phototropins mediate this response. While *phot1* mediates low fluence phototropism, *phot2* is responsible for high fluence phototropism. Given that PHOT1 protein is affected by mutations, it was interesting to examine whether the low fluence phototropism is affected in *phot1*<sup>CR</sup> alleles. The 3-4-day old dark-grown seedlings of AV and *phot1*<sup>CR2</sup>, *phot1*<sup>CR3</sup>, and *phot1*<sup>CR5</sup> alleles were exposed to unilateral blue light of 0.3-1 μmol/m²/s fluence, and after 16 h, the seedlings were examined for any curvature towards blue light. As expected, AV seedlings showed nice curvature towards blue light, while the extent of curvature was affected in *phot1*<sup>CR</sup> alleles (Figure 4.31). More specifically, the extent of bending towards blue light was reduced in *phot1*<sup>CR2</sup> compared to AV, while the curvature was minimal in *phot1*<sup>CR3</sup> and *phot1*<sup>CR5</sup> than AV(Figure 4.31). This suggests that the *phot1* function in mediating low fluence phototropism is compromised in *phot1*<sup>CR</sup> alleles.

## 4.7.3 phot1<sup>CR</sup> alleles show reduced chloroplast accumulation

As phototropins mediate chloroplast relocation responses when exposed to low and high fluence blue light, it is necessary to confirm whether the partial loss of chloroplast accumulation response seen earlier in the T<sub>1</sub> generation is retained in the current generation plants. So, we analyzed chloroplast movement response in phot  $I^{CR}$  alleles. As seen in  $T_1$ , the chloroplast accumulation response mediated by phot1 in response to low fluence blue light was affected in the phot1<sup>CR2</sup>, phot1<sup>CR3</sup>, and phot1<sup>CR5</sup> alleles compared to AV (Figure 4.32A). The mean chloroplast relocation response showed about 40%, 52%, and 58% reduction in the chloroplast accumulation response in the phot1<sup>CR2</sup>, phot1<sup>CR3</sup>, and phot1<sup>CR5</sup> alleles, respectively, compared to AV. In addition, the chloroplast avoidance response mediated by *phot2* in response to high fluence blue light is also affected with a 45%, 50%, and 41% reduction in the mean avoidance response in the phot1<sup>CR2</sup>, phot1<sup>CR3</sup>, and phot1<sup>CR5</sup> alleles, respectively, compared to AV (Figure 4.32B). This suggests the interactions between different phototropins in mediating blue light-specific responses. Consistent with the inheritance of mutations, the loss of phot1 function is also inherited stably from  $T_0$  to  $T_1$ ,  $T_2$ , and  $T_3$  generations.

# 4.7.4 Plant morphology of *phot1<sup>CR</sup>* alleles

The plant phenotype of  $phot1^{CR2}$ ,  $phot1^{CR3}$ , and  $phot1^{CR5}$  alleles was recorded compared to AV at different stages of development-both vegetative and reproductive.



Figure 4.33. Comparision of plant phenotype of 90 day old  $phot1^{CR}$  alleles with wild type A, AV. B,  $phot1^{CR2}$ . C,  $phot1^{CR3}$ . D,  $phot1^{CR5}$ . Note that  $phot1^{CR2}$  and  $^3$  show dwarf phenotype compared to AV

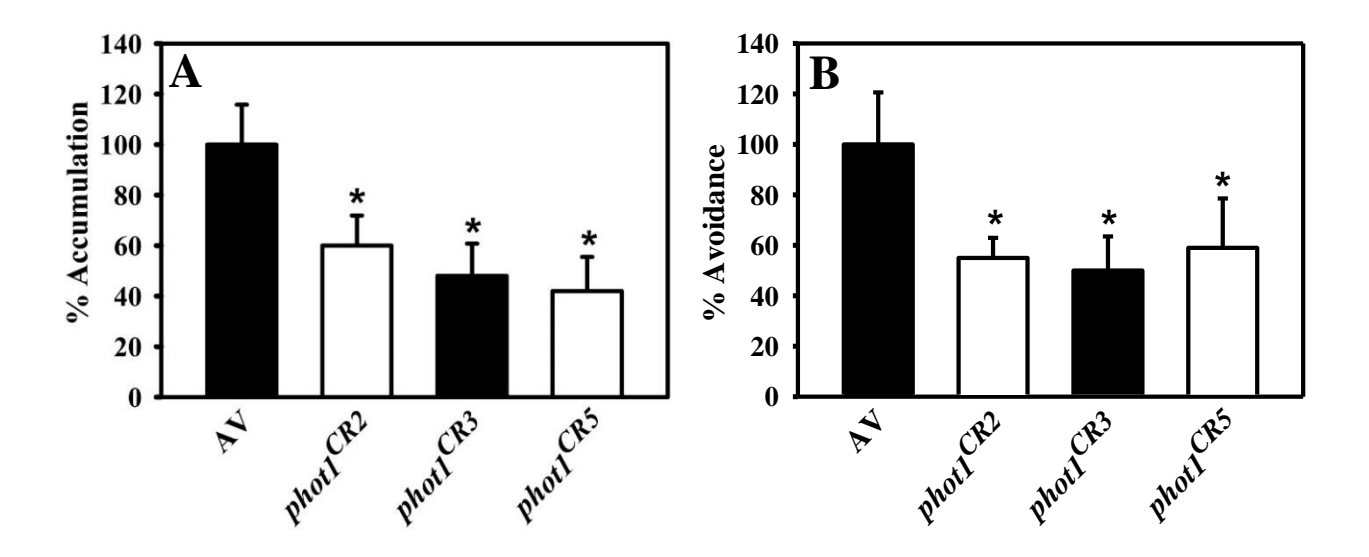


Figure 4.32. Assessment of loss phot1 function by monitoring the chloroplast movement in response to varying BL intensity. A, and B shows chloroplast movement analysis in  $phot1^{CR2}$ ,  $phot1^{CR3}$ , and  $phot1^{CR5}$  plants. Dark adapted tomato leaf discs were placed in 96 well microplate well in the dark, and then red light transmittance was recorded for 20 min for dark reading. The leaf discs were then irradiated sequentially with weak blue light (3.2  $\mu$ mol/m²/s) for 80 min for accumulation induction (Accumulation) and strong blue light (60-80  $\mu$ mol/m²/s) for 40 min each for avoidance induction (Avoidance). The blue light was given during the interval periods between red light transmittance measurements. % accumulation and avoidance was calculated with reference to positive control, AV. Note that chloroplast accumulation response mediated by phot1 is affected in the  $phot1^{CR}$  lines, suggesting impaired function of phot1. We could even see loss of avoidance movement in the stabilized lines of  $phot1^{CR}$  indicating impaired phot2 function. Each data point is a representation of the mean value  $\pm$ S.E of eight replicates.

The plant height of 2.5- month-old *phot1*<sup>CR2</sup>, *phot1*<sup>CR3</sup>, and *phot1*<sup>CR5</sup> alleles was substantially reduced compared to AV (Figure 4.33). A closer examination of the internodes and their lengths revealed that the reduction in the plant height is due to the shorter internodes in these alleles than AV (Figure 4.34 A, B, C and D).

# 4.7.5 Leaf morphology is altered in *phot1<sup>CR</sup>* alleles.

Light interception is very crucial for plant growth and development. Plants use tropic movements to adjust the position of leaves and petioles to maximize light absorption. While the changes in stem curvature are responsible for the directional growth of the plant, petiole curvature influences the directional growth of individual leaves. In addition, leaf shape, expansion, and flattening are also mediated by phototropins. To examine the influence of *phot1* on leaf morphology leaves from the 10<sup>th</sup> node of the 2.5-month-old plants of *phot1*<sup>CR2</sup>, *phot1*<sup>CR3</sup>, and *phot1*<sup>CR5</sup> alleles were compared with AV (Figure 4.35). At first glance, it is apparent that all the *phot1*<sup>CR</sup> alleles show variation in leaf morphology compared to AV. More specifically, compared to AV, the leaves of the *phot1*<sup>CR2</sup> allele are flat and light in color with more leaflets, while in *phot1*<sup>CR3</sup>, the leaves are lighter with a similar leaflet number to that of AV. In the *phot1*<sup>CR5</sup> allele, leaves were curled slightly than AV, while the number of leaflets and color appear identical to AV. This suggests that *phot1* affects leaf morphology, albeit with variations in different alleles.

### 4.7.6 Phototropin1 affects leaf chlorophyll and carotenoid contents.

Carotenoids and chlorophyll are the dominant pigments of the photosynthetic apparatus and are part of light-harvesting complex. Carotenoids help channel high energy from chlorophyll to protect from excess light. Carotenoids are also essential for maximizing carbon fixation. Given the variation seen in the leaf color, we examined the chlorophyll and carotenoid contents of the leaves of  $phot1^{CR}$  alleles. Estimation of chlorophyll a and b from the  $10^{th}$  node leaf of 2.5-month-old plants revealed lower levels in  $phot1^{CR2}$  and  $phot1^{CR3}$  than AV while the chlorophyll a was similar to AV, chlorophyll b content in  $phot1^{CR5}$  was slightly higher than that of AV leaves (Figure 4.36). As expected, this difference was also reflected in the total chlorophyll content, which was lower in  $phot1^{CR2}$  and  $phot1^{CR3}$  alleles and similar to AV in the  $phot1^{CR5}$  allele.

The individual carotenoid profiling in the 10<sup>th</sup> node leaf of 2.5-month-old

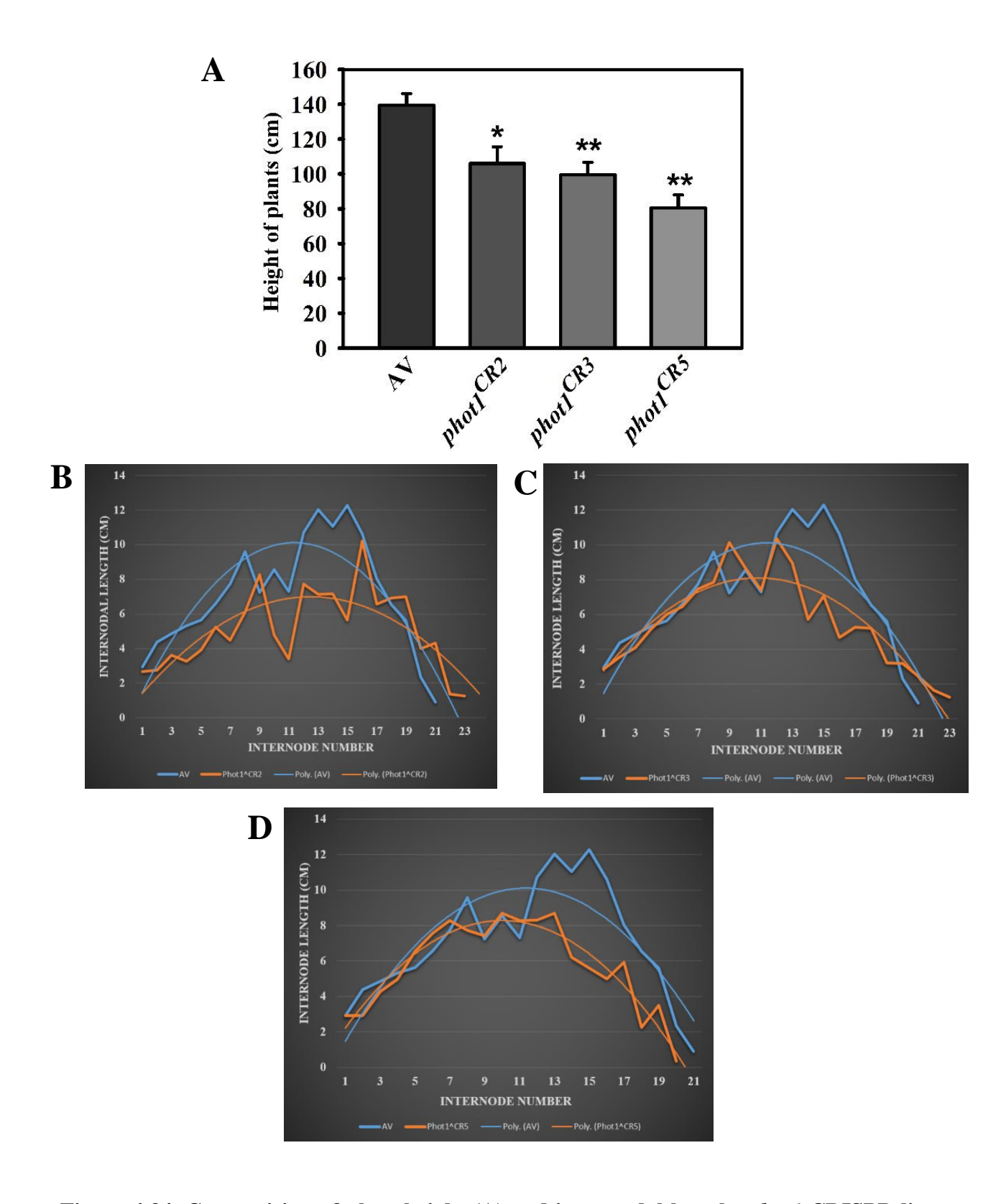


Figure 4.34. Comparision of plant height (A) and intermodal lengths *phot1* CRISPR lines with wild type. A, Plant height (3 month old) is reduced in all the *phot1*<sup>CR</sup> alleles. B, C and D show reduced intermodal length in the *phot1*<sup>CR2, 3 and 5</sup>. Data are means  $\pm$ SE (n=5-10 plants). \*P  $\leq 0.05$ , \*\*P  $\leq 0.01$  and \*\*\*P  $\leq 0.001$ .

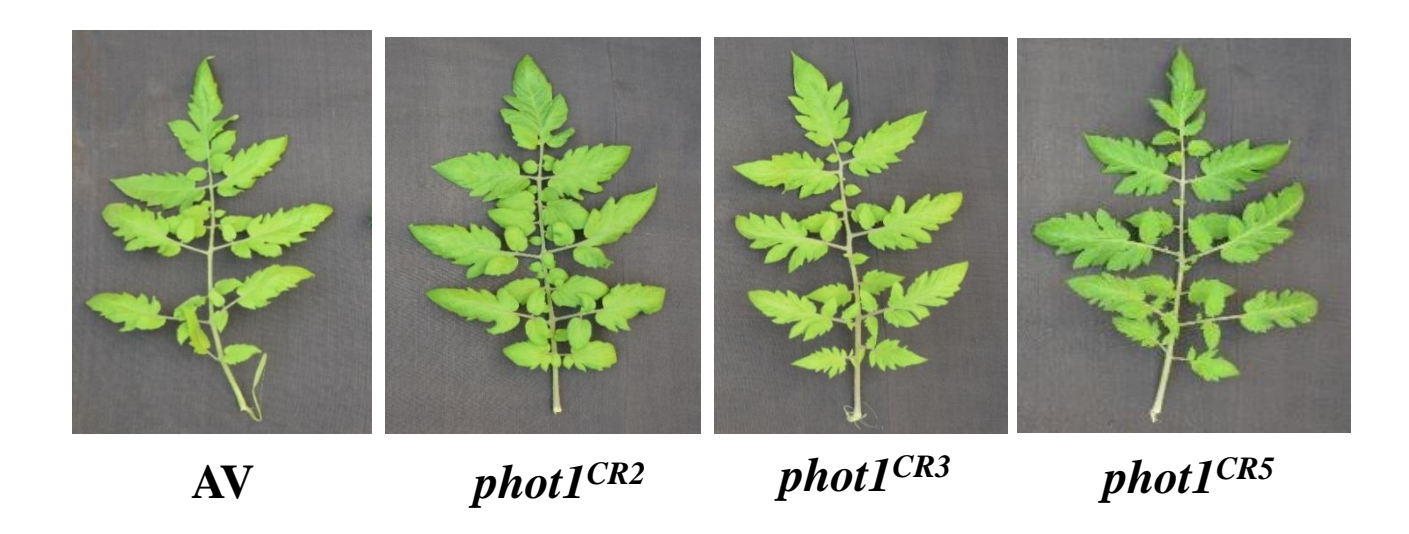


Figure 4.35. Comparision of leaf morphology. The  $10^{\rm th}$  node leaf from the 3 month old plants was examined for any morphological changes. Note that  $phot1^{CR2}$  exhibits more leaflets than AV, while  $phot1^{CR3}$  & 5 are similar to AV.

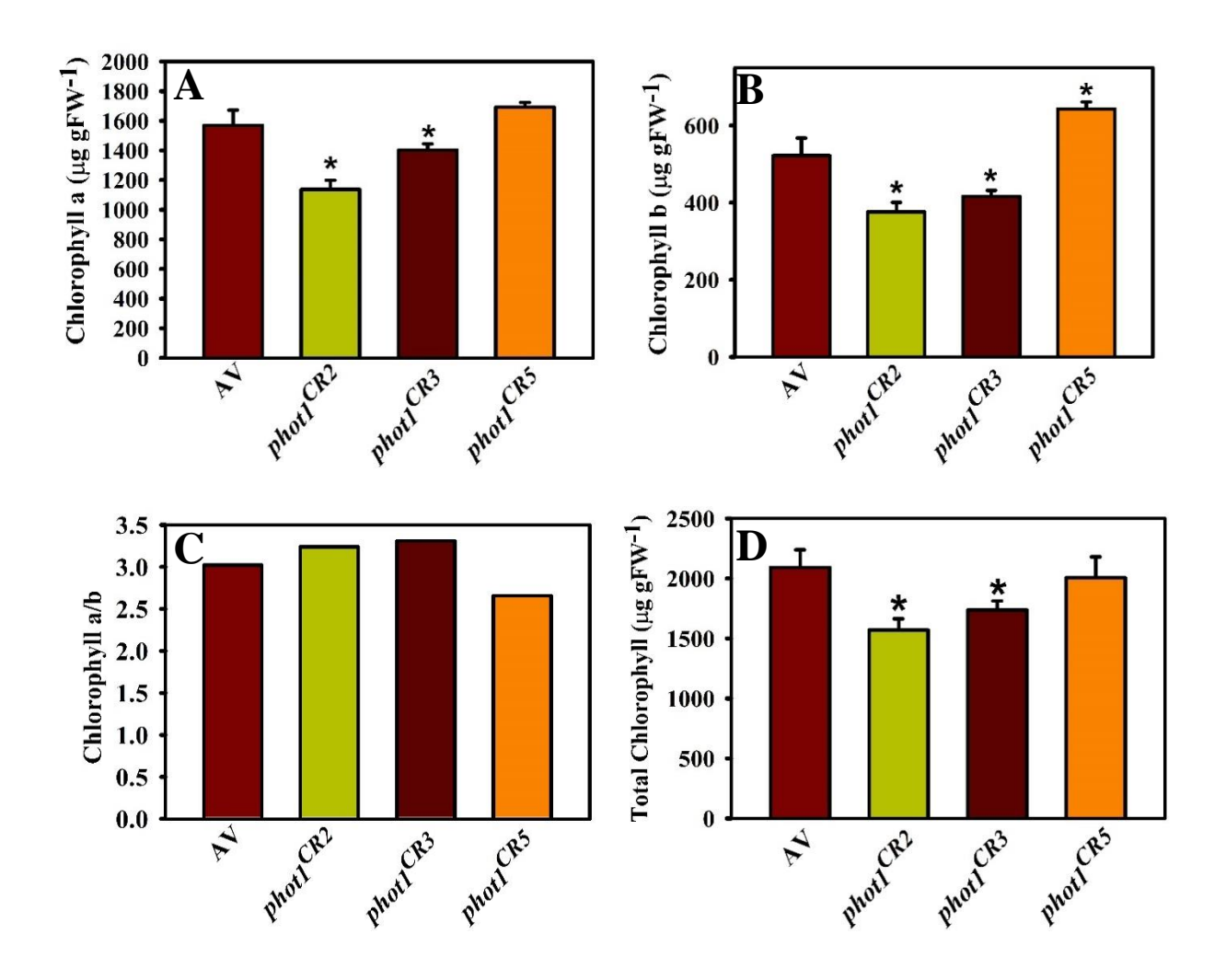


Figure 4.36. Comparision of chlorophyll content from the  $11^{th}$  node of 3 month old plants. A, shows Chla content which is lower in  $phot1^{CR2 \text{ and } 3}$  but similar to AV in  $phot1^{CR5}$ . B, shows Chlb content, which is lower in  $phot1^{CR2 \text{ and } 3}$  but higher in  $phot1^{CR5}$  than AV. C, shows Chla/b ratio, which is similar in all alleles. D, shows total chlorophyll content in all alleles  $phot1^{CR2 \text{ and } 3}$  showed reduction, while  $phot1^{CR5}$  is similar to AV. Data are means  $\pm$ SE (n=5-10 leaves). \*P  $\leq$  0.05, \*\*P  $\leq$  0.01 and \*\*\*P  $\leq$  0.001.

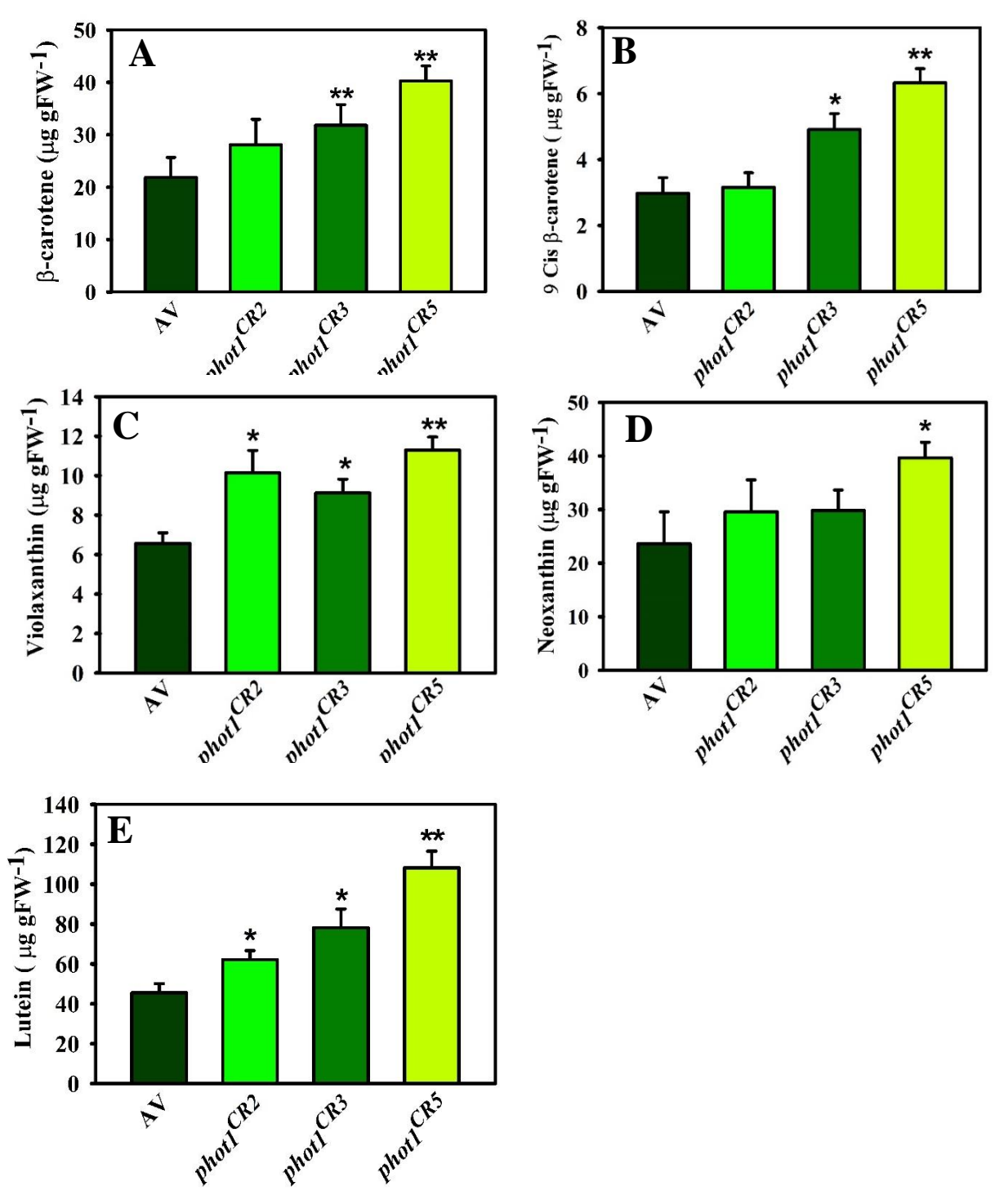


Figure 4.37. Comparision of carotenoid content of leaves (A-E) of  $11^{th}$  node of 3 month old plants in phot CRISPR alleles. A, β-carotene content in all the alleles except in  $phot1^{CR2}$  allele. B, shows higher 9 Cis-β-carotene content in all the alleles except in  $phot1^{CR2}$  allele. C, shows higher violaxanthin content in all the alleles. D, shows higher neoxanthin content in  $phot1^{CR5}$ . E, shows higher lutein content compared to wild type plants in all the alleles. Data are means  $\pm$ SE (n=5-10 leaves). \*P < 0.05, \*\*P < 0.01 and \*\*\*P < 0.001.

plants of AV and  $phot1^{CR}$  alleles (Figure 4.37) was carried out, and it revealed interesting differences. The dominant carotenoids in the leaves were β-carotene, neoxanthin, and lutein. However, the levels of violaxanthin and 9-Cis-β-carotene contents were much lower than these carotenoids. A significant increase in lutein and violaxanthin was observed in all three  $phot1^{CR}$  alleles. Also, the levels of "β- carotene and 9-Cis-β-carotene" increased in all the lines except the  $phot1^{CR2}$  (similar to AV), while neoxanthin content was similar to AV in  $phot1^{CR2}$  and  $phot1^{CR3}$  and higher in  $phot1^{CR5}$  than AV. The total carotenoid content was significantly elevated in the leaves of all the  $phot1^{CR}$  alleles.

# 4.7.7 Fruit development is altered in *phot1<sup>CR</sup>* alleles.

As photoreceptors are known to influence fruit development, ripening, and associated pigmentation, it was interesting to examine the same in the  $phot1^{CR}$  alleles. The flowers were tagged at the time of anthesis in AV and in  $phot1^{CR}$  alleles, and the fruit development and ripening were monitored carefully by visual examination of the fruits daily. Compared to AV, the fruits of all the three  $phot1^{CR}$  alleles required seven days longer post-anthesis to reach the mature green (MG) stage (Figure 4.38). After that, the transition of MG to breaker (BR) stage required a shorter duration in all the three  $phot1^{CR}$  alleles than AV. Further transition of BR to red ripe (RR) stage was extended in all the three  $phot1^{CR}$  alleles than AV.

## 4.7.8 Ethylene and CO<sub>2</sub> emissions from the fruits of *phot1<sup>CR</sup>* alleles

As tomato is a climacteric fruit, the rate of ethylene emission and respiration influence fruit development and ripening. As the fruit development and ripening were delayed in the fruits of *phot1*<sup>CR</sup> alleles, it is expected that the ethylene and CO<sub>2</sub> emission would be lower in these fruits than in AV. However, no difference was observed in the ethylene emission at MG and BR stages in the fruits of AV and *phot1*<sup>CR</sup> alleles, while a slight reduction in the ethylene emission was observed at RR in *phot1*<sup>CR3</sup> and *phot1*<sup>CR5</sup> than AV but not in *phot1*<sup>CR2</sup> (Figure 4.39A). Consistent with this, almost comparable levels of CO<sub>2</sub> were emitted from the fruits of AV and *phot1*<sup>CR</sup> alleles (barring *phot1*<sup>CR2</sup> and *phot1*<sup>CR5</sup> at MG) at MG and BR, with a slight reduction at RR in all three alleles (Figure 4.39B). Based on this, ethylene emission appears not correlated to fruit development and ripening in *phot1*<sup>CR</sup> alleles.

# 4.7.9 Acid and sugar levels in RR fruits of phot1<sup>CR</sup> alleles

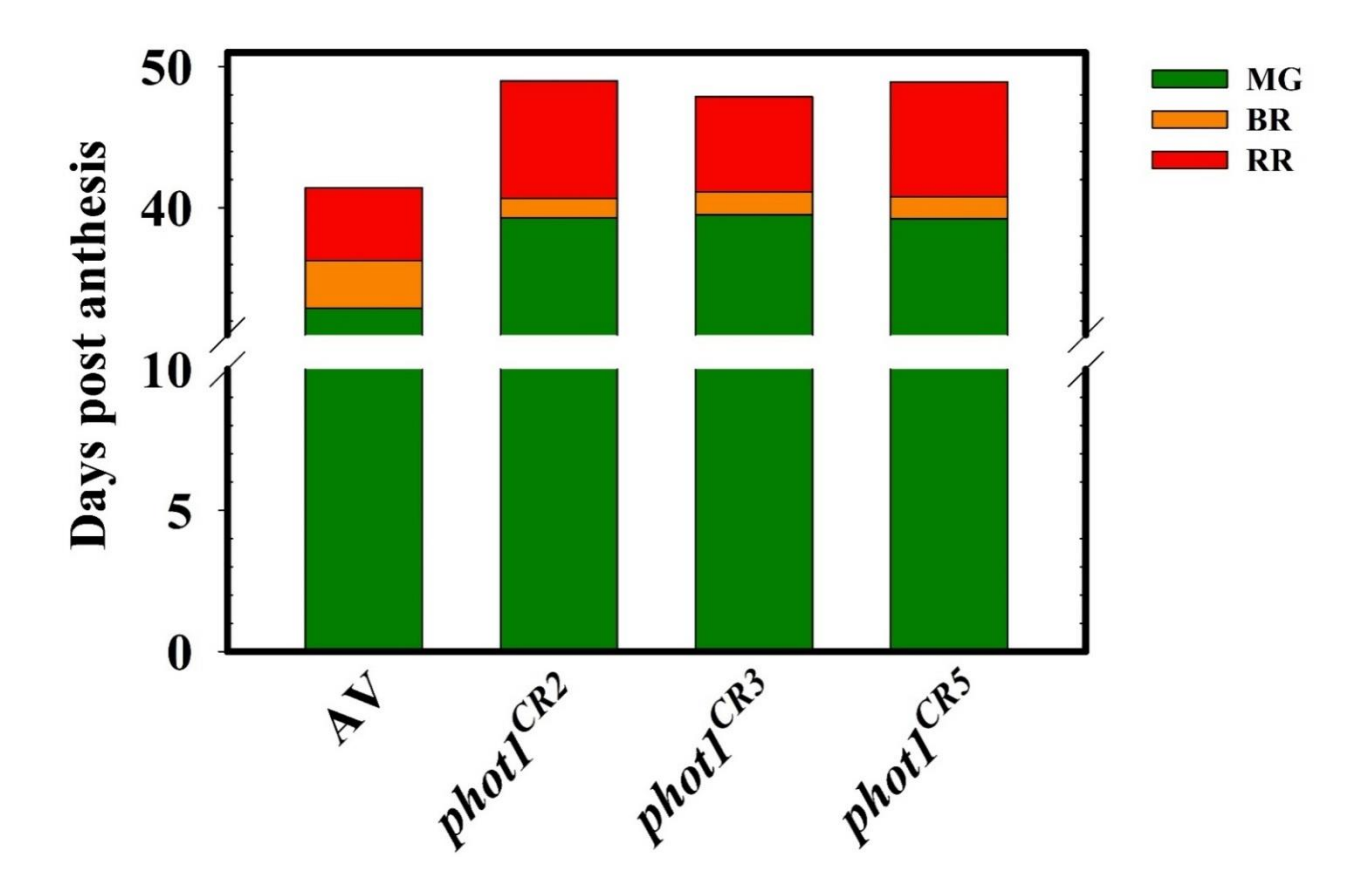


Figure 4.38. Chronological fruit development during ripening in AV and *phot1*<sup>CR</sup> lines. Data are means  $\pm$ SE (n=15 for each ripening stage). AV-32 DPA, *phot1*<sup>CR2,3 & %</sup> -39 DPA for MG, AV-3.3 DPA, *phot1*<sup>CR2,3 & %</sup> -1.5 DPA for BR, AV-5.1 DPA, *phot1*<sup>CR2,3 & %</sup> -7.2 DPA for RR.

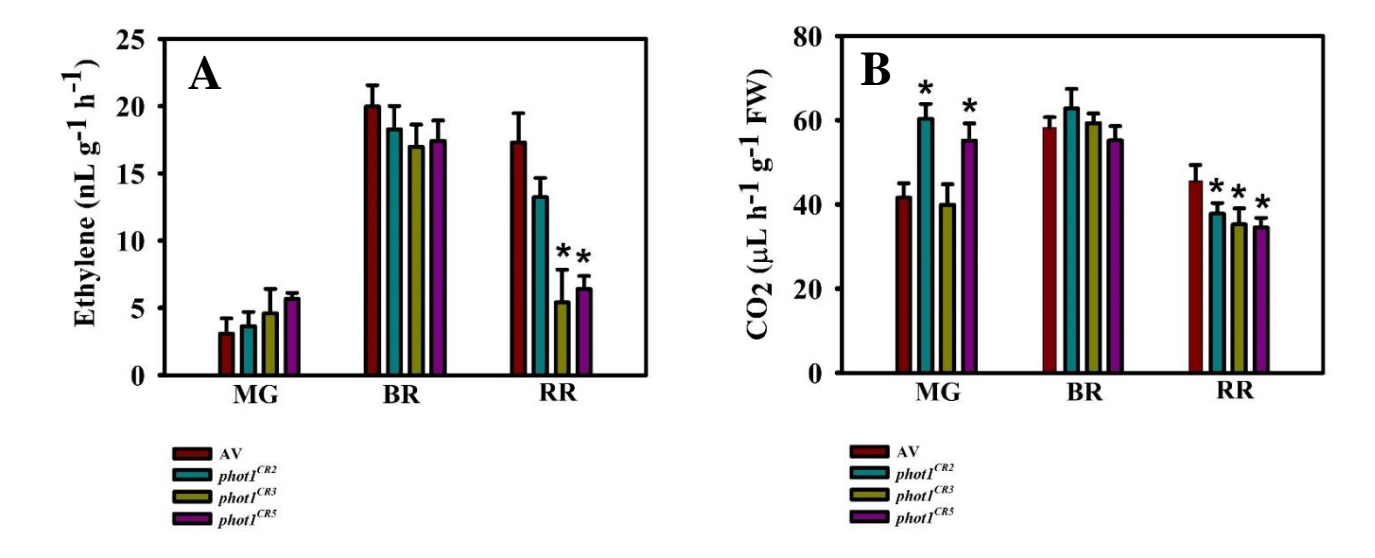
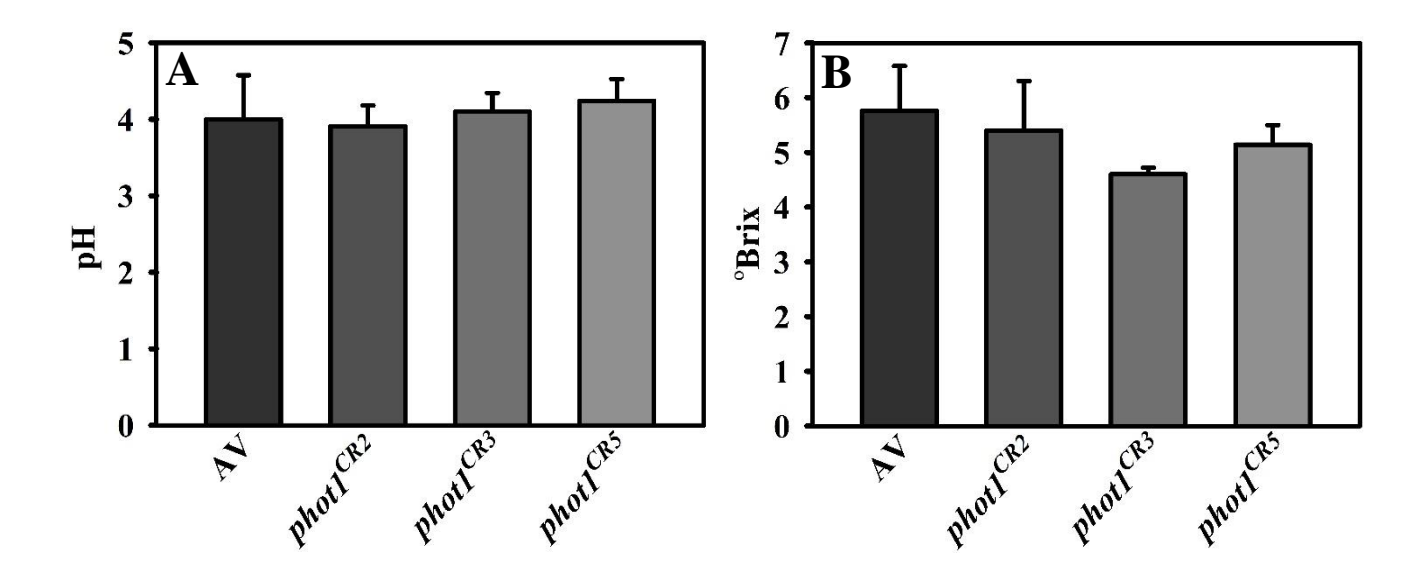


Figure 4.39. Emission of ethylene and  $CO_2$  from the ripening fruits of AV and  $phot1^{CR}$  lines. Fruits were collected at MG, BR and RR stages from AV and  $phot1^{CR}$  lines. Ethylene (A) and  $CO_2$  (B) emission were recorded. Data are means  $\pm SE$  (n=3-5 fruit for each ripening stage). P value \*  $\leq 0.05$ , \*\*  $\leq 0.01$ , \*\*\*  $\leq 0.001$ 



**Figure 4.40.** Measurement of pH (A) and °Brix (B) in red ripe fruits of AV and *phot1*<sup>CR</sup> lines. Data are means  $\pm$ SE (n=5 fruits). \*P  $\leq$  0.05, \*\*P  $\leq$  0.01 and \*\*\*P  $\leq$  0.001.

As °Brix and pH affect the fruit taste and quality, it was interesting to examine if *phot1* affects these parameters. Similar to *phot2*, no influence of *phot1* was observed on the pH and °Brix of the red ripe fruits of *phot1*<sup>CR</sup> alleles (Figure 4.40), as no variation was observed from AV fruits.

## 4.7.10 phot1 mutants show decreased carotenoid levels in fruits

During tomato fruit ripening, red color development is associated with increased carotenoid levels, mainly lycopene and  $\beta$ -carotene. Several reports have indicated that the ripening burst of ethylene is associated with the increased expression of psyl, which may contribute to an increase in lycopene accumulation via phytoene and phytofluene (Bramley, 2002; Giovannoni, 2007). As Npsl mutant is dominant-negative and its fruits show high carotenoids, especially lycopene content at the ripe stage, it was interesting to know whether loss of photl function affects the fruit carotenoid content.

Examination of carotenoid levels in the fruits of AV and  $phot1^{CR}$  alleles at different ripening stages revealed the following. At the MG stage, phytoene, phytofluene, lycopene, and  $\alpha$ - carotene were undetected in AV and  $phot1^{CR}$  alleles (Figure 4.41). While  $\beta$ -carotene, violaxanthin, and neoxanthin (barring  $phot1^{CR2}$ ) levels were similar in AV and  $phot1^{CR}$  alleles at MG, lutein levels were higher in the  $phot1^{CR}$  alleles than in AV. Like MG, phytoene, phytofluene, lycopene, and  $\alpha$ -carotene were below the detection limits in AV and  $phot1^{CR}$  alleles at the BR stage. At the same time, lutein, violaxanthin, and neoxanthin levels were higher in the  $phot1^{CR}$  alleles than in AV. However,  $\beta$ -carotene levels were similar in AV and  $phot1^{CR3}$  while low in  $phot1^{CR2}$  and  $phot1^{CR5}$  alleles. At the RR stage, all the carotenoids, i.e., phytoene, phytofluene, lycopene,  $\beta$ - carotene,  $\alpha$ -carotene, and lutein (barring  $phot1^{CR2}$ ) were lower in abundance in the  $phot1^{CR}$  alleles than AV (Figure 4.42). This suggests that, similar to phot2, phot1 also acts as a positive regulator for carotenogenesis.

# 4.7.11 Carotenogenic gene expression is not correlated to carotenoid content in *phot1*<sup>CR</sup> alleles.

As dxs encodes the rate-limiting enzyme for the MEP pathway, psy1 is rate limiting for lycopene formation, and cycb is critical for  $\beta$ -carotene content, we examined the gene expression for all these in the ripening fruits of  $phot1^{CR}$  alleles

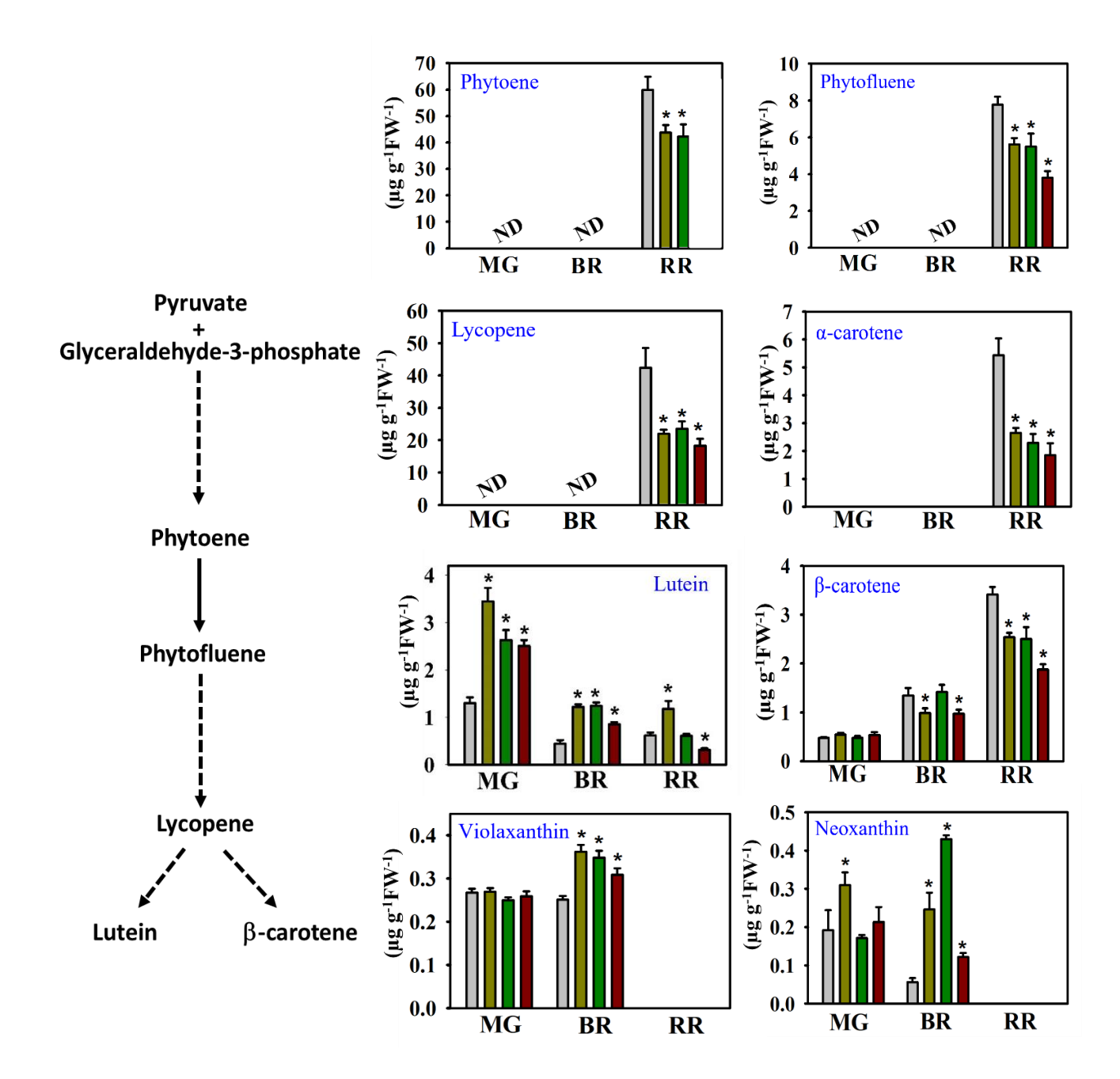


Figure 4.41. Comparision of carotenoid content of fruits of phot CRISPR alleles at three different stages of development. Data are means  $\pm SE$  (n=5-10 leaves). \*P  $\leq$  0.05, \*\*P  $\leq$  0.01 and \*\*\*P  $\leq$  0.001.

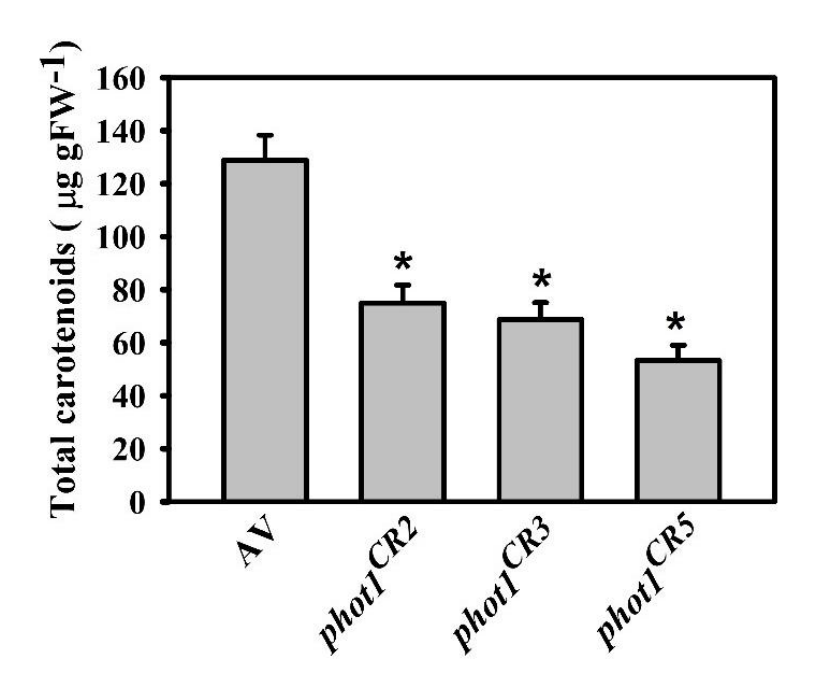


Figure 4.42. Total carotenoid content of red ripe stage fruits of *phot1<sup>CR</sup>* alleles.

Carotenoid content are presented as  $\mu g/g$  fresh weight. Student's *t*-test was used to calculate the significant difference between AV and *phot1*<sup>CR</sup> lines. Data are the means of 6-8 biological replicate  $\pm$ SE. The P values <0.05, <0.01 and <0.001 were indicated by one, two and three asterisks respectively.

# Pyruvate + Glyceraldehyde-3-phosphate

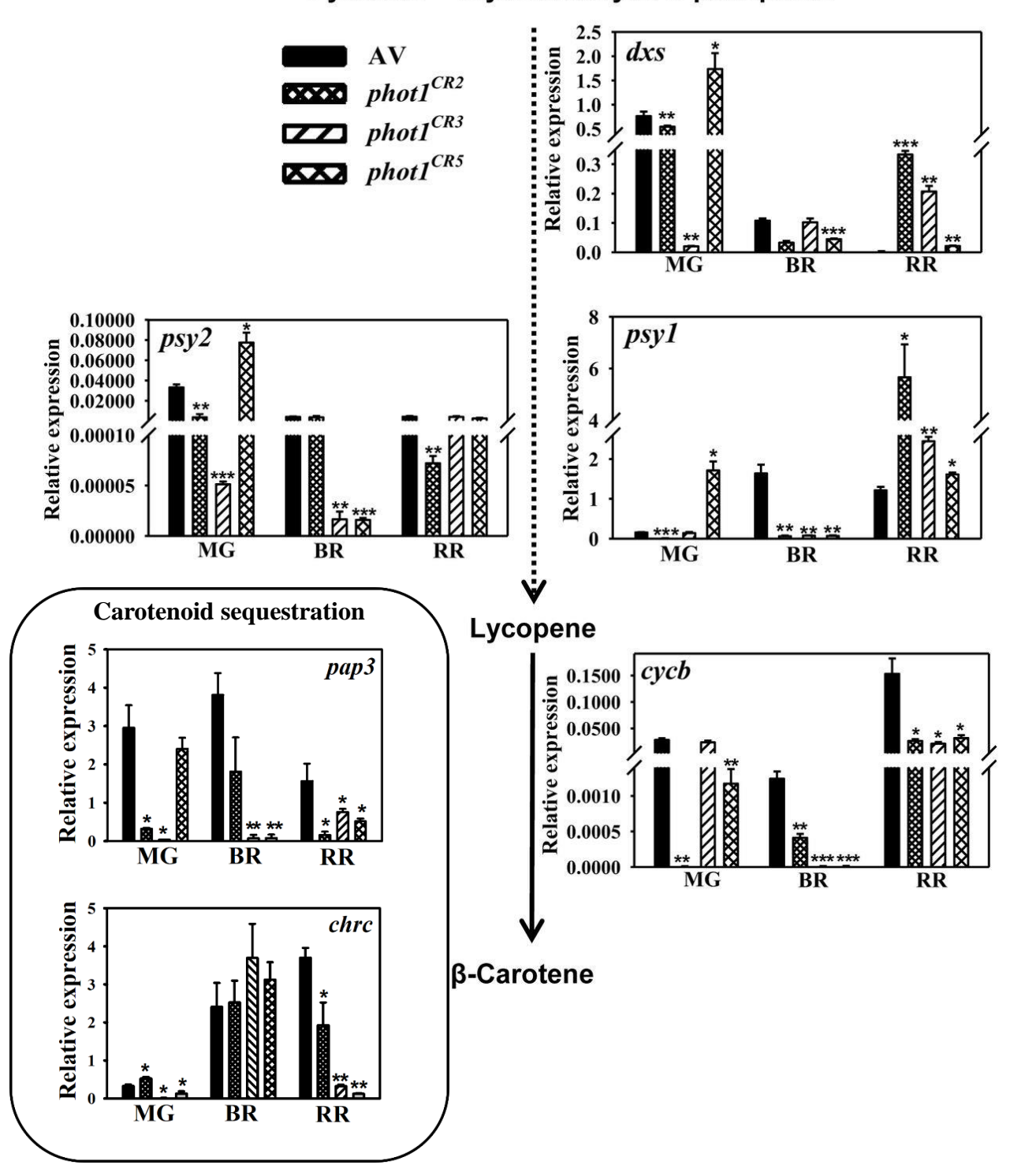


Figure 4.43. qRT-PCR based expression profiling of rate limiting genes of carotenoid biosynthesis and carotenoid sequestration genes in ripening fruits of AV and *phot1*<sup>CR</sup> lines. The graphs indicate relative expression of genes obtained after normalization with  $\beta$ -actin and ubiquitin. Data are means  $\pm$ SE (n=3). \*P  $\leq$  0.05, \*\*P  $\leq$  0.01 and \*\*\*P  $\leq$  0.001.

and AV (Figure 4.43). In addition, we also checked the expression of leaf-specific psy2. At MG and BR stages, the expression of dxs (barring  $phot1^{CR5}$ ), psy1 (barring  $phot1^{CR5}$ ), psy2 (barring  $phot1^{CR5}$ ), and cycb was either similar to or lower

than AV in the  $phot1^{CR}$  alleles (Figure 4.43). However, at the RR stage, the expression of dxs and psy1 was very high in  $phot1^{CR}$  alleles than in AV, while that of psy2 remained similar or lower than in AV (Figure 4.43). The expression of cycb was lower in all the  $phot1^{CR}$  alleles than AV at the RR stage (Figure 4.43). This suggests the absence of correlation between the expression of crucial genes-dxs and psy1 and carotenoid content. In addition, the contribution of psy2 towards fruit carotenoid content also appears to be minimal. However, a weak correlation could be seen between cycb expression and  $\beta$ -carotene content. All these results suggest that in phot1 mutants, carotenogenesis may be regulated post-transcriptionally.

### 4.7.11.1 Mutations in *phot1* down-regulate the carotenoid sequestration genes.

CHRC and PAP3 are the proteins involved in carotenoid sequestration, and their gene expression, as well as protein abundances, were correlated with carotenoid contents in mutants/lines exhibiting high carotenoid content in fruits in earlier studies from our lab (Kilambiet al., 2013; Kilambi et al., 2017; Kilambi et al., 2021). Expression analysis of *chrc* and *pap3* in AV and *phot1*<sup>CR</sup> alleles was conducted to examine the correlation with carotenoid levels (Figure 4.43). Consistent with lower carotenoid levels in *phot1*<sup>CR</sup> alleles than AV, the *chrc* and *pap3* expression were lower or similar to AV at all ripening stages (barring *phot1*<sup>CR2</sup> at MG), with significant downregulation at the RR stage. This suggests a direct correlation between carotenoid content and the expression of carotenoid sequestration genes.

## **4.7.12** *phot1* mutations affect the primary metabolite levels

The onset of ripening in tomato triggers massive metabolic shifts, which ultimately results in increasing the flavor, taste, and palatability of the fruits. Several factors, both external (light, temperature, disease, etc.) and internal (hormones, stress, etc.), influence the above process. Given that Nps1, a dominant negative mutant of phot1, affected the fruit metabolome drastically (Kilambi et al., 2021); we checked the influence of phot1 on the primary metabolome of ripening fruits in AV and  $phot1^{CR}$  alleles. GC-MS analysis in the fruits of AV and  $phot1^{CR}$  alleles at

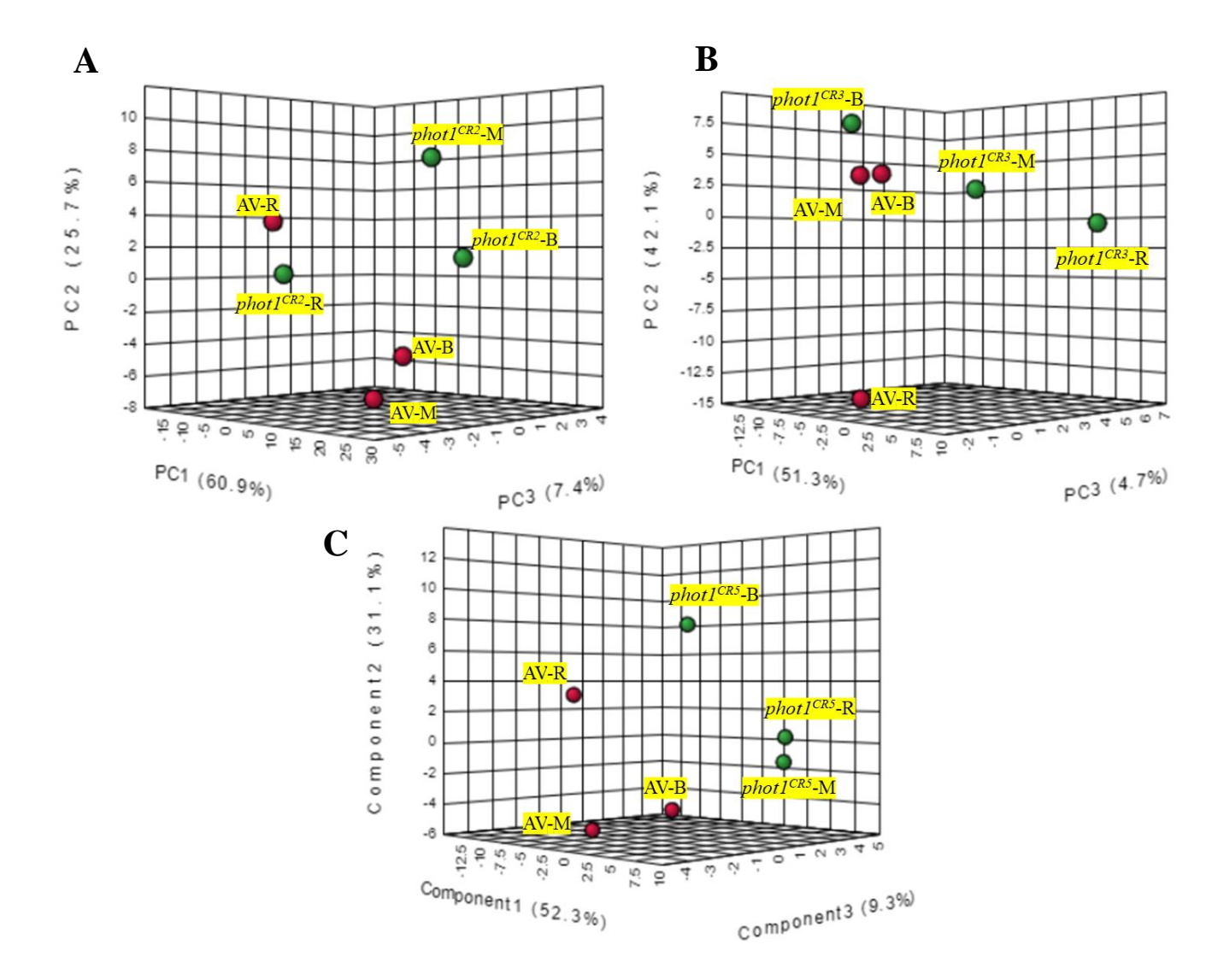


Figure 4.44. The principal component analysis (PCA) of metabolites during different stages of ripening in phot1 CRIPSR lines. Data are means  $\pm$  SE (n=5-8) for each ripening stage.

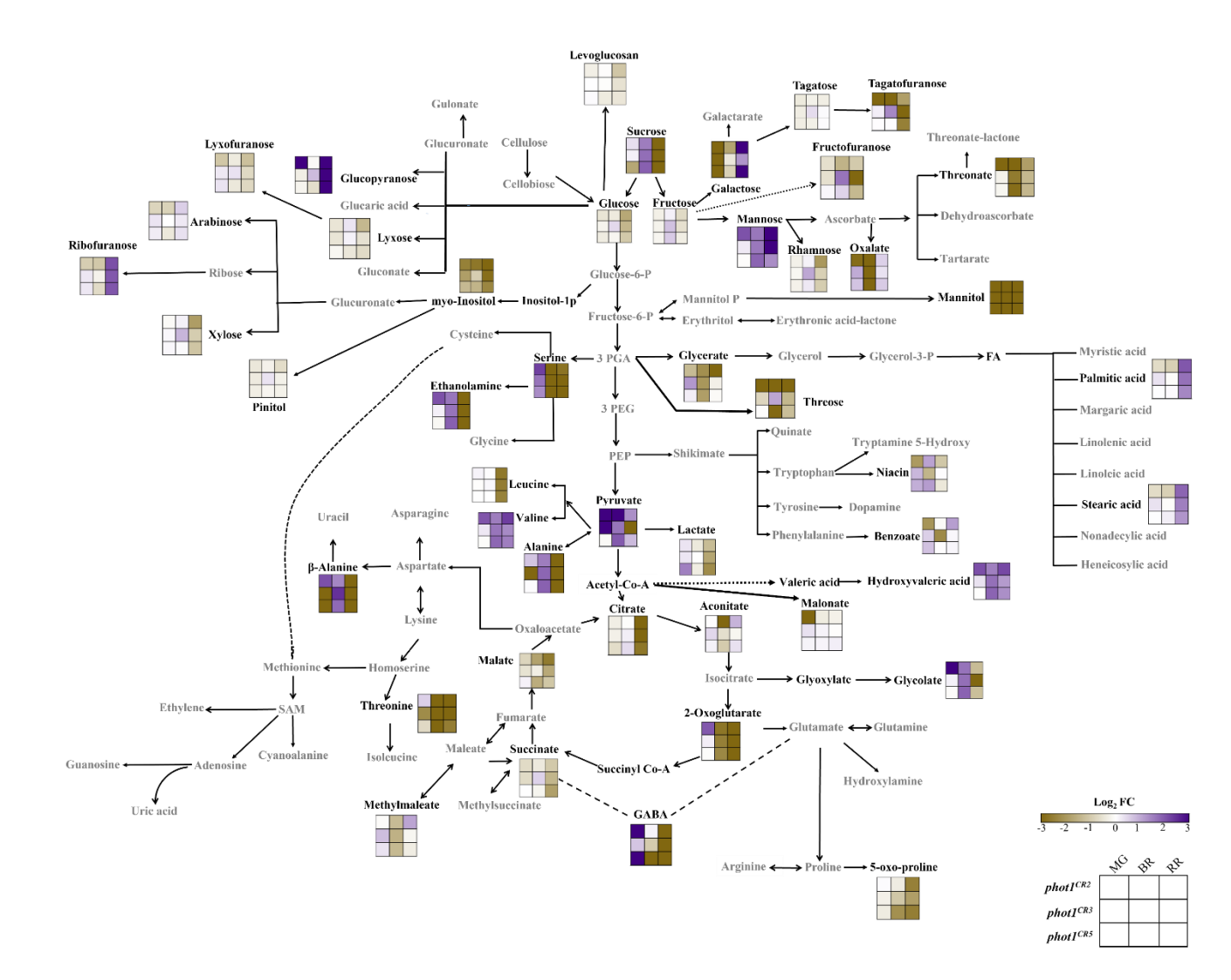


Figure 4.45. The metabolic shifts observed in the ripening fruits of *phot1* CRISPR lines during ripening in comparison to AV. An overview of metabolic pathways representing relative abundance of metabolites at different ripening stages in fruits of WT,  $phot1^{CR2}$ ,  $phot1^{CR3}$ , and  $phot1^{CR5}$  lines is shown. The Y-axis represents the log2 Fold change in metabolites with reference to internal standard ribitol. X-axis denotes metabolite levels at MG-mature green, BR-breaker, and RR-red ripe stages. Data are means  $\pm$ SE (n=5-8). Only those metabolites that are statistically significant minimum 2-fold change are shown here.

different ripening stages led to identifying about 63 metabolites grouped into different chemical classes based on their functional groups. PCA plots revealed vast differences between the metabolite profiles of AV and *phot1*<sup>CR</sup> alleles at different ripening stages, and minimal overlap was observed (Figure 4.44). Like carotenogenesis, we found that the loss of *phot1* function influenced the primary metabolome (Figure 4.45).

Examination of metabolite profiles in the fruits of AV and  $phot1^{CR}$  alleles at different ripening stages revealed significant changes during the transition from BR to RR stage. In contrast, only a minimal difference was observed from MG to BR transition. Among the nine amino acids detected and quantified, only valine was abundant in the  $phot1^{CR}$  alleles, while the rest were downregulated than AV at the RR stage (Figure 4.46A). Similarly, among the 19 organic acids detected, most organic acids, including TCA cycle intermediates like citrate,  $\alpha$ -ketoglutarate, succinate, malate, etc., were downregulated in  $phot1^{CR}$  alleles than AV (Figure 4.46B). The only exception was aconitate, which was higher in  $phot1^{CR2}$  (at RR stage) but similar to AV in the other two alleles. Among 22 sugars identified, most of the sugars were downregulated in the  $phot1^{CR}$  alleles than AV at the RR stage (Figure 4.46C). This includes sucrose, glucose, and fructose which contribute to the sweetness of tomato fruits. Based on the above, there appears to be a vast influence of phot1 on tomato metabolome in the ripening fruits.

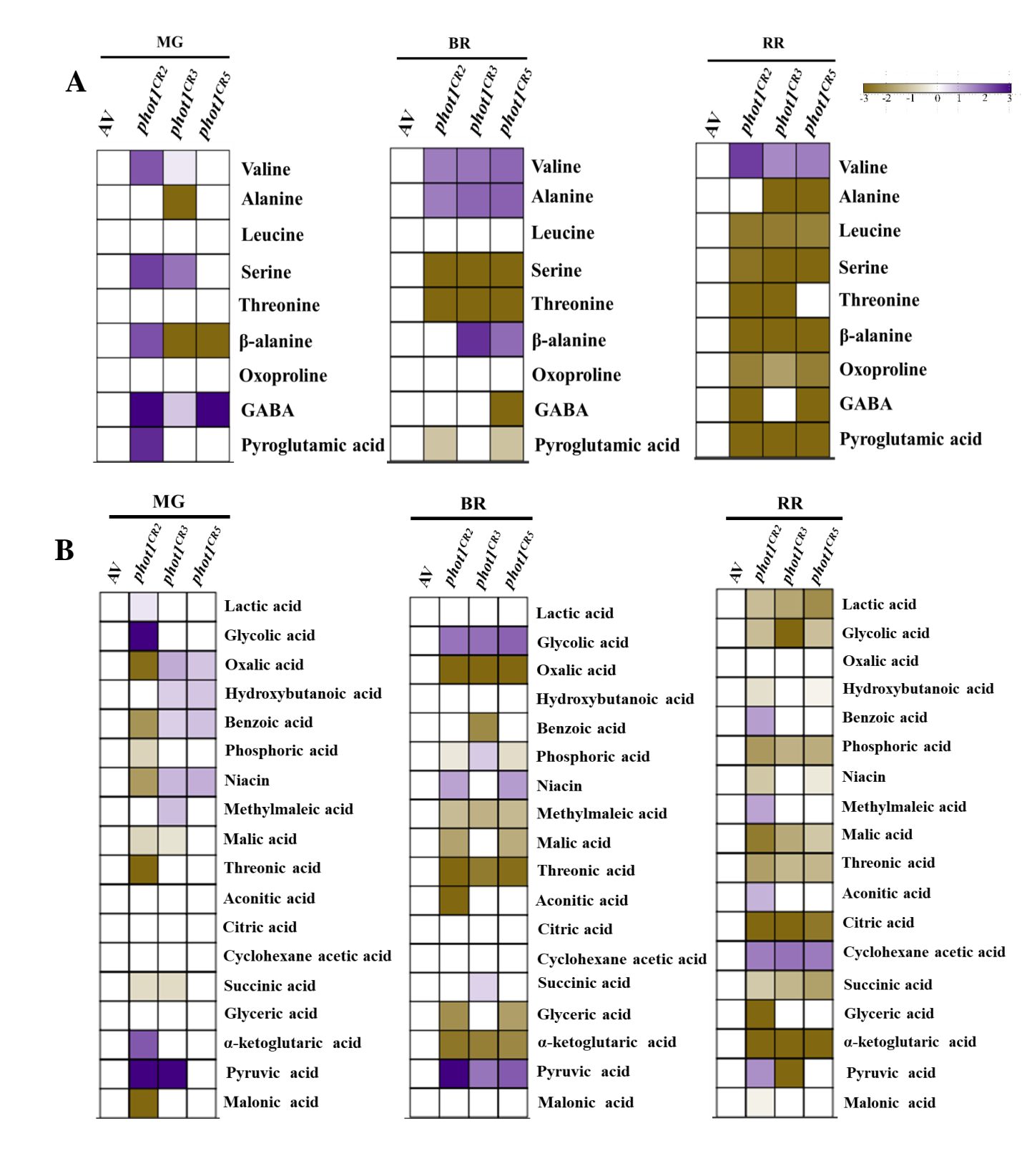


Figure 4.46 Primary metabolites level in ripening fruits of AV and *phot1* CRISPR lines fruits during ripening. Data are means  $\pm$ SE (n=5-8). Only those metabolites that are statistically significant minimum 2-fold change are shown here. A, amino acids. B, Organic acids.

C

Figure 4.46 Primary metabolites level in ripening fruits of AV and *phot1* CRISPR lines fruits during ripening. Data are means  $\pm$  SE (n=5-8). Only those metabolites that are statistically significant minimum 2-fold change are shown here. C, Sugars.

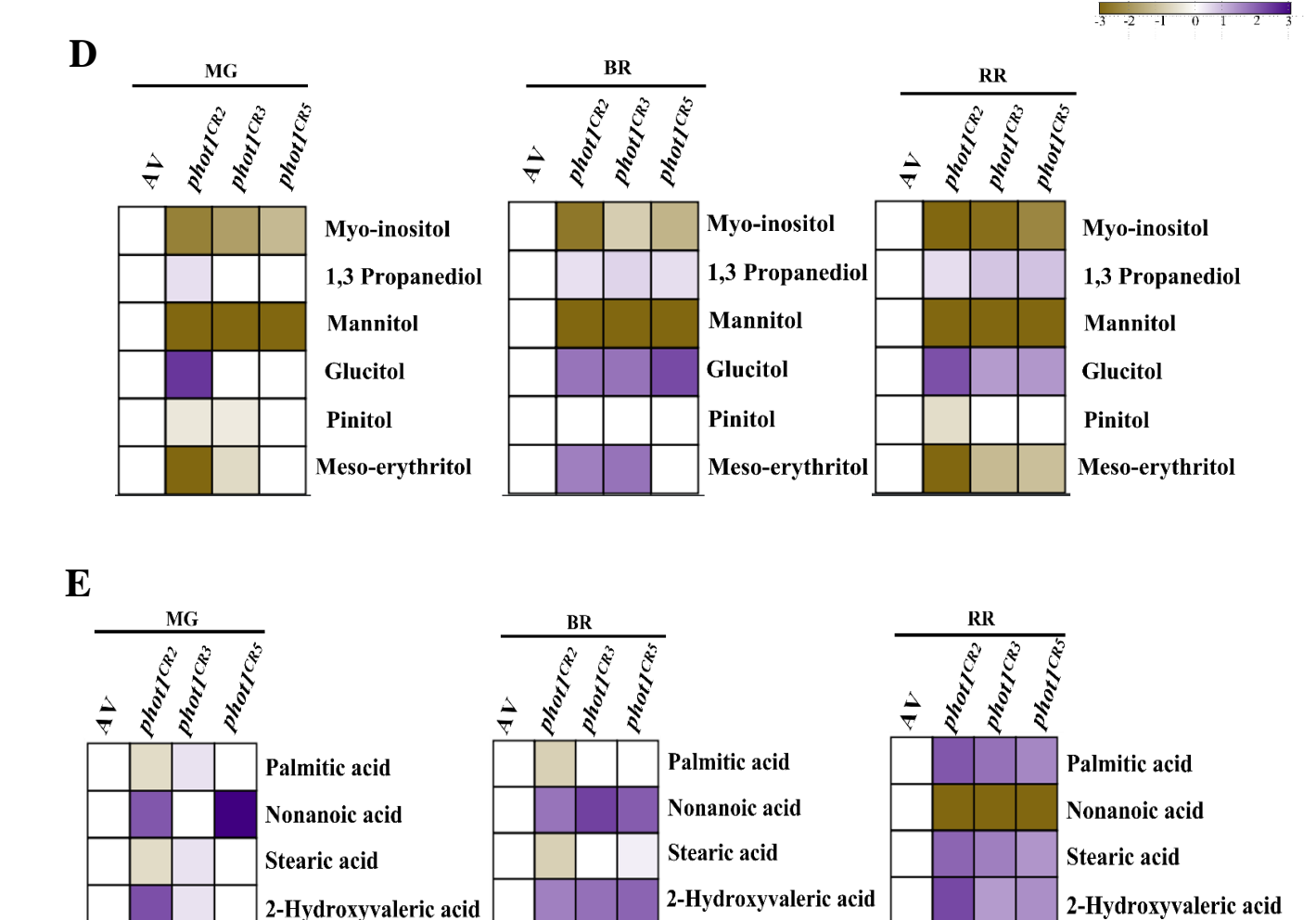


Figure 4.46 Primary metabolites level in ripening fruits of AV and *phot1* CRISPR lines fruits during ripening. Data are means  $\pm$  SE (n=5-8). Only those metabolites that are statistically significant minimum 2-fold change are shown here. D, Alcohols. E, Fatty acids.

#### 5. Discussion

As a model of a fleshy fruit, the tomato has been a target of several scientists to boost its nutritional quality, °Brix, shelf life, etc., using biotechnological approaches (Giuliano, 2017). Of the several players involved in increasing the nutritional quality, especially the carotenoid content, most of the information came from studying natural mutants, overexpression of essential carotenoid biosynthetic genes or transgenic studies using various transcription factors, receptors, etc. (Seymour et al., 2013) Based on these studies, it is apparent that carotenoid content is reduced in fruits having improper ripening, such as *RIPENING INHIBITOR (RIN)* (Vrebalov et al., 2002), *COLORLESS* NON-*RIPENING (CNR)* (Manning et al., 2006), and *NON-RIPENING (NOR)* (Yuan et al., 2016). These mutant loci encode transcription factors that regulate fruit ripening, associated pigmentation, and softening, acting primarily through ethylene synthesis and signaling (Seymour et al., 2013). In addition to ethylene, other hormones like ABA, JA, and auxin appear to be essential factors for fruit ripening and pigmentation (Galpaz et al., 2008; Liu et al., 2013; Su et al., 2015).

Besides the transcription factors, hormones, and their receptors, signaling intermediates, light also plays an essential yet supporting role in boosting carotenoid content in tomato fruits. Tomato fruits can ripen in the absence of light, but the nutritional quality is improved in the presence of light (Raymundo et al., 1976; Gupta et al., 2014). Examination of light signaling and photoreceptor mutants and their transgenics has revealed that light perception and signaling can be manipulated to increase the carotenoid content in tomato fruits. A dominant-negative mutant of *phot1*, *Nps1* in tomato exhibited loss of phototropic curvature, chloroplast accumulation, and enhanced carotenoid content in the ripe fruits (Kilamb et al., 2021). However, as tomato has no other mutants in *phot1* than *Nps1* and none for *phot2*, it is imperative that either gene-silenced or knockouts are needed to validate their functions in overall plant development, including fruit carotenogenesis.

One of the ways to assess a gene function is to isolate mutants using reverse genetics strategies like RNAi or gene editing, etc. While RNAi leads to suppression of gene expression, thereby interfering with the gene function, CRISPR/Cas9 mediated editing mainly results in gene knockouts if the coding sequences are targeted for editing. In this study, we examined the roles of *phot1* and *phot2* in

enhancing the carotenoid content of tomato fruits. To do this, we employed reverse genetics strategies like RNAi and CRISPR/Cas9 to generate gene-silenced lines or knockouts of *phot1* and *phot2* and studied their influence on fruit carotenogenesis and primary metabolite contents.

Since *phot1* and *phot2* share significant sequence homology, the regions that are unique to them, especially between the 5' UTR and 1st exon, were chosen for RNAi-mediated silencing. Around 11 independent *phot2*<sup>RNAi</sup> lines were generated, while *phot1* explants failed to regenerate despite multiple attempts. Hence, CRISPR/Cas9 strategy was used to edit the 1st exon of the *phot1* gene to generate knockouts. CRISPR/Cas9-editing of *phot1* resulted in eight editing events in five plants that were either heterozygous or chimeric. These mutations included five large deletions and two small deletions of 4-5 bp and were confirmed by Sanger sequencing.

Examination of *phot2* expression in 11 independent *phot2*<sup>RNAi</sup> lines revealed variable suppression ranging from zero (four lines) to 87% (6 lines show 44% to 87% silencing). This variation in *phot2* suppression is expected and is most probably due to the position effect of the neighboring genes, T-DNA integration in the genomic region which is transcriptionally inactive, or could be due to unknown factors that might affect RNAi phenomenon (Xiong et al., 2005; Kerschen et al., 2004; Kohli et al., 2003). Given that the *phot2*<sup>RNAi</sup> lines showed several phenotypic changes compared to the empty vector control (pHellsgate line), it is essential to ascertain a tight co-segregation of the genotype and the phenotype. As most of these changes could be due to somaclonal variation, any detailed characterization of the silenced lines can be carried out only in subsequent generations after confirming the loss of function in the highly silenced *phot2* lines. Three *phot2*<sup>RNAi</sup> lines (*phot2*<sup>RNAi-5</sup>, *phot2*<sup>RNAi-6</sup>, and *phot2*<sup>RNAi-9</sup>) were selected for advancing to T<sub>1</sub> generation for further characterization as they had high silencing of the *phot2* gene in T<sub>0</sub> generation.

Similarly, in the case of *phot1* knockouts, a stable inheritance of all eight editing events to T<sub>1</sub> has to be checked. Some editing events might be lost due to efficient repair mechanisms or if editing is observed only in somatic cells but not germ-line cells. Also, the mutations should be homozygous to link the phenotype with the genotype. Once the mutation is confirmed, the *Cas9* gene has to be segregated out, as its continued presence can generate additional editing. To do all

the above, 50 seeds from each of the five lines harboring editing in the *phot1* gene were germinated. Out of 8 editing events observed in T<sub>0</sub>, five were recovered in the homozygous condition in the T<sub>1</sub> generation. From these, only *phot1*<sup>CR2</sup> (Ser84Gly substitution and in-frame deletion of 50 aa from 85-135 aa) became *Cas9*- and *nptII*-free in the T<sub>1</sub> generation, while *phot1*<sup>CR1</sup> (Thr100Cys\*), *phot1*<sup>CR3</sup> (Asp117Cys\*), *phot1*<sup>CR4</sup> (in-frame deletion of 96 aa from 76-171 aa), and *phot1*<sup>CR5</sup> (20 aa in-frame deletion from 111-131 aa) alleles were both *Cas9* and *nptII* positive. As the mutation affected the PHOT1 protein, it may also have affected the *phot1* function. This can be verified by checking the functions mediated by individual phototropins.

Phototropins mediate different responses throughout the plant life cycle, such as long-term and short-term responses. The long-term responses include phototropism, seedling development, and leaf flattening, while the short-term/fast responses include stomatal opening and chloroplast movement (Briggs and Christie, 2002; Wada et al., 2003; Christie, 2007; Shimazaki et al., 2007;Kong and Wada, 2011). Under low light conditions, chloroplast accumulation movement maximizes the light uptake for photosynthesis. In high-intensity light, the chloroplast avoidance reaction is essential to prevent photo-oxidative damage (Jarillo et al., 2001; Kagawa et al., 2001). Both *phot1* and *phot2* mediate the chloroplast accumulation response redundantly, while *phot2* mediates the avoidance response exclusively (Jarillo et al., 2001; Kagawa et al., 2001; Sakai et al., 2001). Based on their role in mediating chloroplast movement, we assessed the loss of either *phot1* or *phot2* function by monitoring the chloroplast movements under changing blue light conditions in *phot2*<sup>RNAi</sup> and *phot1*<sup>CR</sup> lines.

Under low and high light intensities, the chloroplasts of tomato wild-type plants displayed normal accumulation and avoidance responses, respectively (Srinivas et al., 2004). Though chloroplast accumulation is hindered in the *Nps1* mutant of tomato, exposure to high fluence blue light evokes a chloroplast avoidance response, demonstrating a functioning PHOT2 protein in the *phot1* mutant (Sharma et al., 2014). Examining chloroplast accumulation response indicative of the phot1 role revealed that its function was compromised in all five *phot1*<sup>CR</sup> alleles. These five alleles were further advanced to T<sub>2</sub> generation.

The progeny of three  $phot2^{RNAi}$  lines  $(phot2^{RNAi-5}, phot2^{RNAi-6}, and phot2^{RNAi-9})$  in the  $T_1$  generation were examined for the extent of phot2 silencing and loss

of chloroplast avoidance response. As the expressivity of transgene silencing varies between and within the individual lines, it was not surprising to see fewer progeny/ $phot2^{RNAi}$  lines exhibiting good silencing. Suppose the silenced line shows a loss of chloroplast avoidance response on exposure to high fluence blue light indicative of the disruption of phot2 function. In that case, we can then attribute that to the endogenous silencing of the phot2 gene. Consistent with this, highly silenced progeny of each  $phot2^{RNAi}$  line showed loss of chloroplast avoidance response. As no noticeable phenotypic changes in the silenced lines were observed, we advanced highly silenced progeny showing maximal loss of phot2 function/ $phot2^{RNAi}$  lines to  $T_2$  and  $T_3$  generations for further stabilization and characterization.

Though the *phot2* transcript levels were variable between the independent T<sub>3</sub> lines, the majority of the progeny of the three T<sub>3</sub> lines showed a significant reduction in *phot2* gene expression compared to the control, pHellsgate, suggesting the stabilization of the transgene integration. When the chloroplast movement was monitored in the T<sub>3</sub> lines, all the silenced progeny of the 3 RNAi lines showed a significant reduction in *phot2* function, given that the chloroplast avoidance response was impaired in them compared to the control. The above observation suggests that the penetrance of *phot2* silencing was very high, as assessed by the loss of *phot2* function. However, the expressivity of the *phot2* silencing varied in the *phot2*<sup>RNAi</sup> lines. Such a change in the expressivity and penetrance of the transgenesilencing is expected. The same has been reported in earlier studies using the RNAi strategy for functional genomics studies (Wanget al., 2005). In addition, all the T<sub>3</sub> progeny of the three RNAi lines were positive for the transgene presence.

The lines *phot2*<sup>RNAi-5</sup>-#8, *phot2*<sup>RNAi-6</sup>-#1, and *phot2*<sup>RNAi-9</sup>-#2 were characterized for phenotypic variations that differed considerably from the control pHellsgate plants. No significant alterations in phenotype were observed when these three *phot2* transgenic lines were compared to control pHellsgate plants. Although these lines had low levels of *phot2* expression, the plants had a normal phenotype. The lines were then characterized thoroughly for the extent of *phot2* silencing and loss of function at transcript and metabolite levels. Due to the scarcity of seeds, we could not do many experiments on seedling phototropism and vegetative development, as *phot2*<sup>RNAi</sup> affected the seed set in the highly silenced lines.

In the T<sub>2</sub> generation, many progenies of phot1<sup>CR3</sup> and phot1<sup>CR5</sup> became Cas9-

free, and the progeny of  $phot1^{CR2}$  were Cas9-free as this line became transgene-free in the T<sub>1</sub> generation itself. The other two alleles,  $phot1^{CR1}$  and  $phot1^{CR4}$ , still harbored the transgene and were not taken forward for further studies. The  $phot1^{CR2}$ ,  $phot1^{CR3}$ , and  $phot1^{CR5}$  progeny were homozygous for editing. The  $phot1^{CR2}$ ,  $phot1^{CR3}$ , and  $phot1^{CR5}$  progeny also showed loss of phot1 function, indicating stable inheritance of mutations to T<sub>2</sub> generation.

The mutations created by CRISPR/Cas system are not always intended, as they can occur in unintended regions in the genome other than the target site. Such off-target mutations can be detrimental as they can affect the function/regulation of un-targeted genes. However, we took sufficient care during the design of gRNA so that the selected gRNA had up to 4 mismatches with the target sequence. In addition, the chosen gRNAs did not have any predicted off-target effects in the coding sequence of un-targeted genes. Despite all the precautions, off-target editing cannot be completely ruled out, as it can be caused due to many factors (Modrzejewski et al., 2020). Therefore, it is essential to exclude the presence of any off-target editing by sequencing the potential off-target sites in the edited transgene-free plants.

The homozygous Cas9-free plants from *phot1*<sup>CR2</sup>, *phot1*<sup>CR3</sup>, and *phot1*<sup>CR5</sup> alleles were checked for unwanted editing. This was done by amplifying the off-target gene sequences predicted by CRISPR-P and CRISPOR web tools. Sanger sequencing of the amplified PCR products revealed the absence of off-target editing events in *phot1*<sup>CR2</sup>, *phot1*<sup>CR3</sup>, and *phot1*<sup>CR5</sup> alleles. Based on the above experiments, these three alleles, *phot1*<sup>CR2</sup>, *phot1*<sup>CR3</sup>, and *phot1*<sup>CR5</sup> (in T<sub>2</sub>/T<sub>3</sub> generation), were characterized in detail at phenotypic, genotypic, functional, metabolite, and transcript levels.

The tropic response of plants towards the direction of light is fundamental to their survival, and phototropins mediate this response. Though phot1 and phot2 redundantly mediate this response, phot1 is more highly photosensitive than phot2. Consequently, the *phot1* mutant of tomato, *Nps1*, lacks phototropism towards lowintensity blue light (Sharma et al., 2014). As expected, the disruption of the *phot1* gene in *phot1*<sup>CR</sup> alleles affected the phototropism. Significantly, the extent of bending toward blue light was minimal in *phot1*<sup>CR3</sup> and *phot1*<sup>CR5</sup> than AV, while it was reduced in *phot1*<sup>CR2</sup>. As the PHOT1 protein is prematurely truncated in *phot1*<sup>CR3</sup> much before the LOV1 domain, the chromophore binding is affected in the LOV1

and LOV2, and the function is lost. However, in *phot1*<sup>CR2,</sup> an in-frame deletion of 50 aa much before the LOV1 domain reduced its curvature but did not completely inhibit it. In the case of *phot1*<sup>CR5</sup>, the mutation caused an in-frame deletion earlier than the LOV1 domain; however, the curvature is minimal. Possibly, the deletion of 20 aa may have affected the 3D structure of the PHOT1 protein and its binding to FMN. Nevertheless, it should be kept in mind that the LOV2 domain is still intact in *phot1*<sup>CR2</sup> and *phot1*<sup>CR5,</sup> and it has been shown that the LOV2 domain is more critical for phototropin activity than LOV1 (Christie, 2007). Due to this, complete loss of phototropism did not occur in any of these alleles unless the mutation renders a dominant negative function to the PHOT1 protein (Sharma et al., 2014).

Previous studies indicate that in addition to plant movements, phytochromes and cryptochromes influence plant biomass and photosynthesis, especially under shaded conditions (Kharshiing and Sinha, 2016; Yang et al., 2016, Mawphlang and Kharshiing, 2017). Similarly, phot1 and phot2 also increase plant growth under low photosynthetically active radiation, with phot1 being more sensitive than phot2 (Takemiya et al., 2005). Consistent with this, *phot1* mutants of tomato exhibit a dwarf phenotype under greenhouse conditions and are bushy (Sharma et a., 2014; present study). More importantly, this reduction in plant height was due to the reduced internodal lengths in the *phot1*<sup>CR</sup> mutants than AV, revealing a new facet of the phot1 function.

Proper leaf positioning and shape are required for optimal light capture for plant growth and development. Earlier studies in Arabidopsis have revealed the crucial role of phytochromes and phototropins in positioning the leaf and its flattening (Fiorucci and Fankhauser, 2017). While the petiole angle is favorably mediated by *phot1*, leaf positioning and flattening are regulated by both *phot1* and 2 (Sakamoto and Briggs, 2002). The adult *Nps1* plants showed bigger leaflets with reduced serration of the margin and increased size of leaflet lobes with downward curling of leaflets (Sharma et al., 2014, Kilambi et al., 2021). Consistent with this, *phot1*<sup>CR</sup> alleles show variation in leaf morphology compared to AV, albeit with variations among different alleles. While the leaves of *phot1*<sup>CR2</sup> and *phot1*<sup>CR3</sup> are flat and light in color, *phot1*<sup>CR5</sup> leaves were curled slightly, with the same number of leaflets and color as AV. Though no significant change in leaf margin serration was seen, the lobe size of leaflets appears to be slightly bigger in *phot1*<sup>CR</sup> alleles than in

AV. This suggests that *phot1* affects plant height and leaf morphology, albeit with variations in different alleles.

Chlorophyll and carotenoids are the primary photosynthetic pigments in plants and play a vital role in enhancing the net carbon yield. Given that the leaf color was pale, examining chlorophyll levels revealed a reduction in total chlorophyll content in  $phot1^{CR2}$  and  $phot1^{CR3}$  alleles. Contrarily, the total carotenoid content was higher in all the  $phot1^{CR}$  alleles than AV, primarily driven by the increase in violaxanthin and lutein contents. In contrast, other carotenoids like  $\beta$ - carotene and neoxanthin varied allele-specifically. A similar reduction in chlorophyll levels were seen in the cry1a mutant than in MM. However, these mutants also showed decreased  $\beta$ -carotene and lutein contents (Fantini et al., 2019). The phot1 seems to influence the chlorophyll contents similar to that of cry1 and xanthophyll contents differently from cry1 in the tomato leaves. Assuming the variation in chlorophyll, carotenoid contents, and leaf morphology, whether there is an influence of phot1 on photosynthesis remains to be examined.

Though earlier studies indicated the influence of photoreceptors and light signaling components on fruit development and pigmentation, few studies revealed the in vivo functions of photoreceptors. Alba et al. (2000) showed the red/far-red reversibility of lycopene accumulation in an off-vine study when MG fruits were given light treatments. Functional phot1 and phot2 were revealed when the chloroplasts from tomato MG fruits exhibited movement in response to low and high fluence BL; however, this function was compromised in *Nps1* (Kilambi et al., 2021). Like phytochrome mutants and Nps1, phot1<sup>CR</sup> mutants and phot2<sup>RNAi</sup> lines exhibited delayed development of MG fruits. While the subsequent transitions from MG to the BR stage were reduced and from BR to RR stage were increased in *phot1<sup>CR</sup>* mutants and phot2<sup>RNAi</sup> lines, Nps1 did not show any such effect (Kilambi et al., 2021). However, phytochrome mutants show a similar effect, while cry and UVR8 roles remain unknown in influencing fruit development (Gupta et al., 2014). Such an effect on fruit development has alluded to the interaction between light and hormone levels in Nps1; no such correlation can be made in the present study, as the hormone levels barring ethylene during fruit development were not checked in phot1<sup>CR</sup> mutants and  $phot2^{RNAi}$  lines.

Apart from fruit development, the associated pigmentation has been ascribed to several factors, with light being one additional factor and the present study's focus. Though carotenoid accumulation can occur in the dark, light exposure to fruits enhances their carotenoid content (Gupta et al., 2014). Among the five different photoreceptors known, overexpression of phytochromes, cryptochromes, and UVR8 increases the carotenoid content of tomato fruits (Liuet al., 2018; Giliberto et al., 2005, Li et al., 2018, Alves et al., 2020). In contrast, the loss of function of cryptochromes or phytochromes and silencing of UVR8 reduces the carotenoid levels (Fantini et al., 2019, Gupta et al., 2014, Bianchetti et al., 2018, Li et al., 2018). Though the *phot1* function is impaired in *Nps1*, the carotenoid accumulation is considerably stimulated, presumably due to its constitutive activation (Kilambi et al., 2021). The reduced carotenoid content can support the relevance of the above in *phot1*<sup>CR</sup> mutants and *phot2*<sup>RNAi</sup> lines, suggesting the requirement of functional phot1 and phot2 for normal carotenogenesis.

Though there is an obligatory link between ethylene emission and carotenogenesis based on earlier studies using ethylene-deficient lines (Oeller et al., 1991; Lanahan et al., 1994), a reduction in ethylene levels does not necessarily lead to low carotenoid levels, as seen in Nps1, hp1, etc. in tomato (Kilambi et al., 2013, Kilambi et al., 2021, Sharma et al., 2021). Though the ethylene levels were similar in the MG and BR stages of AV and  $phot1^{CR}$  mutants, they were reduced than AV at the RR stage. This reduction in ethylene and reduced  $CO_2$  emission can be correlated to the reduced carotenoid content in  $phot1^{CR}$  lines. Such a conclusion could not be made in  $phot2^{RNAi}$  lines as we could not measure ethylene emission levels due to the scarcity of fruits.

As carotenoid content is reduced in the RR fruits of  $phot1^{CR}$  mutants and  $phot2^{RNAi}$  lines, we can expect that the expression of the MEP pathway and the carotenogenesis pathway genes will be decreased than AV. However, the results reveal a complex regulation. Though there is a stimulation of dxs, the rate-limiting enzyme for MEP pathway in  $phot1^{CR}$  mutants and  $phot2^{RNAi}$  lines, carotenoid content is less. Similarly, stimulation of psy1 in  $phot1^{CR}$  mutants, which is rate-limiting for lycopene formation, but no change in  $phot2^{RNAi}$  lines reveals a post-transcriptional regulation. No role of psy2 in fruit-specific carotenogenesis is shown in this study, contrary to its contribution towards carotenogenesis in Nps1 (Kilambi et al., 2021).

Contrarily, lower expression of *cycb* in *phot1*<sup>CR</sup> mutants and *phot2*<sup>RNAi</sup> lines can be correlated to lower  $\beta$ -carotene levels; the same case is with the carotenoid sequestration genes. All these results indicate a stringent post- transcriptional regulation of MEP and carotenogenesis pathways in *phot1*<sup>CR</sup> mutants and *phot2*<sup>RNAi</sup> lines similar to that seen in *Nps1* (Kilambi et al., 2021), *hp1* (Kilambi et al., 2013), and *DET1*-underexpression lines (Enfissi et al., 2010).

During tomato fruit ripening, complex sugars break down to simple sugars, and the sweetness of fruits increases. Different photoreceptors seem to influence the °Brix content multifariously. While phytochromes do not affect the °Brix content of tomato fruits, cryptochromes seem to regulate it positively; a higher °Brix was reported in the *Nps1* ripe fruits (Gupta et al., 2014; Giliberto et al., 2005; Kilambi et al. 2021). Contrary to *Nps1*, *phot1*<sup>CR</sup> mutants and *phot2*<sup>RNAi</sup> lines have similar °Brix like AV. This suggests the lack of effect of phototropins on this process, while a higher °Brix in *Nps1* can be attributed to the constitutive activation of phot1 (Kilambi et al., 2021).

Many changes accompany the ripening of tomato fruits, resulting in considerable shifts in the metabolites. PCA profiles suggest significant shifts in the metabolite profiles of phot1<sup>CR</sup> mutants, while the changes are purported to be minimal in phot2<sup>RNAi</sup> lines. In phot1<sup>CR</sup> mutants, similar to carotenoids, most amino acids, including γ-amino butyric acid (GABA), were also downregulated at the RR stage except valine. However, in the case of *phot2*<sup>RNAi</sup> lines, only three amino acids, glycine, β-alanine, and GABA, showed significantly high abundance. As gene-edited tomato accumulating high levels of GABA (Waltz, 2022) is commercially approved for release in the market, it will be interesting to examine the influence of phot2 on regulating GABA levels. While the high aminome can be linked to low levels of TCA cycle intermediates in Nps1, the reverse seems true in  $phot2^{RNAi}$  lines, though only a few amino acids and TCA cycle intermediates were differentially expressed. But, both the aminome and TCA cycle intermediates were downregulated in phot1<sup>CR</sup> mutants. While most of the sugars were downregulated in phot1<sup>CR</sup> mutants, only the three detected sugars were lower in phot2<sup>RNAi</sup> lines than the control, and contrarily most sugars were highly abundant in *Nps1* (Kilambi et al., 2021).

The vastly different effects of Nps1 on fruit metabolome than phot1<sup>CR</sup>

mutants can be attributed to the constitutive activation of phot1. A functional phot1 is necessary for normal carotenogenesis and primary metabolome. Based on the above, it can be concluded that phot1 is a significant player in regulating the primary metabolism of ripening tomato fruits; phot2 seems to have a mild effect. Such a differential effect on metabolome was reported with cryptochromes too. cry1 was the dominant photoreceptor affecting the phenylpropanoid metabolism of leaves, while cry2 is prevalent in fruits affecting carotenoids (Fantini et al., 2019).

Our study revealed a new facet of the functions of phototropins in regulating fruit ripening. Such a function could not have been identified in Arabidopsis due to its dehiscent, dry fruit, thus highlighting the importance of studying gene functions in crops. To conclude, our study suggests that as *phot1* and *phot2* positively regulate carotenogenesis, the gain of function mutations in both *phot1* and *phot2* may enhance the carotenoid content in tomato fruits.

### **6 Summary and Conclusion**

### 6.1 Silencing of phototropin1 and phototropin2 genes using RNAi strategy

RNAi strategy was employed to silence both *phototropin1* (*phot1*) and *phototropin2* (*phot2*) genes in tomato. The pHellsgate vector containing the cDNA targeted towards the 3' ends of the *phot1* and *phot2* genes driven by CaMV35S promoter was used for gene silencing. *Agrobacterium tumefaciens* mediated transformation was carried out using tomato (*S. lycoperscicum* cv Arka Vikas) cotyledons. The cotyledons transformed with the *phot1* construct did not regenerate even after multiple attempts, and we could not generate *phot1* gene silenced lines. But, the *phot2* construct was successfully transformed, and 21 *Slphot2* RNAi lines were regenerated and transferred to the greenhouse. The phenotypes of these plants were monitored throughout the life cycle. Out of 21 *phot2* RNAi lines, seven died due to *Tuta absoluta* infection, and three did not set any fruit even after repeated manual pollination. The rest 11 lines were used for further analyses. Similarly, four lines were raised with the pHellsgate empty vector; out of these, only one line survived, set fruit, and gave seeds. This line was used as an empty vector control for further studies in all generations.

A PCR-based screening was carried out using primers specific to the *neomycin phosphotransferase* (*nptII*) gene to check whether the RNAi cassette for silencing the *phot2* gene was integrated into genomic DNA. The *nptII* gene amplification was observed in all the 11 *Slphot2* RNAi lines and one pHellsgate line, confirming the integration of the RNAi cassette. Real-time quantitative PCR was carried out in these RNAi lines to assess whether transgene integration has affected the endogenous *phot2* expression. Of the 11 independent *phot2* RNAi lines examined, the line numbers. 2, 3, 7 and 11 did not show any silencing, while line numbers 1 (50%), 5 (80%), 6 (87%), 8 (60%), 9 (75%) and 10 (44%) showed significant silencing of *phot2* gene. Three highly silenced lines, *phot2*<sup>RNAi-5</sup>, *phot2*<sup>RNAi-6</sup>, *phot2*<sup>RNAi-9</sup>, and pHellsgate line, were advanced to T<sub>1</sub> generation.

Examining *phot2* expression in the  $T_1$  progeny of *phot2*<sup>RNAi-5</sup>, *phot2*<sup>RNAi-6</sup>, and *phot2*<sup>RNAi-9</sup> lines revealed a variation in their expression. Also, *phot2* expression differed between the progeny of single lines. To elaborate, for *phot2*<sup>RNAi-5</sup> progeny, #2 (65%), #3 (67%), #5 (52%) and #7 (56%) showed significant silencing while the rest did not show any effect. For *phot2*<sup>RNAi-6</sup> progeny, only two plants out of eight

showed silencing- #3 (60%) and #7 (90%). For  $phot2^{RNAi-9}$  progeny, out of 8 plants, only four showed significant silencing- # 4 (50%), #5 (70%), #7 (54%) and #8 (60%). Such a variation in the expressivity and penetrance of transgene silencing was expected as many studies using RNAi approaches reported a similar behavior earlier (Wesley et al., 2001; Wang et al., 2005). As we did not observe any noticeable phenotypic changes in the silenced lines, we then assessed the function of phot2 in highly silenced lines among the  $T_1$  progeny as that would indicate whether RNAi silencing affected the gene function.

The phototropins mediate chloroplast movements in response to low light intensity (chloroplast accumulation) and high light intensity (chloroplast avoidance) (Briggs et al., 2001; Sakai et al., 2001) to help the plants optimize their photosynthetic efficiency and growth. While *phot1* and *phot2* contribute to low light-induced chloroplast accumulation, *phot2* specifically plays a role in avoidance responses under high light intensity (Jarillo et al., 2001; Kagawa et al., 2001;Sakai et al., 2001).

Taking advantage of the specific role of phot2 in mediating chloroplast avoidance response under high fluence, we used this assay to assess the loss of phot2 function in the highly silenced phot2 RNAi lines. The red light transmittance was measured for the dark-adapted leaves of pHellsgate and highly silenced progeny from each of the phot2 RNAi lines for dark measurement. After that, the leaf discs were exposed to low fluence blue light (3.2 µmol/m<sup>2</sup>/s), which induced a chloroplast accumulation response, reflected in the reduction of red light transmittance. This was followed by high fluence blue light exposure (60-80 µmol/m<sup>2</sup>/s), which triggers chloroplast avoidance response, and the red light transmittance was measured. Based on this assay, the progeny of *phot2*<sup>RNAi-5</sup>: #2(33%), #3(42%), and #7(100%) showed variable avoidance response compared to 100% avoidance recorded for pHellsgate plant. Similarly, for the progeny of phot2<sup>RNAi-6</sup>: #3 (45%) and #7 (11%) chloroplast avoidance, while the progeny of *phot2*<sup>RNAi-9</sup>: # 478%), #5 (70%), and #8 (50%) showed variable chloroplast avoidance compared to pHellsgate control. As the highly silenced lines showed variable loss of phot2 function, the lines which showed maximal loss of *phot2* function were examined for the presence of the transgene. All the lines which showed loss of *phot2* function also carried the transgene, *nptII*. Based on the above, only those lines which showed high silencing of phot2 gene, followed

by maximal loss of *phot2* function and the presence of transgene, were advanced to  $T_2$  generation for further stabilization and characterization.

As expected, in the T<sub>2</sub> generation, the transgene segregation and a variable loss of *phot2* function were also observed among the progeny of each of the three RNAi lines. Following the same rationale mentioned above, the three T<sub>2</sub> lines showing a significant reduction in *phot2* expression and maximal loss of *phot2* function, transgene presence, and seeds were taken forward to the next generation, T<sub>3</sub>. In the T<sub>3</sub> generation, a minimum of eight to ten seeds were sowed from the lines, *phot2*<sup>RNAi-5</sup>-#8, *phot2*<sup>RNAi-6</sup>-#1, and *phot2*<sup>RNAi-9</sup>-#2 and control, pHellsgate. After transferring to the greenhouse, these lines were characterized for any phenotypic variations that were considerably different from the control plants. No significant alterations in phenotype or development were observed when these three *phot2* transgenic lines were compared to control pHellsgate lines. Although these lines had low levels of *phot2* expression, the plants had a normal phenotype. The lines were then characterized thoroughly for the extent of *phot2* silencing and loss of function and at phenotypic, transcript, and metabolite levels.

Though the transcript levels were variable between the independent T<sub>3</sub> lines, the majority of the progeny of the three T<sub>3</sub> lines showed a significant reduction in *phot2* gene expression compared to the control, pHellsgate, suggesting the stabilization of the transgene integration. When the chloroplast movement was monitored in the T<sub>3</sub> lines, all the silenced progeny of the 3 RNAi lines showed a significant reduction in *phot2* function, given that the chloroplast avoidance response was impaired in them compared to the control. This suggests that the penetrance of *phot2* silencing was very high, as assessed by the loss of *phot2* function, even though the expressivity of the *phot2* silencing varied in the *phot2*RNAi lines. Such a change in the expressivity and penetrance of the transgene-silencing is consistent with earlier studies using the RNAi strategy for functional genomics studies (Wang et al., 2005). In addition, all the T<sub>3</sub> progeny of the three RNAi lines were positive for the transgene presence.

Given that different photoreceptors influence fruit ripening and pigmentation, it was interesting to examine the influence of *phot2* on fruit development and ripening. Flowers from the T<sub>3</sub> generation plants were tagged at the

anthesis, and the fruit developmental stages were monitored. The color transition between different ripening stages was visually observed during the on-vine ripening and recorded. Compared to pHellsgate,  $phot2^{RNAi-6}$  and  $phot2^{RNAi-9}$  lines required a longer duration to attain the mature green stage (MG), while  $phot2^{RNAi-5}$  fruits behaved like control in reaching MG. After that, the fruits of all the three RNAi lines required a slightly lesser duration (~1 day) to attain the breaker stage (BR) than the control and subsequent transition from breaker to the red ripe stage (RR) in the RNAi lines was longer (~2-3 days) than the control fruits. Once the ripe fruits are formed, examination of total soluble sugar content and pH revealed no significant changes in the RNAi lines from the control.

As photoreceptors like phytochromes, cryptochromes and UVR8 are positive regulators of carotenogenesis in tomato fruits, and tomato *phot1* mutant exhibits high carotenoid levels, it was of interest to examine the influence of *phot2* on fruit carotenogenesis. Analysis of total carotenoid content in ripe fruits of *phot2* RNAi lines revealed a decrease compared to pHellsgate fruits; specifically, lycopene ( $\sim$ 1.6-2.2 fold),  $\beta$ -carotene ( $\sim$ 1.53-2.36 fold), and lutein ( $\sim$ 1.6-2 fold) levels were reduced. This suggests that *phototropin2* positively regulates fruit carotenoid accumulation.

To examine the influence of *phot2* on the expression of carotenogenic genes, the gene expression of rate-limiting enzymes of the MEP pathway, dxs (deoxy-xylulose-5-phosphate synthase) and the carotenoid biosynthesis, psyl (phytoene synthase) for lycopene formation and cycb (chromoplast specific lycopene  $\beta$ -cyclase) for  $\beta$ -carotene formation was checked. Compared to the pHellsgate fruits, dxs expression was higher in the ripe fruits of  $phot2^{RNAi}$  lines. Despite high phytoene levels and low levels of lycopene in the  $phot2^{RNAi}$  lines, the psyl expression was similar to that of the control. As  $\beta$ -carotene amounts were lower, the cycb expression would be expected to be lower in the silenced lines. Consistent with this, a lower cycb expression was observed in the silenced lines. In addition, the expression of genes involved in carotenoid sequestration, chromoplast-specific carotenoid-associated protein (chrc), and plastid lipid-associated protein 3 (pap3) were similar to that of control. This suggests that carotenogenesis in  $phot2^{RNAi}$  lines is not regulated at the transcriptional level and may be regulated post-transcriptionally.

To check the influence of *phot2* on metabolite profiles of tomato fruit, we used GC-MS to detect the primary metabolite levels in the red ripe fruits of *phot2* silenced lines. We identified around sixty-five metabolites belonging to different classes such as organic acids, carbohydrates, fatty acids, amino acids, and amines. The PCA showed overlapping metabolite profiles of *phot2*<sup>RNAi</sup> lines with pHellsgate lines, suggesting little differences. Of the eight amino acids detected, only three: Glycine,  $\beta$ -alanine, and  $\gamma$ -aminobutyric acid (GABA), showed significantly high abundance in *phot2*<sup>RNAi</sup> lines, while the rest were similar in abundance to that of pHellsgate fruits, and many were below the detection limits. Similarly, in the case of organic acids, only citrate and aconitate were high in abundance in the fruits of *phot2* silenced lines, and malate levels were similar. In contrast, gluconate levels were lower than the pHellsgate fruits. Most of the twenty-one sugars detected were parallel in abundance to control, and only fructose, xylose, and mannitol were significantly lower in *phot2* silenced lines. All these results suggest a mild influence of *phot2* on the primary metabolome.

### 6.2 CRISPR/Cas9 mediated editing of phototropin1 gene

As the RNAi strategy did not work for silencing the *phot1* gene, CRISPR/CAS9 strategy was used to develop tomato lines with different allelic variations in the *phot1* gene. We targeted the first exon mainly for creating knockouts. We used a double guide RNA-based approach rather than a single guide RNA-based for high editing efficiency. The pCAMBIA2300-CAS9-Phot1 vector harboring double gRNA driven by AtU6 promoter and human codon-optimized Cas9 under the 2x35S CaMV promoter with kanamycin as plant selection marker was used for editing the *phot1* gene. The above construct was transferred into Agrobacterium strain LBA4404, and tomato transformation in AV was carried out according to the protocol of Van Eck et al. (2006). The plants regenerated on kanamycin were screened for the presence of *CRISPR/Cas9* cassette and *nptII* gene before transferring to the greenhouse.

After confirming that the plants were positive for both *Cas9* and *nptII*, these were further screened using *phot1*-specific PCR to check the editing. Analysis of *phot1* amplicons on 2% (w/v) agarose gel revealed a few smaller fragments than the expected size suggesting editing. Sequencing of these smaller fragments revealed

large deletions compared to AV. However, using this gel-based method, as deletions smaller than 50 bp are difficult to visualize compared to large deletions, the sequencing step is essential to identify smaller deletions and point mutations. In cases with no significant mobility shift in the PCR amplicons, we could observe a few base pair changes on sequencing. This strategy helped us to identify at least eight editing events in the T<sub>0</sub> generation, including five large deletions and two small deletions of 4-5 bp. None of these events were homozygous in the T<sub>0</sub> generation; they were either heterozygous or chimeric with one wild- type band and smaller fragments. The eight editing events upon sequence confirmation include phot1<sup>CR1</sup> (97 bp deletion; heterozygous), phot1<sup>CR2</sup> (4, 149 bp deletion; heterozygous), phot1<sup>CR3</sup> (5,46 bp deletion; chimera), phot1<sup>CR4</sup> (288 bp deletion, heterozygous) and phot1<sup>CR5</sup> (56, 63 bp deletion; chimera) alleles. No inversions or insertions in the edited regions were observed in the *phot1* explants. The *phot1*-specific screening of the adult plants (after transferring the hardened rooted explants to the greenhouse) was also carried out to rule out any successful repair of the editing event. At least in the  $T_0$  generation, all the initially observed editing events were also confirmed at the adult stage.

The mutated gene sequences of *phot1* were translated to protein sequences with the EXPASY tool and aligned with the AV PHOT1 protein sequence using MULTIALIGN software. The above-aligned sequences revealed that the deletions induced by CRISPR/Cas9 affected the PHOT1 protein sequence. Among eight editing events, mutations in *phot1* prematurely truncated the PHOT1 protein due to frameshifts resulting in Thre100Cys\* (*phot1*<sup>CR1</sup>), Ala115Gly\*, and Asp117Cys\* (*phot1*<sup>CR3</sup>) and Pro98Gly\* (*phot1*<sup>CR5</sup>). In addition, a Ser84Gly substitution and inframe deletion of 50 aa from 85-135 aa (*phot1*<sup>CR2</sup>), in-frame deletion of 96 aa from 76-171 aa (*phot1*<sup>CR4</sup>), and 21 aa from 111-131 aa (*phot1*<sup>CR5</sup>) were observed.

As phototropins mediate chloroplast relocation responses when exposed to low and high fluence blue light, it was interesting to examine whether the mutations in *phot1*<sup>CR</sup> alleles affected the function of PHOT1 protein, especially the chloroplast accumulation response. As expected, *phot1*<sup>CR1-5</sup> lines showed loss of *phot1* function as evidenced by the 25%, 33%, 40%, 29%, and 25% reduction in the chloroplast accumulation response (partial loss), respectively. This suggests that the mutations induced by CRISPR/Cas9 affected the *phot1* function. These plants and AV were

monitored for any phenotypic changes throughout their life cycle. The seeds were collected for all the alleles to advance them to the next generation.

Fifty seeds from each allele were germinated to raise T<sub>1</sub> *phot1*<sup>CR</sup> plants to generate homozygous edited and Cas9-free lines. These plants were screened to identify the homozygous edited lines that are also Cas9-free. Out of 8 editing events observed in T<sub>0</sub>, five- Thre100Cys\* (*phot1*<sup>CR1</sup>), Ser84Gly substitution and in-frame deletion of 50 aa from 85-135 aa (*phot1*<sup>CR2</sup>), Asp117Cys\* (*phot1*<sup>CR3</sup>), in-frame deletion of 96 aa from 76-171 aa (*phot1*<sup>CR4</sup>), and 21 aa from 111-131 aa (*phot1*<sup>CR5</sup>) could be recovered to a homozygous condition in the T<sub>1</sub> generation. Only *phot1*<sup>CR2</sup> became Cas9-free in the T<sub>1</sub> generation, and the remaining four alleles were both *Cas9* and *nptII* positive. All the homozygous lines were monitored for any phenotypic changes compared to AV. The monitoring of chloroplast movement revealed the loss of *phot1* function with 31%, 30%, 40%, 35%, and 29% reduction in the chloroplast accumulation response in the progeny of *phot1*<sup>CR1-5</sup>, respectively. This reveals the stable inheritance of loss of function in *phot1* alleles from T<sub>0</sub> to T<sub>1</sub> generation.

All the five  $phot1^{CR}$  alleles that are recovered in the homozygous condition in  $T_1$  were advanced to  $T_2$  generation by growing a minimum of 30 plants per line. The genomic DNA was isolated from these plants and was initially screened using PCR for the presence of Cas9. Upon screening for the presence of Cas9, many of the progeny of  $phot1^{CR3}$  and  $phot1^{CR3}$  became Cas9- free, and all the progeny of  $phot1^{CR2}$  were Cas9-free since this line became transgene-free in the  $T_1$  generation itself. The other two alleles,  $phot1^{CR1}$  and  $phot1^{CR4}$ , still harbored the transgene and were not taken forward for further studies. In addition, the editing was also confirmed in these Cas9-free plants by using phot1-specific PCR, subsequent analysis of PCR fragments on agarose gel electrophoresis, and Sanger sequencing. The  $phot1^{CR2}$ ,  $phot1^{CR3}$ , and  $phot1^{CR3}$  progeny were homozygous for editing.

To rule out the presence of any off-target editing, the homozygous Cas9-free plants from  $phot1^{CR2}$ ,  $phot1^{CR3}$ , and  $phot1^{CR5}$  alleles were checked for unwanted editing. This was done by amplifying the off-target gene sequences predicted by CRISPR-P and CRISPOR web tools. Sanger sequencing of the amplified PCR products revealed the absence of off-target editing events in  $phot1^{CR2}$ ,  $phot1^{CR3}$ , and

 $phot1^{CR5}$  alleles. Based on the above experiments, these three alleles,  $phot1^{CR2}$ ,  $phot1^{CR3}$ , and  $phot1^{CR5}$ , were characterized in detail at phenotypic, genotypic, functional, metabolite, and transcript levels. These alleles were also advanced to the next generation to finish the pending experiments that could not be completed in the  $T_2$  generation.

Since phot1 mediates low fluence phototropism and PHOT1 protein is affected by mutations, it was interesting to examine whether the low fluence phototropism is affected in  $phot1^{CR}$  alleles. Exposure of 3-4-day old dark-grown seedlings of AV and  $phot1^{CR2}$ ,  $phot1^{CR3}$ , and  $phot1^{CR5}$  alleles to unilateral blue light of 0.3-1  $\mu$ mol/m²/s fluence for 16 h revealed a nice curvature in AV seedlings. However, the extent of bending towards blue light was reduced in  $phot1^{CR2}$  compared to AV, while the curvature was minimal in  $phot1^{CR3}$  and  $phot1^{CR5}$  than AV. This suggests that the phot1 function in mediating low fluence phototropism is compromised in  $phot1^{CR}$  alleles. In addition, the chloroplast accumulation response to low fluence blue light was affected in the  $phot1^{CR2}$ ,  $phot1^{CR3}$ , and  $phot1^{CR5}$  alleles compared to AV.

The plant phenotype of *phot1*<sup>CR2</sup>, *phot1*<sup>CR3</sup>, and *phot1*<sup>CR5</sup> alleles was recorded compared to AV at different stages of development-both vegetative and reproductive. The plant height of 2.5- month-old *phot1*<sup>CR2</sup>, *phot1*<sup>CR3</sup>, and *phot1*<sup>CR5</sup> alleles was substantially reduced compared to AV. Acloser examination of the internodes and their lengths revealed that the reduction in the plant height is due to the shorter internodes in these alleles than AV. In addition, as leaf shape, expansion, and flattening are also mediated by phototropins, examination of leaf morphology revealed that *phot1* affects leaf morphology albeit with variations in different alleles like the number of leaflets, flat leaves, light-colored leaves, etc. than AV. Estimating total chlorophyll revealed lower levels in *phot1*<sup>CR2</sup> and *phot1*<sup>CR3</sup> alleles and levels similar to AV in the *phot1*<sup>CR5</sup> allele.

In contrast, a significant increase in the amount of lutein and violaxanthin was observed in all three  $phot1^{CR}$  alleles. Also, the levels of  $\beta$ -carotene and 9-Cis- $\beta$ -carotene increased in all the lines than AV except the  $phot1^{CR2}$  (similar to AV), while neoxanthin content was identical to AV in  $phot1^{CR2}$ , and  $phot1^{CR3}$  and higher in  $phot1^{CR5}$  than AV. The total carotenoid content was significantly elevated in all the

phot1<sup>CR</sup> alleles leaves.

Similar to  $phot2^{RNAi}$  lines, the fruits of all the three  $phot1^{CR}$  alleles required seven days' longer time post-anthesis to reach the MG stage compared to AV. After that, the transition of MG to the BR stage required a shorter duration in all the three  $phot1^{CR}$  alleles than AV. The further transition of BR to RR stage was extended in all the three  $phot1^{CR}$  alleles than AV. As the fruit development and ripening were delayed in the fruits of  $phot1^{CR}$  alleles, it was expected that the ethylene and  $CO_2$  emission would be lower in these fruits than in AV. However, no difference was observed in the ethylene emission at MG and BR stages in the fruits of AV and  $phot1^{CR}$  alleles, while a slight reduction in the ethylene emission was observed at RR stage in  $phot1^{CR3}$  and  $phot1^{CR5}$  than AV but not in  $phot1^{CR2}$ .

Consistent with ethylene emission, almost comparable levels of  $CO_2$  were emitted from the fruits of AV and  $phot1^{CR}$  alleles (barring  $phot1^{CR2}$  and  $phot1^{CR5}$  at MG) at MG and BR with slight reduction at RR in all the three alleles. Based on this, ethylene emission appears not correlated to fruit development and ripening in  $phot1^{CR}$  alleles. In addition, similar to phot2, no influence of phot1 was observed on the pH and °Brix of the red ripe fruits of  $phot1^{CR}$  alleles compared to AV fruits.

As Nps1 mutant is dominant-negative and its fruits show high carotenoids, especially lycopene content at the ripe stage (Kilambi et al., 2021), it was interesting to know whether loss of the phot1 function affects the fruit carotenoid content. At the RR stage, phytoene, phytofluene, lycopene,  $\beta$ -carotene,  $\alpha$ -carotene, and lutein (barring  $phot1^{CR2}$ ) were lower in abundance in the  $phot1^{CR}$  alleles than AV. This suggests that, similar to phot2, phot1 also acts as a positive regulator for carotenogenesis. Then th carotenogenic expression was examined at different ripening stages. At MG and BR stages, the expression of dxs1 (barring  $phot1^{CR5}$ ), psy1 (barring  $phot1^{CR5}$ ), psy2 (barring  $phot1^{CR5}$ ), and cycb was either similar to or lower than AV in the  $phot1^{CR}$  alleles. However, at the RR stage, the expression of dxs1 and psy1 was very high in  $phot1^{CR}$  alleles than in AV, while that of psy2 remained similar or lower than in AV. The expression of cycb was lower in all the  $phot1^{CR}$  alleles than AV at the RR stage. This suggests the absence of correlation between the expression of crucial genes-dxs1 and psy1 and carotenoid content. In addition, the contribution of psy2 towards fruit carotenoid content also appears

minimal. However, a weak correlation between cycb expression and  $\beta$ -carotene content could be seen. All these results suggest that in phot1 mutants, carotenogenesis may be post-transcriptionally regulated.

Consistent with lower carotenoid levels in *phot1*<sup>CR</sup> alleles than AV, the carotenoid sequestration genes- *chrc* and *pap3* expression were lower or similar to AV at all ripening stages (barring *phot1*<sup>CR2</sup> at MG), with significant downregulation at the RR stage. This suggests a direct correlation between carotenoid content and the expression of carotenoid sequestration genes.

Given that *Nps1*, a dominant negative mutant of *phot1*, affected the fruit metabolome drastically (Kilambi et al., 2021), we checked the influence of *phot1* on the primary metabolome of ripening fruits in AV and *phot1*<sup>CR</sup> alleles. GC-MS analysis in the fruits of AV and *phot1*<sup>CR</sup> alleles at different ripening stages led to identifying about 63 metabolites grouped into different chemical classes based on their functional groups. PCA plots revealed vast differences between the metabolite profiles of AV and *phot1*<sup>CR</sup> alleles at different ripening stages, and minimal overlap was observed. Examination of metabolite profiles in the fruits of AV and *phot1*<sup>CR</sup> alleles at different ripening stages revealed significant changes during the transition from BR to RR stage. In contrast, only a minimal difference was observed from MG to BR transition. Among the nine amino acids detected and quantified, only valine was abundant in the *phot1*<sup>CR</sup> alleles, while the rest were downregulated than AV at the RR stage.

Similarly, among the 19 organic acids detected, most organic acids, including TCA cycle intermediates like citrate,  $\alpha$ -ketoglutarate, succinate, malate, etc., were downregulated in  $phot1^{CR}$  alleles than AV. Among 22 sugars identified, most of the sugars were downregulated in the  $phot1^{CR}$  alleles than AV at the RR stage. This includes sucrose, glucose, and fructose which contribute to tomato fruits' sweetness. Based on the above, there appears to be a vast influence of phot1 on tomato metabolome in the ripening fruits.

### **6.3 Conclusion**

In the present study, we successfully silenced *phot2* using RNAi strategy and edited *phot1* using the CRISPR/Cas9 approach. Using RNAi strategy, out of the 11 lines generated in T<sub>0</sub> generation, three highly silenced, independent lines were taken

forward to T<sub>3</sub> generation based on the extent of *phot2* silencing, loss of *phot2* function, and the presence of the transgene. The loss of *phot2* function was stably inherited in the T<sub>3</sub> generation. Compared to AV, *phot2*<sup>RNAi</sup> lines exhibited delayed fruit development and had lower carotenoid content in the ripe fruits, with no change in total soluble sugar levels and pH. The lower carotenoid levels in the fruits of *phot2*<sup>RNAi</sup> lines were not correlated to the carotenogenic gene expression or the expression of carotenoid sequestration genes. Such a lack of correlation suggests the probable post-transcriptional regulation of carotenogenesis. The effect of *phot2* silencing on the primary metabolism of ripe fruits appears minimal.

Five of the eight editing events generated by CRISPR/Cas9 in *phot1* in the T<sub>0</sub> generation were recovered to homozygosity in the T<sub>1</sub> generation. Editing of the *phot1* gene resulted in protein truncations and in-frame deletions. In the T<sub>2</sub> generation, three alleles became Cas9-free, and no off-target editing was detected. Detailed analysis of these three alleles in T<sub>2</sub>/T<sub>3</sub> generation revealed the influence of *phot1* on plant height, leaf morphology, leaf pigment levels, and fruit development. Editing of *phot1* gene disrupted phototropism and chloroplast accumulation response. The loss of *phot1* function is stably inherited in successive generations. *phot1* acts as a positive regulator of fruit carotenogenesis, which may be regulated post-transcriptionally. The mutations in *phot1* caused an extensive variation in the fruit metabolome. Our study suggests that as *phot1* and *phot2* positively regulate carotenogenesis, the generation of gain of function mutations in both *phot1* and *phot2* may enhance the carotenoid content in tomato fruits.

### References

Adams DO, Yang SF (1977) methionine metabolism in apple tissue: implication of S-adenosylmethionine as an intermediate in the conversion of methionine to ethylene. Plant Physiol **60(6)**: 892-896

**Alba R, Cordonnier-Pratt MM, Pratt LH** (2000) Fruit localized phytochromes regulate lycopene accumulation independently of ethylene production in tomato. Plant Physiol **123**: 363-370

**Al-Babili S, Hobeika E, Beyer P** (1996) A cDNA encoding lycopene cyclase from Narcissus pseudonarcissus L (PGR96). Plant Physiol **112**:1398

**Alexander L, Grierson D** (2002) Ethylene biosynthesis and action in tomato: A model for climacteric fruit ripening. J Exp Bot **53**: 2039-2055

Alves FRR, Lira BS, Pikart FC, Monteiro SS, Furlan CM, Purgatto E, Pascoal GB, Andrade SC da S, Demarco D, Rossi M, et al (2020) Beyond the limits of photoperception: constitutively active PHYTOCROME B2 overexpression as a means of improving fruit nutritional quality in tomato. Plant Biotechnol J 18: 2027-2041

Ariizumi T, Kishimoto S, Kakami R, Maoka T, Hirakawa H, Suzuki Y, Ozeki Y, Shirasawa K, Bernillon S, Okabe Y, et al (2014) Identification of the carotenoid modifying gene PALE YELLOW PETAL 1 as an essential factor in xanthophyll esterification and yellow flower pigmentation in tomato (Solanum lycopersicum). Plant J 79: 453-465

Atares A, Moyano E, Morales B, Schleicher P, Garcia-Abellan JO, Anton T, Garcia-Sogo B, Perez-Martin F, Lozano R, Flores FB, et al (2011) An insertional mutagenesis programme with an enhancer trap for the identification and tagging of genes involved in abiotic stress tolerance in the tomato wild-related species solanum pennellii. Plant Cell Rep 30: 1865-1879

Azari R, Tadmor Y, Meir A, Reuveni M, Evenor D, Nahon S, Shlomo H, Chen L, Levin I (2010) Light signalling genes and their manipulation towards modulation of phytonutrient content in tomato fruits. Biotechnol Adv 28: 108-118

**Bai Y, Kissoudis C, Yan Z, Visser RGF, van der Linden G** (2018) Plant behaviour under combined stress: tomato responses to combined salinity and pathogen stress. Plant J **93**: 781-793

Bauchet G, Grenier S, Samson N, Bonnet J, Grivet L, Causse M (2017) Use of modern tomato breeding germplasm for deciphering the genetic control of agronomical traits by Genome Wide Association study. Theor Appl Genet 130: 875-889

**Baulcombe D** (1999) Viruses and gene silencing in plants. Arch Virol Suppl 189-201

**Baulcombe D, English J** (1996) Ectopic pairing of homologous DNA and post-transcriptional gene silencing in transgenic plants. f. Curr Opin Plant Biol 7: 173-180

**Beetham PR, Knipp PB, Sawycky XL, Arntzen CJ, May GD** (1999) A tool for functional plant genomics: Chimeric RNA/DNA oligonucleotides cause in vivo genespecific mutations. Proc Natl Acad Sci U S A **96**: 8774-8778

**Belhaj K, Chaparro-Garcia A, Kamoun S, Nekrasov V** (2013) Plant genome editing made easy: Targeted mutagenesis in model and crop plants using the CRISPR/Cas system. Plant Methods **9**: 1

Bernstein E, Caudy AA, Hammond SM, Hannon GJ (2001) Role for a bidentate ribonuclease in the initiation step of RNA interference. Nature 409: 363-366

**Bianchetti RE, Silvestre-Lira B, Santos-Manteiro S, Demarco D, Puragatto E, Rothan C, Rossi M, Freschi L** (2018) Fruit localized phytochrome regulate biogenesis, starch synthesis, and carotenoid metabolism in tomato. J Exp Bot doi: 10.1093/jxb/ery145

**Bibikova M, Golic M, Golic KG, Carroll D** (2002) Targeted chromosomal cleavage and mutagenesis in Drosophila using zinc-finger nucleases. Genetics **161**: 1169-1175

**Bitinaite J, Wah DA, Aggarwal AK, Schildkraut I** (1998) Fok I dimerization is required for dna cleavage. Proc Natl Acad Sci U S A **95**: 10570-10575

**Boggio SB, Palatnik JF, Heldt HW, Valle EM** (2000) Changes in amino acid composition and nitrogen metabolizing enzymes in ripening fruits of Lycopersicon esculentum Mill. Plant Sci **159**:125-133

Bolger A, Scossa F, Bolger ME, Lanz C, Maumus F, Tohge T, Quesneville H, Alseekh S, Sorensen I, Lichtenstein G, et al (2014) The genome of the stress-tolerant wild tomato species Solanum pennellii. Nat Genet 46: 1034-1038

**Botella-Pavia P, Rodriguez-Concepcion M** (2006) Carotenoid biotechnology in plants for nutritionally improved foods. Plant Physiol **123**: 369-381

Bou-Torrent J, Toledo-Ortiz G, Ortiz-Alcaide M, Cifuentes-Esquivel N, Halliday KJ, Martinez-Garcia JF, Rodriguez-Concepcion M (2015) Regulation of carotenoid biosynthesis by shade relies on specific subsets of antagonistic transcription factors and cofactors. Plant Physiol 169: 1584-1594

**Briggs WR and Christie JM** (2002) Phototropins 1 and 2: versatile plant blue light receptors. Trends Plant sci **7**: 204-210.

Briggs WR, Beck CF, Cashmore AR, Christie JM, Hughes J, Jarillo JA, Kagawa T, Kanegae H, Liscum E, Nagatani A, et al (2001) The phototropin family of photoreceptors. Plant Cell 13: 993-997

**Briggs WR, Olney MA** (2001) Photoreceptors inn plant photomorphogenesis to date. Five phytochromes, two cryptochromes, one phototropin, and one superchrome. Plant Physiol **125**: 85-88

**Brocklehurst S, Watson M, Carr IM, Out S, Heidmann I, Meyer P** (2018) Induction of epigenetic variation in Arabidopsis by over-expression of DNA METHYLTRANSFERASE1 (MET1). PLoS One **13**: 1-22

**Brooks C, Nekrasov V, Lippman ZB, Van Eck J** (2014) Efficient gene editing in tomato in the first generation using the clustered regularly interspaced short palindromic repeats/CRISPR-associated9 system. Plant Physiol **166**: 1292-1297

**Brummell DA, Harpster MH** (2001) Cell wall metabolism in fruit softening and quality and its manipulation in transgenic plants. Plant Mol Biol **47**: 311-339

Burch-Smith TM, Anderson JC, martin GB, Dinesh-Kumar SP (2004) Applications and advantages of virus-induced gene silencing for gene function studies in plants. Plant J 39: 734-746

Burch-Smith TM, Schiff M, Liu Y, Dinesh-Kumar SP (2006) Efficient virus-induced gene silencing in Arabidopsis. Plant Physiol 142: 21-2B

Burg SP, Burg EA (1965) The ripening of fruits. Science 28: 148(3674): 11960-6.

Caldwell DG, McCallum N, Shaw P, Muehlbauer GJ, Marshall DF, Waugh R (2004) A structured mutant population for forward and reverse genetics in Barley (Hordeum vulgare L.). Plant J 40: 143-150

Candau R, Bejarano CR, Cerda-Olmedo E (1991) In vivo channeling of substrates in an enzyme aggregate for carotene biosynthesis. Proc Natl Acad Sci U S A 88: 4936-4940

**Carrari F, Fernie AR** (2006) Metabolic regulation underlying tomato fruit development. J Exp Bot **57**: 1883-1897

Carrari F, Nunes-Nesi A, Gibon Y, Lytovchenko A, Ehlers Loureiro M, Fernie AR (2003) Reduced expression of aconitase results in an enhanced rate of photosynthesis and marked shifts in carbon partitioning in illuminated leaves of wild species tomato. Plant Physiol 133: 1322-1335

Carroll D (2011) Genome engineering with zinc-finger nucleases. Genetics 188: 773-782

**Casal JJ Mazella MA** (1998) Conditional synergism between cryptochrome 1 and phytochrome B is shown by the analysis of phyA, phyB and hy4 simple, double and triple mutants in Arabidopsis. Plant Physiology **118**: 19-25

**Casal JJ, Sanchez RA** (1998) Phytochromes and seed germination. Seed Science research. **8**:317-329.

**Cashmore AR, Jarillo JA, Wu YJ and Liu D** (1999) Cryptochromes: Blue light receptors for plants and animals. Science **284**:760-765.

Cermak T, Baltes NJ, Cegan R, Zhang Y, Voytas DF (2015) High-frequency, precise modification of the tomato genome. Genome Biol. Doi: 10.1186/s13059-015-0796-9

Cermak T, Curtin SJ, Gil-Humanes J, Cegan R, Kono TJY, Konecna E, Belanto JJ, Starker CG, Mathre JW, Greenstein RL, et al (2017) A multipurpose toolkit to enable advanced genome engineering in plants. Plant Cell **29:** 1196-1217

Cermak T, Doyle EL, Christian M, Wang L, Zhang Y, Schmidt C, Baller JA, Somia N V., Bogdanove AJ, Voytas DF (2011) Efficient design and assembly of custom TALEN and other TAL effector-based constructs for DNA targeting. Nucleic Acids Res 39: 1-11

Chandrasekaran J, Brumin M, Wolf D, Leibman D, Klap C, Pearlsman M, Sherman A, Arazi T, Gal-On A (2016) Development of broad virus resistance in non-transgenic cucumber using CRISPR/Cas9 technology. Mol Plant Pathol 17: 1140-1153

**Chappell J, Wolf F, Proulx J, Cuellar R, Saunders C** (1995) Is the reaction catalyzed by 3-hydroxy-3-methylglutaryl coenzyme A reductase a rate-limiting step for isoprenoid biosynthesis in plants? Plant Physiol **109**: 1337-1343

Charity JA, Klimaszewska K (2005) Persistence of Agrobacterium tumefaciens in transformed conifers. Environ Biosafety Res 4(3): 167-177.

Chen K, Wang Y, Zhang R, Zhang H, Gao C (2019) CRISPR/Cas Genome editing and precision plant breeding in Agriculture. Annu Rev Plant Biol **70**: 667-697

**Chen M, Chory J, Fankhauser C** (2004) Light signal transduction in higher plants. Annual Review of Genetics **38**: 87-117

Cheung AY, McNellis T, Piekos B (1993) Maintenance of chloroplast components during chromoplast differentiation in the tomato mutant green flesh. Plant Physiol 101: 1223-1229

**Chinnusamy V, Zhu JK** (2009) RNA-directed DNA methylation and demethylation in plants. Sci China, Ser C Life Sci **52:** 331-343

Christian M, Qi Y, Zhang Y, Voytas DF (2013) Targeted Mutagenesis of Arabidopsis thaliana

Christie JM (2007) Phototropins blue-light receptors. Annu Rev Plant Biol 58: 21-45

Christie JM, Reymond P, Powell GK, Bernasconi P, Raibekas AA, Liscum E, Briggs WR (1998) Arabidopsis NPH1: A flavoprotein with the properties of a photoreceptor for phototropism. Science (80-) 282: 1698-1701azari

Christie JM, Yang H, Richter GL, Sullivan S, Thomson CE, Lin J, Titapiwatanakun B Ennis M, Kaiserli E, Lee OR, et al (2011) Phot1 inhibition of ABCB19 primes lateral Auxin Fluxes in the shoot Apex required for Phototropism. PLoS Biol doi: 10.1371/journal.pbio.1001076

Cong L, Ran FA, Cox D, Lin S, Barretto R, Hsu PD, Wu X, Jiang W, Marraffini a, Zhang F (2013). Multiplex genome engineering using CRISPR/Cas systems. Science (New York). Science 339: 819-823

Cooley MB, Goldsbrough AP, Still DW, Yoder JI (1996) Site selected insertional mutagenesis of tomato with maize Ac and Ds elements. Mol Gen Genet 252: 184-194

**Cunningham FX, Gnatt E** (1998) Genes and enzymes of carotenoid biosynthesis in plants. Annu Rev Plant Biol **49**: 557-583

Cunningham J, Gnatt E (2001) One ring or two? Determination of ring number in carotenoids by lycopene ε-cyclases. Proc Natl Acad Sci U S A 98: 2905-2910

Cuttriss AJ, Cazzonelli CI, Wurtzel ET, Pogson BJ (2011) Biosynthesis of vitamins in plants. Elsevier 1-36.

**D'Aoust MA, Yelle S, Nguyen-Quoc B** (1999) Antisense inhibition of tomato fruit sucrose decreases fruit setting and the sucrose unloading capacity of young fruit. Plant Cell **11**: 2407-2418

**DeBolt S, Cook DR, Ford CM** (2006) L-tartaric acid synthesis from vitamin C in higher plants. Proc Natl Acad Sci U S A **103**: 5608-5613

**Dna CNR, Cuerda-gil D, Slotkin RK** (2016) Corrigendum: Non-canonical RNA-directed DNA methylation. Nat Plants **3**: 1

**Dong C, Beetham P, Vincent K, Sharp P** (2006) Oligonucleotide-directed gene repair in wheat using a transient plasmid gene repair assay system. Plant Cell rep **25**: 457-465

**Eisenreich W, Bacher A, Arigoni D, Rohdich F** (2004) Biosynthesis of isoprenoids via the non-mevalonate pathway. Cell Mol Life Sci **61**: 1401-1426

**Eisenreich W, Rohdich F, Bacher A** (2001) Deoxyxylulose phosphate pathway to terpenoids. Trends Plant Sci. **6**: 78-84

Enfissi EMA, Barneche F, Ahmed I, Lichtle C, Gerrish C, Mc Quinn RP, Giovannoni JJ, Lopez-Juez E, Bowler C, Bramley PM, et al (2010) Integrative transcript and metabolite analysis of nutritionally enhanced DE-ETIOLATED1 downregulated tomato fruit. Plant Cell 22: 1190-1215

Fantini E, Sulli M, Zhang L, Aprea G, Jimenez-Gomez JM, Bendahmane A, Perrotta G, Giuliano G, Facella P (2019) Pivotal roles of cryptochromes 1a and 2 in tomato development and physiology 1. Plant Physiol 179: 732-748

**Fernie AR, Carrari F, Sweetlove LJ** (2004b) Respiratory metabolism glycolysis intermediates, nucleotides, sugars, organic acids, amino acids and sugar alcohols in potato tubers using a nonaquous fractionation method. Plant Physiol **127**: 685-700

**Fiorucci AS and Fankhauser C** (2017) Plant strategies for enhancing access to sunlight. Current Biology **27**: R931-940.

**Folta KM and Spalding EP** (2001) Unexpected roles for cryptochrome 2 and phototropin revealed by high-resolution analysis of blue-light mediated hypocotyl growth inhibition. Plant J **26**: 471-478

**Frankel N, Hasson E, Iusem ND, Rossi MS** (2003) Adaptive Evolution of the Water Stress-Induced Gene Asr2 in Lycopersicum species Dwelling in Arid Habitats. Mol Biol Evol **20**: 1955-1962

**Fraser PD, Bramley PM** (2006) metabolic profiling and quantification of carotenoids and related isoprenoids in crop plants. Biotechnol Agric For **57**: 229-242

Fraser PD, Kiano JW, Truesdale MR, Schuh W, Bramley PM (1999) Phytoene synthase enzyme activity in tomato does not contribute to carotenoid synthesis in ripening. Plant Mol Biol 40: 687-698.

Fraser PD, Truesdale MR, Bird CR, Schuh W, Bramley PM (1994) Carotenoid biosynthesis during tomato fruit development (Evidence for tissue specific gene expression). Plant Pysiol **105**: 405-403

- Fridman E, Carrari F, Liu YS, Fernie AR, Zamir D (2004) Zooming in on a quantitative trait for tomato yield using interspecific introgressions. Science (80-) **305**: 1786-1789
- **Fridman E, Pleban T, Zamir D** (2000) A recombination hotspot delimits a wild-species quantitative trait locus for tomato sugar content to 484 bp within an invertase gene. Proc Natl Acad Sci USA **97**: 4718-4723
- **Gaj T, Sirk SJ, Shui S, Liu J** (2016) Genome-Editing Technologies: Principles and Applications.
- Galpaz N, Wang Q, Menda N, Zamir D, Hirschberg J (2008) Abscisic acid deficiency in the tomato mutant high-pigment 3 leading to increased plastid number and higher fruit lycopene content. Plant J 53: 717-730
- **Ganzalez RM, Ricardi MM, Iusem ND** (2013) Epigenetic marks in an adaptive water stress-responsive gene in tomato roots under normal and drought conditions. Epigenetics 8: 864-872
- **Gapper NE, McQuinn RP, Giovannoni JJ** (2013) Molecular and genetic regulation of fruit ripening. Plant Mol Biol **82**: 575-591
- Gascuel Q, Diretto G, Monforte AJ, Fortes AM, Granell A (2017) Use of natural diversity and biotechnology to increase the quality and nutritional content of tomato and grape. Front Plant Sci 8: 11-34
- Giliberto L, Perrotta G, Pallara P, Weller JL, Fraser PD, Bramley PM, Fiora A, Tavazza M, Giuliano G (2005) Manipulation of the blue light photoreceptor cryptochrome 2 in tomato affects vegetative development, flowering time, and fruit antioxidant content. Plant Physiol 137: 199-208
- **Gillaspy G, Ben-David H, Gruissem W** (1993) Fruits: A developmental perspective. Plant Cell **5**: 1439-1451
- Gimenez E, Pineda B, Capel J, Anton MT, Atares A, Perez-Martin F, Garcia-Sogo B, Angosto T, Moreno V, Lozano R (2010) Functional analysis of the Arlequin mutant corroborates the essential role of the ARLEQUIN/TAGL1 gene during reproductive development of tomato. PLos One. doi:10.1371/journal.pone.0014427
- **Giorio G, Stigliani AL, D'Ambrosio C** (2008) Phytoene synthase genes in tomato (Solanum lycopersicum)- new data on the structures, the deduced amino acid sequences and the expression patterns. FEBS J. **275**: 527-535
- Giorio G, Yildirim A, Stigliani AL, D Ambrosio C (2013) Elevation of lutein content in tomato: A biochemical tug-of-war between lycopene cyclases. Metab Eng **20**: 167-176
- **Giuliano G** (2017) Provitamin A biofortification of crop plants: a gold rush with many miners. Curr Opin Biotechnol **44**: 169-180
- **Giuliano G, Bartley GE, Scolnik PA** (1993) regulation of carotenoid biosynthesis during tomato development. The Plant Cell **5**: 379-387

- Greenberg MVC, Deleris A, Hale CJ, Liu A, Feng S, Jacobsen SE (2013) Interplay between active chromatin marks and RNA-directed DNA methylation in Arabidopsis thaliana. PLoS Genet. doi: 10.1371/journal.pgen.1003946
- Greene EA, Codomo CA, Taylor NE, Henikoff JG, Till BJ, Reynolds SH, Enns LC, Burtner C, Johnson JE, Odden AR, et al (2003) Spectrum of chemically induced mutations from a large-scale reverse-genetic screen in Arabidopsis. Genetics 164: 731-740
- **Grzebelus D** (2018) the functional impact of transposable elements on the diversity of plant genomes. Diversity. Doi: 10.3390/d10020018
- Gupta P, Reddaiah B, Salava H, Upadhyaya P, Tyagi K, Sarma S, Datta S, Malhotra B, Thomas S, Sunkum A, et al (2017) Next-generation sequencing (NGS)-based identification of induced mutations in a doubly mutagenized tomato (Solanum lycopersicum) population. Plant J 92: 495-508
- **Gupta RM, Musunuru K** (2014) Expanding the genetic editing tool kit: ZFNs, TALENs, and CRISPR-Cas9. J Clin Invest **124**: 4154-4161
- Gupta SK, Sharma S, Santisree P, Kilambi HV, Appenroth K, Sreelakshmi Y, Sharma R (2014) Complex and shifting interactions of phytochromes regulate fruit development in tomato. Plant, Call Environ 37: 1688-1702
- **Haag JR, Ream TS, Marasco M, Nicora CD, Norbeck AD, Pasa-Tolic L, Pikaard CS** (2012) In vitro Transcription Activities of Pol IV, Pol V, and RDR2 Reveal Coupling of Pol IV and RDR2 for dsRNA Synthesis in Plant RNA Silencing. Mol Cell **48**: 811-818
- **Hayut SF, Bessudo CM, Levy AA** (2017) Targeted recombination between homologous chromosomes for precise breeding in tomato. Nat Commun **8**: 1-9
- Hidema J, Teranishi M, Iwamatsu Y, Hirouchi T, Ueda T, Sato T, Burr B, Sutherland NM, Yamamoto K, Kumagai T (2005) Spontaneously occurring mutations in the cyclobutene pyrimidine dimer photolyase gene cause different sensitivities to ultraviolet-B in rice. Plant J 43: 57-67
- **Hirschberg J** (2001) Carotenoid biosynthesis in flowering plants. Curr Opin Plant Biol **4**: 210-218
- **Hsieh MH, Goodman HM** (2005) The Arabidopsis IspH homolog is involved in the plastid nonmevalonate pathway of isoprenoid biosynthesis. Plant Physiol **138**: 641-653
- **Hu L, Li N, Xu C, Zhong S, Lin X, Yang J, Zhou T, Yuliang A, Wu Y, Chen YR, et al** (2014) Mutation of a major CG methylase in rice causes genome-wide hypomethylation, dysregulated genome expression, and seedling lethality. Proc Natl Acad Sci U S A **111**: 10642-10647
- Hwang WY, Fu Y, Reyon D, Maeder ML, Tsai SQ, Sander JD, Peterson RT, Yeh JRJ, Joung JK (2013) Efficient genome editing in zebrafish using a CRISPR-Cas system. Nat Biotechnol 31: 227-229
- **Iida S, Terada R** (2005) Modification of endogenous natural genes by gene targeting in rice and other higher plants. Plant Mol Biol **59**: 205-219

- Imaizumi T, Tran HG, Swartz TE, Briggs WR, Kay SA (2003) FKF1 is essential for photoperiodic specific light signalling in Arabidopsis. Nature **426**: 302-306
- **Inoue SI, Kinoshita T, Shimazaki KI** (2005) Possible involvement of phototropins in leaf movement of kidney bean in response to blue light. Plant Physiol **138**: 1994-2004
- Inoue SI, Kinoshita T, Takemiya A, Doi M, Shimazaki KI (2008) Leaf positioning of Arabidopsis in response to blue light. Mol Plant 1: 15-16
- **Isaacson T, Ohad I, Beyer P, Hirschberg J** (2004) Analysis in vitro of the enzyme CRITSO pathway establishes a poly-cis-carotenoid biosynthetic pathway in plants. Plant Physiol **136**: 4246-4225
- **Ito H, Yoshida T, Tsukahara S, Kawabe A** (2013) evolution of the ONSEN retrotransposon family activated upon heat stress in Brassicaceae. Gene **518**: 256-261
- **Iwabuchi K, Sakai T, Takagi S** (2007) Blue light dependent nuclear positioning in Arabidopsis thaliana leaf cells. Plant Cell Physiol **48**: 1291-1298
- **Jahns P, Latowski D, Strzalka K** (2009) mechanism and regulation of the violaxanthin cycle: The role of antenna proteins and membrane lipids. Biochim Biophys Act-Bioenerg **1787**: 3-14
- Jarillo JA, Gabrys H, Capel J, Alonso JM, Ecker JR, Cashmore AR (2001) Phototropin related NPL1 controls chloroplast relocation induced by blue light. Nature **410**: 952-954
- **Jia H, Nian W** (2014) Targeted genome editing of sweet orange using Cas9/sgRNA. PLoS One. doi: 10.1371/journal.pone.0093806
- **Jia H, Orbovic V, Jones JB, Wang N** (2016) Modification of the PthA4 effector binding elements in Type I CsLOB1 promoter using Cas9/sgRNA to produce transgenic Duncan grapefruit alleviating XccΔpthA4: DCsLOB1.3 infection. Plant Biotechnol J **14**: 1291-1301
- **Jiao Y, Lau OS, Deng XW** (2007) Light regulated transcriptional networks in higher plants. Nat Rev Genet 8: 217-230
- **Jinek M, Chylinski K, Fonfara I, Hauer M, Doudna JA, Charpentier E** (2012) A programmable dual-RNA guided DNA endonuclease in adaptive bacterial immunity. Science (80-) **337**: 816-821
- Jinek M, Jiang F, Taylor DW, Sternberg SH, Kaya E, Ma E, Anders C, Hauer M, Zhou K, Lin S, et al (2014) Structures of Cas9 endonucelases reveal RNA-mediated conformatiol activation. Science (80-) 343: 1-28
- Just D, Garcia V, Fernandez L, Bres C, Mauxion JP, Petit J, Jorly J, Assali J, Bournonville C, Ferrand C, et al (2013) Micro-Tom mutants for functional analysis of target genes and discovery of new alleles in tomato. Plant Biotechnol 30: 225-231
- Kagawa T, Sakai T, Suetsugu N, Oikawa K, Ishiguro S, Kato T, Tabata S, Okada K, Wada M (2001) Arabidopsis NPL1: A phototropin homolog controlling the chloroplast high-light avoidance response. Science (80-) 291: 2138-2141

Kanegae H, Tahir M, Savazzini F, Yamamoto K, Yano M, Sasaki T, Kanegae T, Wada M and Takano M (2000) rice homologues OsNPH1a and OsNPH1b are differently photoregulated. Plant Cell Physiol 41: 415-423

Karvelis T, Gasiunas G, Young J, Bigelyte G, Silanskas A, Cigan M, Siksnys V (2015) Rapid characterization of CRISPR-Cas9 protospacer adjacent motif sequence elements. Genome Biol 16: 1-13

**Kasai A, Bai S, Hojo H, Harada T** (2016) Epigenome editing of potato by grafting using transgenic tobacco as siRNA donor. PLoS One 11: 1-12

Kaur N, Alok A, Shivani, Kaur N, Pandey P, Awasthi P, Tiwari S (2018) CRISPR/Cas9-mediated efficient editing in phytoene desaturase (PDS) demonstrates precise manipulation in banana cv. Rasthali genome. Funct Integr genomics 18: 89-99

**Kawamata T, Seitz H, Tomari Y** (2009) Structural determinants of miRNAs for RISC loading and slicer-independent unwinding. Nat Struct Mol Biol **16**: 953-960

**Kerschen A, Napoli CA, Jorgensen RA, Muller AE** (2004) Effectiveness of RNA interference in transgenic plants. FEBS Lett **566**: 223-228

**Kharshiing E and Sinha SP** (2016) Deficiency in phytochrome A alters photosynthetic activity, leaf starch metabolism and shoot biomass production in tomato. Photochem J Photobiol B Biol **165**: 157-162

**Kharshiing E, Sreelakshmi Y, Sharma R** (2019) The light awakens! Sensing light anddarkness. In sensory Biology of Plants. Springer, Singapore. Pp 21-57

**Khatodia S, Bhatotia K, Passricha N, Khurana SMP, Tuteja N** (2016) The CRISPR/Cas genome-editing tool: Application in improvement of crops. Front Plant Sci. doi: 10.3389/fpls.2016.00506

Kilambi HV, Dindu A, Sharma K, Nizampatnam NR, Gupta N, Thazath NP, Dhanya AJ, Tyagi K, Sharma S, Kumar S, et al (2021) The new kid on the block: a dominant-negative mutation of phototropin1 enhances carotenoid content in tomato fruits. Plant J 106: 844-961

Kilambi HV, Kumar R, Sharma R, Sreelakshmi Y (2013) Chromoplast specific carotenoid associated protein appears to be important for enhanced accumulation of carotenoids in hp1 tomato fruits. Plant Physiol **161**: 2085-2101

Kilambi HV, Manda K, Rai A, Charakana C, Bagri J, Sharma R et al., (2017) Green-fruited Solanum habrochaites lacks fruit-specific carotenogenesis due to metabolic and structural blocks. Journal of Experimental Botany 68: 4803-4819

Kim SW, Kim JB, Ryu JM, Jung JK, Kim JH (2009) High-level production of lycopene in metabolically engineered E.coli. Process Biochem 44: 899-905

**Kim YG, Cha J, Chandrasegarans S** (1996) Hybrid restriction enzymes: Zinc finger fusions to Fok I cleavage domain. Proc Natl Acad Sci U S A **93**: 1156-1160

Kinoshita T, Doi M, Suetsugu N, Kagawa T, Wada M, Shimazaki K (2001) Phot1 and phot2 mediate blue light regulation of stomatal opening. Nature **414**: 656-660

- **Klee HJ, Giovannoni JJ** (2011) Genetics and control of tomato fruit ripening and quality attributes. Annu Rev Genet **45**: 41-59
- **Knott GJ, Doudna JA** (2018) CRIPSR-Cas guides the future of genetic engineering. Science (80-) **361**: 866-869
- **Kochevenko A, Willmitzer L** (2003) Chimeric RNA/DNA oligonucleotide-based site-specific modification of the tobacco acetolactate synthase gene. Plant Physiol **132**: 174-184
- Kohli A, Twyman RM, Abranches R, Wegel E, Stoger E, and Christou P (2003) Transgene integration, organization and interaction in plants. Plant Mol Biol **52**: 247-258
- **Kong SG and Wada M** (2011) Analysis of chloroplast movement and relocation in Arabidopsis. Methods Mol Biol **774**: 87-102
- **Kostov K, Batchvarova R, Slavov S** (2007) Application of chemical mutagenesis to increase the resistance of tomato to Orobanche ramose L. Bulg J Agric Sci **13**: 505-513
- Kumagai MH, Donson J, Della-Cioppa G, Hanley K, Grill LK (1995) Cytoplasmic inhibition of carotenoid biosynthesis with virus-derived RNA. Proc Natl Acad Sci U S A 92: 1679-1683
- **Lanahan MB, Yen HC, Giovannoni JJ, Klee HJ** (1994) The *never ripe* mutation blocks ethylene perception in tomato. Plant Cell **6**: 521-530
- **Latowski D, Grzyb J** (2004) The xanthophyll cycle-molecular mechanism and physiological significance. Acta Physiol Plant **26**: 197-212
- Leitao JM (2012) Chemical Mutagenesis. Plant Mutat Breed biotechnol 135-158
- **Levin I, Frankel P, Gilboa N, Tanny S, Lalazar A** (2003) the tomato dark green mutation is a novel allele of the tomato homolog of the DEETIOLATED1 gene. Theor Appl Genet **106**: 454-460
- **Li F, Vallabhaneni R, Yu J, Rocheford T, Wurtzel ET** (2008) The maize phytoene synthase gene family: Overlapping roles for carotenogenesis in endosperm, photomorphogenesis, and thermal stress tolerance. Plant Physiol **147**: 1334-1346
- **Li L, Van Eck J** (2007) Metabolic engineering of carotenoid accumulation by creating a metabolic sink. Transgenic Res **16**: 581-585
- Li Q, Eichten SR, Hermanson PJ, Zaunbrecher VM, Song J, Wendt J, Rosenbaum H, Madzima TF, Sloan AE, Huang J et al (2014) Genetic perturbation of the maize methylome. Plant Cell **26**: 4602-4616
- **Li R, Fu D, Zhu B, Luo Y, Zhu H** (2018) CRISPR/Cas9-mediated mutagenesis of IncRNA1459 alters tomato fruit ripening. Plant J **94**: 513-524
- Li T, Liu B, Spalding MH, Weeks DP, Yang B (2012) High-efficiency TALEN-based gene editing produces disease-resistance rice. Nat Biotechnol 30: 390-392
- Li X, Wang Y, Chen S, Tian H, Fu D, Zhu B, Luo Y, Zhu H (2018) Lycopene is enriched in tomato fruit by CRISPR/Cas9-mediated multiplex genome editing. Fron Plant Sci 9: 1-12

- **Lichtenthaler HK** (1999) The 1-deoxy-D-xylulose-5-phosphate pathway of isoprenoid biosynthesis in plants. Annual Reviews in Plant Phys and Plant Mol Bio **50**: 47-65
- **Lino M and Haga K** (2005) Role played by auxin in phototropism and photomorphogenesis in Light Sensing in Plants, Wada M, Shimazaki K and Lino M, eds (Berlin: Springer-Verlag), in press.
- Liu CC, Ahammed GJ, Wang GT, Xu CJ, Chen KS, Zhou YH, Yu JQ (2018) Tomato CRY1a plays a critical role in the regulation of phytohormone homeostasis, plant development, and carotenoid metabolism in fruits. Plant Cell Environ 41: 354-366
- Liu LJ, Zhang YC, Li QH, Sang Y, Mao J, Lian HL, Wang L, Yang HQ (2008) COP1 mediated ubiquitination of CONSTANS is implicated in cryptochrome regulation of flowering in Arabidopsis. Plant Cell **20**: 292-306
- Liu M, Pirrello J, Kesari R, Mila I, Roustan JP, Li Z, Latche A, Pech JC, Bouzayen M, Regad F (2013) A dominant repressor version of the tomato SI-ERF.B3 gene confers ethylene hypersensitivity via feedback regulation of ethylene signaling and response components. Plant J 76: 406-419
- Liu R, How-Kit A, Stammitti L, Teyssier E, Rolin D, Mortain-Bertrand A, Halle S, Liu M, Kong J, Wu C, et al (2015) A DEMETER-like DNA demethylase governs tomato fruit ripening. Proc Natl Acad Sci U S A 112: 10804-10809
- Liu Y, Roof S, Ye Z, Barry C, van Tuinen A, Vrebalov J, Bowler C, Giovannoni J (2004) Manipulation of light signal transduction as a means of modifying fruit nutritional quality in tomato. Proc Natl Acad Sci U S A **101**: 9897-9902
- Liu Y, Schiff M, Marathe R, Dinesh-Kumar SP (2002) Tobacco Rar1, EDS1 and \npr1/NIM1 like genes are required for N-mediated resistance to tobacco mosaic virus. Plant J 30: 415-429
- **Lois LM, Rodriguez-Concepcion M, Gallego F, Campos N, Boronat A** (2000) Carotenoid biosynthesis during tomato fruit development: Regulatory role of 1-deoxy-D-xylulose-5-phosphate synthase. Plant J **22**: 503-513
- Mahfouz MM, Li L, Shamimuzzaman M, Wibowo A, Fang X, Zhu JK (2011) De novoengineered transcription activator-like effector (TALE) hybrid nuclease with novel DNA binding specificity creates double-strand breaks. Proc Natl Acad Sci U S A 108: 2623-2628
- **Majumdar R, Rajasekaran K, Cary JW** (2017) RNA interference (RNAi) as a potential tool for control of mycotoxin contamination in crop plants: Concepts and considerations. Front Plant Sci. doi: 10.3389/fpls.2017.00
- Makarova KS, Wolf YI, Iranzo J, Shmakov SA, Alkhnbashi OS, Brouns SJJ, Charpentier E, Cheng D, Haft DH, Horvath P, et al., (2020) Evolutionary classification of CRIPSR-Cas systems: a burst of class 2 and derived variants. Nat Rev Microbiol 18: 67-83
- Mali P, Aach J, Stranges PB, Esvelt KM, Moosburner M, Kosuri S, Yang L, Church GM (2013) CAS9 transcrptional activators for target specificity screening and paired nickases for cooperative genome engineering. Nat Biotechnol 31: 833-838

Malnoy M, Viola R, Jung MH, Koo OJ, Kim JS, Velasco R, Kanchiswamy CN (2016) DNA-free genetically edited grapevine and apple protoplast using CRISPR/Cas9 ribonucleoproteins. Front Plant Sci 7: 1-9

Manning K, Tor M, Poole M, Hong Y, Thompson AJ, King GJ, Giovannoni JJ, Seymour GB (2006) A naturally occurring epigenetic mutation in a gene encoding an SBP-box transcription factor inhibits tomato fruit ripening. Nat Genet 38: 948-952

Marroni F, Pinosio S, Di Centa E, Jurman I, Boerjan W, Felice N, Cattonaro F, Morgante M (2011) Large-scale detection of rare variants via pooled multiplexed next-generation sequencing: Towards next-generation Ecotilling. Plant J 67: 736-745

**Martin-Pizarro C, Trivino JC, Pose D** (2019) Functional analysis of the TM6 MADS-box gene in the octoploid strawberry by CRSIPR/Cas9-directed mutagenesis. J Exp Bot **70**: 949-961

**Mathieu S, Boutron I, Moher D, Altman DG, Ravaud P** (2009) Comparison of registered and published primary outcomes in randomized controlled trials. Jama **302**: 977-984

Matsukura C, Yamaguchi I, Inamura M, Ban Y, Kobayashi Y, Yin YG, Saito T, Kuwata C, Imanishi S, Nishimura S (2007) generation of gamma irradiation-induced mutant lines of the miniature tomato (Solanum lycopersicum L.) cultivar 'Micro Tom'. Plant Biotechnol 24: 39-44

**Mawphlang OIL, Kharshiing EV** (2017) Photoreceptor mediated plant growth responses: Implications for photoreceptor engineering toward improved performance in crops. Front Plant Sci **8**: 1-14

**McClintock B** (1950) the origin and behavior of mutable loci in maize. Proc Natl Acad Sci U S A **36**: 344-355

Mcclintock B (1983) The significance of Responses of Science (80-) 792-801

McQuinn RP, Gapper NE, Gray AG, Zhong S, Tohge T, Fei Z, Fernie AR, Giovannoni JJ (2020) manipulation of ZDS in tomato exposes carotenoid and ABA-specific effects on fruit development and ripening. Plant Biotechnol J 18: 2210-2224

**Menda N, Semel Y, Peled D, Eshed Y, Zamir D** (2004) In silico screening of a saturated mutation library of tomato. Plant J **38**: 861-872

Menu T, Sagilo P, Granot D, Dai N, Raymond P, Ricard B (2004) High hexokinase activity in tomato fruit perturbs carbon and energy metabolism and reduces fruit and seed size. Plant, Cell Environ 27: 89-98

**Meyer RS, Purugganan MD** (2013) Evolution of crop species: genetics of domestication and diversification. Nat Rev Genet **14**: 840-852

Miao J, Guo D, Zhang J, Huang Q, Qin G, Zhang X, Wan J, Gu H, Qu LJ (2013) Targeted mutagenesis in rice using CRISPR-Cas system. Cell Res **23**: 1233-1236

Minoia S, Petrozza A, D'Onofrio O, Prion F, Mosca G, Sozio G, Cellini F, Bendahmane A, Carriero F (2010) A new mutant genetic resource for tomato crop improvement by TILLING technology. BMC Res Notes. Doi: 10.1186/1756-0500-3-69

**Mirouze M, Vitte C** (2014) Transposable elements, a treasure trove to decipher epigenetic variation: insights from Arabidopsis and crop epigenomes. J Exp Bot **65**: 2801-2812

Modrzejewski D, Hartung F, Lehnert H, Sprink T, Kohl C, Keilwagen J, Wilhelm R (2020). Which factors affect the occurrence of off-target effects caused by the use of CRISPR/Cas: A systematic Review in Plants. Front Plant Sci. doi: 10.3389/fpls.2020.574959

Mogilner N, Zutra D, Gafny R, Bar-Joseph, Moshe (1993) The persistence of engineered Agrobacterium tumefaciens in agroinfected plants. MPMI 6: 673-675.

Mohanta TK, Bashir T, Hashem A, Abd Allah EF, Bae H (2017) Genome editing tools in plants. Genes (Basel). doi: 10.3390/genes8120399

**Mondini L, Noorani A, Pagnotta MA** (2009) Assessing plant genetic diversity by molecular tools. Diversity 1: 19-35

**Moon HS, Li Y, Stewart CN** (2010) Keeping the genie in the bottle: transgene biocontainment by excision in pollen. Trends Biotechnol **28**: 3-8

**Moscou MJ, Bogdanove AJ** (2009) A simple cipher governs DNA recognition by TAL effectors. Science (80-) **326**: 1501

Mushtaq M, Bhat JA, Mir ZA, Sakina A, Ali S, Singh AK, Tyagi A, Salgotra RK, Dar AA, Bhat R (2018) CRIPSR/Cas approach: A new way of looking at plant-abiotic interactions. J Plant Physiol 224-225: 156-162

Mussolino C, Morbitzer R, Lutge F, Dannemann N, Lahaye T, Cathomen T (2011) A novel TALE nuclease scaffold enables high genome editing activity in combination with low toxicity. Nucleic Acids Res **39**: 9283-9293

**Neff MM, Chory J** (1998) genetic interaction between phytochrome A, phytochrome B and cryptochrome 1 during Arabidopsis development. Plant Physiology **118**: 27-36

Nishitani C, Hirai N, Komori S, Wada M, Okada K, Osakabe K, Yamamoto T, Osakabe Y (2016) Efficient genome editing in Apple using a CRISPR/Cas9 system. Sci rep 6: 1-8

**Niyogi KK, Grossman AR, Bjorkman O** (1998) Arabidopsis mutants define a central role for the xanthophyll cycle in the regulation of photosynthetic energy conversion. Plant cell **10**: 1121-1134

Nozue K, Kanegae T, Imaizumi T, Fukuda S, Okamoto H, Yeh KC, Lagarias JC, Wada M (1998) A phytochrome from thr fern Adiantum with features of the putative photoreceptor NPH1. Proc Natl Acad Sci U S A 95: 15826-15830

Nunes-Nesi A, Carrari F, Lytovchenko A, Smith AMO, Loureiro ME, Ratcliffe RG, Sweetlove LJ, Fernie AR (2005) Enhanced photosynthetic performance and growth as a

consequence of decreasing mitochondrial malate dehydrogenase activity in transgenic tomato plants. Plant Physiol **137**: 611-622

Oeller PW, Min-Wong L, Taylor LP, Pike DA, Theologis A (1991) Reversible inhibition of tomato fruit senescence by antisense RNA. **254**: 437-439

**Ohgishi M, Saji K, Okada K and Sakai T** (2004) Functional analysis of each blue light receptor, cry1, cry2, phot1 and phot2, by using combinatorial multiple mutants in Arabidopsis. Proc Natl Acad Sci USA **101**: 2223-2228

Okabe Y, Asamizu E, Saito T, Matsukura C, Ariizumi T, Brs C, Rothan C, Mizoguchi T, Ezura H (2011) Tomato TILLING technology: Development of a reverse genetics tool for the efficient isolation of mutants from micro-tom mutant libraries. Plant Cell Physiol **52:** 1994-2005

**Okamura M, Yasuno N, Ohtsuka M, Tanaka A, Shikazono N, Hase Y** (2003) Wide variety of flower-color and shape mutants regenerated from leaf cultures irradiated with ion beams. Nucl Instruments methods Phys Res Sect B Beam Interact with Mater Atoms 206: 574-578

Okuzaki A, Toriyama K (2004) Chimeric RNA/DNA oligonucleotide-directed gene targeting in rice. Plant Cell Rep 22: 509-512

Oms-Oliu G, hertog MLATM, Van de Poel B, Ampofo-Asiama J, Geeraerd AH, Nicolai BM (2011) Metabolic characterization of tomato fruit during preharvest development, ripening, and postharvest shelf-life. Postharvest Biol Technol 62: 7-16

**Otagaki S, Kawai M, Masuta C, Kanazawa A** (2011) Size and positional effects of promoter RNA segments on virus-induced RNA-directed DNA methylation and transcriptional gene silencing. Epigenetics **6**: 681-691

Park H, Kreunen SS, Cuttriss AJ, DellaPenna D, Pogson BJ (2002) Identification of the carotenoid isomerase provides insight into carotenoid biosynthesis, prolamellar body formation, and photomorphogenesis. Plant Cell 14: 321-332

**Parry AD, Horgan R** (1991a) Carotenoid metabolism and the biosynthesis of abscisic acid. Phytochemistry **30**: 815-821

**Pecker I, Gabbay R, Cunningham FX, Hirschberg J** (1996) Cloning and characterization of the cDNA for lycopene bet-cyclase from tomato reveals decrease in its expression during fruit ripening. Plant Mol Bio **30**: 807-819

Pennisi E (2013) The CRISPR craze. Science (80-) 341: 833-836

Perry JA, Wang TL, Welham TJ, Gardner S, Pike JM, Yoshida S, Parniske M (2003) A TILLING reverse genetics tool and a web-accessible collection of mutants of the legume Lotus japonicus. Plant Physiol 131: 866-871

Persikov A V, Wetzel JL, Rowland EF, Oakes BL, Xu DJ, Singh M, Noyes MB (2015) A systematic survey of the Cys2His2 zinc finger DNA-binding landscape. Nucleic Acids Res 43: 1965-1984

Peterson BA, Haak DC, Nishimura MT, Teixeira PJPL, James SR, Dangl JL, Nimchuk ZL (2016) genome-wide assessment of efficiency and specificity in CRISPR/Cas9 mediated multiple site targeting in Arabidopsis. PLoS One 11: 1-11

**Pratta G, Zorzoli R, Boggio SB, Picardi LA, Valle EM** (2004) Glutamine and glutamate levels and related metabolizing enzymes in tomato fruits with different shelf-life. Sci Hortic **100**: 341-347

**Preuss S and Pikaard CS** (2003) Targeted gene silencing in plants using RNA interference. DNA Press pp 23-36

Pulido P, Toledo-Ortiz G, Philips MA, Wright LP, Rodriguez-Concepcion M (2013) Arabidopsis J-protein J20 delivers the first enzyme of the plastidial isoprenoid pathway to protein quality control. Plant Cell **25**: 4183-4194

**Rabinowitch HD, Budowski P, Kedar N** (1975) Carotenoids and epoxide cycles in mature-green tomatoes. Planta **122**: 91-97

Ramegowda V, Mysore KS, Senthil-Kumar M (2014) Virus-induced gene silencing is a versatile tool for unraveling the functional relevance of multiple abiotic stress-responsive genes in crop plants. Front Plant Sci 5: 1-12

Ran FA, Cong L, Yan WX, Scott DA, Gootenberg JS, Kriz AJ, Zetsche B, Shalem O, Wu X, Makarova KS, et al (2015) In vivo genome editing using Staphylococcus aureus Cas9. Nature 520: 186-191

**Raymundo LC, Chichester CO, Simpson KL** (1976) Light-dependent carotenoid synthesis in the tomato fruit. J Agri Food Chem **24(1)**: 59-64 doi: 10.1021/jf60203a28

Reyon D, Tsai SQ, Khgayter C, Foden JA, sander JD, Joung JK (2012) FLASH assembly of TALENs for high-throughput genome editing. Nat Biotechnol 30: 460-465

**Richardson DL, Davies HV, Ross HA, Mackay GR** (1990) Invertase activity and its relation to hexose accumulation in potato tubers. J Exp Bot **41(1)**: 95-99

**Rodriguez-Concepcion M** (2010) Supply of precursors for carotenoid biosynthesis in plants. Arch. Biochem Biophys **504**: 118-122

**Rodriguez-Concepcion M, Boronat A** (2002) Elucidation of the methylerythritol phosphate pathway for isoprenoid biosynthesis in bacteria and plastids. A metabolic milestone achieved through genomics. Plant Physiol **130**: 1079-1089

Rodriguez-Leal D, Lemmon ZH, Man J, Bartlett ME, Lippman ZB (2017) Engineering quantitative trait variation for crop improvement by genome editing. Cell 171: 470-480.e8

Roessner-Tunali U, Hegemann B, Lytovchenko A, Carrari F, Bruedigam C, Granot D, Fernie AR (2003) Metabolic profiling of transgenic tomato plants overexpressing hexokinase reveals that the influence of hexose phosphorylation diminishes during fruit development. Plant Physiol 133: 84-99

Ronen G, Carmel-Goren L, Zamir D, Hirschberg J (2000) An alternative pathway to β-carotene formation in plant chromoplasts discovered by map-based cloning of Beta and old-gold color mutations in tomato. Proc Natl Acad Sci U S A 97: 11102-11107

Rontein D, Dieuaide-Noubhani M, Dufourc EJ, Raymond P, Rolin D (2002) the metabolic architecture of plant cells: stability of central metabolism and flexibility of anabolic pathways during the growth cycle of tomato cells. J Biol Chem 277: 43948-43960

**Rossi M, Iusem ND** (1994) Tomato (Lycopersicon esculentum) genomic clone homologous to a gene encoding an abscisic acid-induced protein. Plant Physiol **104**: 1073-1074

**Rothan C, Diouf I, Causse M** (2019) Trait discovery and editing in tomato. Plant J **97**: 73-90

Roux F, Giancola S, Durand S, Reboud X (2006) Building of an experimental cline with Arabidopsis thaliana to estimate herbicide fitness cost. Genetics 173: 1023-1031

**Ruiz MT, Vionnet O, Baulcombe DC** (1998) Initiation and maintenance of virus-induced gene silencing. Plant Cell **10**: 937-946

**Ruiz-Sola MA, Rodriguez-Concepcion M** (2012) Carotenoid biosynthesis in Arabidopsis: A colorful pathway. Arab B 10: e0158

Saito T, Ariizumi T, Okabe Y, Asamizu E, Hiwasa-Tanase K, Fukuda N, Mizoguchi T, Yamazaki Y, Aoki K, Ezura H (2011) TOMATOMA: A novel tomato mutant database distributing micro-tom mu collections. Plant Cell Physiol **52**: 282-296

Sakai T, Kagawa T, Kasahara M, Swartz TE, Christie JM, Briggs WR, Wada M, Okada K (2001) Arabidopsis nph1 and npl1: Blue light receptors that mediate both phototropism chloroplast relocation. Proc Natl Acad Sci U S A 98: 6969-6974

**Sakamoto K, Briggs WR** (2002) Cellular and subcellular localization of phototropin 1. Plant Cell **14**: 1723-1735

Sarsu F, Penna S, Atomic B, Ibrahim R, Agency MN, Sangwan RS (2018) Manual on mutation breeding.

**Sasaki T, Burr B** (2000) international Rice genome Sequencing Project: the effort to completely sequence the rice genome. Curr Opin Plant Biol 3: 138-142

Sauer NJ, Narvaez-Vasquez J, Mozoruk J, Miller RB, Warburg ZJ, Woodward ZJ, Mihiret YA, Lincoln TA, Segami RE, Sanders SL, et al (2016) Oligonucleotidw-mediated genome editing provides precision and function to engineered nucleases and antibiotics in plants. Plant Physiol 170: 1917-1928

**Schauer N, Zamir D, Fernie AR** (2005) Metabolic profiling of leaves and fruit of wild species tomato: A survey of the Solanum lycopersicum complex. J Exp Bot **56**: 297-307

Schneiders H, Der HJA Van, Rigola D, Oeveren J, Van Janssen A, Bonne A, Orsouw NJ Van (2009) High-Throughput Detection of Induced Mutations and Natural Variation Using KeyPoint Technology.

**Schofield A, Paliyath G** (2005) Modulation of carotenoid biosynthesis during tomato fruit ripening through phytochrome regulation of phytoene synthase activity. Plant Physiol Biochem **43(12)**: 1052-1060.

**Schwechheimer C, Deng XW** (2000) The COP/DET/FUS proteins-regulators of eukaryotic growth and development. Semin Cell Dev Biol **11**: 495-503

**Senthil-Kumar M, Mysore KS** (2011) Virus-induced gene silencing can persist for more than 2 years and also be transmitted to progeny seedlings in Nicotiana benthamiana and tomato. Plant Biotechnol J **9**:797-806

**Senthil-Kumar M, Mysore KS** (2013) RNAi in plants: Recent developments and applications in agriculture. Gene Silenc theory, Tech Appl 183-200

**Seymour GB, Ostergaard L, Chapman NH, Knapp S, Martin C** (2013) Fruit development and ripening. Annu rev Plant Biol **64**: 219-241

**Shah SA, Erdmann S, Mojica FJM, Garrett RA** (2013) protospacer recognition motifs: Mixed identities and functional diversity. RNA Biol **10**: 891-899

**Shan Q, Wang Y, Li J, Gao C** (2014) Genome editing in rice and wheat using the CRISPR/Cas system. Nat Protoc **9**: 2395-2410

Sharma K, Gupta S, Sarma S, Rai M, Sreelakshmi Y, Sharma R (2021) Mutations in tomato 1-aminocyclopropane carboxylic acid synthase2 uncover its role in development beside fruit ripening. Plant J 106: 95-112

Sharma S and Sharma RP LePHOT1 EF063359 (2006) World Wide Web, <a href="http://www.ncbi.nlm.nih.gov">http://www.ncbi.nlm.nih.gov</a>

**Sharma S and Sharma RP** LePHOT2 EF021291 (2007) World Wide Web, http://www.ncbi.nlm.nih.gov

Sharma S, Kharshiing E, Srinivas A, Zikihara K, Tokutomi S, Nagatani A, Fukayama H, Bodanapu R, Behera RK, Sreelakshmi Y, et al (2014) A dominant mutation in the light-oxygen and voltage2 domain vicinity impairs phototropin1 signalling in tomato. Plant Physiol **164**: 2030-2044

Shimazaki K, Doi M, Assmann SM, Kinoshita T (2007) Light regulation of stomatal movement. Annu Rev Biol 58: 219-247

Shukla VK, Doyon Y, Miller JC, Dekelver RC, Moehle EA, Worden SE, Mitchell JC, Arnold NL, Gopalan S, Meng X, et al (2009) Precise genome modification in the crop species Zea mays using zinc-finger nucleases. Nature **459**: 437-441

Sijen T, Vijn I, Rebocho A, Van Blokland R, Roelofs D, Mol JNM, Kooter JM (2001) Trsnacriptional and posttranscriptional gene silencing are mechanistically related. Curr Biol 11: 436-440

**Simkin AJ, Zhu C, Kuntz M, Sandmann G** (2003) comparison of carotenoid content, gene expression and enzyme levels in tomato (Lycopersicon esculentum) leaves. Z Naturforsch C **58(5-6)**: 371-380

**Slade AJ, Fuerstenberg SI, Loeffler D, Steine MN, Facciotti D** (2005) A reverse genetic, nontransgenic approach to wheat crop improvement by TILLING. Nat Biotechnol 23: 75-81

- Smith HH (1958) Radiation in the production of useful mutations. Bot. rev 24: 1-24
- **Spooner DM, Anderson GJ, Jansen RK** (1993) Chloroplast DNA evidence for the interrelationships of tomatoes, potatoes and pepinos (Solanaceae). Am J Bot **80**: 676-688
- **Srinivas A, Behera RK, Kagawa T, Wada M, Sharma R** (2004) High Pigment1 mutation negatively regulates phototropic signal transduction in Tomato seedlings. Plant Physiol 134: 790-800
- Stadler LJ (1928) Genetic effects of X-rays in maize. Genetics 14: 69-75
- Su L, Diretto G, Purgatto E, Danoun S, Zouine M, Li Z, Roustan JP, Bouzayen M, Giuliano G Chervin C (2015) Carotenoid accumulation during tomato fruit ripening is modulated by the auxin-ethylene balance. BMC Plant Biol 15: 1-12
- Suetsugu N, Mittmann F, Wagner G, Hughes J, Wada M (2005) A chimeric photoreceptor gene, NEOCHROME, has arisen twice during plant evolution. Proc Natl Acad Sci USA **102**: 13705-13709.
- Sun L, Yuan B, Zhang M, Wang L, Cui M, Wang Q, Leng P (2012) Fruit specific RNAi-mediated suppression of SINCED1 increases both lycopene and β-carotene contents in tomato fruit. J Exp Bot 63: 3097-3108
- Symons GM, Chua YJ, Ross JJ, Quittenden LJ, Davis NW, Reid JB (2012) Hormonal changes during non-climacteric ripening in strawberry. J Exp Bot 63: 4741-4750.
- **TAGI** (2000) Analysis of the genome sequence of Arabidopsis thaliana. Nature **408**: 796-815
- **Takemiya A, Inoue S, Doi M, Kinoshita T and Shimazaki K** (2005) Phototropins promote plant growth in response to blue light in low light environments. Plant Cell **17**:1120-1127
- **Tepperman JM, Hudson ME, Khanna R, Zhu T, Chang SH, Wang X, Quail PH** (2004) Expression profiling of phyB mutant demonstrates substantial contribution of other phytochromes to red-light-regulated gene expression during seedling de-etiolation. The Plant Journal **38**:725-739
- **Tepperman JM, Zhu T, Chang HS, Wang X, Quail PH** (2001) Multiple transcription-factor genes are early targets of phytochrome A signalling. Proceedings of the National Academy of Sciences, USA **98**: 9437-9442.
- Tian S, Jiang L, Gao Q, Zhang J, Zong M, Zhang H, Ren Y, Guo S, Gong G, Liu F, et al (2017) Efficient CRISPR/Cas9 based gene knockout in watermelon. Plant Cell Rep 36: 399-406
- **Till BJ, Cooper J, Tai TH, Colowit P, Greene EA, Henikoff S, Comai L** (2007) Discovery of chemically induced mutations in rice by TILLING. BMC Plant Biol 7: 1-12
- Till BJ, Reynolds SH, Greene EA, Codomo CA, Enns LC, Johnson JE, Burtler C, Odden AR, Young K, Taylor NE, et al (2003) large-scale discovery of induced point mutations with high-throughput TILLING. Genome Res 13: 524-530

Till BJ, Reynolds SH, Weil C, Springer N, Burtner C, Young K, Bowers E, Codomo CA, Enns LC, Odden AR, et al (2004) Discovery of induced point mutations in maize genes by TILLING. BMC Plant Biol 4: 1-8

**Toledo-Ortiz G, Huq E, Rodriguez-Concepcion M** (2010) Direct regulation of phytoene synthase gene expression and carotenoid biosynthesis by phytochrome-interacting factors. Proc Natl Acad Sci U S A **107**: 11626-11631

**Ueta R, Abe C, Watanabe T, Sugano SS, Ishihara R, Ezura H, Osakabe Y, Osakabe K** (2017) rapid breeding of parthenocarpic tomato plants using CRISPR/Cas9. Sci Rep 7: 1-8

Using Engineered TAL Effector Nucleases. G3 Genes, Genomes, Genet 3: 1697-1705

**Valle EM, Boggio SB, Heldt HW** (1998) Free amino acids content of phloem sap and fruits in *Lycopersicon esculentum*. Plant Cell Physiol **39**: 485-461

Van Der Biezen EA, Brandwagt BF, Van Leeuwen W, Nijkamp HJJ, Hille J (1996) Identification and isolation of the FEEBLY gene from tomato by transposon tagging. Mol Gen Genet 251: 267-280

Van Eck J, Kirk DD, Walmsley AM (2006) Tomato (Lycopersicum esculentum). Methods Mol Biol. **343**:459-73 doi: 10.1385/1-59745-130-4

**Van Kammen A** (1997) Virus induced gene silencing in infected and transgenic plants. Trends Plant sci. **2**:409-411

Varsha Wesley S, Helliwell CA, Smith NA, Wang M, Rouse DT, Liu Q, Gooding PS, Singh SP, Abbott D, Stoutjesdijk PA, et al (2001) Construct design for efficient, effective and high-throughput gene silencing in plants. Plant J 27: 581-590

Vats S, Kumawat S, Kumar V, Patil GB, Joshi T, Sonah H, Sharma TR, Deshmukh R (2019) Genome editing in Plants: Exploration of. 8: 1386

**Veillet F, Perrot L, Chauvin L, Kermarrec MP, Guyon-Debast A, Chauvin JE, Nogue F, Mazier M** (2019) Transgene-free genome editing in tomato and potato plants using Agrobacterium-mediated delivery of a CRISPR/Cas9 cytidine base editor. Int J Mol Sci. doi: 10.3390/ijms20020402

**Voinnet O.** (2001) RNA silencing as a plant immune system against viruses. TRENDS Genet **17**: 449-459

Von Lintig J, Welsch R, Bonk M, Giuliano G, Batschauer A, Kleinig H (1997) Light-dependent regulation of carotenoid biosynthesis occurs at the level of phytoene synthase expression and is mediated by phytochrome in Sinapis alba and Arabidopsis thaliana seedlings. Plant J 12: 625-634.

Vrebalov J, Ruezinsky D, Padmanabhan V, White R, Medrano D, Drake R, Schuch W, Giovannoni J (2002) A MADS-box gene necessary for fruit ripening at the tomato ripening-inhibitor (rin) locus. Science (80-) 296: 343-346

**Wada M and Kagawa T and Sato Y** (2003) Chloroplast movement. Annu Rev Plant Biol **54**:455-468

- **Waltz, Emily** (2021) GABA-enriched tomato is first CRISPR-edited food to enter market. Nature Biotechnology 40- 10.1038/d41587-021-000262
- Wang H, Yang H, Shivalila CS, Dawlaty MM, Cheng AW, Zhang F, Jaenisch R (2013) One-step generation of mice carrying mutations in multiple genes by CRISPR/casmediated genome engineering. Cell **153**: 910-91
- **Wang MB, Metzlaff M** (2005) RNA silencing and antiviral defense in plants. Curr Opin Plant Biol **8(2)**:216-22 doi: 10.1016/j.pbi.2005.01.006
- Wang S, Liu J, Feng Y, Niu X, Giovannoni J, Liu Y (2008) Altered plastid levels and potential for improved fruit nutrient content by downregulation of the tomato DDB1-interacting protein CUL4. Plant J 55: 89-103
- Wang Y, Wang Z, Chen Y, Hua X, Yu Y, Ji Q (2019) A highly efficient CRISPR-Cas9 based genome engineering platform in Acinetobacter baumannii to understand the H2O2-sensing mechanism of OxyR. Cell Chem Biol 26: 1732-1742.e5
- Wang Z, Mo Y, Qian S, Gu Y (2002) Negative phototropism of rice root and its influencing factors. Sci China, Ser C Life Sci 45: 485-496
- Wang Z, Wang S, Li D, Zhang Q, Li L, Zhong C, Liu Y, Huang H (2018) Optimized paired-sgRNA/Cas9 cloning and expression cassette triggers high-efficiency multiplex genome editing in kiwifruit. Plant Biotechnol J 16: 1424-1433
- Welsch R, Beyer P, Hugueney P, Kleinig H, von Lintig J (2000) Regulation and activation of phytoene synthase, a key enzyme in carotenoid biosynthesis, during photomorphogenesis. Planta 211: 846-854
- Welsch R, Medina J, Giuliano G, Beyer P, von Lintig J (2003) Structural and functional characterization of the phytoene synthase promoter from Arabidopsis thaliana. Planta **216**: 523-534
- Wendt T, Holm PB, Starker CG, Christian M, Voytas DF, Brinch-Pedersen H, Holme IB (2013) TAL effector nucleases induce mutations at a pre-selected location in the genome of primary barley transformants. Plant Mol Biol 83: 279-285
- **Wenzel G** (2006) Molecular plant breeding: Achievements in green biotechnology and future perspectives. Appl Microbiol Biotechnol **70**: 642-650
- Wiedenheft B, Sternberg SH, Doudna JA (2012) RNA-guided genetic silencing systems in bacteria and archaea. Nature **482**: 331-338
- Wienholds E, van Eeden F, Kosters M, Mudde J, Plasterk RHA, Cuppen E (2003) Efficient target-selected mutagenesis in zebrafish. Genome Res 13: 2700-2707
- Wisman E, Koornneef M, Chase T, Lifshytz E, Ramanna MS, Zabel P (1991) Genetic and molecular characterization of an Adh-1 null mutant in tomato. MGG Mol gen Genet **226**: 120-128
- Woitsch S, Romer S (2003) Expression of xanthophyll biosynthetic genes during light-dependent chloroplast differentiation. Plant Physiol **132(3)**: 1508-1517

- **Wyllie SG, Fellman JK** (2000) Formation of volatile branched chain esters in bananas (Musa sapientum L.). J Agric Food Chem **48**: 3493-3496
- Xie M, Yu B (2015) siRNA-directed DNA Methylation in Plants. Curr Genomics 16: 23-31
- Xie Z, Johansen LK, Gustafson AM, Kasschau KD, Lellis AD, Zilberman D, Jacobsen SE, Carrington JC (2004) Genetic and functional diversification of small RNA pathways in plants. PLoS Biol 2: 642-652
- **Xiong Y, Contento AL, Bassham DC** (2005) AtATG18a is required for the formation of autophagosomes during nutrient stress and senescence in Arabidopsis thaliana. Plant J **42**: 535-546
- Xu C, Liberatore KL, Macalister CA, Huang Z, Chu YH, Jiang K, Brooks C, Ogawa-Ohnishi M, Xiong G, Pauly M, et al (2015) A cascade of arabinosyltransferases controls shoot meristem size in tomato. Nat genet 47: 784-792
- **Xu C, Park SJ, Van Eck J, Lippman ZB** (2016) Control of inflorescence architecture in tomato by BTB/POZ transcriptional regulators. Genes Dev **30**: 2048-2061
- Yang D Seaton DD, Krahme J Halliday KJ (2016) Photoreceptors effects on plant biomass, resource allocation, and metabolic state. Proc Natl Acad Sci U S A 113: 7667-7672
- **Yanovsky MJ, Kay SA** (2003) Living by the calendar: How plants know when to flower. Nat Rev Mol Cell Biol **4**: 265-275
- Yen HC, Shelton BA, Howard LR, Lee S, Vrebalov J, Giovannoni JJ (1997) the tomato high-pigment (hp) locus maps to chromosome 2 and influences plastome copy number and fruit quality. Theor Appl Genet 95: 1069-1079
- **Yoder JI** (1990) rapid proliferation of the maize transposable elements Activator in transgenic tomato. Plant Cell **2**: 723-730
- **Yoon K, Cole-Strauss A, Kmiec EB** (1996) Targeted gene correction of episomal DNA in mammalian cells mediated by a chimeric RNA DNA oligonucleotide Proc Natl Acad Sci U S A **93**: 2071-2076
- **Yu Q and Beyer P** (2012) Reaction specificities of the ionone forming lycopene cyclase from rice (Oryza sativa) elucidated in vitro. FEBS Lett. **586**: 3415-3420
- Yuan XY, Wang RH, Zhao XD, Luo YB, Fu DQ (2016) Role of the tomato Non-Ripening mutation in regulating fruit quality elucidated using iTRAQ protein profile analysis. PLoS One 11: 1-21
- Zanor MI, Osorio S, Nunes-Nesi A, Carrari F, Lohse M, Usadel B, Kuhn C, Bleiss W, Giavalisco P, Willmitzer L et al (2009) RNA interference of LIN5 in tomato confirms its role in controlling brix content, uncovers the influence of sugars on the levels of fruit hormones, and demonstrates the importance of sucrose cleavage for normal fruit development and fertility. Plant Physiol 150: 1204-1218

- **Zhang F, Wen Y, Guo X** (2014) CRISPR/Cas9 for genome editing: Progress, implications and challenges. Hum Mol Genet **23**: 40-46
- **Zhang H, Lang Z, Zhu JK** (2018) Dynamics and function of DNA methylation in plants. Nat Rev Mol Cell Biol **19**: 489-506
- **Zhao TY, Thacker R, Corum JW, Snyder JC, Meeley RB, Obendorf RL, Downie B** (2004) Expression of the maize GALACTINOL SYNTHASE gene family: (I) Expression of two different genes during seed development and germination. Physiol Plant **121**: 634-646
- Zhong S, Fei Z, Chen YR, Zheng Y, Huang M, Vrebalov J, McQuinn R, Gapper N, Liu B, Xiang J, et al (2013) Single-base resolution methylomes of tomato fruit development reveal epigenome modifications associated with ripening. Nat Biotechnol 31: 154-159
- **Zhou L, Tian S, Qin G** (2019) RNA methylomes reveal the m6A-mediated regulation of DNA demethylase gene SlDML2 in tomato fruit ripening. Genome Biol **20**: 1-23
- Zhu C, Yamamura S, Nishihara M, Koiwa H, Sandmann G (2003) cDNAs for the synthesis of cyclic carotenoids in petals of Gentiana lutea and their regulation during flower development. Biochim Biophys Acta- Gene Struct Expr 1625: 305-308
- Zhu T, Peterson DJ, Tagliani L, St. Clair G, Baszczynski CL, Bowen B (1999) Targeted manipulation of maize genes in vivo using chimeric RNA/DNA oligonucleotides. Proc Natl Acad Sci U S A **96**: 8763-8733

### References

## Probing structural organisation of chromatin during B cell development through mechanistic modelling

by Anubhooti.

Indira Gandhi Memorial Library UNIVERSITY OF HYDERABAD Central University P.O. HYDERABAD-500 046.

Submission date: 27-Dec-2022 12:28PM (UTC+0530)

**Submission ID:** 1986849759

File name: Thesis\_Anubhooti\_13LAPH19\_Final.pdf (26.87M)

Word count: 21571 Character count: 118580

# Targeted gene Silencing/Knockout of tomato phototropins to decipher their role in fruit carotenogenesis

**ORIGINALITY REPORT** 

6% SIMILARITY INDEX

4%
INTERNET SOURCES

5%
PUBLICATIONS

%
STUDENT PAPERS

**PRIMARY SOURCES** 

1 V

www.biorxiv.org

Internet Source

1 %

2

www.ncbi.nlm.nih.gov

Internet Source

<1%

Himabindu Vasuki Kilambi, Alekhya Dindu, Kapil Sharma, Narasimha Rao Nizampatnam et al. "The new kid on the block: a dominant negative mutation of phototropin1 enhances carotenoid content in tomato fruits", The Plant Journal, 2021

Publication

4

Hymavathi Salava, Sravankumar Thula, Vijee Mohan, Rahul Kumar, Fatemeh Maghuly. "Application of Genome Editing in Tomato Breeding: Mechanisms, Advances, and Prospects", International Journal of Molecular Sciences, 2021

<1%

Publication

5

Himabindu Vasuki Kilambi, Alekhya Dindu, Kapil Sharma, Narasimha Rao Nizampatnam

<1%

Exclude quotes On Exclude matches < 14 words

Exclude bibliography On

The Plant Journal (2021) 106, 844-861

doi: 10.1111/tpj.15206

1365313x, 2021, 3. Downloaded from https://onlinelibrary.wiley.com/doi/10.1111/tpj.15206 by University Of Hyderabad. Wiley Online Library on [29/12/2022]. See the Terms and Conditions (https://onlinelibrary.wiley.com/rems-a-d-conditions) on Wiley Online Library for rules of use; OA articles are governed by the applicable Creative Commons License

## The new kid on the block: a dominant-negative mutation of phototropin1 enhances carotenoid content in tomato fruits

Himabindu Vasuki Kilambi<sup>†,\*</sup>, Alekhya Dindu, Kapil Sharma (D), Narasimha Rao Nizampatnam<sup>†,\*</sup>, Neha Gupta<sup>†</sup>, Nikhil Padmanabhan Thazath, Ajayakumar Jaya Dhanya<sup>†</sup>, Kamal Tyagi<sup>†,\*\*</sup>, Sulabha Sharma<sup>†,\*\*</sup>, Sumit Kumar<sup>‡,\*</sup>, Rameshwar Sharma (D) and Yellamaraju Sreelakshmi<sup>\*</sup>

Repository of Tomato Genomics Resources, Department of Plant Sciences, University of Hyderabad, Hyderabad 500046, India

Received 26 October 2020; revised 15 January 2021; accepted 10 February 2021; published online 17 February 2021.

#### **SUMMARY**

Phototropins, the UVA-blue light photoreceptors, endow plants to detect the direction of light and optimize photosynthesis by regulating positioning of chloroplasts and stomatal gas exchange. Little is known about their functions in other developmental responses. A tomato *Non-phototropic seedling1* (*Nps1*) mutant, bearing an Arg495His substitution in the vicinity of LOV2 domain in phototropin1, dominant-negatively blocks phototropin1 responses. The fruits of *Nps1* mutant were enriched in carotenoids, particularly lycopene, compared with its parent, Ailsa Craig. On the contrary, CRISPR/CAS9-edited loss of function *phototropin1* mutants displayed subdued carotenoids compared with the parent. The enrichment of carotenoids in *Nps1* fruits is genetically linked with the mutation and exerted in a dominant-negative fashion. *Nps1* also altered volatile profiles with high levels of lycopene-derived 6-methyl 5-hepten2-one. The transcript levels of several MEP and carotenogenesis pathway genes were upregulated in *Nps1*. *Nps1* fruits showed altered hormonal profiles with subdued ethylene emission and reduced respiration. Proteome profiles showed a causal link between higher carotenogenesis and increased levels of protein protection machinery, which may stabilize proteins contributing to MEP and carotenogenesis pathways. The enhancement of carotenoid content by *Nps1* in a dominant-negative fashion offers a potential tool for high lycopene-bearing hybrid tomatoes.

Keywords: Solanum lycopersicum, tomato, phototropins, fruit ripening, carotenoid content, gene editing, primary metabolites, protein protection machinery.

### INTRODUCTION

Light is an omnipresent environmental signal that is very effectively utilized by plants to modulate a variety of growth and developmental responses. The capacity to sense light endows plants to monitor seasonal changes, detect the canopy shade, and orient their growth towards or away from light (Nemhauser and Chory, 2002; Kharshing et al., 2019). In young germinating seedlings, the availability of light is necessary to initiate photomorphogenic development, wherein seedlings become photoautotrophic by transforming plastids to fully functional chloroplasts (Jenkins et al., 1983; Waters and Langdale, 2009). The

formation of chloroplasts is preceded by light-triggered activation of chlorophyll and carotenoid biosynthesis (Kasemir, 1983; Bartley and Scolnik, 1995; von Wettstein et al., 1995; Llorente et al., 2017).

Extensive studies on the light-mediated formation of photosynthetic pigments in seedlings revealed that specific photoreceptors activate key genes involved in chlorophyll and carotenoid biosynthesis (llag *et al.*, 1994; Von Lintig *et al.*, 1997; Huq *et al.*, 2004; Yuan *et al.*, 2017). At least five different classes of photoreceptors have been reported in plants viz., phytochromes, cryptochromes, phototropins, zeitlupe/FKF1/LKP1 and UVR8 (Galvão and Fankhauser, 2015; Kharshiing *et al.*, 2019). Among these, phytochrome

<sup>\*</sup>For correspondence (e-mail syellamaraju@gmail.com).

<sup>&</sup>lt;sup>†</sup>These authors contributed equally to this study.

<sup>&</sup>lt;sup>‡</sup>Present address: School of Plant Sciences and Food Security, Tel Aviv University, Tel Aviv, 6997801, Israel

<sup>\$</sup>Present address: Department of Plant and Environmental Sciences, Weizmann Institute of Science, Rehovot, 7610001, Israel

<sup>&</sup>lt;sup>1</sup>Present address: ATGC Biotech Pvt. Ltd, Hyderabad, India

<sup>\*\*</sup>Present address: Department of Postharvest Science, ARO, Volcani Center, Rishon LeZion, 7505101, Israel

<sup>&</sup>lt;sup>††</sup>Present address: Applied Plant Science, Technical University Darmstadt, Schnittspahnstr. 10, Darmstadt, D-64287, Germany

<sup>&</sup>lt;sup>‡‡</sup>Present address: Department of Botany, Nalanda College, Patliputra University, Bihar, India

specifically influences the chlorophyll and carotenoids formation in young seedlings (Von Lintig et al., 1997; Hug et al., 2004). The synthesis of chlorophylls and carotenoids in photosynthetic tissues are tightly coupled and regulated in a stoichiometric fashion. Carotenoids act as photosynthetic accessory pigments and protect chlorophylls from photooxidation (Bartley and Scolnik, 1995; Frank and Cogdell, 1996). Consequently, inhibition of carotenoid biosynthesis leads to photooxidation of chloroplasts with albino or pale green seedlings (Mayfield and Taylor, 1984; Mayfield et al., 1986).

While chlorophyll accumulation is obligatorily linked with carotenoid biosynthesis (Mayfield and Taylor, 1984; Bartley and Scolnik, 1995), the carotenoid biosynthesis can occur independently of chlorophylls. The organs like carrot roots or tomato fruits make high amounts of carotenoids in the chromoplasts (Llorente et al., 2017). Given the diversity of genetic resources available, tomato has emerged as a model to study the regulation of carotenogenesis (Seymour et al., 2013; Barry, 2014). The molecular-genetic studies established that carotenogenesis in tomato employs the same biosynthetic pathway as in leaves, albeit with modification. The first enzyme of the pathway – phytoene synthase (PSY) - is replaced by a chromoplast-specific PSY1, and conversion of lycopene to β-carotene is mediated by chromoplast-specific lycopene β-cyclase (CYCB; Hirschberg, 2001). The carotenoids complement of tomato fruits is also distinctly different from leaves, with lycopene and upstream precursors constituting principal carotenoids rather than xanthophylls.

Besides, the initiation of carotenogenesis in tomato fruits is obligatorily coupled with the induction of ripening. Consequently, the non-ripening mutants, such as Rin, Nor and Cnr, fail to accumulate carotenoids in fruits (Seymour et al., 2013). Downstream to ripening regulators, the accumulation of carotenoids is also linked with the climacteric rise of ethylene. Therefore, ethylene-insensitive mutant such as Nr does not accumulate carotenoids (Barry et al., 2005). Even total suppression of ethylene biosynthesis by transgenic means leads to fruits bereft of carotenoids (Oeller et al., 1991). While ripening regulators and ethylene are essential for the induction of carotenogenesis in fruits, other hormones also modulate carotenoid biosynthesis. The ABA-deficient mutants of tomato fruits show higher carotenoids (Galpaz et al., 2008). Similarly, jasmonic acid also influences fruit carotenoid biosynthesis (Liu et al., 2012). The carotenoid levels in fruits are also dependent on the auxin-ethylene balance, indicating an antagonistic role of indole-3-acetic acid (IAA; Su et al., 2015), even second messengers like NO affect accumulation of fruit carotenoids (Bodanapu et al., 2016).

Though multiple factors modulate carotenoid levels in tomato fruits, the light too retains a modulatory role. Tomato fruits grown or incubated in darkness develop a normal complement of carotenoids, albeit at lower levels than light-grown plants (Raymundo et al., 1976; Gupta et al., 2014). The mutants defective in light signaling such as hp1 and hp2 accumulate a high amount of carotenoids in fruits, indicating a negative influence of light on carotenogenesis (Kilambi et al., 2013). This influence seems to be indirect as the higher level of carotenoids is ascribed to an increased number of plastids (Azari et al., 2010) and a higher level of carotenoid sequestration proteins in ripened fruits (Kilambi et al., 2013). Among the plant photoreceptors, only cryptochromes, phytochromes and UVR8 seem to influence carotenogenesis in tomato fruits. The loss of function mutants of cryptochromes and phytochromes and silencing of UVR8 reduces carotenoid levels in fruits (Gupta et al., 2014; Bianchetti et al., 2018; Li et al., 2018; Fantini et al., 2019). Conversely, the overexpression of the above photoreceptors increases the fruit carotenoids level (Giliberto et al., 2005; Li et al., 2018; Liu et al., 2018; Alves et al., 2020).

Among the plant photoreceptors, phototropin is considered as a receptor that specifically modulates movement responses (Galvão and Fankhauser, 2015), such as phototropic seedling curvature, negative phototropism of roots, stomatal movements and chloroplast relocation to adapt to high or low light intensity. Though phototropins regulate chloroplast movements, they do not seem to play a role in chloroplast development and function, as the photosynthetic efficiency of phot2 mutants is not compromised (Gotoh et al., 2018). The studies concerning phototropin function are limited to vegetative tissues, and their role in other organs such as fruits is not known.

The uncovering of physiological functions can be best executed by the use of mutants. In an earlier study, we described the isolation and characterization of the Nps1 mutant bearing a mutation in phototropin1 (Sharma et al., 2014). Nps1 mutant bearing an Arg 495 His substitution in the vicinity of LOV2 domain dominant-negatively blocked phot1-mediated responses in tomato such as chloroplast movement and seedling phototropic curvature. In this study, we show that Nps1 also influenced fruit carotenogenesis in a dominant-negative fashion. The stimulation of carotenogenesis was specific to Nps1, as loss of function phot1 alleles displayed reduced carotenoids levels. Genetic analysis using the introgression of Nps1 in two distinct cultivars revealed that enhancement of carotenoids is tightly linked to Nps1 mutation. The influence of Nps1 was not limited to carotenogenesis; analysis of proteome, metabolome and volatiles revealed broad spectrum influence of Nps1 specifically on protein quality control machinery.

### **RESULTS**

Carotenogenesis in tomato fruits is governed by a complex interaction between endogenous and environmental factors, including light acting via phytochromes and cryptochromes (Liu *et al.*, 2015). Conversely, it is not known whether phototropins contribute to carotenogenesis. In this study, we show that a dominant-negative mutation in phototropin1-*Nps1*, which suppresses phototropin1 function, influences fruit development and considerably enhances carotenoids.

#### Nps1 impedes phototropin1 function in fruits

To monitor whether phototropins are functional in fruits, we examined chloroplast accumulation and avoidance mediated by phototropin1 and phototropin2, respectively. In dark-adapted Nps1 and its parent Ailsa Craig (AC), chloroplasts were localized on the cell periphery (Figure 1a). Low-fluence blue-light-mediated chloroplast accumulation in the center of cells was seen only in AC but not in Nps1. Consequently, high-fluence blue-light-mediated chloroplast avoidance was also confined to AC. The absence of chloroplast movement indicated that, similar to leaves, phototropin1 function is compromised in Nps1 fruits (Sharma et al., 2014). We then examined whether Nps1 affected fruit development and attainment of ripening stages viz. mature-green (MG), breaker (BR) and redripe (RR). Interestingly, days post-anthesis (dpa) to attain MG was 8 days longer in Nps1 than AC (34 dpa). However, post-MG, duration to MG→BR and BR→RR in Nps1 and AC were nearly similar (Figure 1b).

# Increased carotenogenesis in *Nps1* is linked to its dominant-negative function

Though MG fruits of *Nps1* were pale-green, on-vine ripened RR fruits exhibited intense-red coloration with 3.1-fold higher lycopene than AC (Figure 1c; Table 1). Similarly, levels of precursors to lycopene were high in *Nps1* RR fruits. Although *Nps1* had higher β-carotene, its increase was subdued compared with lycopene. The contribution of carotenoids downstream to lycopene to the carotenoid pool was minor. To ascertain that elevated carotenogenesis is genetically linked with *Nps1*, we crossed it with its parent AC. We also crossed *Nps1* with Arka Vikas (AV) to establish whether its dominant-negative effect is retained in distant genetic background.

Akin to reported residual phototropism in F<sub>1</sub> (Sharma et al., 2014), F<sub>1</sub> seedlings showed slight curvature. In consonance with the dominant nature of Nps1, F<sub>1</sub> RR fruits exhibited high lycopene (Tables 1 and S1). Analysis of phototropism of F<sub>2</sub> seedlings along with CELI endonuclease assay revealed a segregation ratio for dominant mutation close to 3:1 (non-phototropic: phototropic; Figure S1; Table S2). Ripening stages of BC<sub>1</sub>F<sub>2</sub> (Nps1/Nps1) and its progeny were similar to Nps1 with delayed MG (Figure 1d, e). The mutation was also confirmed by Sanger sequencing of Nps1/Nps1 plants in both AC and AV backgrounds (Figure 1f-i).

Alike *Nps1*, in BC<sub>1</sub>F<sub>2</sub> (*Nps1*/*Nps1*) RR fruits, lycopene was considerably higher. Similarly, BC<sub>2</sub>F<sub>1</sub> and BC<sub>2</sub>F<sub>2</sub> (*Nps1*/*Nps1*) progeny RR fruits also had higher lycopene and its precursors (Tables 1 and S1). Similar to *Nps1*, backcrossed plants retained epinasty-like downward inclination of expanding apical leaves and had increased branching compared with AC (Figure 1j,k). However, levels of chlorophylls/carotenoids in *Nps1* and BC<sub>2</sub>F<sub>4</sub> *Nps1* leaves were akin to AC (Table S3). Further studies were carried out using BC<sub>2</sub>F<sub>2</sub> (*Nps1*/*Nps1*) and its F<sub>3</sub>/F<sub>4</sub> progeny in AC, which, altogether for convenience, is referred to as *Nps1*\*.

# Loss-of-function of *phot1* reduces carotenoid levels in fruits

To ascertain whether enriched carotenoids in *Nps1\** is specific to its dominant-negative action, we generated CRISPR/Cas9-edited loss-of-function alleles. Out of eight editing events in T<sub>0</sub> plants, five were recovered to homozygosity in T<sub>1</sub> progeny (Figure 2). Among five alleles, T100Cys\* (phot1<sup>CR1</sup>) and D117Cys\* (phot1<sup>CR3</sup>) had truncated PHOT1 protein, while the other three had an in-frame deletion of 50 (phot1<sup>CR2</sup>), 96 (phot1<sup>CR4</sup>) and 21 (phot1<sup>CR3</sup>) amino acids. In the T<sub>2</sub> generation, phot1<sup>CR2</sup>, phot1<sup>CR3</sup> and phot1<sup>CR5</sup> became Cas9-free with no off-target editing (Figure S2). All alleles showed reduced chloroplast accumulation and avoidance in leaf (Figure S3), which confirms that phot1 and phot2 redundantly regulate chloroplast relocation.

Though all alleles showed delayed attainment of MG similar to  $Nps1^*$ , post-MG, unlike Nps1, the transition to BR was shorter (less short in  $phot1^{CR1}$ ), and BR to RR was marginally extended (excepting  $phot1^{CR1}$ ) compared with AV (Figure S4a). Importantly, opposite to  $Nps1^*$ , in all alleles, fruit color at RR was lighter, indicating a reduction in accumulation of carotenoids (Figure S4b). Particularly lycopene, phytoene, phytofluene,  $\beta$ -carotene and  $\alpha$ -carotene were lower than AV in all alleles (Table S4). The opposite influence on carotenoids in  $Nps1^*$  vis-a-vis  $phot1^{CR1-5}$  lines entails that carotenoids increase in  $Nps1^*$  was specific to its dominant-negative action. We then characterized in detail the influence of  $Nps1^*$  on phytohormones, metabolome and proteome, including transcript levels of selected genes vis-à-vis AC.

### Nps1\* fruits show reduced ethylene emission

Though ripening duration from MG to RR in AC and Nps1\* was nearly similar, system II ethylene emission was highly subdued in Nps1\* (Figure 3). In tomato, system II ethylene is mainly contributed by 1-aminocyclopropane-1-carboxylate synthase 2 and 4 (acs2, acs4), 1-aminocyclopropane-1-carboxylic acid oxidase 1 and 3 (aco1, aco3; Barry et al., 2000). Compared with AC, acs2 and acs4 transcripts were higher in Nps1\* at MG and BR but nearly similar at RR

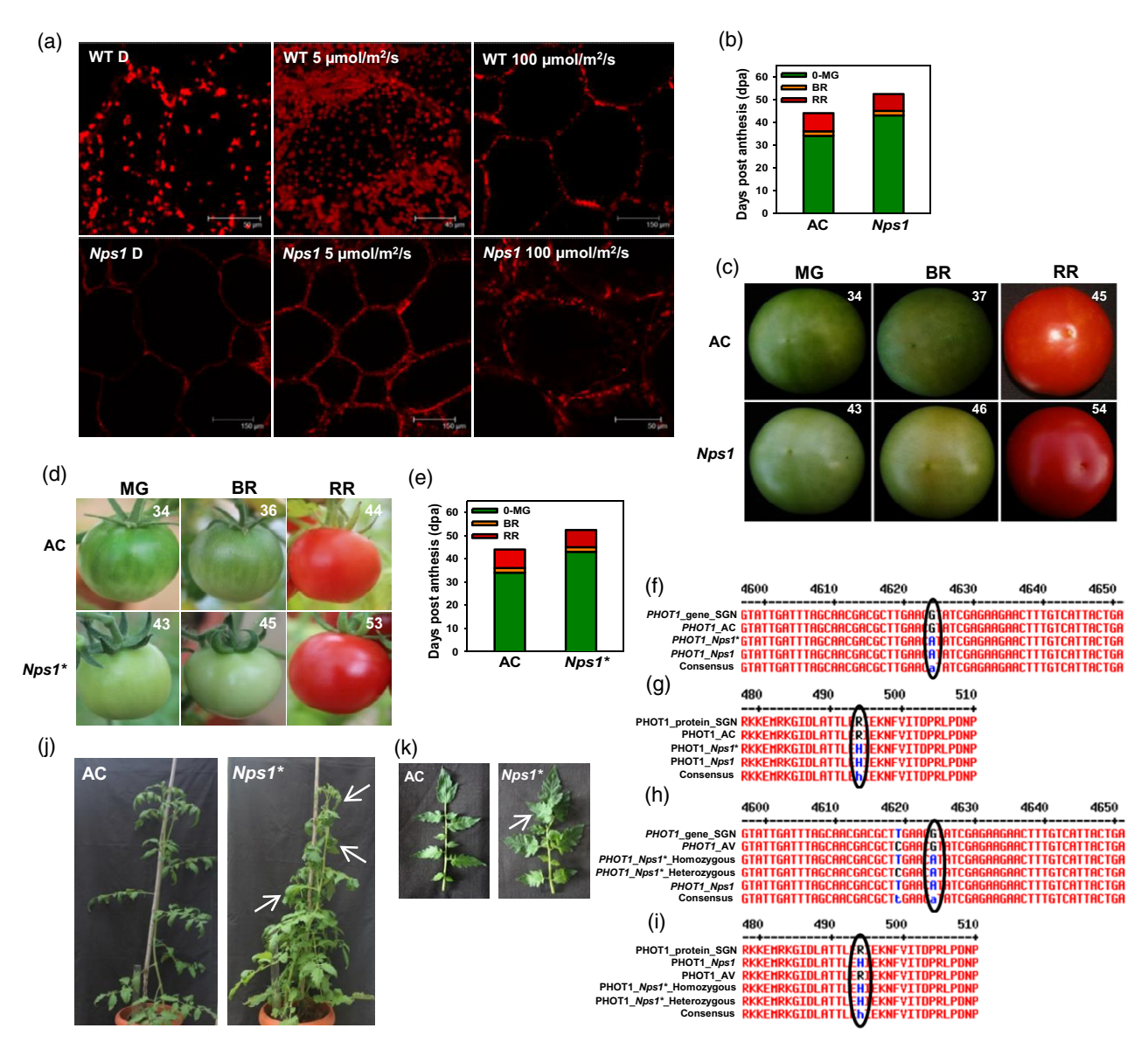


Figure 1. Blue-light-induced chloroplast relocations in the fruit pericarp of Ailsa Craig (AC) and Nps1, fruit development and ripening in AC and Nps1 and Nps1 introgressed plants.

- (a) The pericarp slices from dark-adapted mature-green (MG) fruits were exposed to low-fluence blue light (5 µmol m<sup>-2</sup> sec<sup>-1</sup>) to induce chloroplast accumulation. Thereafter, slices were exposed to high-fluence (100 µmol m<sup>-2</sup> sec<sup>-1</sup>) blue light to induce chloroplast avoidance. Photographs shown are the representative images taken after 30 min of light treatment.
- (b) Chronological development of fruits. Note: while Nps1 is delayed in attaining the MG stage, the duration to attain breaker (BR) and red-ripe (RR) stages was similar to AC (n = 15-20 fruits from 30 plants).
- (c) Development of fruit color in AC and Nps1. Days post-anthesis are indicated on the top right corner of photos.
- (d) Development of fruit color in AC and Nps1\*. Days post-anthesis are indicated on the top right corner of photos.
- (e) Chronological development of fruits (n = 15-20 fruits from 30 plants). Note: fruit development and ripening duration in Nps1\* is similar to Nps1.
- (f-i) Confirmation of introgression of Nps1\* mutation in AC (f, g) and AV (h, i). (f, h) Alignment of phot1 gene (Solyc11g072710) sequence. (g, i) Alignment of PHOT1 amino acid sequences. Note: in recent ITAG3.2 annotation the mutation is located at R494H.
- (j, k) Phenotype of AC and Nps1\* (BC2F3) plants (j) and leaves (k). Note: Nps1\* shows more biomass. White arrows point to leaf curling and epinasty in Nps1\* (j, k). Note: Nps1\* leaves show twisted rachis (k).

(barring lower acs2; Figure S5). Conversely, aco1 and aco3 transcripts were highly reduced in Nps1\* (barring aco1 at BR). Seemingly, reduced aco expression in Nps1\* may have lowered ethylene emission. Nps1\* also emitted less CO<sub>2</sub>, signifying reduced respiration (Figure 3). Nps1\* RR fruits were more firm and had higher °Brix. Though the acidity of fruits differed in AC and Nps1\* at MG and BR, it was similar at RR (Figure S6). In contrast to Nps1\*, in RR fruits of phot1<sup>CR</sup> alleles, °Brix and pH was akin to AV (Figure S4c,d).

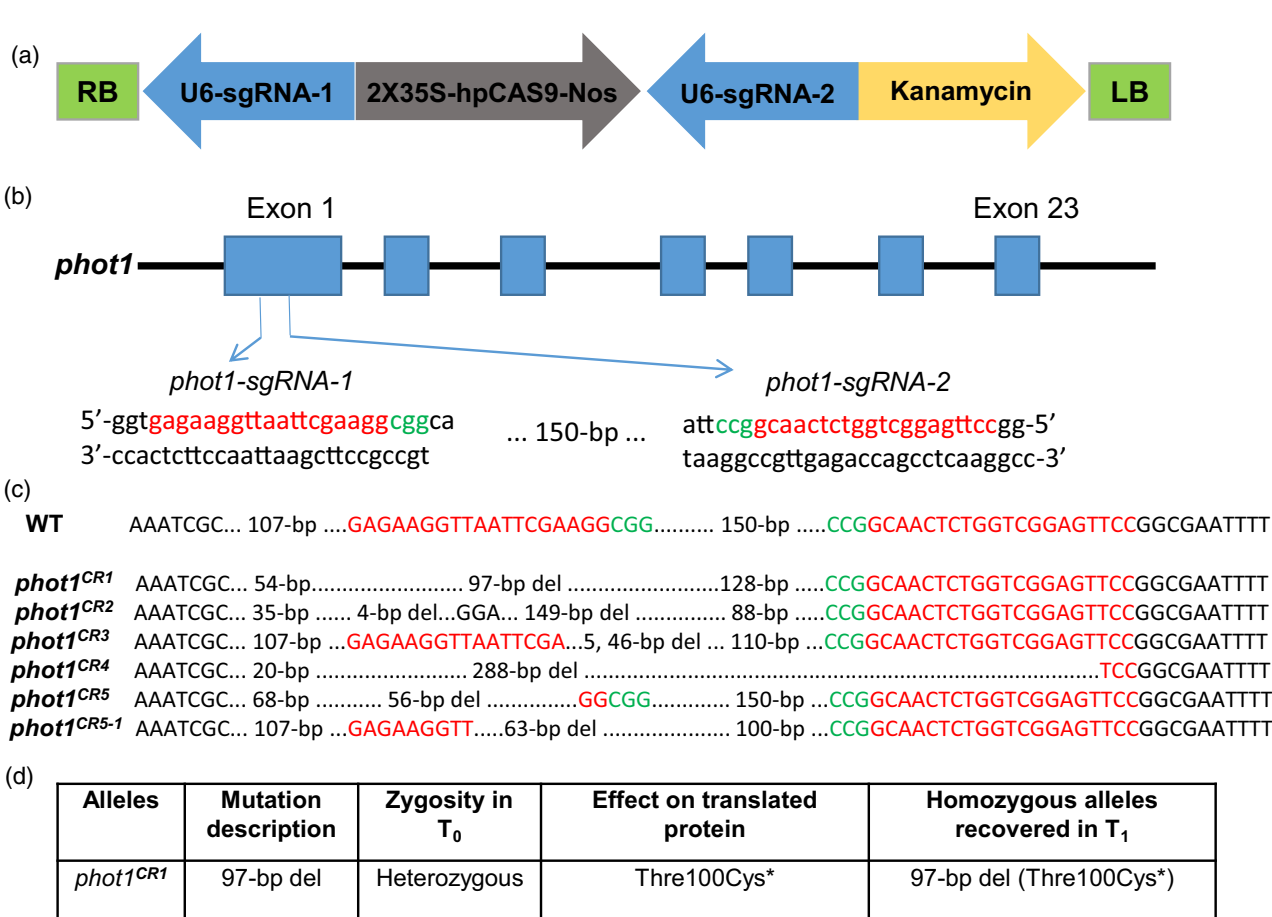
1365313x, 2021, 3. Downloaded from https://onlinelibrary.wiley.com/doi/10.1111/tpj.15206 by University Of Hyderabad. Wiley Online Library on [29/1/20222]. See the Terms and Conditions (https://onlinelibrary.wiley.com/terms-and-conditions) on Wiley Online Library for rules of use; OA articles are governed by the applicable Creative Commons. License

8

Table 1 Carotenoid and chlorophyll contents in the fruits of AC and Nps1 at different ripening stages

1	AC			Nps1			L	L	L	BC <sub>2</sub> F <sub>2</sub> Nps1		
Metabolite (μg gFW <sup>-1</sup> )	MG	BR	RR	MG	BR	RR	BC <sub>1</sub> F <sub>1</sub> RR	BC <sub>1</sub> F <sub>2</sub> <i>Nps1</i> RR	BC₂F₁ RR	MG	BR	RR
Phytoene	N	ND	$13.16 \pm 0.97$	ND	ND	$\textbf{48.13}\pm\textbf{2.78}^*$	$65.94 \pm 0.98*$	$\textbf{39.67} \pm \textbf{1.2}*$	46.97 ± 1.2***	ND	ND	33.26 ± 1.83***
Phytofluene	N	ND	$2.13 \pm 0.31$	ND	ND	$\textbf{11.07}\pm\textbf{0.44}*$	$\textbf{16.69} \pm \textbf{0.38}*$	$6.73\pm0.12*$	$\textbf{1.56}\pm\textbf{0.04}*$	ND	ND	$\textbf{3.46} \pm \textbf{0.26}*$
ζ-Carotene	ND	ND	$\textbf{3.58} \pm \textbf{0.05}$	ND	ND	$\textbf{4.52}\pm\textbf{0.26}*$	$\textbf{9.01}\pm\textbf{0.09}*$	$\textbf{7.38}\pm\textbf{0.09}*$	$\textbf{1.40} \pm \textbf{0.06} ***$	ND	ND	$\textbf{1.75} \pm \textbf{0.13} ***$
Neurosporene	ND	ND	ND	ND	ND	ND	$\textbf{5.58} \pm \textbf{0.07}*$	$\textbf{6.94}\pm\textbf{0.13}*$	$\bf 2.91 \pm 0.41 ***$	ND	$\textbf{4.23}\pm\textbf{0.20}*$	19.02 $\pm$ 0.69**
Lycopene	N	$0.99 \pm 0.06$	$40\pm1.18$	$0.31\pm0.004$	$\textbf{1.06} \pm \textbf{0.1}$	$\textbf{123.46}\pm5.71^*$	$\textbf{134.78}\pm\textbf{2.7}*$	129.78 $\pm$ 1.32*	119.43 ± 4.36***	ND	$0.65 \pm 0.06**$	113.96 $\pm$ 3.71***
α-Carotene	$\textbf{0.43} \pm \textbf{0.02}$	$\textbf{0.44}\pm\textbf{0.06}$	$\textbf{2.13} \pm \textbf{0.04}$	$\textbf{0.26}\pm\textbf{0.02}*$	$0.48 \pm 0.03$	$\textbf{2.34}\pm\textbf{0.04}*$	$\textbf{4.25}\pm\textbf{0.17}*$	$\textbf{2.26}\pm\textbf{0.08}$	$\bf 2.64 \pm 0.08***$	$\textbf{0.20} \pm \textbf{0.01} ***$	$\textbf{0.46} \pm \textbf{0.03}***$	$\textbf{2.96} \pm \textbf{0.34} ***$
γ-Carotene	ND	ND	ND	ND	ND	ND	ND	ND	$\textbf{1.33} \pm \textbf{0.09} ***$	ND	$4.93 \pm 0.19***$	$5.08\pm0.48**$
β-Carotene	$\textbf{1.53} \pm \textbf{0.21}$	$2.3\pm0.46$	$\textbf{6.12} \pm \textbf{0.35}$	$3.74\pm0.33$	$3.53\pm0.42$	$8.00\pm0.49*$	$\textbf{8.22}\pm\textbf{0.01}*$	$\textbf{11.92}\pm\textbf{0.26}*$	$\textbf{3.40} \pm \textbf{0.18} ***$	$\textbf{2.06}\pm\textbf{0.45}*$	$4.88\pm0.20^{**}$	$3.45 \pm 0.59 ***$
Lutein	$4.40\pm0.49$	$3.33\pm0.17$	$\textbf{3.03} \pm \textbf{0.01}$	$\textbf{1.39} \pm \textbf{0.10}*$	$\textbf{1.17}\pm\textbf{0.08}*$	$\textbf{0.62}\pm\textbf{0.07}*$	$\textbf{0.13}\pm\textbf{0.005}*$	$\textbf{0.83}\pm\textbf{0.01}*$	1.54 $\pm$ 0.11***	$\textbf{1.35} \pm \textbf{0.13} ***$	$3.23\pm0.13$	$\textbf{1.58} \pm \textbf{0.18**}$
Violaxanthin	$\textbf{1.45} \pm \textbf{0.16}$	$\textbf{0.68}\pm\textbf{0.10}$	$\textbf{0.0} \pm \textbf{0.0}$	$\textbf{0.75}\pm\textbf{0.06}$	$\textbf{0.40} \pm \textbf{0.05}$	ND	ND	ND	ND	$\textbf{0.53} \pm \textbf{0.08}$	$\textbf{0.55}\pm\textbf{0.04*}$	ND
Neoxanthin	ND	ND	ND	ND	ND	ND	ND	ND	ND	$\textbf{0.42}\pm\textbf{0.06}*$	$0.56 \pm 0.11***$	$0.0\pm0.0$
β-Cryptoxanthin	$\textbf{0.16} \pm \textbf{0.004}$	$\textbf{0.24}\pm\textbf{0.07}$	$\textbf{2.94} \pm \textbf{0.002}$	$0.0\pm0.0$	$\textbf{0.18} \pm \textbf{0.006}$	$5.46 \pm 0.12*$	$\textbf{2.24}\pm\textbf{0.10}*$	$\textbf{6.43}\pm\textbf{0.16}*$	$\textbf{0.49} \pm \textbf{0.03}$	$\textbf{0.14} \pm \textbf{0.007}$	$\textbf{0.18} \pm \textbf{0.003} **$	$\textbf{0.61} \pm \textbf{0.07}$
Total CAR	$\textbf{8.26} \pm \textbf{0.89}$	$\textbf{7.98}\pm\textbf{0.92}$	$\textbf{73.09} \pm \textbf{2.91}$	$6.45\pm0.51$	$\textbf{6.82} \pm \textbf{0.68}$	$\textbf{203.6}  \pm  \textbf{9.91***}$	237.84 ± 4.5***	$\textbf{212}\pm\textbf{3.3}***$	181.67 ± 6.56***	$\textbf{4.7}\pm\textbf{0.73}*$	$19.67 \pm 0.96***$	185.13 $\pm$ 8.28***
Chlorophyll a	$124.48 \pm 13.21$	$97.74\pm3.82$	$25.47\pm0.31$	$108.5\pm4.7$	$57.5\pm0.79***$	$\textbf{23.32}\pm\textbf{0.19}**$	$\textbf{21.44} \pm \textbf{0.37} ***$	$\textbf{24.65} \pm \textbf{0.81}$	$\bf 21.66 \pm 0.68**$	102.74 $\pm$ 5.84	$\bf 39.82 \pm 6.52^{**}$	$\textbf{21.09}  \pm  \textbf{0.43} ***$
Chlorophyll b	$202.69 \pm 21.58$	$\textbf{159.04} \pm \textbf{6.16}$	$40.97\pm0.49$	$176.79 \pm 7.73$	$93.38 \pm 1.28 ***$	$\textbf{37.48}\pm\textbf{0.32}^{**}$	$34.49 \pm 0.62 ***$	$39.63 \pm 1.3$	$34.83 \pm 1.1^{**}$	$\textbf{167.36} \pm \textbf{9.62}$	$64.32 \pm 10.73^{**}$	$33.86 \pm 0.73 ***$
Chl a: Chl b	$0.6142\pm0.0001$	$0.6145\pm0.0002$	$\textbf{0.62} \pm \textbf{0.0009}$	$0.6141\pm0.0001$	$\bf 0.6158 \pm 0.0001^*$	$\textbf{0.6223} \pm \textbf{0.01}$	$0.6217\ \pm\ 0.0004$	$0.6221\pm0.0001$	$0.6218\pm0.0008$	$0.6139\pm0.0004$	$\bf 0.6197  \pm  0.001^*$	$\textbf{0.6229} \pm \textbf{0.0006}$
Total Chi	$327.17 \pm 34.79$	$256.78 \pm 9.98$	$66.44 \pm 0.80$	$285.35\pm12.44$	$150.88 \pm 2.07^{***}$	$60.81\pm0.51**$	$55.94 \pm 0.99 ***$	$64.28 \pm 2.12$	$56.49 \pm 1.78 **$	$270.10 \pm 15.46$	104.15 $\pm$ 17.2**	$54.95 \pm 1.17^{***}$
CHL:CAR	$\textbf{39.6} \pm \textbf{3.56}$	$32.55\pm0.099$	$\textbf{0.9} \pm \textbf{0.037}$	$44.24\pm1.29$	$\textbf{22.12}  \pm  \textbf{0.27} ***$	$\textbf{0.298}  \pm  \textbf{0.014***}$	$\textbf{0.24}\pm\textbf{0.12} **$	$\textbf{0.3}  \pm  \textbf{0.05***}$	$\textbf{0.31}\pm\textbf{0.08**}$	$57.46 \pm 1.61 ^{**}$	$5.29 \pm 0.18 ***$	$0.29 \pm 0.009 ***$

Carotranid and chlorophyll contents are presented as  $\mu g^{-1}$  fresh weight. Data are means  $\pm$  SE (n = 3). Chl, chlorophyll: CAR, carotranid; ND, not detected as no peak was discernible on the chromatogram. Student's frest was used to determine the significant differences have been found. The P-values < 0.05, < 0.01 and < 0.001 were indicated by one, two or three asterisks, respectively.



Alleles	Mutation description	Zygosity in T <sub>0</sub>	Effect on translated protein	Homozygous alleles recovered in T <sub>1</sub>
phot1 <sup>CR1</sup>	97-bp del	Heterozygous	Thre100Cys*	97-bp del (Thre100Cys*)
phot1 <sup>CR2</sup>	4, 149-bp del	Heterozygous	Ser84Gly and in-frame deletion of 50 aa from 85- 135 aa	4, 149-bp del (Ser84Gly and 50 aa deletion from 85-135 aa)
phot1 <sup>CR3</sup>	5, 46-bp del	Chimera	Ala115Gly* Asp117Cys*	46-bp del (Asp117Cys*)
phot1 <sup>CR4</sup>	288-bp del	Heterozygous	In-frame deletion of 96 aa from 76-171 aa	288-bp del (96 aa deletion from 76-171 aa)
phot1 <sup>CR5</sup>	56, 63-bp del	Chimera	Pro98Gly* In-frame deletion of 21 aa from 111-131 aa	63-bp del (21 aa deletion from 111-131 aa)

Figure 2. The CRISPR/CAS9-mediated editing in the tomato phot1 gene.

### Hormonal balance is altered in Nps1\*

In seedling phototropism, it is surmised that phototropins affect the transport of auxins (Fankhauser and Christie, 2015); however, the influence of phototropins on other

phytohormones is uncharacterized. We examined whether, in conjunction with ethylene, Nps1\* also modulated other phytohormones (Figure 3). Higher IAA level in Nps1\* at MG and BR is consistent with the antagonistic action of ethylene and auxin. Higher levels were also observed for

<sup>(</sup>a) Schematic representation of binary vectors used in this study. phot1-sgRNA-1 and 2: Arabidopsis U6 promoter and the gRNA sequence; 2X 35S-hpCAS9-Nos: 2X CaMV35S promoter sequence; hpCas9: human-codon optimized SpCas9; Nos: nos terminator; kanamycin: the kanamycin-resistant marker expression cassette; RB: right border of T-DNA; LB: left border of T-DNA.

<sup>(</sup>b) Schematic view of sgRNA1 and sgRNA2 target sites in the phot1 gene. Boxes indicate exons, red color indicates 19-20-bp target sequences, and green indicates the protospacer-adjacent motif (PAM).

<sup>(</sup>c) Sequence alignment of the target regions. The wild-type sequence is shown at the top, with the target sequence in red and the PAM in green. Nucleotide variations at the targets of T<sub>0</sub> mutant lines, 'del' - base deletion.

<sup>(</sup>d) The table shows the alleles identified in T<sub>0</sub>, the effect of editing on the phot1 gene and protein sequences, and the recovered alleles in the T<sub>1</sub> generation.

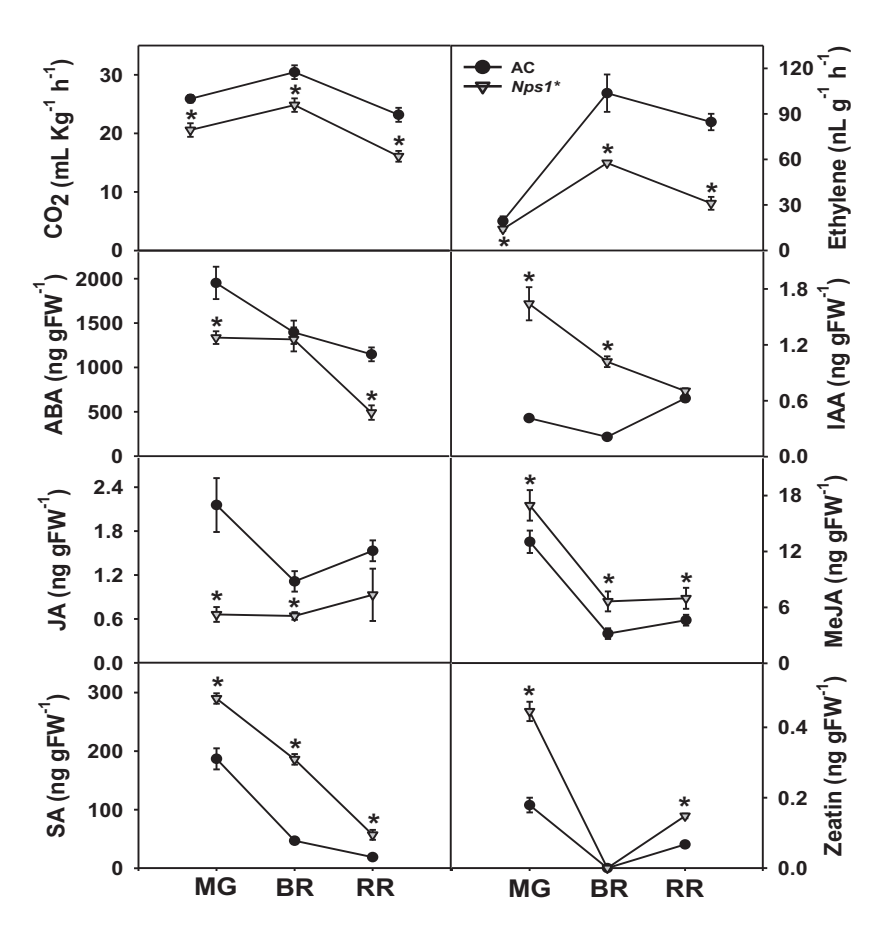


Figure 3. Rate of respiration and hormonal levels in ripening fruits of Ailsa Craig (AC) and Nps1\*. Data are means  $\pm$  SE (n = 5),  $P \le 0.05$ .

methyl jasmonate (MeJA), salicylic acid (SA) and zeatin (barring BR). In contrast, abscisic acid (ABA; barring BR) and jasmonic acid (JA) levels were lower in Nps1\*. Ostensibly, in addition to ethylene, Nps1\* also affected the overall hormonal homeostasis of fruits.

### Nps1\* upregulates several MEP and carotenogenesis pathway genes

Consistent with high lycopene content, Nps1\* also modulated the expression of carotenoid biosynthesis genes. The precursor for carotenoid biosynthesis, geranylgeranyl diphosphate (GGPP), is derived from the methylerythritol-4-phosphate (MEP) pathway. Barring deoxy-xylulose 5phosphate synthase (dxs) that had lower expression, other genes, deoxy-xylulose 5-phosphate reductase (dxr), 4-hydroxy-3-methyl but-2-enyl diphosphate reductase (hdr), isopentenyl diphosphate isomerase 5g (idi5g) (BR, RR) and geranylgeranyl pyrophosphate synthase 2 (ggpps2) (MG) were upregulated in Nps1\* (Figure 4).

Like the MEP pathway, Nps1\* differentially regulated genes mediating fruit-specific carotenogenesis. Though the expression of psy1, which converts GGPP to phytoene was lower (barring BR) in Nps1\*, other downstream genes, phytoene desaturase (pds), ζ-carotene isomerase (ziso), \(\zeta\)-carotene desaturase (zds) and carotenoid isomerase (crtiso) leading to lycopene were

upregulated (barring pds at RR, ziso at MG, zds at BR). Oddly, psy2, a leaf carotenogenesis gene, was uprequlated in Nps1\*. Seemingly, desaturation steps are more crucial than phytoene formation for enhanced lycopene levels in Nps1\* fruits.

Downstream to the lycopene, the expression of all four lycopene cyclases was higher in Nps1\* at BR and RR stages. Remarkably, Nps1\* also showed stage-specific higher expression of genes mediating β-carotene branch – leading to violaxanthin, neoxanthin; and α-carotene branch - leading to lutein. Out of four carotenoid cleavage dioxygenases (ccd) genes examined, three (ccd1b, ccd4a, ccd4b) were upregulated in Nps1\*. The expression of genes encoding carotenoid sequestration proteins, chromoplastspecific carotenoid-associated protein (chrc), and pap3 (at RR), was considerably higher in *Nps1*\*.

Consistent with low carotenoid content, the expression of key carotenogenesis genes in phot1CR alleles was distinct from Nps1\* (Figure S7). Though in phot1<sup>CR2</sup>, phot1<sup>CR3</sup> and phot1<sup>CR5</sup>, dxs expression varied at MG, BR, it was upregulated at RR compared with AV. Likewise, psy1 expression was lower at MG (except phot1<sup>CR5</sup>) and BR and higher at RR. Compared with AV, psy2 expression was either similar or lower (barring MG in phot1<sup>CR5</sup>), and chromoplast-specific *lycopene-β-cyclase* (*cycb*) was lower at all ripening stages (barring MG in phot1<sup>CR3</sup>).

1365313x, 2021, 3. Downbaded from https://onlinelibrary.wiley.com/doi/10.1111/tpj.15206 by University Of Hyderabad, Wiley Online Library on [29/122022]. See the Terms and Conditions (https://onlinelibrary.wiley.com/rems-and-conditions) on Wiley Online Library for rules of use; OA articles are governed by the applicable Creative Commons License

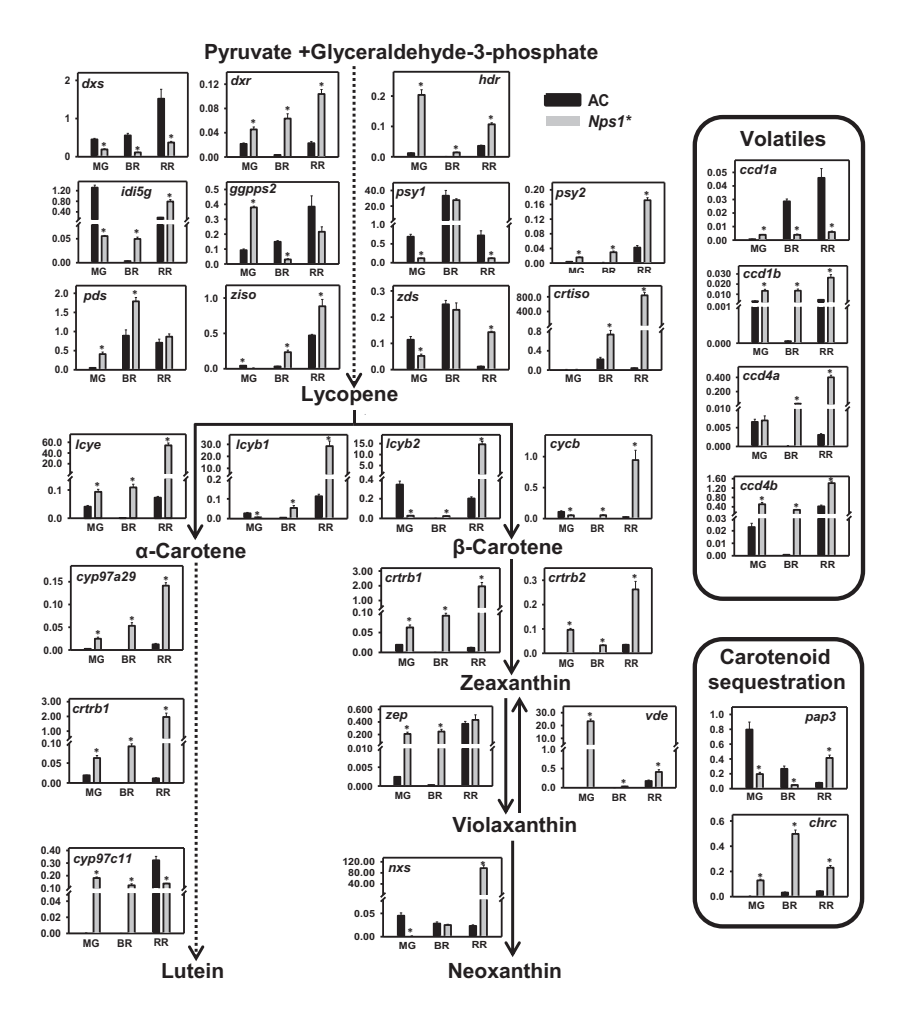


Figure 4. Relative expression of genes mediating carotenoid biosynthesis, sequestration and carotenoid-derived volatile formation in ripening fruits of AC and

Dotted arrows indicate multiple steps in the carotenoid biosynthesis pathway. The genes mediating carotenoid sequestration and volatile formation are enclosed in separate rectangles. The y-axis indicates the relative expression of genes obtained after normalization with \( \beta - actin \) and \( ubiquitin. \) Data are means  $\pm$  SE (n = 3), \* $P \le 0.05$ .

### Nps1\* influences gene expression of ripening regulators

The influence of Nps1\* was not limited to carotenoid biosynthesis genes; it stimulated its expression along with phot2 (Figure S8). Consistent with reduced ethylene emission, ethylene response factor 6 (erf6) expression was lower in Nps1\*. It differentially modulated ripening regulators, with higher expression of ripening inhibitor (rin) and tomato agamous-like 1 (tagl1), (barring BR) and lower expression of Nonripening (nor), fruitful 1 (ful1) and fruitful 2 (ful2) at MG and BR. Similarly, genes regulating chloroplast numbers - golden 2-like (glk2) and Arabidopsis pseudo response regulator 2-like (aprr2) had lower expression at BR and RR. Other carotenoid biosynthesis regulatory genes, Cys-rich zinc finger domain-containing protein (Or), phytochrome interacting factor1 (pif1), had higher (MG, BR) and lower expression (RR) in *Nps1*\*.

### Nps1\* upregulates fruit aminome and sugars

Nps1\* also influenced the metabolome, as evident by distinct principal component analysis (PCA) of Nps1\*, prominently at RR (Figure S9). The diversity in metabolome was contributed by higher levels of amino acids and sugars in Nps1\* (Figures 5 and S10; Table S5). Consistent with the higher Brix, the sucrose level was higher in Nps1\*. Likewise, lower levels of organic acids belonging to the TCA cycle, such as citrate and aconitate, may be related to reduced respiration rate of Nps1\*.

### Nps1\* also influences volatiles

Akin to metabolites, the volatiles of Nps1\* were distinct from AC (Figures 5 and S11; Table S6). Among detected volatiles, the majority were from the phenolics pathway, followed by lipid, terpenoid and phenylpropanoid pathways. Among carotenoid-derived volatiles, only 6-methyl

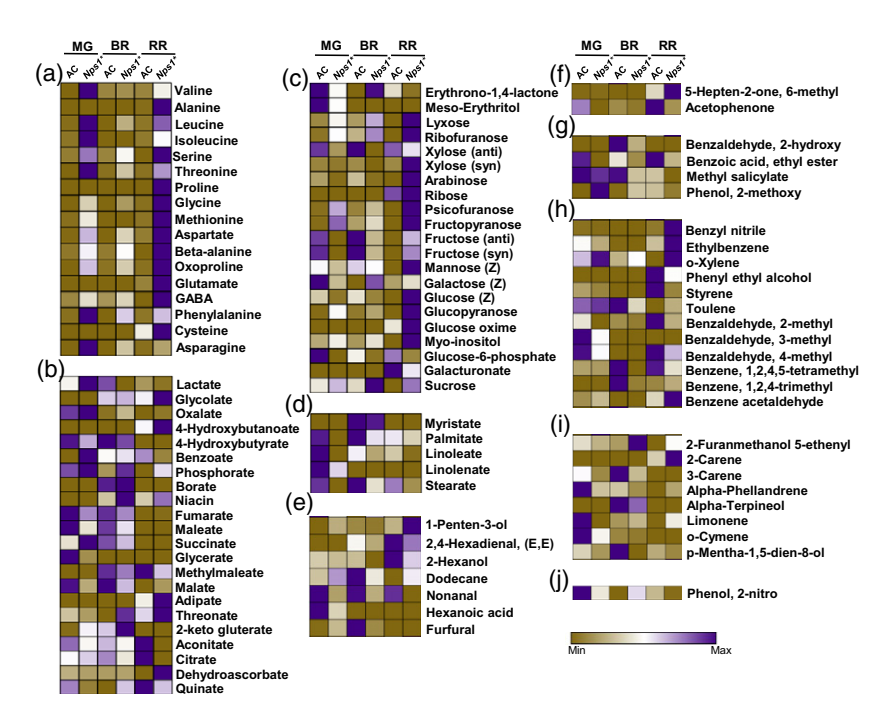


Figure 5. Primary metabolites and volatiles levels in ripening fruits of Ailsa Craig (AC) and  $Nps1^*$ . Only significantly different metabolites ( $\geq$  1.5-fold) are depicted in heat maps. Data are means  $\pm$  SE (n=5 for primary metabolites and n=8 for volatiles),  $P \leq 0.05$ .

(a-d) Primary metabolites: (a) amino acids; (b) organic acids; (c) sugars; (d) fatty acids.

(e-j) Volatiles: (e) lipid-derived; (f) open-chain carotenoid derived; (g) phenylpropanoid-derived; (h) phenolic-derived; (i) terpenoid-derived; (j) aminoacid-derived volatiles.

5-hepten-2-one (MHO) and acetophenone were detected. Consistent with high lycopene, the level of lycopenederived MHO was 2.7-fold high in *Nps1\**. Among odorand taste-contributing volatiles, methyl salicylate, phenylethanol, hexanal and *p*-menth-1-en-9-al were lower in *Nps1\**. Compared with metabolites, *Nps1\** influence on volatiles was subdued.

### Nps1\* upregulates abiotic stress-related proteins

We profiled the proteome of AC and Nps1\* fruits to decipher its contribution to enhanced carotenogenesis. The proteome (≥ 2 peptide hits) comprised of about 2336 (MG), 2375 (BR) and 2318 (RR) proteins (Figure S12). Label-free quantification identified several upregulated (MG-190, BR-167, RR-139) or downregulated (MG-113, BR-126, RR-92) proteins in Nps1\* compared with AC (Table S7). Additionally, Nps1\* and AC also had proteins uniquely associated with them. The proteins identified uniquely in Nps1\* (MG-131, BR-95, RR-72) and in AC (MG-177, BR-117, RR-98) varied in a stage-specific fashion (Table S8). Relatively, Nps1\* had fewer unique proteins, but lost several proteins compared with AC. Functional annotation highlighted differences between Nps1\* and AC proteome (Figure S13), particularly greater up- and downregulation abiotic stress (barring BR) and biotic stress categories in Nps1\*. Consistent with enhanced aminome, the amino acid metabolism category was downregulated in Nps1\*.

### Nps1\* upregulates carotenoid sequestration proteins

Contrary to the expectation that Nps1\* may enhance carotenogenic proteins, proteome profiling revealed GGR,

DXS, PSY1, ZISO, ZDS, CRTISO only in AC (RR), but not in *Nps1\** (Figure 6; Tables S7–S9). Among the MEP pathway, plastidic HDR was fivefold downregulated (RR) in *Nps1\**; however, isopentenyl diphosphate isomerase (IDI1) was exclusively identified in *Nps1\**. In addition, two carotenoid sequestration proteins were upregulated in *Nps1\**. Prominently, CHRC, a protein associated with high lycopene (Kilambi *et al.*, 2013), was 4.7-fold higher in *Nps1\**. Likewise, CHRD (Leitner-Dagan *et al.*, 2006a) was exclusively detected in *Nps1\** RR fruits.

# Molecular chaperones maintaining protein stability are abundant in Nps1\*

A prominent function of abiotic stress proteins is to protect functional proteome by being molecular chaperones. Consistent with this, Nps1\* showed stage-specific upregulation of several Hsps (MG- 17; BR-17; RR-11 Hsps) compared with AC (Figure S14; Table S9), with few Hsps upregulated at two or more stages. Specifically, Hsp21 was abundantly present only in Nps1\*, and levels of Hsp70.2 were considerably higher. Despite Hsp21 being present only in Nps1\*, its transcript level was low, and expression of Hsp70.2 declined during ripening (Figure S15), indicating posttranscriptional regulation. Nps 1\* also upregulated protein-folding chaperones, such as peptidyl-prolyl isomerase (PPI), 14-3-3 proteins, protein disulfide isomerase (PDI) and methionine sulfoxide reductase (MSR; Figure S14). Strikingly, OR was not detected in Nps1\* and AC. The absence of proteases in Nps1\*, particularly at the RR, aided to the protection of proteins, and the converse was seen in AC (Tables S7 and S8).

1365313x, 2021, 3. Downloaded from https://onlinelibrary.wiley.com/doi/10.1111/tpj.15206 by University Of Hyderabad, Wiley Online Library on [29/12/2022]. See the Terms and Conditions (https://onlinelibrary.wiley.com/rems-and-conditions) on Wiley Online Library for rules of use; OA articles are governed by the applicable Cretaive Commons License

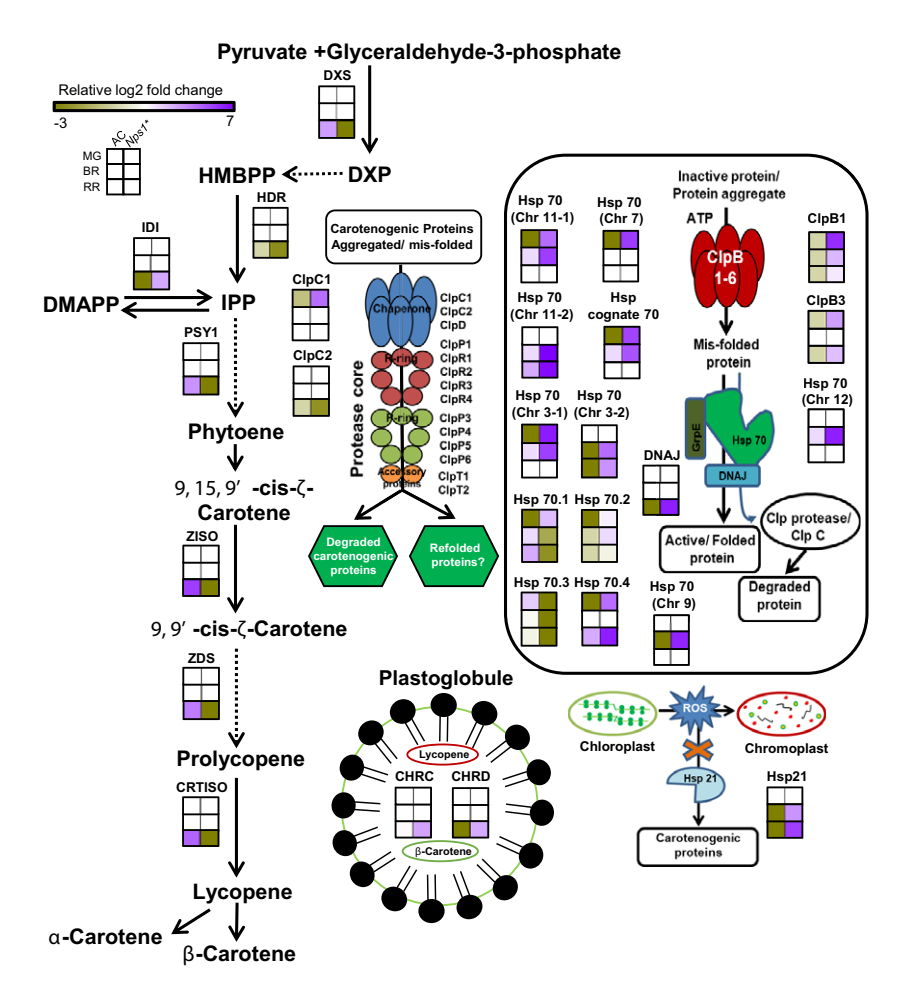


Figure 6. Schematic representation of relative abundances of proteins involved in carotenoid biosynthesis, sequestration, protein folding, degradation and heat shock proteins in Ailsa Craig (AC) and Nps1\* fruits at different stages of ripening.

Heat maps were generated using normalized log2-fold changes for differentially expressed proteins. For proteins detected only in Nps1\* or in AC, the missing values were replaced with 1/10 of the lowest value in the dataset, and the heat maps were generated with normalized log2 abundances. Carotenogenic proteins that are aggregated or misfolded can be folded into their active conformation by Clp B protease system in the presence of ATP together with Hsp 70 and DNAJ proteins (Maurizi and Xia, 2004). Alternatively, the above misfolded or aggregated proteins can be degraded by Clp C/Clp protease system or facilitated for refolding (Nishimura and van Wijk, 2015; Pulido et al., 2016; D'Andrea et al., 2018). CHRC and CHRD are plastid lipid-associated proteins that can be localized to the plastoglobule and assist in the sequestration of carotenoids (Leitner-Dagan et al., 2006a,b; Kilambi et al., 2013). Chloroplast to chromoplast conversion involves the generation of reactive oxygen species (ROS) that may induce either degradation or inactivation of carotenogenic proteins. This action of ROS can be prevented by Hsp 21, which may thus protect carotenogenic proteins from degradation (Neta-Sharir et al., 2005)

The levels of several Clp components, purported to regulate the activity of carotenogenic proteins, were altered in Nps1\* (Figures 6 and S14; Table S9). While ClpB3 protease (Solyc12g0426060) was sixfold high in Nps1\* during early ripening, ClpB1 (Solyc03q115230.3.1) was upregulated throughout ripening. The downregulation of ClpC2 (Solyc12g0426060) in Nps1\* was seen only at RR, while ClpC1 (Solyc03g0118340) in Nps1\* was nearly similar to AC. Akin to Hsp21, transcripts of ClpC1 and ClpB3 lacked correlation with respective protein levels during ripening (Figure S15).

### DISCUSSION

The capability to enhance the carotenoid levels in fleshy fruits is an important biotechnological target (Giuliano, 2017). In tomato, analysis of high-pigment and -

photoreceptor mutants, including transgenics, has demonstrated a causal link between light signaling and carotenogenesis. It alludes to the fact that manipulation of photoreceptors and associated signaling partners can be an effective means for boosting carotenoids levels in fruits. In this study, we show an original function for plant photoreceptor phototropin1, wherein a dominant-negative mutant - Nps1 - considerably enhances the carotenoid levels in tomato fruits, whereas the loss of function alleles reduce the carotenoid content.

## Altered hormonal balance seemingly delays attainment of MG in Nps1

The role of phytochrome and cryptochrome in tomato fruit is mainly inferred by mutant analysis. Alba et al. (2000)

demonstrated functional phytochromes by red/far-red reversible accumulation of lycopene in MG tomato fruits. Similarly, both phototropin1 and phototropin2 are functional in tomato fruits, as MG fruits display chloroplast accumulation and avoidance, respectively. On the contrary, *Nps1* seems to be compromised in functional phototropin1 as blue-light failed to elicit chloroplast movement in its fruits. Unlike deep-green colored MG fruits of tomato *hp1* and *hp2* mutants, *Nps1\** MG fruits were pale-green colored. Considering that phytochromes modulate chlorophyll accumulation in tomato fruits (Bianchetti *et al.*, 2018; Gupta *et al.*, 2014), reduced chlorophylls in *Nps1\** fruits indicate phototropin1 role in this process.

Little is known about the interaction between light and phytohormones in tomato fruit development. Similar to phytochrome mutants (Gupta et al., 2014), Nps1\* fruits are delayed in attaining the MG. Nonetheless, the alluded linkage between phototropins and phytochromes is limited to the pre-MG stage. Post-MG, unlike delayed progression to BR and RR in phytochrome mutants (Gupta et al., 2014), the transition to BR and RR was not altered in Nps1\*. Similar to Nps1\*, an auxin-resistant (Balbi and Lomax, 2003) and a NO-overproducing mutant (Bodanapu et al., 2016) show prolonged pre-MG phase implying hormonal participation. In tomato fruits, enhanced ethylene emission coupled with high ABA and low IAA levels accelerated the attainment of MG (Liang et al., 2020; Sharma et al., 2020). Conversely, reduced ABA, ethylene levels, and high auxin levels may delay the transition to MG in Nps1\*. Seemingly, Nps1\* impairs the hormonal balance, consequently delaying attainment of the MG.

# High aminome seems to be linked to reduced levels of TCA cycle proteins

Parallel to carotenoids,  $Nps1^*$  considerably increases several amino acids. Considering that amino acids are derived from glycolysis and the TCA cycle, their elevation would reduce flux into the TCA cycle. Reduced  $CO_2$  emission from  $Nps1^*$  fruits also implied a subdued TCA cycle. Consistent with this, levels of citrate, aconitate and  $\alpha$ -ketoglutarate were low in  $Nps1^*$  fruits. Likewise, several proteins related to the TCA cycle or its derivatives were also affected in  $Nps1^*$ . Lower levels of citrate may ensue from a higher level of aconitase. Similarly, a low level of isocitrate dehydrogenase may lower  $\alpha$ -ketoglutarate levels. Moreover, reduced levels of  $\alpha$ -ketoglutarate dehydrogenase may divert  $\alpha$ -ketoglutarate to amino acids. Consistent with this, amino acids derived from  $\alpha$ -ketoglutarate such as glutamate and proline were substantially high in  $Nps1^*$ .

The slackened TCA cycle may ensue from a reduced abundance of pyruvate dehydrogenase that may limit pyruvate flux into the TCA cycle. In *Nps1\**, reduction in malate dehydrogenase isoforms likely leads to a build-up of malate. In turn, an abundance of malic enzyme isoforms

may accelerate the conversion of malate into pyruvate (Osorio *et al.*, 2013). Seemingly, increased pyruvate boosts an abundance of pyruvate-derived amino acids — alanine, valine, leucine in *Nps1\**. Consistent with this, proteins involved in amino acid biosynthesis show higher levels in *Nps1\**. In parallel, increased pyruvate can boost the MEP pathway, thus enhancing the level of carotenoids in *Nps1\**.

# Nps1\* dominant-negatively enhances carotenogenesis in tomato

At times, the influence of dominant-negative mutation such as *Nac-Nor* or dominant mutation *Nr* may vary in different genetic backgrounds (Elkind *et al.*, 1990; Lanahan *et al.*, 1994; Rodríguez *et al.*, 2010; Wang *et al.*, 2020). Such influence was not conspicuous for *Nps1\**, as in two different genetic backgrounds it dominant-negatively stimulated carotenoids. Altered volatile profiles with increased MHO level derived from lycopene, higher amino acids and sugars coupled with reduced CO<sub>2</sub> emission indicated that *Nps1\** affected a broad spectrum of responses. In *Nps1\**, high lycopene is accompanied by a decrease in fatty acids, while a converse is seen in *cry2* mutant (Fantini *et al.*, 2019). It is plausible that a decrease in fatty acids reflects metabolites diversion towards the carotenoid pathway.

In tomato fruits, carotenoid synthesis does not obligatorily require light, nonetheless light is necessary for maximal carotenoid production (Raymundo et al., 1976; Gupta et al., 2014). In general, deficiency of photoreceptors such as UVR8 (Li et al., 2018), or cryptochromes (Giliberto et al., 2005; Liu et al., 2018; Fantini et al., 2019) or phytochromes (Gupta et al., 2014; Bianchetti et al., 2018) lead to reduced carotenoid levels. Conversely, the phytochromeB2-overexpressor line stimulated the carotenoid level (Alves et al., 2020). Unlike other photoreceptors, Nps1\*, while impairing phototropin1 functioning, considerably stimulates carotenoid accumulation. The recreation of tomato Nps1 mutation (Arg495His) in Arabidopsis phot1 (Arg472His) and Chlamydomonas phot (Arg210His) conferred constitutively active kinase activity to phototropin1 (Aihara et al., 2012; Petersen et al., 2017). Seemingly, upregulation of carotenoids by Nps1\* is linked with constitutively active phototropin1, as loss of function phot1 alleles displayed reduced carotenoids. Ostensibly, a functional phot1 is necessary for normal fruit carotenogenesis, while constitutively active phot1 in Nps1\* exacerbates accumulation of carotenoids.

# Ethylene emission and carotenogenesis are not linked in Nps1\*

Unlike other photoreceptors that can translocate to the nucleus, phototropins are membrane-bound (Liscum *et al.*, 2020), thus may only influence the biosynthesis of carotenoids indirectly. Unfortunately, the constituents linking phototropin activation to gene expression are not yet

known. Considering that activation of phototropins generates an asymmetric auxin gradient that upregulates transcription of auxin-associated genes culminating in hypocotyl curvature (Esmon et al., 2006), it is plausible that Nps1\* may stimulate carotenogenesis by altering the hormonal balance. In tomato, carotenoid accumulation is modulated by auxin-ethylene interaction, wherein high auxin suppresses ethylene action and reduces carotenoid accumulation (Su et al., 2015). On the contrary, in Nps1\* though auxin level is high and ethylene emission is reduced, fruits accumulate a high amount of carotenoids. Though total suppression of ethylene biosynthesis reduces carotenoids in tomato fruits (Oeller et al., 1991; Lanahan et al., 1994), reduced ethylene emission does not lead to reduced carotenoids, as seen in Nps1\* and other tomato mutants (Kilambi et al., 2013; Sharma et al., 2020). The role of other hormones in increasing carotenoid levels in Nps1\* is also equivocal. Nps1\* fruits accumulate a much higher level of carotenoids than the JA-overexpressor line (Liu et al., 2012), ABA-deficient mutants (Galpaz et al., 2008) or transgenics (Sun et al., 2012). Therefore, it seems unlikely that reduced ABA, JA or high MeJA levels in fruits contributed to carotenoid stimulation. In sum, though Nps1\* strongly affects the hormonal balance of tomato fruits, its influence on carotenoid accumulation is not strictly dependent on it.

## Nps1\* upregulates several MEP and carotenogenesisrelated genes

Though the identity of the signal chain components emanating from Nps1\* is arcane, it upregulated key ripening regulators, rin, and tagl1, which are known to promote carotenogenesis. The above cohort also included Or and pif1, known to modulate carotenogenesis. Reduced expression of glk2 and aprr2 confirmed that high carotenoid levels in Nps1\* are unrelated to chloroplast numbers. Considering that expression of *nor* and *ful1*, 2 were lower, they seem not to participate in Nps1\*-mediated carotenogenesis.

Though phototropins mediate chloroplast movements, they seem not to affect leaf chlorophyll levels (Gotoh et al., 2018). Similarly, Nps1\* and AC leaves had no discernible difference in chlorophyll levels. Nonetheless, reduced chlorophylls in Nps1\* MG fruits suggest that phototropin1 action in fruit is distinct from leaves. The onset of fruitripening triggers in parallel chlorophyll catabolism (Kilambi et al., 2017) and the transformation of chloroplasts to chromoplasts. Ripening also shifts major flux from the MEP pathway towards carotenoids providing its primary precursor GGPP. Consistent with this, Nps1\* influenced MEP pathway genes such as dxs1 and ggpps2, which were downregulated, while dxr, hdr and idi1 are upregulated. Because overexpression of hdr and dxr boosts carotenoid levels (Estévez et al., 2001; Botella-Pavía et al., 2004),

elevated carotenoids in Nps1\* can ensue from their upregulation. The upregulation of idi1 transcript was also reflected in Nps1\* proteome, where IDI1 protein was exclusively detected. Because IDI1 disruption reduces carotenoid content in fruits (Pankratov et al., 2016), plausibly high IDI1 in Nps1\* also directs the flux towards carotenoids. Opposite to IDI1, reduced dxs expression lowered its protein levels, but such a correlation between transcript and protein was amiss for DXR. In essence, Nps1\* seems to modulate the MEP pathway at multiple levels, thus affecting precursor supply towards the carotenoids pathway.

In ripening tomato fruits, carotenoid formation is mediated by a fruit-specific PSY1 (Fray and Grierson, 1993) distinct from leaf-specific PSY2 (Fraser et al., 1999; Fantini et al., 2013). Excepting psy1, Nps1\* upregulated expression of carotenogenesis genes upstream of lycopene. While transgenic psy1-overexpressor lines stimulate lycopene levels (Fraser et al., 2007), the lowered expression does not inevitably lower the lycopene level. Consistent with this, in phot1<sup>CR</sup> loss of function alleles, though psv1 expression was high at RR, the lycopene content was low. A similar negative correlation between psy1 expression and lycopene content was observed in the hp1 mutant (Kilambi et al., 2013) and DET1-underexpression lines (Enfissi et al., 2010). Current evidence indicates that psy2 does not contribute to fruit-specific carotenogenesis (Fraser et al., 1999; Fantini et al., 2013). However, it may have a hitherto undiscovered role in fruits. Given that Cao et al. (2019) showed tomato PSY2 to be functionally more active than PSY1, it is plausible that a high psy2 expression in Nps1\* fruits may contribute towards high carotenoid levels in concert with PSY1.

Emerging evidence indicates that in addition to psv1. other intermediary genes also contribute to the elevation of lycopene levels (Fantini et al., 2013), Consistent with this, overexpression of pds in tomato enhances lycopene and β-carotene in the fruits (McQuinn et al., 2018), while suppression of zds reduces lycopene level (McQuinn et al., 2020). Higher expression of intermediary genes, especially crtiso in Nps1\*, signifies that these genes also can contribute to high lycopene levels. Though the genes downstream to lycopene showed higher expression levels in Nps1\*, it had little correlation with downstream carotenoid levels, except ccd1b. Among CCDs, CCD1 degrades lycopene-releasing volatiles such as MHO (Vogel et al., 2008; llg et al., 2014). Markedly, higher expression of the ccd1b gene in Nps1\* seems to correlate with high MHO levels.

### Nps1\* shows enrichment of carotenoid sequestration proteins

Recent studies have highlighted a major role of posttranscriptional regulation in accumulation of carotenoids, such as mRNA modification (Tan et al., 2017; Li et al., 2018),

protein abundance and stability (D'Andrea *et al.*, 2018; Yazdani *et al.*, 2019). Despite the genetic and transgenic intervention, little is known about the contribution of proteins and enzymes in carotenogenesis. For most carotenogenesis genes, the correlation was amiss between transcript levels and the respective protein abundances in *Nps1\**. Despite the high expression of several carotenogenic genes, none of the corresponding proteins was detected in *Nps1\** proteome. Unlike MEP pathway proteins, carotenogenic pathway protein abundance may be too low, thus escaping detection.

The above lack of transcript/protein abundance correlation signifies that enhanced carotenoids in *Nps1\** likely arise from the maintenance of their function rather than their relative abundance. Current evidence favors that the protection of carotenogenic proteins is also an essential part of higher carotenoids synthesis in tomato fruits (D'Andrea and Rodriguez-Concepcion, 2019). Alternatively, higher carotenoid levels can also ensue from increased carotenoid sequestration. Consistent with this, tomato fruits bearing high carotenoid levels also have increased carotenoid sequestration proteins (Kilambi *et al.*, 2013, 2017; Nogueira *et al.*, 2013). As, in *Nps1\**, CHRC and CHRD levels are high, increased sequestration seems to contribute to higher carotenoid content.

# Higher carotenogenesis in *Nps1*\* may ensue from protein protection

Remarkably, *Nps1*\* proteome was enriched in chaperones, proteins mediating protein folding and proteinase inhibitors. Emerging evidence indicates that chaperones and proteases play a pivotal role in sustaining the activity of rate-limiting MEP pathway enzymes such as DXS and DXR (Flores-Pérez et al., 2008; Pulido et al., 2016, 2017) and carotenogenic enzymes like PSY1 (Welsch et al., 2018). Thus, reduction in Clp and Hsp70.2 activities by mutations or by transgenic means leads to the accumulation of enzymatically active DXS and DXR (Flores-Pérez et al., 2008; Pulido et al., 2016), PSY1, PDS, ZDS, etc. (Welsch et al., 2018), and carotenoids enrichment (D'Andrea et al., 2018; D'Andrea and Rodriguez-Concepcion, 2019). Consistent with this, increased ClpB3 protease, Hsp70.2, and reduced ClpC1, ClpC2 protease levels in Nps1\* may sustain the activity of DXS and other carotenogenic proteins (D'Andrea and Rodriguez-Concepcion, 2019).

In tomato, chaperones like *Hsp21* (Neta-Sharir *et al.*, 2005; Carvalho *et al.*, 2012) and *Or* (Yazdani *et al.*, 2019) are implicated in chromoplast formation and enhancing carotenoids. Hsp21 was abundantly present solely in *Nps1\**; therefore, it is plausible that Hsp21 may contribute to enhanced lycopene levels in *Nps1\**. Considering that there is an overlap between components of protein stability/protection machinery for PSY in Arabidopsis leaves (Welsch *et al.*, 2018) and in tomato fruits (D'Andrea *et al.*, 2018;

D'Andrea and Rodriguez-Concepcion, 2019), the likelihood of upregulation of above components by *Nps1\** is very high. Indeed, most of these components were highly abundant in *Nps1\** fruits, except OR. Though OR was below the detection limit, the enhanced transcript levels of *Or* in *Nps1\** indicate a probable transient upregulation of its protein level. In such a case, it may protect both PSY1 and PSY2 (Welsch *et al.*, 2018), thus contributing to high carotenoids in *Nps1\** fruits. Considering the importance of chaperones/protein folding in maintaining the MEP pathway and carotenogenic proteins, these proteins in *Nps1\** may play a similar role. Plausibly, in *Nps1\**, these proteins provide a protective microenvironment allowing efficient functioning of carotenogenic proteins leading to carotenoid enrichment.

It remains to be determined how *Nps1\** influences broad-spectrum responses encompassing increased carotenogenesis, metabolic and proteomic shifts. Within the constraints of limited knowledge about phototropin signaling, we can only make a conjecture. Phototropins function as light and temperature sensors, and loss of this sensing capability by dominant-negative mutation may create a stressful situation. While other regulatory mechanisms may alleviate the stress in vegetative tissues, during fruit ripening absence of such compensation may amplify the stress. Because this stress is within, it is construed as abiotic stress, leading to the upregulation of abiotic stress-related proteins and protein protection mechanisms.

In summary, our results highlight that phototropins play an important role in the regulation of carotenoid biosynthesis during fruit ripening. Besides bringing a new photoreceptor regulating carotenogenesis in tomato, our study unfolds a potential biotechnological tool to enhance the carotenoid levels in fruits. The dominant-negative feature of *Nps1\** makes it an attractive tool for enhancing carotenoid levels in heterozygous fruits, thus has considerable value for the hybrid industry. Our work adds to the current impetus to generate tomato with health-promoting carotenoids, and advances the repertories available for making more nutritious tomato.

### **EXPERIMENTAL PROCEDURES**

### Plant material

Tomato (*Solanum lycopersicum*) cultivar Ailsa Craig (LA2838, TGRC, Davis, CA), Arka Vikas (IIHR, Bengaluru, India) and *non-phototropic seedling 1* mutant, *Nps1* (Sharma *et al.*, 2014) were used. Seeds germination and low-fluence blue-light-induced phototropic curvature analysis of parents and backcrossed progeny was carried out as described in Sharma *et al.* (2014). After the phototropic screening, seedlings were transferred to white light (100  $\mu$ mol  $m^{-2}$  sec $^{-1}$ ) for 1 week and then transferred to a greenhouse (28  $\pm$  1°C day/ambient at night).

Reciprocal crosses were made between wild-type (AC and AV) and Nps1 plants. The BC<sub>1</sub>F<sub>1</sub> plants were self-pollinated to generate

BC<sub>1</sub>F<sub>2</sub> plants, which were backcrossed again to raise BC<sub>2</sub>F<sub>2</sub> progeny. The homozygous BC<sub>2</sub>F<sub>2</sub> (Nps1: Nps1) plants were then advanced to BC2F3 and BC2F4 progeny, and the zygosity of progeny for Nps1 at each stage was identified by low-fluence phototropism and CELI endonuclease assay (Mohan et al., 2016; see Table S10 for primers). The zygosity of plants was also confirmed by Sanger sequencing of polymerase chain reaction (PCR)-amplified Phot1 gene products (Macrogen, Seoul, Korea).

### Chloroplast relocation

The MG fruits after harvest were dark-adapted for 12 h. The fruits were cut into two identical halves under green safe light. For chloroplast accumulation, after obtaining the dark position of chloroplasts, the slices were exposed to low-fluence blue light (5 μmol m<sup>-2</sup> sec<sup>-1</sup>) for 30 min. Thereafter, slices were exposed to high-fluence (100  $\mu mol\ m^{-2}\ sec^{-1})$  blue light for 30 min to induce chloroplast avoidance. The positioning of chloroplasts was observed in a Zeiss confocal microscope as described in Sharma et al. (2014).

Chloroplast movement in tomato leaf was monitored by the measurement of red light transmittance through leaf discs at 25°C using a microplate reader (Biotek, Synergy HT), as described by Wada and Kong (2011).

### Generation of gene-edited lines of phot1 by CRISPR-Cas9

Double-guide RNAs (sgRNA) for the phot1 gene (Solyc11g072710) with GC content between 40 and 60% were selected using the CRISPR-P web tool (http://cbi.hzau.edu.cn/crispr; Lei et al., 2014; Phot1-sgRNA-1: GAGAAGGTTAATTCGAAGG and Phot1-sgRNA-2: GGAACTCCGACCAGAGTTGC).

The human codon-optimized CAS9 with 2x35S CaMV promoter and Nos terminator was amplified from pAGM4723 plasmid (Addgene# 49772) using Kpnl forward, and Pacl reverse primers (Table S11). The amplified products were cloned into the pCAM-BIA2300 vector. The gRNA expression cassette was developed through overlap extension PCR as described in Nekrasov et al. (2013). Using Pacl forward and Spel reverse primers, the Phot1sgRNA-1, and with Kpnl forward and Kpnl reverse primers, the Phot1-sgRNA-2 expression cassettes were amplified and cloned into a pCAMBIA2300-CAS9 vector. The final vector pCAMBIA2300-CAS9-Phot1 was verified by sequencing (see Table S11 for primers).

The pCAMBIA2300-CAS9-Phot1 vector was transferred into Agrobacterium strain LBA4404, and tomato transformation in AV was carried out according to the protocol of Van Eck et al. (2006). Transgenic plants were recovered in the medium supplemented with kanamycin and transferred into the soil. Genomic DNA was isolated, according to Sreelakshmi et al. (2010), from 8-12-weekold plants. The CRISPR/Cas9-induced mutations were screened by amplifying a region of about 546 bp surrounding both the gRNAs in the phot1 and separation of fragments on agarose gel (Table S11). Sanger sequencing of six individual clones/editing event was performed after cloning the PCR product into InsTAclone PCR Cloning Kit (Thermo Scientific, Waltham, MA, USA) using the M13 forward primer. The confirmed edited lines were advanced to T<sub>1</sub> generation, and the homozygous mutants were identified by PCR followed by sequencing. The Cas9-free homozygous lines were identified in the T2 generation and were further characterized for fruit characteristics as described below.

Off-targets for the phot1 sgRNAs were identified using CRISPR-P and CRISPOR web tools (http://cbi.hzau.edu.cn/crispr; http://cris por.tefor.net; Lei et al., 2014; Haeussler et al., 2016). A list of 33

potential off-targets was predicted for the target locus with up to four mismatches. Further, based on high cutting frequency distribution (CFD) off-target score (Haeussler et al., 2016), seven potential off-targets were selected (four for Phot1-sgRNA-1; three for Phot1-sgRNA-2; Table S12). The genomic DNA surrounding the potential off-target locus was amplified using specific primers (Table S11), and the PCR products were analyzed by Sanger sequencing.

### Fruit ripening

For the fruit ripening study, AC, AV, Nps1\* and phot1<sup>CR1-5</sup> plants were grown in three randomized blocks (each block constitutes one biological replicate) as described previously (Kilambi et al., 2013; Figure S16). The flowers were tagged at anthesis for chronological monitoring of fruit development. The time points of attainment of different ripening stages viz, MG, BR and RR were identified, and fruits were harvested, flash-frozen in liquid nitrogen and stored at -80°C until further use as described previously (Kilambi et al., 2013).

### Estimation of carotenoids, transcripts, hormones, metabolites, °Brix, firmness and respiration rate

The carotenoid and chlorophyll levels were determined from leaves and fruits using the protocols of Gupta et al. (2015) and Wellburn (1994), respectively. Real-time (RT)-PCR analysis (for primers, see Table S11) and ethylene emission estimation were carried out as described in Kilambi et al. (2013). The hormone estimation and metabolite analysis were carried out as described by Bodanapu et al. (2016). Metabolites were extracted from the fruits of AC and Nps1\* (BC2F2 homozygous), and identified by gas chromatography-mass spectrometry (GC-MS). Sugar content, pH and firmness of fruits were determined as described by Gupta et al. (2014). The respiration rate of tomato fruits was measured as described by Sharma et al. (2020).

### Proteome profiling

Protein isolation, separation and digestion were carried out as described earlier by Kilambi et al. (2013, 2016, 2017). Proteins (70  $\mu$ g) were first separated by one dimensional sodium dodecyl sulfate-polyacrylamide gel electrophoresis (SDS-PAGE). Thereafter, in-gel digestion was carried out using trypsin, and peptides were extracted. After desalting by C18 spin columns (Thermo Scientific), peptides were aliquoted, dried and stored at -80°C.

## Mass spectrometry, data analysis and label-free quantification

Peptides were analyzed using Easy nanoLC-II coupled with LTQ Velos Pro mass spectrometer (Thermo Scientific). Peptides (350 ng) were separated using a C18 column setup, the 118 min gradient with all the other mass spectrometric parameters, as mentioned in Kilambi et al. (2016). Data analysis was done using Sorcerer (version 5.1 release, Sage-N Research). Solanum lycopersicum iTAG3.2 proteome sequence (ftp://ftp.solgenomics.net/toma to\_genome/annotation/ITAG3.2\_release/ITAG3.2\_proteins.fasta, downloaded on 18 July 2017, 35 673 sequences and 12 210 990 residues) was used as the database. The searches were done with Sequest with the parameters described in Kilambi et al. (2016). The mass spectrometry proteomics data are available via ProteomeXchange (Vizcaíno et al., 2014) with the dataset identifier PXD018150. Label-free quantitation was carried out using Scaffold software (version 4.7.5, Proteome Software), as described previously in Kilambi et al. (2016).

### Extraction of volatile compounds and their identification

The volatile compounds from the fruits were extracted as described in Rambla et al. (2016), and were adsorbed to a 50-µm divinylbenzene/Carboxen/Polydimethylsiloxane (DVB/CAR/PDMS) SPME fiber assembly (Supelco, Bellefonte, PA, USA) for 20 min at 50°C under continuous agitation. The fiber was inserted into GC 7890A (Agilent Technologies, Palo Alto, CA, USA) coupled with MS Pegasus 4D with Time of Flight as the detector (LECO Corporation, MI, USA). The volatiles were desorbed at 250°C for 1 min. The volatiles were then separated using the following program: 5 min at 45°C with a linear ramp of 5°C min<sup>-1</sup> to 250°C and held at 250°C for 5 min. Both the injector and detector temperatures were set at 260 and 250°C, respectively. Helium was used as carrier gas at a flow rate of 1.5 ml min<sup>-1</sup>. Ionization energy (EI) of 70 eV was used for mass spectrometry detector, with a source temperature of 250°C, a scan range of 35-600 m/z, and the mass spectra were recorded at a 2 scans/sec speed.

The raw data were processed by ChromaTOF software 2.0 (Leco) and further analyzed using the MetAlign software package (Lommen and Kools, 2012; www.metalign.nl). The Metalign results were processed with MSClust software for the reduction of data and compound mass extraction (Tikunov *et al.*, 2012). The mass spectra extracted by MSClust were searched in NIST MS Search v 2.2 software for the identification of compound names within the NIST (National Institute of Standard and Technology) Library and Golm Metabolome Database Library. The compound hits, which showed the maximum matching factor (MF) value (>600) and the least deviation from the retention index were used for metabolite identity.

### Statistical analysis

Unless otherwise specified, a minimum of three biological replicates was used for every experiment. A Student's *t*-test was performed to determine significant differences using Sigma plot (version 11.0). Where required, the *P*-values < 0.05, < 0.01, < 0.001, are indicated by one, two or three asterisks, respectively. Heat maps were made using Morpheus software (https://software.b roadinstitute.org/morpheus/).

### **AUTHOR CONTRIBUTIONS**

The whole study was conceived and designed by YS. HVK performed genetic and phenotypic segregation, ethylene evolution, fruit carotenoid, transcript profiling, proteome analyses. AD characterized the gene-edited lines. KS performed metabolite, volatile and hormone analyses. NRN designed the CRISPR constructs, off-target analysis. NG generated edited plants, and performed initial screening for editing in tissue culture explants. NPT performed initial proteome analyses, Brix, firmness, pH and leaf carotenoid profiling. AJD performed sequencing and transcript profiling of selected genes. SS and KT performed fruit chloroplast movement assay and initial fruit ripening. KT made the first cross between AV and Nps1. SK performed leaf chlorophyll estimation and carbon dioxide evolution from fruits. Data were interpreted by HVK, KS, NRN, AD, RS and YS. YS and RS wrote the manuscript with inputs from HVK and NRN. All authors read and approved the manuscript.

### **ACKNOWLEDGEMENTS**

The authors thank Ms Hemalatha for technical help with GeLCMS, and Dr Eros Kharshiing for the critical reading of the manuscript. This work was supported by the Department of Biotechnology (DBT), India (BT/PR11671/PBD/16/828/2008, BT/PR/6983/PBD/16/1007/2012, and BT/COE/34/SP15209/2015) to YS and RS; University Grants Commission, India, research fellowship to HVK; Council of Scientific and Industrial Research, India research fellowship to KT; Department of Biotechnology research fellowship to AD, NPT and AJD.

### **CONFLICT OF INTEREST**

The authors declare no conflict of interests.

### **DATA AVAILABILITY STATEMENT**

All relevant data can be found within the manuscript and its supporting materials. The proteome data were uploaded on the PRIDE repository and the details are given above.

### SUPPORTING INFORMATION

Additional Supporting Information may be found in the online version of this article.

**Figure S1.** CELI endonuclease assay for the detection of *phot1* mutation and its zygosity in backcrossed plants.

**Figure S2.** Identification of homozygous edited and CAS9-free plants in  $T_1$  and  $T_2$  generations, and screening for potential off-tarqet effects in *phot1*<sup>CR</sup> lines.

Figure S3. Chloroplast relocation response in the leaf discs of AV, Nps1 and  $phot1^{CR}$  alleles.

Figure S4. Chronological development of fruits in AV and *phot1*<sup>CR</sup> lines, and the color, pH and °Brix of their ripe fruits.

Figure S5. Relative transcript levels of genes mediating system II ethylene biosynthesis in ripening fruits of AC and Nps1\*.

Figure S6. Fruit firmness, Brix and pH of ripening fruits of AC and Nos1\*.

**Figure S7.** Relative expression of rate-limiting genes mediating carotenoid biosynthesis in ripening fruits of AV and  $phot^{CR}$  lines.

Figure S8. Relative expression of ripening regulators, modulators of carotenogenesis and phototropin genes in ripening fruits of AC and Nps1\*.

**Figure S9.** The principal component analysis (PCA) of primary metabolites detected in ripening fruits of AC and *Nps1\**.

Figure S10. The metabolic shifts in AC and Nps1\* fruits during ripening.

**Figure S11.** The principal component analysis (PCA) of volatiles detected in ripening fruits of AC and *Nps1\**.

Figure S12. Proteome profiling in ripening fruits of AC and Nps1\*.

Figure S13. Functional annotation of differentially expressed proteins and proteins present solely in ripening fruits of AC and Nps1\*.

**Figure S14.** Relative abundances of heat shock proteins and proteins involved in protein folding and degradation in AC and *Nps1\** fruits at different stages of ripening.

**Figure S15.** Relative expression of selected *Clp* proteases and *Hsps* in ripening fruits of AC and *Nps1\**.

**Figure S16.** The randomized block design for growing AC and *Nps1\** plants.

- Table S1. Carotenoid and chlorophyll contents in the fruits of AV and Nps1 at different ripening stages.
- Table S2. The genetic segregation of Nps1 in BC<sub>1</sub>F<sub>2</sub> generation in AC and AV backgrounds.
- Table S3. The carotenoid and chlorophyll contents in the leaves of 70-day-old AC, Nps1 and Nps1\*( $BC_2F_3$ ).
- Table S4. Carotenoid content in the red ripe fruits of AV and homozygous phot  $1^{CR}$  lines in the  $T_2$  generation.
- Table S5. List of primary metabolites identified in the fruits of AC and Nps1\* during ripening.
- Table S6. List of volatiles identified in ripening fruits of AC and
- Table S7. Differentially expressed proteins in ripening fruits of Nps1\* compared with AC.
- Table S8. List of proteins identified solely in Nps1\* and solely in AC during ripening.
- Table S9. List of carotenoid-related proteins, TCA cycle proteins, Hsps, and other proteins involved in protein folding and degradation in the ripening fruits of Nps1\* and AC.
- **Table S10**. The primers used for detection of *phot1* mutation by CELI endonuclease assay and sequencing.
- Table S11. List of primers used for generating gene-edited phot1 plants, their confirmation, and detection of potential off-target sites by PCR followed by sequencing.
- Table S12. List of potential off-targets predicted for phot1gRNA1 and phot1gRNA2.
- Table S13. The primers used for quantitative real-time PCR in this

#### **REFERENCES**

- Aihara, Y., Yamamoto, T., Okaiima, K., Yamamoto, K., Suzuki, T., Tokutomi, S. et al. (2012) Mutations in N-terminal flanking region of blue light-sensing light-oxygen and voltage 2 (LOV2) domain disrupt its repressive activity on kinase domain in the Chlamydomonas phototropin. Journal of Biological Chemistry, 287, 9901-9909.
- Alba, R., Cordonnier-Pratt, M.M. & Pratt, L.H. (2000) Fruit-localized phytochromes regulate lycopene accumulation independently of ethylene production in tomato. Plant Physiology, 123, 363-370.
- Alves, F.R.R., Lira, B.S., Pikart, F.C., Monteiro, S.S., Furlan, C.M., Purgatto, E. et al. (2020) Beyond the limits of photoperception: constitutively active PHYTOCHROME B2 overexpression as a means of improving fruit nutritional quality in tomato. Plant Biotechnology Journal, 18(10), 2027–2041.
- Azari, R., Tadmor, Y., Meir, A., Reuveni, M., Evenor, D., Nahon, S. et al. (2010) Light signaling genes and their manipulation towards modulation of phytonutrient content in tomato fruits. Biotechnology Advances, 28, 108-118
- Balbi, V. & Lomax, T.L. (2003) Regulation of early tomato fruit development by the diageotropica gene. Plant Physiology, 131, 186-197.
- Barry, C.S. (2014) Ripening mutants. In: Nath, P., Bouzayen, M., Mattoo, A.K. & Pech, J.C. (Eds.) Fruit ripening: physiology, signalling and genomics (pp. 246-258). Wallingford: CABI.
- Barry, C.S., Llop-Tous, M.I. & Grierson, D. (2000) The regulation of 1aminocyclopropane-1-carboxylic acid synthase gene expression during the transition from system-1 to system-2 ethylene synthesis in tomato. Plant Physiology, 123, 979-986.
- Barry, C.S., McQuinn, R.P., Thompson, A.J., Seymour, G.B., Grierson, D. & Giovannoni, J.J. (2005) Ethylene insensitivity conferred by the green-ripe and never-ripe 2 ripening mutants of tomato. Plant Physiology, 138, 267–275.
- Bartley, G.E. & Scolnik, P.A. (1995) Plant carotenoids: pigments for photoprotection, visual attraction, and human health. The Plant Cell, 7, 1027-
- Bianchetti, R.E., Silvestre-Lira, B., Santos-Monteiro, S., Demarco, D., Purgatto, E., Rothan, C. et al. (2018) Fruit-localized phytochromes regulate plastid biogenesis, starch synthesis, and carotenoid metabolism in tomato. Journal of Experimental Botany, 69, 3573-3586.

- Bodanapu, R., Gupta, S.K., Basha, P.O., Sakthivel, K., Sadhana, Sreelakshmi, Y. et al. (2016) Nitric oxide overproduction in tomato shr mutant shifts metabolic profiles and suppresses fruit growth and ripening. Frontiers in Plant Science, 7, 1714.
- Botella-Pavía, P., Besumbes, Ó., Phillips, M.A., Carretero-Paulet, L., Boronat, A. & Rodríguez-Concepción, M. (2004) Regulation of carotenoid biosynthesis in plants: evidence for a key role of hydroxymethylbutenyl diphosphate reductase in controlling the supply of plastidial isoprenoid precursors. The Plant Journal, 40, 188-199.
- Cao, H., Luo, H., Yuan, H., Eissa, M.A., Thannhauser, T.W., Welsch, R. et al. (2019) A neighboring aromatic-aromatic amino acid combination governs activity divergence between tomato phytoene synthases. Plant Physiology, 180, 1988-2003.
- Carvalho, L.J.C.B., Lippolis, J., Chen, S., de Souza, C.R.B., Vieira, E.A. & Anderson, J.V. (2012) Characterization of carotenoid-protein complexes and gene expression analysis associated with carotenoid sequestration in pigmented cassava (Manihot Esculenta Crantz) storage root. Open Biochemistry Journal, 6, 116-130.
- D'Andrea, L. & Rodriguez-Concepcion, M. (2019) Manipulation of plastidial protein quality control components as a new strategy to improve carotenoid contents in tomato fruit. Frontiers in Plant Science, 10, https://doi. org/10.3389/fpls.2019.01071.
- D'Andrea, L., Simon-Moya, M., Llorente, B., Llamas, E., Marro, M., Loza-Alvarez, P. et al. (2018) Interference with Clp protease impairs carotenoid accumulation during tomato fruit ripening. Journal of Experimental Botanv. 69, 1557-1568.
- Elkind, Y., Cahaner, A. & Kedar, N. (1990) A mixed model for the effects of single gene, polygenes and their interaction on quantitative traits. 2. The effects of the nor gene and polygenes on tomato fruit softness. Heredity (Edinh), 64, 205-213.
- Enfissi, E.M.A., Barneche, F., Ahmed, I., Lichtlé, C., Gerrish, C., McQuinn, R.P. et al. (2010) Integrative transcript and metabolite analysis of nutritionally enhanced de-etiolated1 downregulated tomato fruit. The Plant Cell, 22, 1190-1215.
- Esmon, C.A., Tinsley, A.G., Ljung, K., Sandberg, G., Hearne, L.B. & Liscum, E. (2006) A gradient of auxin and auxin-dependent transcription precedes tropic growth responses. Proceedings of the National Academy of Sciences of the United States of America, 103, 236-241.
- Estévez, J.M., Cantero, A., Reindl, A., Reichler, S. & León, P. (2001) 1-Deoxy-d-xylulose-5-phosphate Synthase, a limiting enzyme for plastidic isoprenoid biosynthesis in plants. Journal of Biological Chemistry, 276, 22901-22909.
- Fankhauser, C. & Christie, J.M. (2015) Plant phototropic growth. Current Biology, 25, R384-R389.
- Fantini, E., Falcone, G., Frusciante, S., Giliberto, L. & Giuliano, G. (2013) Dissection of tomato lycopene biosynthesis through virus-induced gene silencing. Plant Physiology, 163, 986-998.
- Fantini, E., Sulli, M., Zhang, L., Aprea, G., Jiménez-Gómez, J.M., Bendahmane, A. et al. (2019) Pivotal roles of cryptochromes 1a and 2 in tomato development and physiology. Plant Physiology, 179, 732-748.
- Flores-Pérez, Ú., Sauret-Güeto, S., Gas, E., Jarvis, P. & Rodríguez-Concepción, M. (2008) A mutant impaired in the production of plastome-encoded proteins uncovers a mechanism for the homeostasis of isoprenoid biosynthetic enzymes in Arabidopsis plastids. The Plant Cell, 20, 1303-1315.
- Frank, H.A. & Cogdell, R.J. (1996) Carotenoids in photosynthesis. Photochemistry and Photobiology, 63, 257-264.
- Fraser, P.D., Enfissi, E.M.A., Halket, J.M., Truesdale, M.R., Yu, D., Gerrish, C. & et al. (2007) Manipulation of phytoene levels in tomato fruit: effects on isoprenoids, plastids, and intermediary metabolism. The Plant Cell, 19, 3194-3211.
- Fraser, P.D., Kiano, J.W., Truesdale, M.R., Schuch, W. & Bramley, P.M. (1999) Phytoene synthase-2 enzyme activity in tomato does not contribute to carotenoid synthesis in ripening fruit. Plant Molecular Biology,
- Fray, R.G. & Grierson, D. (1993) Identification and genetic analysis of normal and mutant phytoene synthase genes of tomato by sequencing, complementation and co-suppression. Plant Molecular Biology, 22, 589-602.
- Galpaz, N., Wang, Q., Menda, N., Zamir, D. & Hirschberg, J. (2008) Abscisic acid deficiency in the tomato mutant high-pigment 3 leading to increased plastid number and higher fruit lycopene content. The Plant Journal, 53, 717-730.

- Galvão, V.C. & Fankhauser, C. (2015) Sensing the light environment in plants: photoreceptors and early signaling steps. Current Opinion in Neurobiology, 34, 46–53.
- Giliberto, L., Perrotta, G., Pallara, P., Weller, J.L., Fraser, P.D., Bramley, P.M. et al. (2005) Manipulation of the blue light photoreceptor cryptochrome 2 in tomato affects vegetative development, flowering time, and fruit antioxidant content. Plant Physiology, 137, 199–208.
- **Giuliano, G.** (2017) Provitamin A biofortification of crop plants: a gold rush with many miners. *Current Opinion in Biotechnology*, **44**, 169–180.
- Gotoh, E., Suetsugu, N., Yamori, W., Ishishita, K., Kiyabu, R., Fukuda, M. et al. (2018) Chloroplast accumulation response enhances leaf photosynthesis and plant biomass production. Plant Physiology, 178, 1358–1369.
- Gupta, P., Sreelakshmi, Y. & Sharma, R. (2015) A rapid and sensitive method for determination of carotenoids in plant tissues by high performance liquid chromatography. *Plant Methods*, 11, 5.
- Gupta, S.K., Sharma, S., Santisree, P., Kilambi, H.V., Appenroth, K., Sreelak-shmi, Y. et al. (2014) Complex and shifting interactions of phytochromes regulate fruit development in tomato. Plant, Cell and Environment, 37, 1688–1702.
- Haeussler, M., Schönig, K., Eckert, H., Eschstruth, A., Mianné, J., Renaud, J.B. et al. (2016) Evaluation of off-target and on-target scoring algorithms and integration into the guide RNA selection tool CRISPOR. Genome Biology, 17, 148.
- Hirschberg, J. (2001) Carotenoid biosynthesis in flowering plants. *Current Opinion in Plant Biology*, **4**, 210–218.
- Huq, E., Al-Sady, B., Hudson, M., Kim, C., Apel, K. & Quail, P.H. (2004) Phytochrome-interacting factor 1 is a critical bHLH: regulator of chlorophyll biosynthesis. *Science*, 305, 1937–1941.
- Ilag, L.L., Kumar, A.M. & Soll, D. (1994) Light regulation of chlorophyll biosynthesis at the level of 5-aminolevulinate formation in Arabidopsis. The Plant Cell, 6, 265–275.
- Ilg, A., Bruno, M., Beyer, P. & Al-Babili, S. (2014) Tomato carotenoid cleavage dioxygenases 1A and 1B: relaxed double bond specificity leads to a plenitude of dialdehydes, mono-apocarotenoids and isoprenoid volatiles. FEBS Open Bio, 4, 584–593.
- Jenkins, G.I., Hartley, M.R. & Bennett, J. (1983) Photoregulation of chloroplast development: transcriptional, translational and post-translational controls? *Philosophical Transactions R Society London B, Biological Sciences*, 303, 419–431s.
- Kasemir, H. (1983) Light control of chlorophyll accumulation in higher plants. In: Shropshire, W. and Mohr, H. (Eds.) Photomorphogenesis. Encyclopedia of plant physiology (new series). Berlin, Heidelberg: Springer, pp. 662–686.
- Kharshiing, E., Sreelakshmi, Y. & Sharma, R. (2019) The light awakens! Sensing light and darkness. In S.K. Sopory (Ed.), Sensory biology of plants (pp. 21–57). Singapore: Springer.
- Kilambi, H.V., Kumar, R., Sharma, R. & Sreelakshmi, Y. (2013) Chromoplast-Specific carotenoid-associated protein appears to be important for enhanced accumulation of carotenoids in hp1 tomato fruits. *Plant Physiology*, 161, 2085–2101.
- Kilambi, H.V., Manda, K., Rai, A., Charakana, C., Bagri, J., Sharma, R. et al. (2017) Green-fruited Solanum habrochaites lacks fruit-specific carotenogenesis due to metabolic and structural blocks. Journal of Experimental Botany, 68, 4803–4819.
- Kilambi, H.V., Manda, K., Sanivarapu, H., Maurya, V.K., Sharma, R. & Sree-lakshmi, Y. (2016) Shotgun proteomics of tomato fruits: Evaluation, optimization and validation of sample preparation methods and mass spectrometric parameters. Frontiers in Plant Science, 7, 969.
- Lanahan, M.B., Yen, H.C., Giovannoni, J.J. & Klee, H.J. (1994) The never ripe mutation blocks ethylene perception in tomato. The Plant Cell, 6, 521–530.
- Lei, Y., Lu, L., Liu, H., Sen, L., Xing, F. & Chen, L. (2014) CRISPR-P: A web tool for synthetic single-guide RNA design of CRISPR-system in plants. *Molecular Plant*, 7, 1494–1496.
- Leitner-Dagan, Y., Ovadis, M., Shklarman, E., Elad, Y., David, D.R. & Vainstein, A. (2006b) Expression and functional analyses of the plastid lipid-associated protein CHRC suggest its role in chromoplastogenesis and stress. Plant Physiology, 142, 233–244.
- Leitner-Dagan, Y., Ovadis, M., Zuker, A., Shklarman, E., Ohad, I., Tzfira, T. et al. (2006a) CHRD, a plant member of the evolutionarily conserved YjgF family, influences photosynthesis and chromoplastogenesis. Planta, 225, 89–102.

- Li, R., Fu, D., Zhu, B., Luo, Y. & Zhu, H. (2018) CRISPR/Cas9-mediated mutagenesis of IncRNA1459 alters tomato fruit ripening. *The Plant Journal*, 94, 513–524.
- Liang, B., Zheng, Y., Wang, J., Zhang, W., Fu, Y., Kai, W. et al. (2020) Over-expression of the persimmon abscisic acid β-glucosidase gene (DkBG1) alters fruit ripening in transgenic tomato. The Plant Journal, https://doi.org/10.1111/tpj.14695.
- Liscum, E., Nittler, P. & Koskie, K. (2020) The continuing arc toward phototropic enlightenment. *Journal of Experimental Botany*, 71, 1652–1658.
- Liu, C.C., Ahammed, G.J., Wang, G.T., Xu, C.J., Chen, K.S., Zhou, Y.H. et al. (2018) Tomato CRY1a plays a critical role in the regulation of phytohormone homeostasis, plant development, and carotenoid metabolism in fruits. Plant, Cell and Environment, 41, 354–366.
- Liu, L., Shao, Z., Zhang, M. & Wang, Q. (2015) Regulation of carotenoid metabolism in tomato. *Molecular Plant*, 8, 28–39.
- Liu, L., Wei, J., Zhang, M., Zhang, L., Li, C. & Wang, Q. (2012) Ethylene independent induction of lycopene biosynthesis in tomato fruits by jasmonates. *Journal of Experimental Botany*, 63, 5751–5761.
- Llorente, B., Martinez-Garcia, J.F., Stange, C. & Rodriguez-Concepcion, M. (2017) Illuminating colors: Regulation of carotenoid biosynthesis and accumulation by light. *Current Opinion in Plant Biology*, 37, 49–55.
- Lommen, A. & Kools, H.J. (2012) MetAlign 3.0: Performance enhancement by efficient use of advances in computer hardware. *Metabolomics*, 8, 719–726.
- Maurizi, M.R. & Xia, D. (2004) Protein binding and disruption by Clp/Hsp100 chaperones. Structure, 12, 175–183.
- Mayfield, S.P., Nelson, T. & Taylor, W.C. (1986) The fate of chloroplast proteins during photooxidation in carotenoid-deficient maize leaves. *Plant Physiology*, 82, 760–764.
- Mayfield, S.P. & Taylor, W.C. (1984) Carotenoid-deficient maize seedlings fail to accumulate light-harvesting chlorophyll a/b binding protein (LHCP) mRNA. European Journal of Biochemistry, 144, 79–84.
- McQuinn, R.P., Gapper, N.E., Gray, A.G., Zhong, S., Takayuki, T., Fei, Z. et al. (2020) Manipulation of ZDS in tomato exposes carotenoid- and aba-specific effects on fruit development and ripening. Plant Biotechnology Journal, 18(11), 2210–2224. https://doi.org/10.1111/pbi.13377.
- McQuinn, R.P., Wong, B. & Giovannoni, J.J. (2018) AtPDS overexpression in tomato: Exposing unique patterns of carotenoid self-regulation and an alternative strategy for the enhancement of fruit carotenoid content. Plant Biotechnology Journal, 16, 482–494.
- Mohan, V., Gupta, S., Thomas, S., Mickey, H., Charakana, C., Chauhan, V.S. et al. (2016) Tomato fruits show wide phenomic diversity but fruit developmental genes show low genomic diversity. PLoS One, 11, e0152907.
- Nekrasov, V., Staskawicz, B., Weigel, D., Jones, J.D. & Kamoun, S. (2013)
  Targeted mutagenesis in the model plant *Nicotiana benthamiana* using
  Cas9 RNA-guided endonuclease. *Nature Biotechnology*, 31, 691–693.
- Nemhauser, J. & Chory, J. (2002) Photomorphogenesis. The Arabidopsis Book, 1, e0054.
- Neta-Sharir, I., Isaacson, T., Lurie, S. & Weiss, D. (2005) Dual role for tomato heat shock protein 21: Protecting photosystem ii from oxidative stress and promoting color changes during fruit maturation. *The Plant Cell*, 17, 1879–1838.
- Nishimura, K. & van Wijk, K.J. (2015) Organization, function and substrates of the essential Clp protease system in plastids. *Biochimica et Biophysica Acta*, 1847, 915–930.
- Nogueira, M., Mora, L., Enfissi, E.M.A., Bramley, P.M. & Fraser, P.D. (2013) Subchromoplast sequestration of carotenoids affects regulatory mechanisms in tomato lines expressing different carotenoid gene combinations. *The Plant Cell*, 25, 4560–4579.
- Oeller, P.W., Lu, M.W., Taylor, L.P., Pike, D.A. & Theologis, A. (1991) Reversible inhibition of tomato fruit senescence by antisense RNA. Science, 254 437–439
- Osorio, S., Vallarino, J.G., Szecowka, M., Ufaz, S., Tzin, V., Angelovici, R. et al. (2013) Alteration of the interconversion of pyruvate and malate in the plastid or cytosol of ripening tomato fruit invokes diverse consequences on sugar but similar effects on cellular organic acid, metabolism, and transitory starch accumulation. Plant Physiology, 161, 628–643.
- Pankratov, I., McQuinn, R., Schwartz, J., Bar, E., Fei, Z., Lewinsohn, E. et al. (2016) Fruit carotenoid-deficient mutants in tomato reveal a function of the plastidial isopentenyl diphosphate isomerase (IDI1) in carotenoid biosynthesis. The Plant Journal, 88, 82–94.

- Petersen, J., Inoue, S.I., Kelly, S.M., Sullivan, S., Kinoshita, T. & Christie, J.M. (2017) Functional characterization of a constitutively active kinase variant of Arabidopsis phototropin 1. *Journal of Biological Chemistry*, 292, 13843–13852.
- Pulido, P., Llamas, E., Llorente, B., Ventura, S., Wright, L.P. & Rodríguez-Concepción, M. (2016) Specific Hsp100 chaperones determine the fate of the first enzyme of the plastidial isoprenoid pathway for either refolding or degradation by the stromal clp protease in arabidopsis. *PLoS Genetics*, 12, e1005824.
- Pulido, P., Llamas, E. & Rodriguez-Concepcion, M. (2017) Both Hsp70 chaperone and Clp protease plastidial systems are required for protection against oxidative stress. *Plant Signaling & Behavior*, 12, e1290039.
- Rambla, J.L., Medina, A., Fernández-del-Carmen, A., Barrantes, W., Grandillo, S., Cammareri, M. et al. (2016) Identification, introgression, and validation of fruit volatile QTLs from a red-fruited wild tomato species. Journal of Experimental Botany, 68, 429-442.
- Raymundo, L.C., Chichester, C.O. & Simpson, K.L. (1976) Light-dependent carotenoid synthesis in the tomato fruit. *Journal of Agriculture and Food Chemistry*, 24, 59–64.
- Rodríguez, G.R., Pratta, G.R., Liberatti, D.R., Zorzoli, R. & Picardi, L.A. (2010) Inheritance of shelf life and other quality traits of tomato fruit estimated from F1's, F2's and backcross generations derived from standard cultivar, nor homozygote and wild cherry tomato. *Euphytica*, 176, 137–147.
- Seymour, G.B., Chapman, N.H., Chew, B.L. & Rose, J.K.C. (2013) Regulation of ripening and opportunities for control in tomato and other fruits. *Plant Biotechnology Journal*, 11, 269–278.
- Sharma, K., Gupta, S., Sarma, S., Rai, M., Sreelakshmi, Y. & Sharma, R. (2020) Mutations in tomato 1-aminocyclopropane carboxylic acid synthase2 uncover its role in development beside system II responses. *Plant Journal*. https://doi.org/10.1111/tpj.15148.
- Sharma, S., Kharshiing, E., Srinivas, A., Zikihara, K., Tokutomi, S., Nagatani, A. et al. (2014) A dominant mutation in the light-oxygen and voltage2 domain vicinity impairs phototropin1 signaling in tomato. Plant Physiology, 164, 2030–2044.
- Sreelakshmi, Y., Gupta, S., Bodanapu, R., Chauhan, V., Hanjabam, M., Thomas, S. et al. (2010) NEATTILL: A simplified procedure for nucleic acid extraction from arrayed tissue for TILLING and other high-throughput reverse genetic applications. Plant Methods, 6, 3.
- Su, L., Diretto, G., Purgatto, E., Danoun, S., Zouine, M., Li, Z. et al. (2015) Carotenoid accumulation during tomato fruit ripening is modulated by the auxin-ethylene balance. BMC Plant Biology, 15, 114.
- Sun, L., Yuan, B., Zhang, M., Wang, L., Cui, M., Wang, Q. et al. (2012) Fruit-specific RNAi-mediated suppression of SINCED1 increases both lycopene and β-carotene contents in tomato fruit. Journal of Experimental Botany, 63. 3097–3108.

- Tan, J., Zhou, Z., Niu, Y., Sun, X. & Deng, Z. (2017) Identification and functional characterization of tomato circRNAs derived from genes involved in fruit pigment accumulation. *Scientific Reports*, 7, 8594.
- Tikunov, Y.M., Laptenok, S., Hall, R.D., Bovy, A. & de Vos, R.C.H. (2012) MSClust: A tool for unsupervised mass spectra extraction of chromatography-mass spectrometry ion-wise aligned data. *Metabolomics*, 8, 714– 718
- Van Eck, J., Kirk, D.D. & Walmsley, A.M. (2006) Tomato (Lycopersicum esculentum). Methods in Molecular Biology, 343, 459–473.
- Vizcaíno, J.A., Deutsch, E.W., Wang, R., Csordas, A., Reisinger, F., Ríos, D. et al. (2014) ProteomeXchange provides globally coordinated proteomics data submission and dissemination. *Nature Biotechnology*, 32, 223–226.
- Vogel, J.T., Tan, B.C., McCarty, D.R. & Klee, H.J. (2008) The carotenoid cleavage dioxygenase 1 enzyme has broad substrate specificity, cleaving multiple carotenoids at two different bond positions. *Journal of Biologi*cal Chemistry, 283, 11364–11373.
- Von Lintig, J., Welsch, R., Bonk, M., Giuliano, G., Batschauer, A. & Kleinig, H. (1997) Light-dependent regulation of carotenoid biosynthesis occurs at the level of phytoene synthase expression and is mediated by phytochrome in Sinapis alba and Arabidopsis thaliana seedlings. The Plant Journal, 12, 625–634.
- Von Wettstein, D., Gough, S. & Kannangara, C.G. (1995) Chlorophyll biosynthesis. The Plant Cell, 7, 1039–1057.
- Wada, M. & Kong, S.G. (2011) Analysis of chloroplast movement and relocation in Arabidopsis. *Methods in Molecular Biology*, 774, 87–102. https://doi.org/10.1007/978-1-61779-234-2\_6
- Wang, R., Angenent, G.C., Seymour, G. & de Maagd, R.A. (2020) Revisiting the role of master regulators in tomato ripening. *Trends in Plant Science*, 25, 291–301.
- Waters, M.T. & Langdale, J.A. (2009) The making of a chloroplast. *EMBO Journal*, 28, 2861–2873.
- Wellburn, A.R. (1994) The spectral determination of chlorophylls a and b, as well as total carotenoids, using various solvents with spectrophotometers of different resolution. *Journal of Plant Physiology*, **144**, 307–313.
- Welsch, R., Zhou, X., Yuan, H., Álvarez, D., Sun, T., Schlossarek, D. (2018) Clp protease and OR directly control the proteostasis of phytoene synthase, the crucial enzyme for carotenoid biosynthesis in Arabidopsis. Molecular Plant, 11, 149–162.
- Yazdani, M., Sun, Z., Yuan, H., Zeng, S., Thannhauser, T.W., Vrebalov, J. et al. (2019) Ectopic expression of ORANGE promotes carotenoid accumulation and fruit development in tomato. Plant Biotechnology Journal, 17, 33–49.
- Yuan, M., Zhao, Y.Q., Zhang, Z.W., Chen, Y.E., Ding, C.B. & Yuan, S. (2017) Light regulates transcription of chlorophyll biosynthetic genes during chloroplast biogenesis. *Critical Reviews in Plant Sciences*, 36, 35–54.